Exciplex OLEDs: Strategies for White Emission and Multifunctional Devices

By

Kavya Rajeev
Registration No: 10PP18A39025

A thesis submitted to the
Academy of Scientific & Innovative Research
for the award of the degree of

DOCTOR OF PHILOSOPHY

in

SCIENCE

Under the supervision of
Dr. K. N. Narayanan Unni

CSIR-National Institute for Interdisciplinary Science and Technology (CSIR-NIIST), Thiruvananthapuram - 695019

Academy of Scientific and Innovative Research
AcSIR Headquarters, CSIR-HRDC Campus
Sector 19, Kamla Nehru Nagar,
Ghaziabad, U.P. – 201 002, India

October 2024

Dedicated to Achan, Amma, Janya & Rahul

राष्ट्रीय अंतर्विषयी विज्ञान तथा प्रौद्योगिकी संस्थान
वैज्ञानिक तथा औद्योगिक अनुसंधान परिषद् | विज्ञान तथा प्रौद्योगिकी मंत्रालय, भारत सरकार
इंडस्ट्रियल इस्टेट पी.ओ., पाप्पनंकोड, तिरुवनंतपुरम, भारत-695 019

CSIR-NATIONAL INSTITUTE FOR INTERDISCIPLINARY SCIENCE AND TECHNOLOGY (CSIR-NIIST)
Council of Scientific & Industrial Research | Ministry of Science and Technology, Govt. of India
Industrial Estate P.O., Pappanamcode, Thiruvananthapuram, India-695 019

डॉ. के एन नारायणन उण्णी
वरिष्ठ प्रिंसिपल वैज्ञानिक एवं प्रमुख
सतत ऊर्जा प्रौद्योगिकी केंद्र

Dr. K. N. Narayanan Unni
Senior Principal Scientist and Head
Centre for Sustainable Energy Technologies (C-SET)

October 28, 2024

CERTIFICATE

*This is to certify that the work incorporated in this Ph.D. thesis entitled," **Exciplex OLEDs: Strategies for White Emission and Multifunctional Devices**" submitted by **Ms. Kavya Rajeev** to the Academy of Scientific and Innovative Research (AcSIR), in fulfilment of the requirements for the award of the Degree of **Doctor of Philosophy in Science,** embodies original research work carried out by the student. We further certify that this work has not been submitted to any other University or Institution in part or full for the award of any degree or diploma. Research materials obtained from other sources and used in this research work have been duly acknowledged in the thesis. Images, illustrations, figures, tables, etc., used in the thesis from other sources have also been duly cited and acknowledged.*

Ms. Kavya Rajeev
(Student)

24/10/2024
Dr. K. N. Narayanan Unni
(Thesis Supervisor)

STATEMENTS OF ACADEMIC INTEGRITY

I Kavya Rajeev, a Ph.D. student of the Academy of Scientific and Innovative Research (AcSIR) with Registration No. 10PP18A39025 hereby undertake that, the thesis entitled *"**Exciplex OLEDs: Strategies for White Emission and Multifunctional Devices**"* has been prepared by me and that the document reports original work carried out by me and is free of any plagiarism in compliance with the UGC Regulations on *"Promotion of Academic Integrity and Prevention of Plagiarism in Higher Educational Institutions (2018)"* and the CSIR Guidelines for "*Ethics in Research and in Governance (2020)*".

28/10/2024

Kavya Rajeev

October 28, 2024

Thiruvananthapuram

It is hereby certified that the work done by the student, under my supervision, is plagiarism-free in accordance with the UGC Regulations on *"Promotion of Academic Integrity and Prevention of Plagiarism in Higher Educational Institutions (2018)"* and the CSIR Guidelines for "*Ethics in Research and in Governance (2020)*".

28/10/2024

Dr. K. N. Narayanan Unni

October 28, 2024

Thiruvananthapuram

ACKNOWLEDGEMENTS

I have great pleasure in expressing my deep sense of gratitude to Dr. K. N. Narayanan Unni, my thesis supervisor, for suggesting the research topic and for his constant guidance, endearing care, valuable support, and encouragement, leading to the successful completion of this work.

I wish to thank Dr. C. Anandharamakrishnan, Director and Dr. A. Ajayaghosh, former Director of the CSIR-National Institute for Interdisciplinary Science and Technology, Thiruvananthapuram, for providing me the necessary facilities for carrying out the work.

My sincere thanks to:

- *Dr. Biswapriya Deb., Dr. Joshy Joseph and Dr. Subrata Das., Doctoral Advisory Committee (DAC) members for their informative discussions in the DAC meetings.*
- *Dr. Jayamurthy P, Dr. V. Karunakaran, Dr. C. H. Suresh and Dr. R. Luxmi Varma present and former AcSIR co-ordinators for the timely help and advice for the academic procedures of AcSIR.*
- *Dr. K. V. Radhakrishnan, Dr. P. Sujatha Devi, and Dr. R. Luxmi Varma present and former Heads, Chemical Sciences and Technology Division for their endless support.*
- *All the AcSIR faculty members of CSIR-NIIST for their help and support during the course work period.*
- *Dr. K. R. Gopidas, Dr. Karunakaran Venugopal, Dr. Vijayakumar C, Dr. Jubi John, Dr. Sreejith Shankar, Dr. V. K. Praveen, Dr. Suraj Soman, Dr. Ishita Neogi, Dr. Adersh Asok, ,Dr. K. Yoosaf, Dr. Rakhi R. B., present and former scientists of the Chemical Sciences and Technology Division, for all the help and support extended to me.*
- *Dr. Atul Shukla , Dr. Ebinazar B. Namdas at University of Queensland, Australia for the collaboration, fruitful discussions and suggestions.*
- *Mr. Robert Philip, Mr. Kiran Mohan and Mr. Peer Mohamed A. for helping in material and thin-film characterization*
- *Mr. Nidhin, Mr. Jerin, Mr. Merin, Ms. Gayathri, Mr. Prasad, Ms. Viji and Ms. Aswathi for the general help*
- *Dr. Saurav, Dr. Swetha, Dr. Anooja J, Ms.Sruthi M M, Ms. Ramees Jebin, Mr. Andrew, Ms. Drishya, Mr. Nayan Dev, Dr.Thejus, Mr. Thejas, Ms.Shisina, Ms. Malini, Ms.*

Sruthi, Ms. Ragi, Ms. Angitha, Ms. Anjali, Ms. Lakshmi, Ms. Adithya, Ms. Lekshmi, etc..for helping with various experiments

- *Mr. Nandu, Mr. Shashwath, Mr. Vipin C K, Dr. Manuraj, Dr. Jayadev, Dr. Rajeev V R, Dr. Anjali Soman, Dr Hanna B and all other former group members for their cooperation and companionship in the lab.*
- *Anagha, Rani, Megha, Riya, Navin, Mani and Akshay for their constant support, and affection throughout my stay at NIIST and all other present and former members of CSTD, C-SET & friends at CSIR-NIIST for their good companionship, care, love, and support throughout my PhD period.*
- *Ms. Devika and Dr. Krishnapriya for their constant care and companionship throughout my stay in Lakshmi Nilayam*
- *CSIR-JRF and SRF for financial assistance.*

I extend my heartfelt thanks to Dr. Anjali K Sajeev and Dr. Vibhu Dharshan for their unwavering support and genuine companionship, which has truly made this journey feel like being part of a cherished family.

I am deeply indebted to my Achan , Amma and Janya for their unconditional love, and unerring support in my life. I am deeply grateful to my partner Rahul for all the patience, understanding, love, and support. I would also like to extend my thanks and appreciation to all my teachers and friends for their help and support.

Kavya Rajeev

TABLE OF CONTENTS

LIST OF ABBREVIATIONS

Å	Angstrom
A	Acceptor
AFM	Atomic-force microscopy
$Al(DBM)_3$	tris(dibenzoyl methane)-aluminum
Alq_3	Tris(8-hydroxyquinoline)aluminium
AMOLED	Active-Matrix OLED
BAlq	Bis(8-hydroxy-2-methylquinoline)-(4-phenylphenoxy)aluminum
BCP	2,9-Dimethyl-4,7-diphenyl1,10phenanthroline
BczVBi	4,4'-Bis(9-ethyl-3-carbazovinylene)-1,1'-biphenyl
BCzPh	9,9'-Diphenyl-9H,9'H-3,3'-bicarbazole
BPhen	4,7-Diphenyl-1,10-phenanthroline
CBP	4,4′-Bis(carbazol-9-yl)biphenyl
CCT	Correlated Color Temperature
CDBP	4,4'-Bis(9-carbazolyl)-2,2'-dimethylbiphenyl
CE	Current Efficiency
CGL	Charge Generation Layer
CIE-1931	Commission Internationale de l'Eclairage-1931
CRI	Color Rendering Index
CS_2CO_3	Caesium Carbonate
CT	Charge Transfer
C545T	2,3,6,7-Tetrahydro-1,1,7,7,-tetramethyl-1H,5H,11H-10-(2benzothiazolyl)quinolizino[9,9a,1gh]coumarin
CzPN	4,5-Bis(carbazol-9-yl)-1,2-dicyanobenzene
D	Detectivity
D	Donor
D-A-D	Donor-Acceptor-Donor
DCJTB	4-(Dicyanomethylene)-2-tert-butyl-6-(1,1,7,7-tetramethyljulolidin-4-yl-vinyl)-4H-pyran
DCQTB	(E)-2-(2-tert-Butyl-6-(2-(2,6,6-trimethyl-2,4,5,6-tetrahydro-1H-pyrrolo[3,2,1-ij]quinolin-8-yl)vinyl)-4H-pyran-4-ylidene)malononitril
3,5-DCzPPy	3,5-Bis(3-(9H -carbazol-9-yl)phenyl)pyridine

DDCzTrz	9,9',9",9"'-((6-Phenyl-1,3,5-triazine-2,4-diyl)bis(benzene-5,3,1-triyl))tetrakis(9H -carbazole)
DNPhB	difluoroboron(Z)-3-(diphenylamino)-3-hydroxy-N,N-diphenylacrylamide
DPNC	3,6-di (4,4′-dimethoxydiphenylaminyl)-9-(1-naphthyl) carbazole
EML	Emissive Layer
EL	Electroluminescence
EQE	External Quantum Efficiency
F8BT	Poly(9,9-dioctylfluorene-alt-N-(4-sec-butylphenyl)-diphenylamine)
FCNIrPic	Bis(3,5-difluoro-4-cyano-2-(2-pyridyl)phenyl-(2-carboxypyridyl) iridium(III)
FIrpic	Bis[2-(4,6-difluorophenyl)pyridinato-C2,N](picolinato)iridium(III)
FWHM	Full width at half maximum
HBL	Hole Blocking Layer
HIL	Hole Injection Layer
HAT-CN	1,4,5,8,9,11-Hexaazatriphenylenehexacarbonitrile
HOMO	Highest Occupied Molecular Orbital
HTM	Hole transporting layer
I_{ph}	Photocurrent
IQE	Internal Quantum Efficiency
$Ir(btp)_2(acac)$	Bis(2-benzo[b]thiophen-2-ylpyridine) (acetylacetonate)iridium(III)
$Ir(MDQ)_2acac$	2-methyldibenzo[f,h]quinoxaline
$Ir(mppy)_3$	Tris[2-(p-tolyl)pyridine]iridium(III)
$Ir(piq)_3$	Tris(1-phenylisoquinoline) iridium(III)
$Ir(ppy)_3$	Tris(2-phenylpyridine)iridium(III)
$(Ir(ppy)_2acac)$	bis[2-(2-pyridinyl-N)phenyl-C](acetylacetonato)iridium(III)
ISC	Inter System Crossing
ITO	Indium doped Tin Oxide
J	Current Density
J_d	Dark current density
KPFM	Kelvin Probe Force Microscopy

L	Luminance
LiF	Lithium Fluoride
LUMO	Low Unoccupied Molecular Orbital
MC	Magneto-Conductance
MCP	1,3-Bis(carbazol-9-yl)benzene
m-CBP	3,3′-Di(9H-carbazol-9-yl)-1,1′-biphenyl
MEL	Magneto- electroluminescence
m-MTDATA	4,4',4"-Tris[phenyl(m-tolyl)amino]triphenylamine
MoO_3	Molybdenum trioxide
NEP	Noise Equivalent Power
NPB	N,N′-Di(1-naphthyl)-N,N′-diphenyl-(1,1′-biphenyl)-4,4′-diamine
OFETs	Organic field-effect transistors
OLEDs	Organic Light Emitting Diodes
OPDs	Organic photodetectors
OPVs	Organic Photovoltaics
OXD-7	1,3-Bis[2-(4-tert-butylphenyl)-1,3,4-oxadiazo-5-yl]benzene
P_0	Incident optical power
PBD	2-(4-Biphenyl)-5-(4-tert -butylphenyl)-134-oxadiazole
PDM	permanent dipole moment
PE	Power efficiency
PEDOT	poly(3,4-ethylenedioxythiophene)
PhOLED	Phosphoroscent OLED
PL	Photoluminescence
PO-T2T	(2,4,6-tris[3-(diphenylphosphinyl)phenyl]-1,3,5-triazine)
PO-01	Bis(4-phenylthieno[3,2-c]pyridinato-N,C2') (acetylacetonate) iridium(III)
PO15	2,8-Bis(diphenyl-phosphoryl)-dibenzo[b,d]thiophene
PPh_3O	Triphenylphosphine oxide
PSS	Polystyrene sulfonate
PtOEP	Platinum(II) octaethylporphine
PVK	Poly(9-vinylcarbazole)
q	electron charge
R	Responsivity
Rb_2CO_3	Rubidium carbonate

RD071	iridium III)bis[2,-4-dimethyl-6-[5-(2-methylpropyl)-2-quinolinyl-N]phenyl-C]-(2,4-pentanedionato-O2,O4)
RGB	Red Green Blue
Rubrene	5,6,11,12)-tetraphenyl-naphthacene
STO	2,5-bis(trimethylsilyl)-thiophene-1,1-dioxide
SOP	Spontaneous Orientation Polarization
SP	surface potential
TADF	Thermally Activated Delayed Fluorescence
TAPC	4,4′-Cyclohexylidenebis[N,N-bis(4 methylphenyl)benzenamine]
TAZ	3-(biphenyl-4-yl)-5-(4-tert-butylphenyl)-4-phenyl-4H-1,2,4-triazole
TBRb	2,8-Di-tert-butyl-5,11-bis(4-tert -butylphenyl)-6,12-diphenyltetracene
TCTA	tris(4-carbazoyl-9-ylphenyl)amine
TCPZ	2,4,6-tris(3-(carbazol-9-yl)phenyl)-triazine
TFB	Poly(9,9-dioctylfluorene-alt-N-(4-sec-butylphenyl)-diphenylamine)
T_g	glass transition temperature
TiO_2	Titanium dioxide
TmPyPB	1,3,5-Tri(m-pyridin-3-ylphenyl)benzene
TPBi	1,3,5-Tris(1-phenyl-1H-benzimidazol-2-yl)benzene
TPD	N,N′-Bis(3-methylphenyl)-N,N′-diphenylbenzidine
Tris-PCz	9-Phenyl-3,6-bis(9-phenyl-9Hcarbazol-3-yl)-9H-carbazole
V	Voltage
WOLEDs	White OLEDs
$Zns(BZT)_2$	zinc bis-2-shydroxyphenyld benzothiazole

PREFACE

Organic electronics is a rapidly growing field that involves the use of carbon-based semiconducting materials to develop flexible, lightweight and cost-effective electronic devices enabling innovations in areas such as displays, lighting, photovoltaics, bioelectronics, etc. Among the various advancements in organic electronics, organic light emitting diodes (OLEDs) have emerged as key players, for high quality displays in consumer electronics and as potential candidates for efficient lighting solutions. However, despite their remarkable progress, OLEDs still face critical challenges including high production costs and limited lifespan, which have hindered their broader commercial adoption. This thesis explores recent progress in exciplex based OLEDs, focuses on novel and simplified device architectures for white emission and explores the idea of multifunctionality in devices.

In **Chapter 1,** an introduction to organic electronics, OLEDs and the concept of exciplex emission are presented. Recent advancements in exciplex-based OLEDs are discussed in detail, highlighting their potential for simple device architectures eliminating the need for a separate emissive layer. Exciplex formed at the interface of transport layers, can act as emitter as well as host for phosphorescent, fluorescent or thermally activated delayed fluorescence (TADF) dopants. By strategically combining the exciplex emission with the emission of dopants, white emission can be acheived without complex device architectures. The existing literature on exciplex based OLEDs; both as emitters and hosts has been thoroughly reviewed to identify commercially available transport materials that are yet to be explored for forming novel exciplex pairs. This opens up new opportunities for developing efficient and cost-effective OLED architectures by utilizing the hitherto unexplored combinations of transport materials.

In **chapter 2**, the issues with the blue emitters and complex device structures of white OLEDs (WOLEDs) are addressed to some extent. A blue exciplex emission at the interface of NPB

(N,N'-bis(naphthalen-1-yl)-N,N'-bis(phenyl)benzidine) and TAZ (3-(biphenyl-4-yl)-5-(4-tert-butylphenyl)-4H-1,2,4-triazole) was obtained. The NPB/TAZ exciplex was utilized as emitter and as well as a host with a yellow phosphorescent dopant, iridium (III) bis(4-phenylthieno[3,2-c]pyridinato-N,C2')acetylacetonate (PO-01). The device design consists of an emissive layer containing both blue and yellow emitting units. By strategically incorporating tetracene as a spacer layer in between the blue and yellow emitting units, we achieved a white emission with CIE coordinates (0.36, 0.39) and a correlated color temperature (CCT) of 4643 K. This approach simplifies the device architecture by utilizing a spacer layer instead of a charge generation layer (CGL), thereby reducing complexity while enhancing white emission.

In **chapter 3**, Solution-processing method was employed, aiming to reduce process complexity and to minimize material usage. The concept of multifunctionality in exciplex based OLEDs is also explored. The combination of NPB and OXD-7 (1,3-bis[2-(4-tert-butylphenyl)-1,3,4-oxadiazo-5-yl]benzene) was utilized for the blue exciplex emission, which could function as an emitter as well as a host with a yellow phosphoroscent dopant, PO-01. A maximum brightness of 36,000 cd/m^2 was achieved for the yellow OLED with an external quantum efficieny (EQE) of 11%. The dual functionality of an NPB:OXD-7 exciplex was also investigated, which acts both as an OLED and a UV photodetector. This multifunctionality is attributed to the strong UV absorption and high surface potential of OXD-7. The surface potential in organic semiconductor thin films originates from the spontaneous orientation polarization (SOP), which facilitates exciplex dissociation and subsequent generation of photocurrent. By judiciously varying the raio of NPB:OXD mixture, either the light emission or the light detection can be made prominent. A multifunctional device, acting as a self-powered UV detector, exhibited a detectivity of 4×10^{11} Jones, responsivity of 17 mA/W and an ON-OFF ratio of 3×10^3 with a reasonable OLED performance.

In **chapter 4**, Single emissive layer WOLEDs are presented by integrating exciplex and excitonic emissions within an emissive layer. The study investigates two blue-emitting hole transport materials (HTMs), TPD (N,N′-Bis(3-methylphenyl)-N,N′-diphenylbenzidine) and TFB (Poly(9,9-dioctylfluorene-alt-N-(4-sec-butylphenyl)-diphenylamine), together with the electron transport material (ETM), PO-T2T (2,4,6-tris[3-(diphenylphosphinyl)phenyl]-1,3,5-triazine). WOLED with a simplified device architecture is demonstrated that combines yellow emission from the TPD:PO-T2T exciplex with blue emission at the TPD/TPBi interface exciplex combined with the emission of TPD. WOLED achieved a high color rendering index of 78 and a maximum brightness of 3358 cd/m². Additionally, it was observed that the incorporation of TFB into the emissive layer resulted in a voltage-dependent emission shift from blue to cool white, showcasing the potential for tunable white light emission within a single emissive layer.

Chapter 1

Introduction to organic electronics, organic light emitting diodes (OLEDs) and exciplex OLEDs

1.1 Abstract

Organic electronic devices utilizing carbon-based materials are an alternative to traditional electronics, especially in flexible displays and solar energy applications. Organic light emitting diode (OLED) is the key application using organic semiconductors. This chapter explores recent advancements in exciplex based OLEDs, emphasizing their potential in cost-effective fabrication by eliminating the need for separate emissive layers. Exciplex emissions, which occur at the molecular interface of a hole transport material (HTM) and electron transport material (ETM), can act as a host for phosphorescent, fluorescent, and thermally activated delayed fluorescence (TADF) dopants, contributing to efficient white OLED (WOLED) designs avoiding complex tandem structures. The strategic selection of exciplex combination is crucial for achieving complementary color emissions and advancing the development of non-tandem white OLEDs. Exciplexes find application not only in OLEDs but also in organic photovoltaic cells as well as photodetectors and it is possible to develop multifunctional devices using exciplexes.

1.2 Introduction

OLEDs have become an inevitable component in the smart electronic world, especially information displays in various electronic gadgets as well as in solid state lighting. The evolution of display technology has progressed from traditional LEDs to advanced OLEDs, marking a significant shift in the capabilities and performance of modern displays. The first LED television was developed in 1977 by James P. Mitchell. Over time, LED technology evolved and was integrated with liquid crystal display (LCD) TVs to provide backlighting for the LCD screen pixels. LEDs produce light through electroluminescence, a process where a semiconductor material emits light when an electric current passes through it. White edge LEDs, LED Arrays, and dynamic LEDs are primarily used LED technologies used by TV manufacturers. LEDs in lighting surpass incandescent, halogen, and other conventional lighting technologies. In recent years, hybrid LEDs combining quantum dots (QDs) and organic emitters, called quantum dot OLEDs (QD-OLEDs)[2] have been the focus of extensive research due to their promising applications in lighting and display technologies. QD-OLEDs offer several advantages, including high efficiency, stable emission, high brightness, and exceptional color rendering capabilities. Various QD types include cadmium-based QDs[3], indium phosphide-based QDs[4], perovskite QDs[5], etc. However, the toxicity of heavy metals like cadmium (Cd), lead (Pb), etc. and intrinsic instability of the QDs and perovskites have significantly impeded the commercial applications of hybrid LEDs[6, 7]. OLEDs, which rely exclusively on organic materials are self-illuminating with several key benefits over LEDs. OLED technology enables the creation of flexible, foldable, thinner, and lighter displays compared to LEDs. OLEDs provide a much wider viewing angle, a wider range of colors and

are more energy-efficient, making them a better choice for both performance and sustainability. This chapter discusses various aspects of OLEDs, including their structure, working principle, emission mechanisms etc. and give a comprehensive understanding on employing exciplex emission in OLEDs and its significance in modern OLED technology.

1.3 Organic electronics - an overview

Organic electronics is a rapidly evolving field that integrates materials science, polymer chemistry and electronics. Unlike inorganic electronics, organic electronics utilizes carbon-based materials such as polymers and small molecules. Like their inorganic counter parts, organic semiconductors also possess semiconductor properties such as a bandgap, mobility, and a negative temperature coefficient of resistance. Organic electronic devices offer several unique advantages including flexibility, low-cost manufacturing and compatibility with large area and low-temperature processing techniques, making it a promising alternative to inorganic electronics. Their inherent flexibility enables the development of flexible devices, making them ideal for applications such as flexible displays and wearable gadgets. Organic electronic devices are characterized by their ability to be processed using solution-based techniques like inkjet printing, spin coating and spray deposition. These methods significantly reduce production costs and enable large area and roll-to-roll fabrication facilitating high-volume manufacturing. Applications of organic electronics are diverse and include OLEDs for displays and lighting, OPV devices for solar energy harvesting and organic field-effect transistors (OFETs) for logic and memory applications. Organic sensors, neuromorphic devices and robotics represent other emerging areas of interest. In summary, organic semiconductor materials are central to the field of organic electronics offering flexibility, low-cost

manufacturing, and tunable properties compatible with diverse substrates. This makes them a versatile platform for developing next-generation electronic devices with wide variety of applications across consumer electronics, healthcare and beyond. In the world of smart gadgets, organic electronics hold significant promise for contributing to technology and sustainability addressing various societal challenges and expanding the potential of electronic devices.

1.4 An introduction to organic light emitting diodes (OLEDs)

The use of electronic gadgets has significantly increased in the post-pandemic world. Smart phones, smart TVs, smart watches etc. have become inevitable consumer electronics components of day-to-day life. OLED displays have become integral to nearly all smart gadgets worldwide due to their superior image quality, vibrant colors, and flexibility. Additionally, OLED technology enables thinner and lighter designs and consumes less power making it ideal for portable devices. The evolution of OLEDs has started with the invention of first OLED by Tang and Vanslyke in 1987[8]. They used an aromatic diamine as the hole transporting or electron blocking layer and tris(8-hydroxyquinoline) aluminum (Alq_3) as the electron transporting and emitting layer. They could obtain an external quantum efficiency (EQE) of 1% and brightness of over 1000 cd/m^2. The Figure 1.1(a) shows the photographs of the OLED inventors and the device architecture of the first OLED. This is considered as a mile-stone in the history of organic electronics. Thereafter, it started bringing tremendous contributions in the display and lighting technology. The first polymer OLED was developed by Burroughes *et al.* in 1990. By 1997, Kido *et al.* demonstrated the first active-matrix OLED (AMOLED), paving the way for advanced display technology. In 1998, Baldo *et al.* introduced

phosphorescent OLEDs, further enhancing the efficiency and performance of OLEDs. World's first OLED display was incorporated in a car audio screen and commercialization of OLED technology took a major leap in 2007 with Sony's release of the first OLED TV; photographs of the display and TV are shown in Figure 1.1 (b).

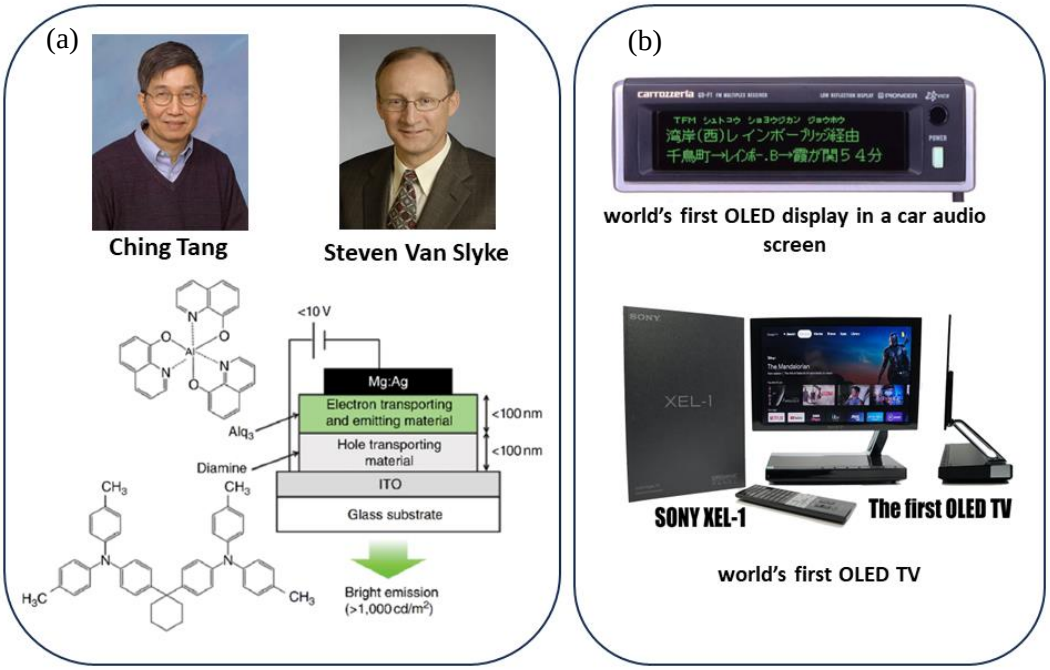

Figure 1.1. (a) The photographs of the OLED inventors Ching Tang and Steven Van Slyke and the device architecture of the first OLED (adapted from ref.8). (b) photograph of the first OLED display in a car audio screen and world's first OLED TV (adapted from ref.9).

The evolution continued with the development of TADF OLEDs by Adachi *et al.* in 2012, which improved the practical applications of OLEDs[9]. Over time, OLED technology has become widespread in consumer electronics, demonstrating its versatility and superior performance compared to traditional display technologies. Attractive properties of OLEDs include self-emitting property, high contrast, high color gamut, light weight, low-power consumption etc. and it can create potentially large area, flexible as well as transparent devices.

However, cost challenge in OLEDs is still a major bottleneck for this fast-growing technology. Inorder to achieve cost-effectiveness, we need to simplify the processing techniques for manufacturing of OLEDs and novel and simplified device architectures are to be employed.

1.4.1 OLEDs : Structure, working principle and parameters

A typical OLED consists of an emissive layer sandwiched between transport as well as injection layers on both sides followed by anode and cathode as shown in Figure 1.2 (a). The injection layers lower the energy barrier for hole/electron injection from anode/cathode to the transport layers. Lithium fluoride (LiF) and cesium carbonate (Cs_2CO_3) are the commonly used electron injection layers (EILs) and PEDOT: PSS (poly (3,4-ethylenedioxythiophene: polystyrene sulfonate) and molybdenum trioxide (MoO_3) are used as hole injection layers (HILs). The selection of suitable transporting layers is based on matching energy levels to lower the energy barriers. The hole transport layer (HTL) transport holes as well as blocks electrons from the emissive layer and electron transport layer (ETL) transport electrons and block holes from the emissive layer towards anode. The transport layers ensure overall charge balance, efficiency, and stability of the devices. Commonly used HTLs are N,N′-Di(1-naphthyl)-N,N′-diphenyl-(1,1′-biphenyl)-4,4′-diamine (NPB), N,N′-Bis(3-methylphenyl)-N,N′-diphenylbenzidine (TPD), 4,4',4"-Tris[phenyl(m-tolyl)amino]triphenylamine (m-MTDATA), tris(4-carbazoyl-9-ylphenyl)amine (TCTA) , poly(9-vinylcarbazole) (PVK), poly(9,9-dioctylfluorene-alt-N-(4-sec-butylphenyl)-diphenylamine) (TFB), poly(9,9-dioctylfluorene-alt-N-(4-sec-butylphenyl)-diphenylamine) (F8BT)[10] and ETLs are 1,3,5-Tris(1-phenyl-1H-benzimidazol-2-yl)benzene (TPBi), 4,7-Diphenyl-1,10-phenanthroline (BPhen) , Alq_3, 1,3-Bis[2-(4-tert-butylphenyl)-1,3,4-oxadiazo-5-yl]benzene (OXD-7), bis(8-

hydroxy-2-methylquinoline)-(4-phenylphenoxy)aluminum (BAlq), 1,3,5-Tri(m-pyridin-3-ylphenyl)benzene (TmPyPB), (2,4,6-tris[3-(diphenylphosphinyl)phenyl]-1,3,5-triazine) (PO-T2T) etc[11-15]. The holes are injected from anode and electrons are injected from cathode. These carriers get transported through the transport layers to reach the emissive layer. At the emissive layer, the exciton recombination and radiative emission occur. The working of a typical OLED with its energy level schematic is illustrated in Figure 1.2 (b).

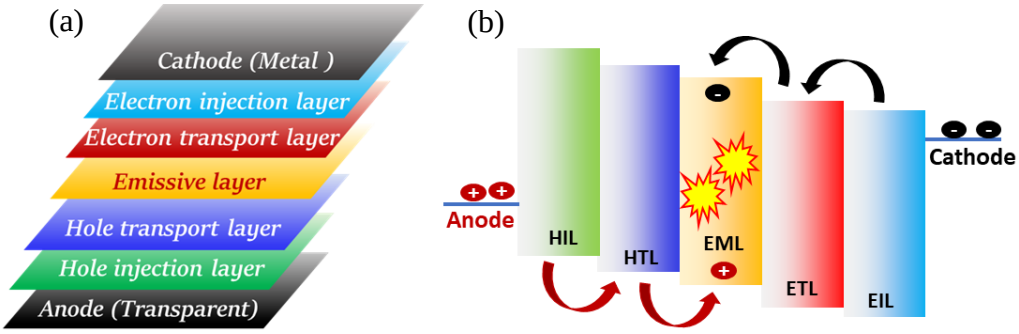

Figure 1.2. (a) Device architecture and (b) working principle of a typical OLED.

Luminance is the key parameter of an OLED which is the light emitted per unit area of the device. The current density (J)- voltage (V)- luminance (L) characteristics show the variation in current density and luminance with respect to the applied bias. The main efficiency parameters of an OLED are current efficiency (CE), power efficiency (PE), internal quantum efficiency (IQE) and EQE. CE is the ratio of luminance to the current density, represents how effectively electrical energy is converted into light. IQE gives the ratio of number of photons generated within the OLED to the number of electrons injected into it. While EQE measures the number of photons emitted from the OLED in the forward direction compared to the number of electrons injected into the device. EQE of an OLED depends on several factors such as charge balance factor (γ), singlet to triplet ratio of excitons ($\eta_{S/T}$), photoluminescence

quantum yield of the emitter (η_{PL}) and out-coupling efficiency (η_{out}). EQE can be represented as the product of IQE and out-coupling efficiency. Hence the maximum EQE of a fluorescent OLED, which uses only singlet excitons, is limited to 5% by considering the emission losses due to these factors within the device. However, the efficiency in phosphorescent OLEDs can be substantially higher as it employs triplet excitons also for emission via spin-orbit coupling. In addition, there are some other parameters defining the emission of the device. Correlated color temperature (CCT) describes the temperature of a blackbody which emits the same wavelength as that of the device. The color rendering index (CRI) evaluates how accurately the emission of the device reveals the colors of objects in comparison to a natural light source. Color purity, which refers to how pure or monochromatic a color is at a certain level of brightness. If the spectrum consists of equal intensities of all colors, the result would be grey, indicating low purity or saturation. Conversely, if the spectrum features a single intense peak with a narrow Full width at half maximum (FWHM), it represents high purity or saturation. Efficiency roll-off refers to the decrease in current efficiency with increase in brightness. In addition to efficiency and color properties, another important parameter for evaluating OLED performance is its lifetime. Lifetime refers to the time elapsed until the OLED either fails entirely or its efficiency drops below a predefined level[16].

1.4.2 Characteristics and hurdles of OLED technology

In the fast-paced realm of display technology, OLED displays have emerged as a groundbreaking innovation, revolutionizing our interaction with digital devices. This advanced technology, renowned for its superior image quality and energy efficiency is reshaping the user experience across various sectors from smartphones to televisions and gaming devices.

Innovations include flexible OLEDs for roll-up TVs, bendable smartphones, transparent OLEDs for smart windows, augmented reality, etc. OLEDs provide more energy efficient lighting by redefining light quality and lighting design. OLED lights offer unique design, flexibility and produce warm, pleasant, and even lighting that mimics the characteristics of natural light. Some of the commercial products using OLEDs in the display and lighting industry are shown in Figure 1.3. The OLED industry is indeed facing several challenges despite its promising technology. OLED products are more expensive compared to traditional LCDs, due to the complex fabrication procedures, complicated multilayer structures and high cost emitter materials involved.

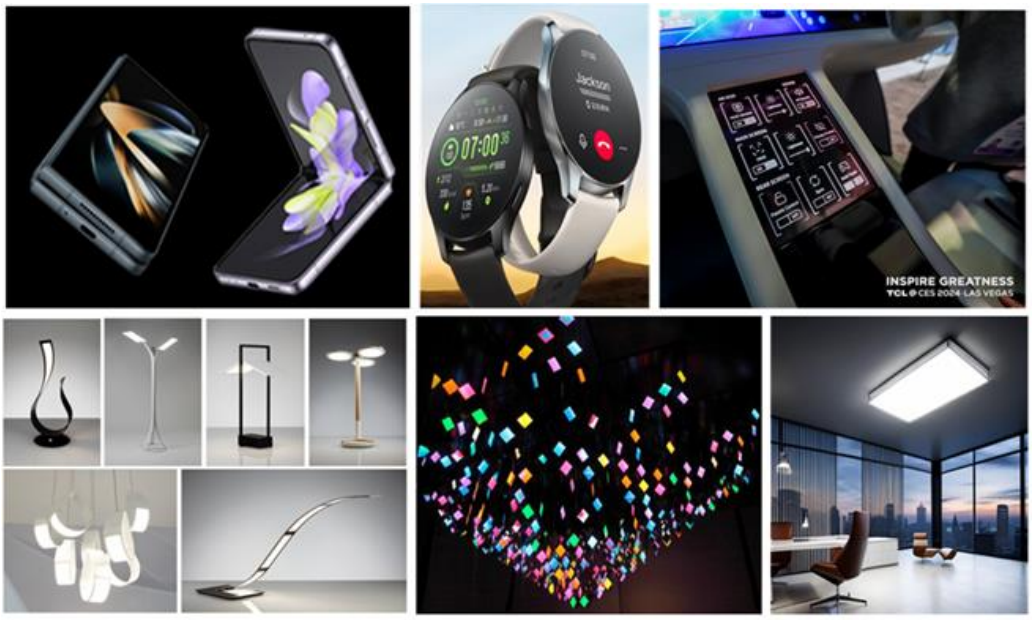

Figure 1.3. Commercially available products using OLEDs in the display and lighting industry.

Future advancements aim to improve energy efficiency, extend display lifespan, enhance color accuracy and brightness promising a more immersive and sustainable user experience and cost-effectiveness. Lack of stable blue emitters is another major issue which affects the overall

display quality[17]. Blue emitting materials are less stable with wider band gap and often have lower energy transfer efficiency compared to red and green emitters[18, 19]. Innovative approaches in material design and advanced manufacturing techniques are needed to achieve stable and efficient blue emitting OLED materials suitable for commercial applications.

1.4.3 Emission mechanisms in OLEDs

To obtain satisfying device performances with high efficiencies, OLEDs must have the potential to fully harvest the singlet and triplet excitons generated in the emissive layer. Based on the emission mechanisms, different generations of emitters are defined[20]. Fluorescent emitters[21-23] are considered as the first generation emitters where only the transition of singlet excitons to the singlet ground state (S_1 to S_0) is theoretically allowed. The maximum theoretical EQE is 25% as the singlet to triplet ratio is 1:3 in OLEDs. However, considering all other loss mechanisms, the EQE is generally limited to 5%. Phosphorescent emitters[24-26] are the second generation emitters in which intersystem crossing (ISC) from S_1 to T_1 transition occurs. As a result, triplet state becomes radiative after a transition from T_1 to S_0. Since the triplet excitons (75%) are also utilized, the theoretical IQE is up to 100%. Third generation of TADF emitters[27-29] have a small energy gap between S_1 and T_1 (ΔE_{ST}), hence thermally activated reverse inter system crossing (RISC) occurs from T_1 to S_1. Hence, theoretical IQE up to 100% is possible in the case of TADF emitters. Hyperfluoroscene[30-32] or thermally-assisted fluorescence is considered as the fourth generation emitters. Here a fluorescent emitter is combined with a TADF assistant dopant to utilize 100% excitons for high efficiencies. QDs are regarded as promising alternative emissive materials for next generation hybrid LEDs. QDs

exhibit quantum confinement effect and the tuning of emission by controlling their size. The EQE of QD LEDs depends on the quantum yield of the QDs.

In this context, concepts such as excimer[33, 34],electromer[35, 36],exciplex[37, 38] and electroplex[39, 40] hold significant importance as they can be triggered using common transport materials and the need of a separate emissive layer can be eliminated. Excimer and exciplex represent excited state emissions achievable through both optical and electrical excitation, whereas electromer and electroplex is exclusively obtained via electrical excitation. This chapter provides a detailed discussion on the concept of exciplex emission, recent advancements in exciplex-based OLEDs, and their role in cost-effective fabrication.

1.5 Exciplex OLEDs : An alternate route towards cost-effectiveness

An exciplex is described as an excited state complex which is formed at the interface of a donor and an acceptor molecule. Consider a pair of donor and acceptor molecules designated as D and A. Under photo-excitation, donor will get excited to form a ground state complex with the acceptor as shown in Figure 1.4. This collision complex is stabilized by charge transfer interaction (CT interaction), called exciplex[41]. This energetic stabilization causes the collision complex to have a longer lifetime compared to the molecular excited states of the component molecules. Exciplex has observable spectroscopic and chemical properties which are distinct from its component molecules.

When we employ the concept of exciplex emission in OLEDs, an excited state complex is formed at the molecular interface of hole and electron transport materials. This points towards the possibilities for simplified device architectures by eliminating separate emissive layer. The

selection of suitable donor and acceptor materials for an efficient exciplex system is done based on the moderate highest occupied molecular orbital (HOMO)-HOMO and low unoccupied molecular orbital (LUMO)-LUMO offset values and at the HTM/ETM interface[42-44]. The broad and red shifted photoluminescence emission spectrum of the exciplex film compared to its that of the component molecules is considered as an evidence for exciplex emission[45, 46].

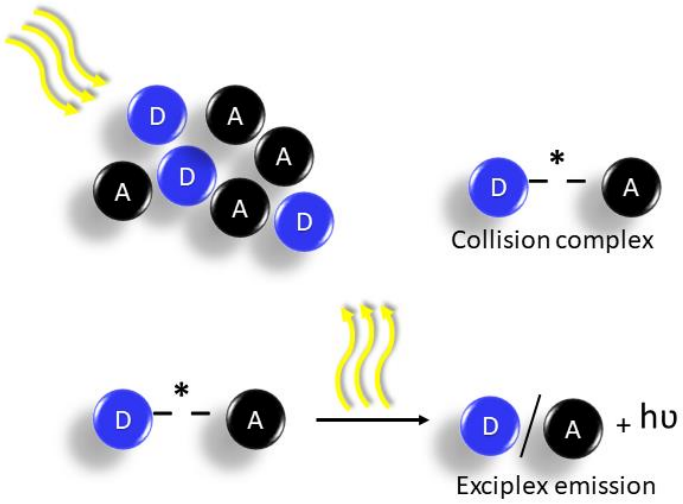

Figure 1.4. Illustration of the mechanism of exciplex emission between a donor molecule (represented as D) and an acceptor molecule (represented as A).

Exciplex can be used either as an emitter or as a host with phosphorescent, TADF or fluorescent dopants. The ability for bipolar transport ability of exciplex system can help to use it as a host with suitable dopants. Highly efficient exciplex OLEDs can be achieved by effectively transferring its energy to suitable emitters. By utilizing exciplex systems of complementary colors, white light emission can also be achieved. Several reports on exciplex-based OLEDs adopting simplified device architectures have been published. This may address the problem of high cost in OLED display as well as lighting industry. Exciplex-based systems with small singlet-triplet energy gap or ΔE_{ST}, can offer 100% exciton harvesting ability in these

systems. Previously, the appearance of exciplex in OLEDs was considered as a major concern for reduced device performance. In 2005, Y. N. Mohapatra and his team at IIT Kanpur reported the spectral broadening in electroluminescent (EL) spectra of the devices due to interfacial exciplex formation[47]. Broad and red shifted EL spectrum was proposed to be due to the formation of exciplex at the TPD /zinc bis-2-shydroxyphenyld benzothiazole ($Zns(BZT)_2$) interface. When they apply an electric field, charge carriers had maximum probability to form the exciplexes at the molecular interfaces, also the dimeric structure of $Zns(BZT)_2$ gives multiple sites for the carriers to bind. This work has pointed towards the strategies for the improvement of device efficiency without losing the wide spectral width of exciplexes. Later in 2012, Goushi *et al.* demonstrated a new strategy for radiative exciton production by using the high RISC efficiency of exciplex state[48]. They achieved a promising EQE via RISC to enhance the radiative exciton production efficiency. This report has shed light on the possibilities of exciplex emission in OLEDs. Since 2015, a growing number of reports on exciplex-based OLEDs have been published.

1.5.1 Exciplex as emitters – literature review

1.5.1.1 Monochrome OLEDs

Revolutionary concepts of exciplex-based approach in efficient OLED architectures have attracted the interest of many researchers since 2015. There are reports on highly efficient and simplified monochromatic OLEDs by utilizing exciplex as a host. Exciplex can also be formed by blending bipolar materials which involves the selection of a suitable donor-acceptor-donor (D-A-D) type molecule. By utilizing exciplex emitters of complementary colors, simplified WOLED structures can also be adopted. Full exciplex-based WOLEDs have become an

alternative for full-tandem WOLEDs, in which the additional task of incorporation of charge generation layer (CGL) can be avoided. Several donor-acceptor combinations have come up with promising performance for exciplex emitter-based OLEDs. However, proper selection criteria for a suitable donor and acceptor combination and high efficiency OLEDs using exciplex as an emitter are yet to be explored.

In 2007, Su *et al.* have reported the effect of acceptors on the efficiency of exciplex emission[49]. Here they used electron transport materials such as Alq_3, TPBi, 2,9-Dimethyl-4,7-diphenyl1,10-phenanthroline (BCP), 2-(4-Biphenyl)-5-(4-tert -butylphenyl)-134-oxadiazole (PBD), etc., with a commonly used hole transport material m-MTDATA. They found that the intermolecular contact between the donor and acceptor molecules is preferred for efficient exciplex formation and minimum barriers at the interfaces are also needed to avoid the uncontrolled flow of carriers. However, this study has brought a lot of attention in employing exciplex emission in efficient OLED designs. Later in 2014, Jankus *et al.* have come up with the concept of exciplex formation in a D-A-D molecule and also with a commonly used host 4,4′-Cyclohexylidenebis[N,N-bis(4-methylphenyl)benzenamine](TAPC)[50]. Liu *et al.* have presented three exciplex emitters consisting of one electron acceptor 3-(4,6-Diphenyl-1,3,5-triazin-2-yl)-9-phenyl-9H-carbazole (DPTPCz) with three different electron donors TAPC, NPB and TPBi[51]. The TAPC device got an EQE of 15.4% with an excellent EL. Santos *et al.* have demonstrated that the locally excited triplet states would undergo RISC to form locally excited (LE) singlet states to give TADF [52]. The delayed emission in exciplex is depending on the CT and LE energy difference rather than the ΔE_{ST} value. In 2017, Pang *et al.* have introduced the concept of magneto electroluminescence (MEL) in exciplex OLEDs[53]. The ΔE_{ST} in exciplexes can allow the magnetic field to manipulate the singlet-triplet populations,

and this type of devices are called 'spin XOLEDs'. An extrinsic MEL can be generated by connecting this through a magnetic tunnel junction as shown in Figure 1.5 (a). The color changing was observed with a sweeping magnetic field. Solution-processed exciplex-based OLEDs were reported by using a solvent-mixing method[54]. Here they have achieved better results by mixing two solvents chlorobenzene and chloroform. The results were comparable to evaporated devices as well. This has pointed towards the possibilities of solution-processable exciplex OLEDs. In 2018, Yuan *et al.* have presented an effective method to enhance the exciplex formation by co-doping an organic spacer molecule into the exciplex mixture as shown in Figure 1.5 (b)[55]. This work showed the possibilities of novel EML designs for efficient exciplex formation. The lack of deep blue emitters in the OLED industry can be addressed by the investigation on exciplex combinations giving deep blue emissions. Hippola *et al.* have come up with a deep blue emitting exciplex consisting of NPB/TPBi: triphenylphosphine oxide (PPh_3O). They have also studied the exciplex formation between NPB:TPBi and NPB:PPh_3O. They observed more delayed exciplex emission in N_2 compared to that in air. A delayed component of 2000 ns was observed in the case of NPB:PPh_3O. The deep blue emission with a maximum brightness of 14,000 cd/m^2 with commission Internationale de l'Eclairage-1931 (CIE) coordinates of (0.1525, 0.0820) was obtained. Schleper *et al.* have introduced the concept of hot exciplexes; with both fast emission and high color purity[56]. Here, the donor and acceptor moieties are coupled with an anthracene bridge. It results in a large T_1 to T_2 gap and hence RISC occurs fast from T_3 to S_1 as depicted in Figure 1.5 (c). The characterization and evolution of excited state is done with quantum chemical simulations. This report shed light on more possibilities of modified molecular designs for exciplex emitters in OLED. By considering the lack of high yield exciplex systems, Wei *et al.*

have come up with an idea of stacking donor and acceptor moieties in a CT chromophore[57]. Here, they have developed an electron acceptor TXO-P-Si by mixing thioxanthen-9-one 10,10-dioxide (TXO) and N-phenyl carbazole (PhCz) units based on the DFT calculations. Exciplex emission was observed in four different donors with a newly designed acceptor. The selected donors are 1,3-Bis(carbazol-9-yl)benzene (mCP), 4,4′-Bis(carbazol-9-yl)biphenyl (CBP), 3,5-Bis(3-(9H -carbazol-9-yl)phenyl)pyridine (3,5-DCzPPy) and 3-(Diphenylphosphoryl)-9-(4 (diphenylphosphoryl)phenyl)-9H -carbazole (PPO21), respectively. An EQE of 16.9% was obtained for the green exciplex emission from TXO-P-Si: 3,5-DCzPPy combination with a low efficiency roll-off. Later in 2022, a solution-processed exciplex OLED was reported by Kesavan *et al.* with a high EQE of 20% solely by pure exciplex as emitter[58]. The exciplex combination consisted of carbazole-based molecule BCC-36 with triazine-based materials PO-T2T and (2,4,6-tris(2-(1H-pyrazol-1-yl) phenyl)-1,3,5-triazine) 3P-T2T with a high PLQY of 90% and EQEs with various dopants as shown in Figure 1.5 (d). Exciplex-based monochrome OLEDs are still in its growing stage. The main challenge is to enhance its quantum yield via proper selection of materials and novel device design strategies and techniques. Weber *et al.* explored the multifunctionality in exciplex emitter OLEDs. The development of multifunctional blue OLEDs using TADF-exciplex materials was presented, where the devices exhibit sensitivity to external stimuli and maximum EQE of 11.6% was achieved. The devices show responses to low external magnetic fields up to 100 mT with magneto-conductance efficiency reaching up to 2.5% and magneto-electroluminescence effects up to 4.1% were detected. The insights gained a fundamental understanding of the exciplex combinations for fully solution-processed OLEDs and a significant advancement towards multifunctional

OLED technology. Table 1.1 shows the summary of major reports on monochrome OLEDs where exciplex is used as an emitter.

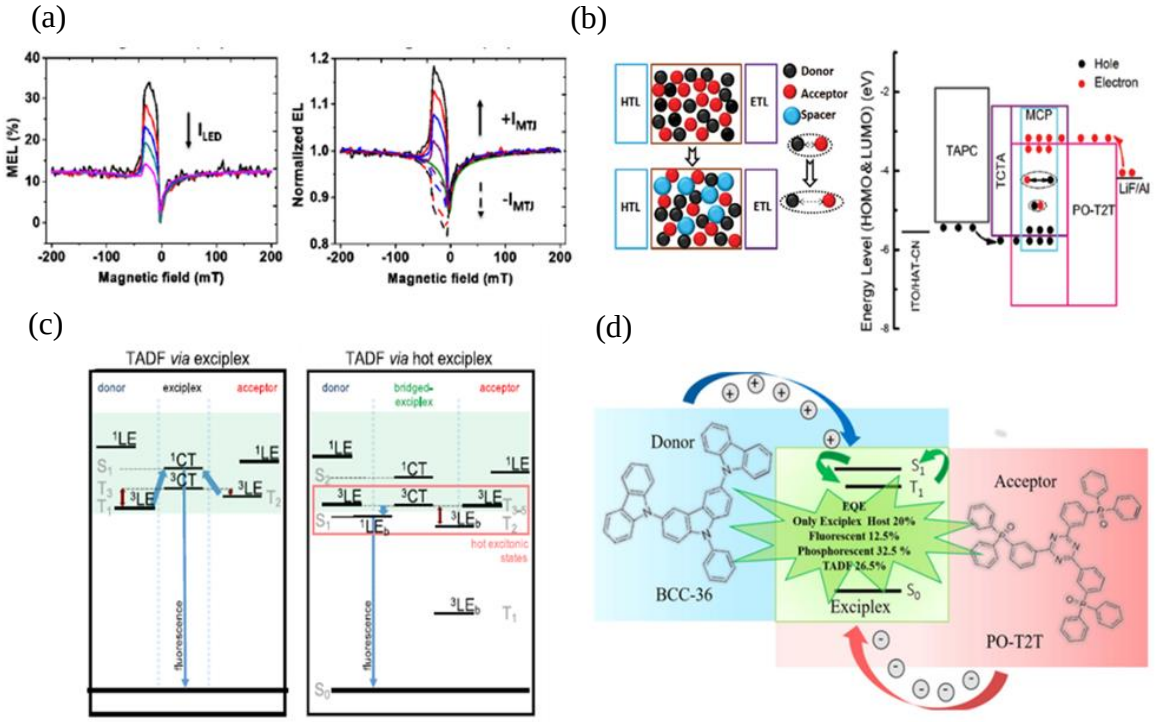

Figure 1.5. (a) The MEL *vs.* magnetic field plot in spin-XOLEDs (adapted from ref. 53) (b) illustration of an organic spacer co-doped in to the exciplex matrix and energy level diagram of the OLED (adapted from ref. 55) (c) demonstration of the mechanism of TADF via exciplex and the concept of hot exciplex (adapted from ref. 56) (d) representation of the exciplex emission and the EQEs achieved with different dopants with exciplex (BCC-36:PO-T2T) as host (adapted from ref. 58).

1.5.1.2 White OLEDs

White emission in OLEDs is achieved by using tandem structures which involves stacking multiple (red, green, blue) emitting units in series within a single device to achieve white light. The individual emission of component molecules can be combined with the exciplex emissions to achieve white light.

Table 1.1. Summary of major reports on monochrome OLEDs where exciplex is used as an emitter without any dopant materials.

Sl No.	EML configuration	Remarks on device design strategy	Maximum (EQE, CE, PE)	Ref	Chemical structures
1	TAPC:DPTPCz TCTA:DPTPCz NPB:DPTPCz	Three different HTMs mixed with a common high T1 bipolar host	15.4%	51	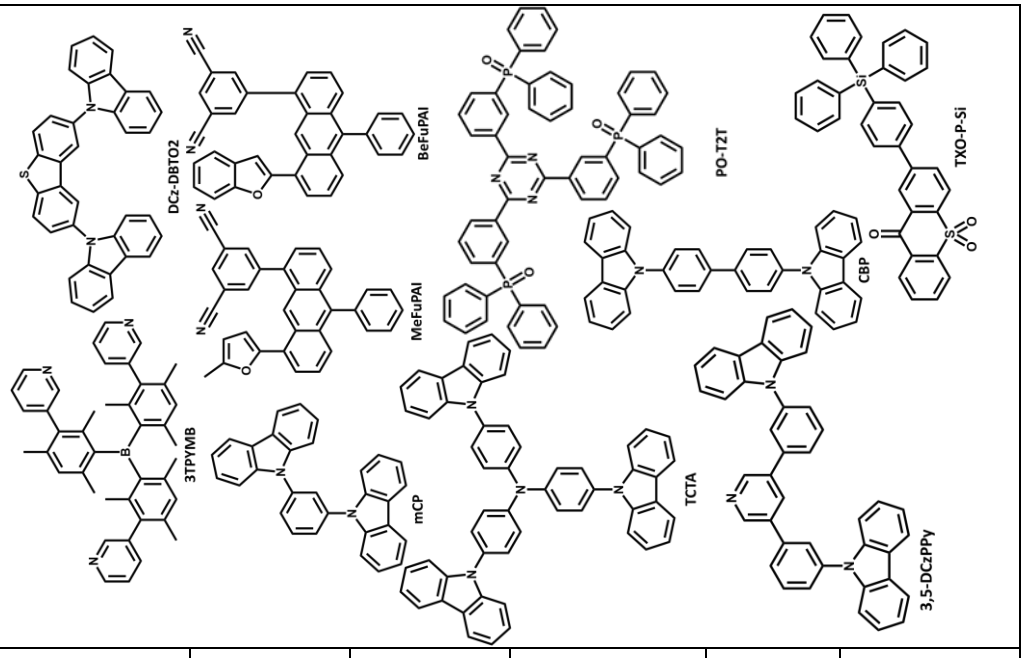
2	[1]MeO-TPD: 3TPYMB	HTM and ETM mixture gives magneto electroluminescence	....	53	
3	TAPC: [2]DCz-DBTO$_2$ (30:70)	HTM and ETM are mixed by the solvent mixing method	8.9% 27.5 cd/A 16.5 lm/W	54	
4	TCTA:PO-T2T	An organic spacer mCP was incorporated in the co-deposited layer	8%	55	
5	[3]MeFuPAI, [4]BeFuPAI	Novel molecules as exciplex emitters	....	56	
6	mCP:[5]TXOPSi, CBP:TXOPSi, 3,5-DCzPPy: TXO-P-Si	A novel acceptor molecule with three different donors	16.9% 53.8 cd/A 48.3 lm/W	57	

([1]N,N,N,N-Tetrakis (4-methoxyphenyl)benzidine, [2]9-[2,8]-9-carbazole-[dibenzothiophene-S,S-dioxide]-carbazole, [3]MeFuPAI (5-(8-(5-methylfuran-2-yl)-10-phenylanthracen-1-yl)isophthalonitrile), [4]BeFuPAI (benzofuran), [5](2-(4-(triphenylsilyl)phenyl)-9H-thioxanthen-9-one 10,10-dioxide).

In 2003, M. Mazzeo *et al.* have fabricated a single layered WOLED by utilizing exciplex emission at the molecular interface between two blue emitting compounds: TPD and 2,5-bis(trimethylsilyl)-thiophene-1,1-dioxide (STO) [59]. The blue emitting donor molecule and the green-red emitting exciplex emission together give white light. Zhu and his team have reported a WOLED from four different exciplex combinations[60]. They observed exciplex emissions at the following molecular interfaces; TPD/Bphen (blue), m-MTDATA/Bphen (green), TPD/$Al(DBM)_3$ (orange) and m-MTDATA/$Al(DBM)_3$ (red). The WOLED achieved CIE coordinates of (0.33, 0.35) and CCT of 3376 K. An all-exciplex tandem WOLED has been reported, combining blue and yellow emissions from two different exciplex layers; mCP:PO-T2T and 4,4'-(9H-fluoren-9-ylidene)bis[N,N-bis(4-methylphenyl)-benzenamine (DTAF):PO-T2T, respectively[61]. They used Liq(1nm)/Al (1nm)/ MoO_3(5 nm) as the CGL. In 2015, Zhao *et al.* have presented a tandem WOLED structure by combining orange and blue exciplex emitting units[62]. TCTA:Bphen and TAPC:3P-T2T were used as blue and orange exciplex combinations respectively; connected through a CGL composed of 2,4,6-tris(3-(1H-pyrazol-1-yl)phenyl)-1,3,5-triazine (3P-T2T): Cs_2CO_3, Al and MoO_3. The tandem device gives twofold current efficiency and EQE compared to the single colour OLEDs at the same current. In the year 2016, Angioni *et al.* presented a single emitting layer WOLED by using a newly synthesized triaryl molecule-based on a benzene-benzothiadiazole-benzene core[63]. The EL spectra comprise of different emission bands; the electromer formed in the novel molecule is responsible for the band at 520 nm and the peak at 580 nm was due to the exciplex formed at the interface between TPD and the novel molecule and a shoulder peak at 635 nm is due to the electroplex. The proposed WOLED could provide an EQE of 2.39% and PE of 2.6 lm/W. In 2019, Xiaozhen Wei and co-workers have come up with a new strategy for structuring

WOLEDs by combining complementary emissions [64]. Commercially available electron transport materials TPBi and PO-T2T combined with the HTL, TAPC give complementary exciplex emissions. They have realized the blue and orange exciplex emissions from TAPC:TPBi and TAPC:PO-T2T combinations. The EL spectra of the devices and the energy level diagram involving the mechanism of white light emission is shown in Figure 1.6 (a). This work has provided a new EML configuration for white emission by proper arrangement of different layers. The optimized WOLED showed the maximum luminance and CE of 3206 cd/m^2 and 3.17 cd/A, respectively. The CIE coordinates of (0.365, 0.393) and CRI index of 73 was obtained. In 2020, our group have introduced a novel idea of combining exciplex and electromer emission to achieve white light[65]. The combination of TAPC:TPBi gives blue exciplex emission, combining with yellow electromer emission of TAPC leads to white emission with the CIE coordinates (0.31, 0.34). The EL spectra and the photographs of the devices are shown in Figure 1.6 (b). This report suggests the possibilities of simplified device designs by utilizing monomer emissions of the component molecules along with the exciplex emission. Dong *et al.* presented a pure white OLED by using spacer materials ; 2,6-Bis(3-(9H-carbazol-9-yl)phenyl)pyridine (26DCzPPy) and Bis[2-(diphenylphosphino)phenyl]ether oxide (DPEPO)[66]. The combination of blue (26DCzPPy:PO-T2T) and orange (TAPC:PO-T2T) exciplexes were combined to generate white light emission. The energy level diagram of the devices with spacer is shown in Figure 1.6 (c). Table 1.2 summarizes the major reports on WOLEDs where exciplex is used as an emitter.

All exciplex-based white OLEDs can address the issue of lack of blue emitters. It can avoid complicated synthetic procedures for high quantum yield dopant materials. The main challenge in exciplex-based WOLEDs is the trade-off between device efficiency and quality of white

light. Many studies are focusing on novel device architecture designs to circumvent this problem.

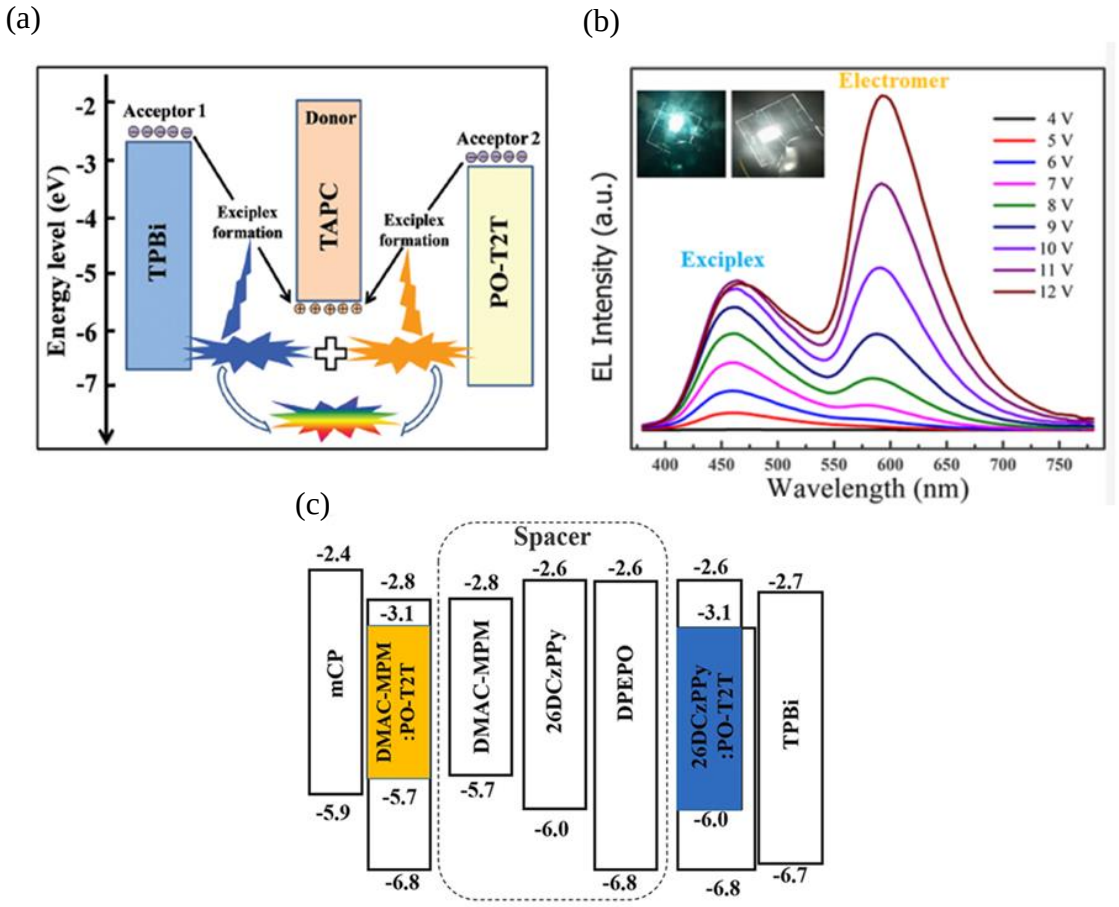

Figure 1.6. (a) The energy level diagram showing the mechanism of white emission by combining blue and yellow exciplex emissions at TAPC/TPBi and TAPC/PO-T2T interfaces, respectively (adapted from ref. 64) (b) EL spectra of the WOLEDs combining yellow electromer emission of TAPC and blue exciplex emission from TAPC:TPBi (adapted from ref. 65) (c) The energy level diagram of all exciplex-based WOLED with spacer layers (adapted from ref. 66).

Table 1.2. Summary of major reports on WOLEDs where exciplex is used as an emitter without any dopant materials.

Sl No.	EML configuration	Remarks on device design strategy	Maximum Efficiency (EQE, CE, PE)	CIE coordinates	Ref.	Chemical structures
1	mCP:POT2T DTAF: PO-T2T	Tandem WOLED using Parallel blend layers of blue and yellow exciplex emissions.	11.6% 27.7 cd/A 15.8 lm/W	(0.29,0.35)	61	
2	TCTA:Bphen TAPC:3P-T2T	Tandem WOLED combining blue and yellow exciplex emissions	9.17% 25.4 cd/A 11.5 lm/W	(0.41,0.44)	62	
3	TPD:1(a new triaryl molecule)	Non-tandem WOLED combining blue electromer emission and yellow exciplex emission	2.39% 2.6 cd/A 11.5 lm/W	(0.38,0.45)	63	
4	TAPC:TPBi TAPC:PO-T2T	Non-tandem WOLED by using two acceptor layers vertically on the same donor layer	1.65% 4.49 cd/A 4.21 lm/W	(0.36,0.39)	64	
5	TAPC:TPBi	Non-tandem WOLED combining blue exciplex emission and yellow electromer emission	0.707% 1.867 cd/A 1.119 lm/W	(0.34,0.31)	65	
6	26DCzPPy: POT2T DMAC-MPM: PO-T2T	Non-tandem WOLED by using blue and yellow exciplex emissions using spacer layer	8% 20 cd/A 20 lm/W	……..	66	

1.5.2 Exciplex as host – literature review

Exciplex emission can be effectively utilized by combining it with phosphorescent, fluorescent or TADF dopants as depicted in shown in Figure 1.7. The spectral overlap between the absorption spectra of the dopant and exciplex emission is considered as the basic criteria for energy transfer from exciplex to the selected dopant. In exciplex host devices, energy transfer occurs through Förster resonance energy transfer (FRET)[67-69] and Dexter energy transfer (DET)[67, 68, 70]. In the case of WOLEDs, complex tandem device architectures and use of high cost phosphorescent emitter materials are the main challenges for cost-effectiveness. These problems can be addressed by employing the exciplex emission mechanism in WOLEDs. Here, the exciplex can be used as an emitter as well as host with suitable phosphorescent dopants of complementary colors. In exciplex-based OLEDs transporting layers contributing to emission and function as a host in the same device. Hence, the device complexity can be minimized to an extent. Exciplex host-based monochrome as well as WOLEDs in combination with various types of emitters are discussed here. Exciplex host systems have a lot of advantages over traditional hosts. The comparison between an exciplex host and a traditional host is summarized in Table 1.3.

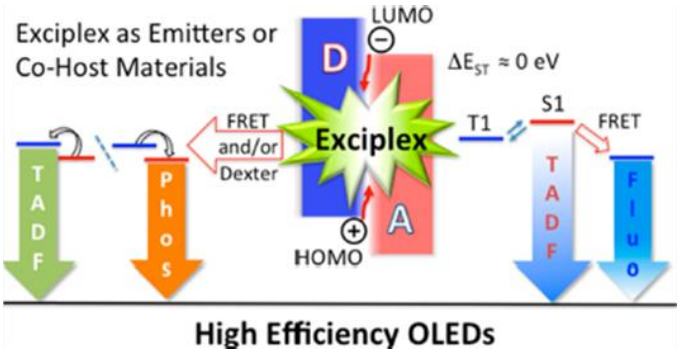

Figure 1.7. Illustration of using exciplex as a host with phosphorescent, TADF, or fluorescent emitters.

Traditional host	Exciplex host
Both charge trapping and energy transfer occur	Energy transfer dominates
Trap assisted recombination leads to high driving voltage	Langevin recombination gives reduced driving voltage
Efficiency is limited since majority are fluorescent materials	High power efficiency by utilizing 100 % electrogenerated exciton energy
Narrow recombination zone	Broadened recombination zone due to balanced charge
Due to weak charge blocking effect, blocking layers are needed	Transport layers have charge blocking effect. Hence, additional layers are not needed
High efficiency roll-off	Low efficiency roll-off due to broad recombination zone
Chances for the formation of additional exciplex	Exciton confinement in dopants and avoid the formation of additional exciplex

Table 1.3. Comparison between traditional and exciplex host

1.5.2.1 Monochrome OLEDs

There are several reports on exciplex host OLEDs in which exciplex act as a host with phosphorescent emitters for highly efficient devices. Commercially available phosphorescent dopants include bis[2-(2-pyridinyl-N)phenyl-C](acetylacetonato)iridium(III) ($Ir(ppy)_2acac$)[71, 72],$Ir(ppy)_3$[73, 74] and tris[2-(p-tolyl)pyridine]iridium(III) ($Ir(mppy)_3$)[75, 76] (green) and 2-methyldibenzo[f,h]quinoxaline ($Ir(MDQ)_2acac$)[77-79],bis(2-benzo[b]thiophen-2-ylpyridine) (acetylacetonate)iridium(III) ($Ir(btp)_2(acac)$)[80, 81], platinum(II) octaethylporphine (PtOEP)[82, 83] (red) etc.. Bis[2-(4,6-difluorophenyl)pyridinato-C2,N](picolinato)iridium(III) (FIrpic)[83-86] and bis(4-phenylthieno[3,2-c]pyridinato-N,C2') (acetylacetonate) iridium(III) (PO-01)[87-90] are blue

and yellow phosphorescent emitters, respectively; which are widely used in OLEDs. Red, green, and blue phosphorescent emitters together in suitable host matrices can yield white emission, although, the high cost of these materials is still a bottleneck in this scenario. Simplified non-tandem device architectures of WOLEDs using exciplex emitters with suitable phosphorescent dopants in exciplex host can yield efficient white light. For the energy transfer to occur, the triplet energy of the formed exciplex must be less than that of its individual components and higher than that of the dopant molecule[91, 92]. In 2011, Park *et al.* effectively utilized the exciplex formed at the molecular interface of CBP and 4,6-Bis(3,5-di(pyridin-3-yl)phenyl)-2-methylpyrimidine (B3PYMPM) and the energy transfer to $Ir(ppy)_3$[93]. They got an EQE exceeding 20% for a doping concentration of 6 mol%. Lee *et al.* presented a color stable orange OLED where red and green phosphorescent emitters doped in exciplex co-host[94]. This co-host system minimizes the triplet quenching by providing a wide recombination zone. Exciplex formation in devices can be in two different ways; bulk and interface types. Several reports on exciplex host with phosphorescent dopants have come up with high EQEs. In 2017, Lee *et al.* have presented a combination of NPB and PO-T2T as the exciplex host with phosphorescent dopants, ($Ir(MDQ)_2(acac)$) and Bis[2-(3,5-dimethylphenyl)-4-methyl-quinoline] (acetylacetonate)iridium(III) ($Ir(mphmq)_2(tmd)$)[95]. The device architecture was optimized as follows; ITO/TAPC/NPB/NPB:PO-T2T:5wt% dopant/POT2T /0.5% rubidium carbonate (Rb_2CO_3):PO-T2T /Al and could achieve maximum EQE of 34.1%. Balanced carrier mobilities in the emissive layer can provide balanced electron-hole capture in devices where exciplex is used as the host, giving high efficiencies. Hung *et al.* have reported a new star shaped molecule, CN-T2T (1,3,5-triazine/cyano hybrid molecule) and it is used as an electron acceptor with a donor 9-Phenyl-3,6-bis(9-phenyl-9Hcarbazol-3-yl)-9H-carbazole (Tris-PCz)

to form an exciplex[96]. The charge carrier mobility in the device could be attributed to their individual mobilities with same magnitudes. They could achieve EQEs of 6.9% and 9.7% by using 1wt% of rubrene ((5,6,11,12)-tetraphenyl-naphthacene) and DCJTB in to the exciplex matrix, respectively as shown in Figure 1.8 (a). A deep blue emitting exciplex consisting of mCP and BM-A10 (phosphine-oxide-based ETM) was used as a host with a blue phosphorescent dye Bis(3,5-difluoro-4-cyano-2-(2-pyridyl)phenyl-(2-carboxypyridyl) iridium(III) (FCNIrPic)[97]. Luminance *vs.* EQE as well as PE plots are shown in Figure 1.8 (b). The EQE of 19% with CIE coordinates of (0.15, 0.19) indicates improved performance and higher color purity compared to FIrpic-based blue devices. By modifying a conventional electron donating material TCTA, exciplex with high triplet energy was achieved.[98]. Here, Ph-O-TCTA (modified TCTA analog) and Tris(4-(diphenylphosphoryl)phenyl)benzene (PhPO) together give exciplex emission, which is used as a host with dopants FIrpic and 2,3,4,5,6-pentakis(3,6-di-tert-butyl-9H-carbazol-9-yl)benzonitrile (5TCzBN). They could get maximum current efficiency of 35.3 cd/A. Chiu *et al.* have reported an exciplex host OLED with an extremely low efficiency roll-off [99]. They have modified donor molecules by adding an electron withdrawing benzimidazole moiety in donor molecule leading to a reduced hole mobility and hence balanced charge recombination. The exciplex system consists of 9,9'-Diphenyl-9H,9'H-3,3'-bicarbazole (BCzPh-pim) as the donor and B3PyMPM as the acceptor with the green dopant $Ir(ppy)_2(acac)$. A deep blue exciplex system was designed by Xia *et al.* in 2023, consisting of mCBP as the electron acceptor and difluoroboron(Z)-3-(diphenylamino)-3-hydroxy-N,N-diphenylacrylamide (DNPhB) as the donor[100]. This system exhibits deep blue emission at 444 nm and a high PLQY of 56%. Wide color phosphorescent OLEDs were fabricated using the exciplex as a host, achieving a brightness of up to 1,50,000

cd/m^2 for a green PhOLED using Ir(ppy)$_3$. This work paves the way for achieving high performance deep blue exciplex OLEDs, meeting the demands for potential applications such as wide color displays. Exciplex hosts with fluorescent dopants were also investigated in parallel with the phosphorescent dopants. In 2015, Zhao *et al.* have reported an efficient red fluorescent OLED by using TCTA:3P-T2T as the host and DCJTB as the dopant[101]. They got an EQE of 10.15% and a lower efficiency roll-off compared to conventional devices. Liu *et al.* have come up with the concept of 100% exciton harvesting by using an exciplex host along with a conventional fluorescent host[102]. The EML configuration is as follows: TAPC: (3-(4,6-diphenyl-1,3,5-triazin-2-yl)-9-phenyl-9Hcarbazole) DPTPCz: x wt% 2,3,6,7-Tetrahydro-1,1,7,7, -tetramethyl-1H,5H,11H-10 (2benzothiazolyl)quinolizino[9,9a,1gh] coumarin (C545T) (30nm) where x = 0.2, 0.4 and 0.8 wt%. In this case, exciton harvesting is achieved via up-conversion of singlet excitons by the exciplex host with energy levels similar to that of the dopant. The minimized exciton trapping leads to high efficiency of the device. In 2019, Liang *et al.* have developed a novel electron accepting molecule along with a donor to form the exciplex host[103]. They got a power efficiency approaching 100 lm/W by using the green fluorescent dopant C545T. The luminance *vs.* EQE plot is shown in Figure 1.8 (c). The exciplex combination was TAPC: 2-(3-(4,6-Diphenyl-1,3,5-triazin-2-yl) phenyl)-1-phenyl-1H-benzo[d]imidazole) (PIM-TRZ), in which PIM-TRZ was a newly synthesized electron acceptor with high electron accepting nature. The utilization of triplet excitons in a fluorescent OLED is a cost-effective strategy for efficient OLEDs. An electro-optical device model has been presented by Regnat *et al.*, which account for triplet harvesting and exciton quenching[104]. The model gives the parameters like RISC rate, TTA rate, etc. which accounts for the details on charge carrier and exciton dynamics in the device. This work suggests the possibilities of

theoretical modeling in predicting exciton dynamics in exciplex-based OLEDs. Also, by utilizing fluorescent dopants can achieve cost-effectiveness compared to Ir or Pt based phosphorescent dopants. Phosphorescent OLEDs have made a revolutionary improvement in the efficiency of OLEDs, though the high cost issue of phosphorescent materials remained. It has led to the beginning of third generation OLED materials by utilizing TADF emission mechanism. Here, all the triplet excitons can be converted into singlets via RISC. Hence, achieving maximum efficiencies. There are several reports on the designing and synthesis of novel TADF molecules. TADF-based OLEDs had reached an EQE of 37%. Several new strategies and device engineering techniques for more efficient TADF OLEDs has also been coming up. In general, TADF emitters-based OLEDs require host with deep lying HOMO level and high singlet energy without forming an exciplex. In 2014, Kim *et al.* have reported a green exciplex host-based OLED with a TADF dopant[105]. They used mCP: 1,3-bis[3,5-di(pyridin-3-yl)phenyl]benzene (BmPyPb) as the host and 1,2,3,5-Tetrakis(carbazol-9-yl)-4,6-dicyanobenzene (4CzIPN) as the green emitter to get an EQE of 28.6%. In 2016, Sun *et al.* have reported a blue TADF OLED using an exciplex combination of mCP: 2,8-Bis(diphenyl-phosphoryl)-dibenzo[b,d]thiophene (PO15) as a host with a TADF emitter, 4,5-Bis(carbazol-9-yl)-1,2-dicyanobenzene (2CzPN)[106]. However, the device showed high efficiency roll-off even with a good charge balance. This might be due to the triplet exciton quenching due to low RISC rate of 2CzPN. Hence, for an exciplex host-based TADF OLED, the dopant must have a high RISC rate to avoid the efficiency roll-off. A different approach with double dopant TADF-sensitized system for exciplex OLED was introduced by Li *et al.*[67]. Here, a multi process energy transfer occurs which offers effective triplet harvesting. The novel double dopant EML offers two additional FRET process compared to a conventional TADF OLED

with one-step process. Yang *et al.* have presented a solution-processed green TADF OLED with an interfacial exciplex host[107]. They have reported a new TADF emitter 2'-(10H-phenoxazin-10-yl)-[1,1':3′,1″-terphenyl]-4,4″,5′-tricarbonitrile (oPTBC) and doped it in CBP/PO-T2T interfacial exciplex host. An EQE of 16.2% was achieved with a low turn-on voltage of 3V. This shows the potential of interfacial exciplex hosts for developing high efficiency OLEDs. Subsequently, a dendritic interfacial exciplex as a host with green emitting a TADF material 5,10-Bis (4-(3,6-di-tert-butyl-9H-carbazol-9-yl)-2,6-dimethylphenyl)-5,10-dihydroboranthrene(tBuCzDBA) was reported by Chen *et al*.[108]. The exciplex system consists of a dendritic oligocarbazole donor with two acceptors 4,6-Bis(3,5-di-4-pyridinylphenyl)-2-methylpyrimidine (B4PyMPM) and B3PyMPM. For enhancing carrier balancing between the donor and acceptor system, a small structural variation has been made in B4PyMPM to get B3PyMPM. The mechanism of exciplex formation and energy transfer to the TADF emitter is depicted in the Figure 1.8 (d). They could achieve a power efficiency of 95 lm/W and EQE of 26.4%. The progress in TADF emitter-based exciplex host OLEDs are less compared to those with phosphorescent emitters. This might be due to the lack of efficient novel TADF emitters. In 2022, Zhou *et al.* reported interface exciplex OLEDs doped with fluorescent, phosphorescent, and thermally activated delayed fluorescence (TADF) emitters to investigate the relationship between their excited state properties and electroluminescence efficiencies[109]. This report demonstrated that careful consideration of the photophysical process is essential in designing high performance emitters for exciplex host materials. This approach provided an in depth understanding on improving exciton utilization and electroluminescence efficiency in interface exciplex OLEDs.

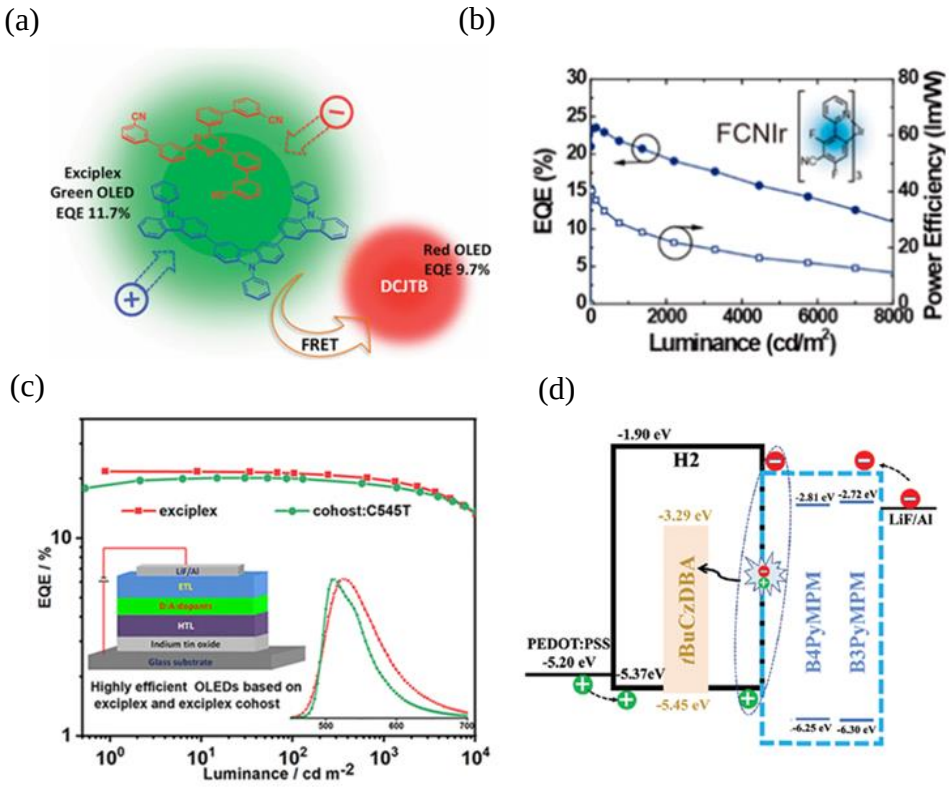

Figure 1.8. (a) The illustration of exciplex emission at the interface of molecules DN-T2T and Tris-PCz and FRET to the dopant (DCJTB) (adapted from ref. 96) (b) luminance *vs.* EQE and power efficiency of the FCNIr doped blue exciplex OLED. molecular structure of the blue dopant is shown in the inset. (adapted from ref. 97) (c) EQE versus luminance plot of the device. the device architecture and the EL spectra are shown in the inset. (adapted from ref. 103) (d) representation of exciplex formation in terms of energy levels between a dendritic oligocarbazole donor (H2) with two acceptors B4PyMPM and B3PyMPM and the energy transfer to the TADF dopant tBuCzDBA (adapted from ref. 108).

Recently, Yin *et al.* reported HLCT-type acceptor molecule-based exciplex system for highly efficient solution-processable OLEDs with low efficiency roll-offs. Solution-processable OLEDs using these TADF exciplexes achieved a maximum EQE of 20.8%. Additionally, a high EQE > 25% with low efficiency roll-off (≈ 3.5% at 1000 cd /m^2) was obtained for solution -processable phosphorescent devices using HLCT-based exciplexes as the host matrix. This

study paves the way for designing effective TADF molecules and host matrices for solution - processable OLEDs. Table 1.4 shows the summary of major reports on monochrome OLEDs where exciplex is used as a host with dopant materials.

Sl No	**EML configuration**	**Remarks on device design strategy**	**Maximum efficiency (EQE, CE, PE)**	**ref**
With Phosphorescent emitters				
1	CBP: B3PYMPM: 6 mol% $Ir(ppy)_3$	Exciplex as a host with a green phosphorescent emitter	20.1% …. ….	93
2	TCTA: B3PYMPM: 3wt% $Ir(mphq)_2(acac)$ and 8wt% $Ir(ppy)_2(acac)$	Color stable orange emission by using red and green emitters in exciplex forming co-host	22.8% 50.9 lm/W ….	94
3	NPB:PO-T2T:5 wt % $Ir(mphmq)_2(tmd)$ and $Ir(MDQ)_2(acac)$	Exciplex as a host with red emitters	34.1% 62.2 lm/W ….	95
4	^{1}TrisPCz: CNT2T: 1wt% Rubrene 1wt% DCJTB	A novel donor molecule is synthesized; exciplex as host with green and red emitters	9.7% 21.4 cd/A 28.1 lm/W	96
5	mCP:BM-A10: 12 wt% FCNIr	Deep blue emitting exciplex as a host and as an emitter	24% 41 lm/W ….	97
6	Ph-O-TCTA: PhPO:10 wt% FIrpic	Efficient exciplex formation by modifying an electron acceptor; exciplex as host with a blue emitter	16.5% 33.6 cd/A 20.6 lm/W	98
7	BCzPh-mimi: B3PyMPM: 8 wt% $Ir(ppy)_2(acac)$	Efficient exciplex formation by modifying an electron donor; exciplex as host with a green emitter	22.31% …. ….	99

With Fluorescent emitters				
1	TCTA:3P-T2T: 1% DCJTB	Exciplex as a host with red fluorescent emitter	10.15% 22.7 cd/A 21.5 lm/W	101
2	TAPC:DPTPCz: 0.8 wt% C545T	Low dopant concentration in exciplex host to minimize the triplet- triplet energy transfer from host to dopant	14.5%, 44 cd/A 46.1 lm/W	102
3	TAPC:PIM-TRZ: 0.6 wt% C545T	A novel electron acceptor is synthesized. exciplex as host with green emitter	20.2%, 68.3 cd/A 86.4 lm/W	103
4	TCTA:B4PYMPM: 0.5 wt% DCJTB	Exciplex as a host with red emitter. An electro-optical device model is presented	…. …. ….	104
With TADF emitters				
1	mCP: BmPyPb: 3% 4CzIPN	Exciplex as a host with blue TADF emitter	28.8%, 56.6 lm/W ….	105

([1]TrisPCz: 9-Phenyl-3,6-bis(9-phenyl-9Hcarbazol-3-yl)-9H-carbazole)

Table 1.4. Summary of major reports on monochrome OLEDs where exciplex is used as a host with dopant materials.

1.5.2.2 White OLEDs

White OLEDs and their dynamic applications in the general lighting industry have been growing fast. WOLED possesses true color qualities, high uniformity, more brightness and is highly energy efficient compared to conventional lighting technologies. These features have made WOLEDs an alternative for other lighting sources in solid-state lighting. Achieving long operational lifetime without compromising power efficiency at high brightness is a

considerable challenge. In the display market, the additional costs for RGB OLEDs can be addressed by WOLEDs to some extent. In 2012, Su *et al.* have come up with a hybrid WOLED structure by utilizing two phosphorescent emitters with a newly synthesized host material containing a triazine core and three phenyl carbazole arms, called 2,4,6-tris(3-(carbazol-9-yl)phenyl)-triazine (TCPZ)[110]. The exciplex emission was obtained from TCPZ:FIrpic combination which covers the green-light region along with blue and red emissions from phosphorescent dopants FIrpic and tris(1-phenylisoquinoline) iridium(III) ($Ir(piq)_3$), respectively. The EL spectra of the device consist of a yellow peak at 540 nm combined with the blue and red bands, rendering white emission. A slight variation for CIE coordinates from (0.39, 0.45) at 100 cd/m^2 to (0.42, 0.46) at 1000 cd/m^2 has been observed. The efficiency achieved was quite low with EQE = 5.4% and PE = 9.4 lm/W at 100 cd/m^2. However, this work offers strategies of device engineering for obtaining stable white light emission with simple device architecture. Later in 2014, Duan *et al.* have reported a unique WOLED device consisting of a blue emitter of singlet state exciplex in combination with phosphorescent emitters[111] . TCTA: Bphen was used as the blue exciplex EML and as a host for the green and red phosphorescent emitter layers; $Ir(ppy)_3$ and $Ir(piq)_3$ respectively. The maximum EQE and PE of 7.1% and 11.4 lm/W at 1000 cd/cm^2 was achieved. The CIE coordinates obtained were slightly changing from (0.39, 0.43) at 10 cd/m^2 to (0.37,0.44) at 10000 cd/m^2 with a corresponding CRI of 62. Zhang *et al.* have presented a hybrid WOLED by utilizing energy transfer from the exciplex to an orange emitter[112]. Blue exciplex combination consists of 3,3′-Di(9H-carbazol-9-yl)-1,1′-biphenyl (mCBP) and PO-T2T as the donor and acceptor materials. The orange phosphorescent dopant bis(2-phenyl-1,3-benzothiozolato-N,C2') iridium (acetylacetonate) ($Ir(bt)_2(acac)$) of 2 nm is inserted in the EML and an excellent warm

WOLED with CIE coordinates of (0.42, 0.43) was obtained. Further simplification of the device structure was carried out by doping a small percentage of the emitter in the whole EML and a brightness up to 40,000 cd/m^2 was obtained. A new technique for complete harvesting of singlet and triplet excitons to generate white light was demonstrated. A blue exciplex was observed between (4,5-Bis(carbazol-9-yl)-1,2-dicyanobenzene) CDBP and PO-T2T. Green and red phosphorescent emitters $Ir(ppy)_2acac$ and ($Ir(MDQ)_2acac$), respectively were used as dopants in the exciplex host matrix[113] . They divided the emissive region into three different zones- zone 1: excitons transfer energy to the respective emitters, zone 2: only triplet excitons can be transferred, zone-3: no exciton can reach the dopant. Proper involvement of the three zones gives an efficient white emission. This single EML hybrid WOLED showed a maximum EQE of 25.5%. The CIE coordinates showed a slight variation from (0.41, 0.45) to (0.38, 0.42) when the luminance increases from 10 to 10000 cd/m^2 with CRI of 72 at 10 cd/m^2 to 76 at 10000 cd/m^2. A blue device with an EML of mCP: B3PYMPM: FIrpic (1:1:0.4%, 10nm)/ B3PYMPM (15 nm) was fabricated, where exciplex excitons were transferred to FIrpic via FRET. In 2017, Dongxiang and his co-workers have presented a blue molecular emitter-free hybrid white OLED[114]. Yellow and red phosphorescent dopants were combined with a blue exciplex or electroplex emission at the TAPC/TmPyPB interface. The phosphorescent layers can effectively harvest triplet exciplex excitons via diffusion process and hence the distance between the dopant layers and exciton forming molecular interface has a crucial role in the performance. An additional TmPyPB layer at n-side and TAPC at p-side has enhanced EQE. The device exhibited a PE of 28.2 lm/W with a high CRI (92.1). In 2018, Ying *et al.* have reported a WOLED by introducing ultra-thin phosphorescent layers in exciplex host[115]. Emissive layer consists of an ultra-thin orange and green phosphorescent emitters in the

exciplex host. Firstly, they fabricated a blue exciplex device in which, a thin layer of mCBP was inserted between TCTA and emissive layer to prevent the exciplex formation at the TCTA/PO-T2T interface. A blue phosphorescent device was also fabricated in which mCBP: PO-T2T: FIrpic (1:1:10%, 15 nm) was used as the EML. It exhibited an improved efficiency-roll-off compared to the exciplex device. Inorder to obtain the exciton diffusion profile, they fabricated a series of white OLEDs by inserting an ultrathin orange sensing layer at different locations within the EML. The optimized double ultra-thin layer (UTL) WOLED exhibited maximum EQE, PE and CE of 22.8%, 953 lm/W and 72.8 cd/A, respectively. Zhang *et al.* have presented a high-performance WOLEDs by using sequential arrangements of blue, green and red ultra-thin phosphorescent layers in an exciplex host[116], as shown in Figure 1.9 (a) The exciplex excitons were efficiently transferred to blue, green and red emitters; FIrpic, $Ir(ppy)_2acac$ and iridium (III)bis[2,-4-dimethyl-6-[5-(2-methylpropyl)-2-quinolinyl-N]phenyl-C]-(2,4-pentanedionato-O2,O4) (RD071) respectively. The thickness of UTLs in EML were optimized. The resulting WOLEDs achieve the maximum EQE, PE and CE of 26.1%, 50 lm/W and 40 cd/A, respectively. Most of the high efficiency OLEDs among the exciplex WOLEDs are based on phosphorescent emitters. One of the major drawbacks is the trade-off between the low cost and high efficiency. This could be addressed via novel device designs for dopant - free exciplex only OLEDs.

Zhang *et al.* in 2018 have reported a pure fluorescent WOLED by using an exciplex host (mCP:PO-T2T) and fluorescent dopant. The traditional fluorescent material, rubrene was used as the orange emitter[117]. The energy transfer ability of the blue exciplex to rubrene was confirmed by the spectral overlap existing between the PL spectrum of the blue exciplex and the absorption spectrum of the dopant. The proposed WOLED structure was as follows:

ITO/MoO_3(3 nm)/mCP(20 nm)/mCP : PO-T2T (1 : 1): x wt% rubrene (15 nm)/PO-T2T (35 nm)/LiF (1 nm)/Al (where the x = 0.8, 1.6 and 2.4, respectively). The device showed an EQE, PE and CE of 4.90%,12.8 lm/W and 14.2 cd/A, respectively. The EL spectra and the CIE diagram for white OLED with 2.4% of dopant is shown in Figure 1.9 (b). Ivaniuk and his team have demonstrated a combination of a yellow-green exciplex emission with blue pure fluorescence[118]. Exciplex emission was observed at the interface of 3,6-di (4,4′-dimethoxydiphenylaminyl)-9-(1-naphthyl) carbazole (DPNC)/BPhen. The blue and green emissions were obtained via pure fluorescence of m-MTDATA and DPNC respectively. The proposed hybrid-WOLED exhibited maximum brightness of 10,000 cd/m^2 with an EQE and CE of 5.3% and 5 cd/A, respectively. The CIE coordinates which is close to pure white emission (0.31,0.34) were obtained. Zhao *et al.* have introduced a yellow emitter to fabricate a series of all-fluorescent WOLEDs by doping it in in blue emitting exciplex host mCP:PO-T2T[119]. The device showed a maximum EQE of 5.65% and maximum brightness of 74,820 cd/m^2. The EL spectra of the yellow and white device are shown in Figure 1.9 (c). Better strategies for TADF-Phosphorescent-fluorescent dopants with exciplex hosts can be adopted for stable white light emission. Fluorescent emitters : DCJTB[120-122], Rubrene [123-125], (E)-2-(2-tert-Butyl-6-(2-(2,6,6-trimethyl-2,4,5,6-tetrahydro-1H-pyrrolo[3,2,1-ij]quinolin-8-yl)vinyl)-4H-pyran-4ylidene)malononitrile (DCQTB)[126] (red dopants) and 4,4'-Bis(9-ethyl-3-carbazovinylene)-1,1'-biphenyl (BczVBi)[22, 127-129], Perylene (blue) and green emitters like C545T[33, 130, 131] can be effectively utilized to create hybrid WOLEDs with exciplex host. Acquiring good spectral stability with simple device structures for WOLEDs is in progress. By employing TADF emission mechanism, WOLEDs based on TADF-phosphorescence or fluorescence hybrid structures can be adopted. In 2016, Liu *et al.* have reported a WOLED by

employing three different TADF emitters with an exciplex host[132]. The doping concentrations of the TADF emitters 2CzPN and 4CzIPN were optimized to 6 and 4 wt %. The device exhibited an extremely low turn-on voltage of 2.3 V and maximum EQE, CE and PE of 19.0%, 50.1 cd/A and 63.0 lm/W, respectively. In 2018, Luo Dongxiang have introduced an idea of single TADF emitter to develop high quality WOLEDs[133]. A TADF emitter 9,9',9",9"'-((6-Phenyl-1,3,5-triazine-2,4-diyl)bis(benzene-5,3,1-triyl))tetrakis(9H -carbazole) (DDCzTrz) is placed in between p-type and n-type layers. The blue emission peak at 462 nm was originated from the TADF emitter DDCzTrz, which combined with an orange emission generated from an exciplex formed at the TAPC/DDCzTrz interface. This can be due to the p-type TAPC and the high electron barrier between TAPC and DDCzTrz. The molecular structures, device architecture and energy level diagram are shown in Figure 1.9 (d). The maximum EQE and PE of 28.4% and 68.5 lm/W were achieved with ultrahigh CRIs of 90. Kaminskiene *et al.* have reported a warm white OLED based on a novel TADF emitter[134]. Here, they utilize the contribution of TADF emission of the molecule as well as its exciplex forming ability. An exciplex emission was confirmed at the molecular interface of 4,4′-(9H,9′H-[3,3′-bicarbazole]-9,9′-diyl)bis(3-(trifluoromethyl) benzonitrile) (pCNBCzoCF_3)/m-MTDATA. The white emission was obtained via the combined effect of a green-blue emission of the pCNBCzoCF_3 with the orange exciplex emission of the m-MTDATA/pCNBCzoCF_3 interface. The device exhibited an EQE, CE and PE of 18.8%, 53.8 cd/A and 19.3 lm/W, respectively. Maximum brightness of 40,900 cd/m^2 was achieved.

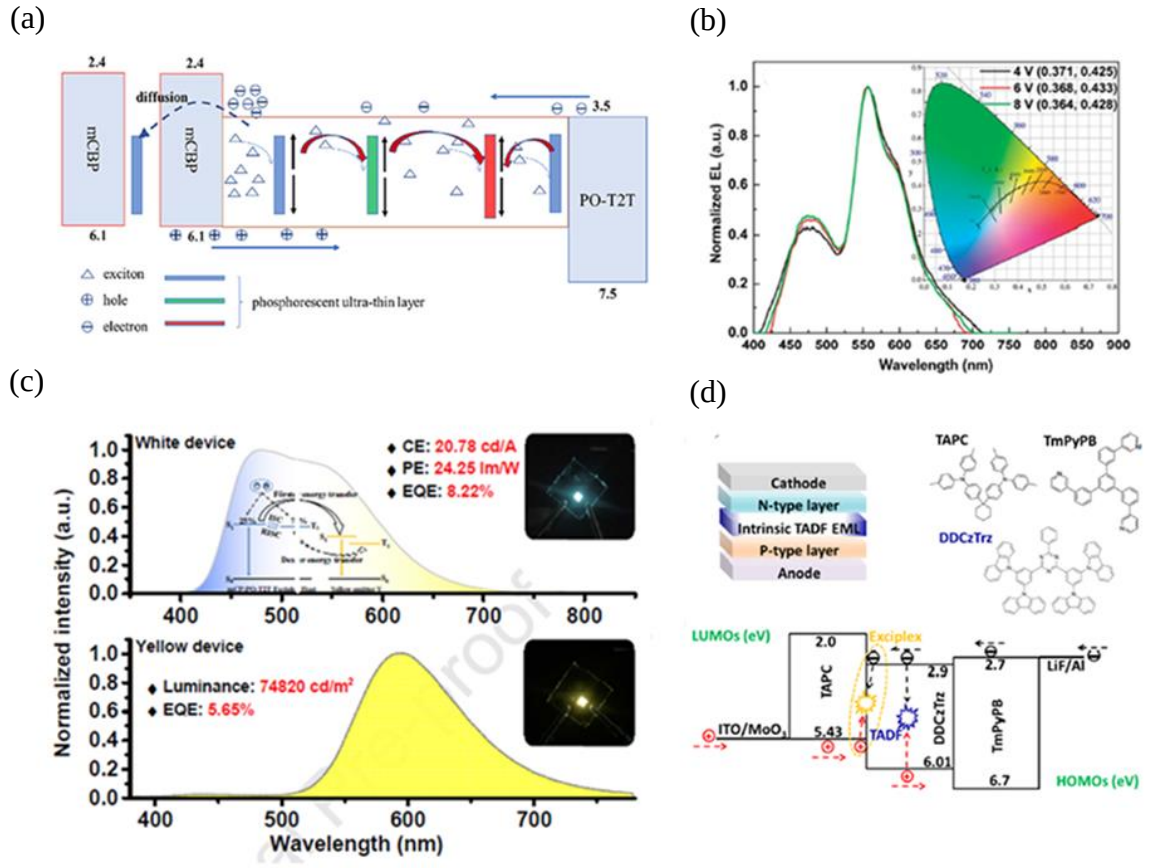

Figure 1.9. (a) The illustration of EML configuration in terms of energy levels by using sequential arrangements of blue, green, and red ultra-thin phosphorescent layers in the exciplex host (mcBP:PO-T2T) in WOLEDs (adapted from ref. 116) (b) The EL spectra of the WOLED where mCP:PO-T2T blue exciplex is used as the host with an orange dopant rubrene. CIE diagram is shown in the inset. (adapted from ref. 118) (c) The EL spectra of the white and yellow OLEDs where blue emitting exciplex as a host with a yellow emitter. The photographs of the devices are shown in the inset. (adapted from ref. 119) (d) The device architecture, molecular structures, and energy level diagram of the WOLED combining the blue emission of TADF emitter DDCzTrz and orange exciplex emission of TAPC/DDCzTrz. (adapted from ref. 133).

Solution-processed WOLEDs have lower efficiency compared to the vacuum-deposited devices[135]. Chen *et al.* have reported solution-processed WOLED by using an interfacial exciplex host with a TADF emitter. A record PE of 93.5 lm/W was achieved, comparable to

vacuum-deposited OLEDs. In 2023, Lu *et al.* have introduced a new strategy to develop simple and efficient exciplex-based monochrome and WOLEDs. In this work, a simpler device structure was developed to achieve high performance white OLEDs by demonstrating vertically stacked multiple interfacial exciplexes. By cleverly arranging donor and acceptor layers and inserting ultra-thin blue phosphorescent emitting layers, a blue phosphorescent OLED achieved a maximum EQE of 28.15%. This approach was employed for other color phosphorescent OLEDs, leading to the development of four-color WOLEDs with maximum EQEs of 21.33%, 25.38% and 24.15%, respectively. A high color stability with CRI exceeding 80 was obtained. This work presents a significant strategy for developing simple and efficient monochrome and white OLEDs via doping-free technology. Recently, Wei *et al.* evaluated the impact of exciton dynamics on the efficiency roll-off properties of exciplex OLEDs using four different exciplex emitters. Insights into exciton behavior were provided by simulating the diffusion lengths of singlet and triplet excitons based on their annihilation rate constants. Additionally, blue, green, yellow, and red phosphorescent OLEDs with high efficiency and low efficiency roll-off were fabricated by optimizing exciplexes as hosts for different color phosphors. The understanding of exciton dynamics in exciplexes was enhanced, contributing to the development of high efficiency, low roll-off phosphorescent OLEDs. Table 1.5. shows the summary of major reports on WOLEDs where exciplex is used as a host with various dopant materials.

Sl No	EML configuration	Remarks on device design strategy	CIE coordinates	Maximum efficiency (EQE, CE, PE)	ref
With phosphorescent emitters					
1	TCPZ:FIrpic (11wt%) /TCPZ:Ir(piq)$_3$ (4wt%) /TCPZ:FIrpic (11 wt%)	Non-tandem multi-EML WOLED by utilizing green exciplex emission with blue and red dopant emissions	(0.39,0.45)	11.6% 27.7 cd/A 15.8 lm/W	110
2	6%Ir(piq)$_3$: TCTA:Bphen/ 6%Ir(ppy)$_3$: TCTA:Bphen /TCTA:Bphen	Non-tandem WOLED with simple device structure by using exciplex and dopant emissions	(0.45,0.39)	10.5%, 10.39 lm/W ….	112
3	CDBP: PO-T2T :Ir(ppy)$_2$acac :Ir(MDQ)$_2$acac	Non-tandem WOLED by using exciplex and dopant emissions	(0.40,0.43)	25.5%, 67 cd/A, 84.1 lm/W	113
4	TAPC: Ir(dmppy)$_2$(dpp)/ TAPC/TmPyPB /TmPyPB :Ir(dmppy)$_2$(dpp)	Non-tandem doping-free hybrid WOLED by utilizing exciplex/electroplex emissions	(0.48,0.40)	15.1% 26.9 cd/A 28.2 lm/W	114
With Fluorescent emitters					
1	mCP:PO-T2T: 1.6 wt% rubrene	All-fluorescent non-tandem WOLEDs with blue emitting exciplex host.	(0.38,0.44)	4.9% 14.2 cd/A 12.8 lm/W	117

2	m-MTDATA (blue) /TCTA/ DPNC (green) /Bphen	Yellow interface exciplex emission combined with fluorescence emissions for non-tandem WOLED.	(0.31,0.34)	5.3%, 5 cd/A ….	118
3	mCP:PO-T2T: 0.5wt% (novel yellow emitter-Y)	Non-tandem WOLED by using blue exciplex as an emitter and host with a yellow emitter.	(0.29,0.39)	8.22%, 20.78 cd/A 24.25 lm/W	119
With TADF emitters					
1	CDBP:PO-T2T: 6 wt% 2CzPN 6 wt% 4CzIPN 4 wt% AnbCz	Non-tandem WOLED by utilizing three different TADF emitters with an exciplex host.	(0.29,0.39)	19%, 50.1 cd/A 63.1 lm/W	132
2	TAPC/DDCzTrz	Exciplex consists of a TADF emitter. Non-tandem WOLED by utilizing orange exciplex and blue dopant emissions.	(0.34,0.35)	28.4% 65.4 cd/A 68.5 lm/W	133
3	mMTDATA/ pCNBCzoCF$_3$	Exciplex consists of a TADF emitter. Non-tandem WOLED by utilizing orange exciplex and green-blue dopant emissions.	(0.4,0.44)	18.8% 53.8 cd/A 19.3 lm/W	134

Table 1.5. Summary of major reports on WOLEDs where exciplex is used as a host with dopants.

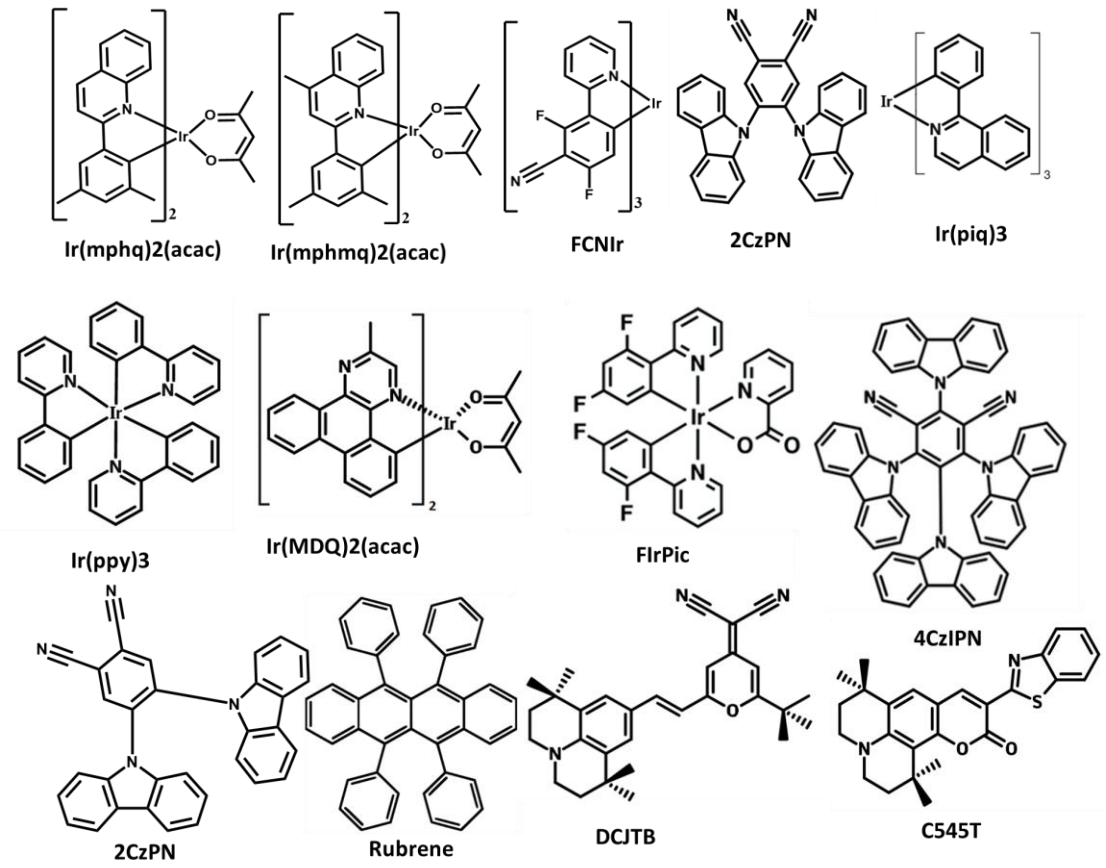

Figure 1.10. The chemical structures of the dopants listed in Tables 1.4 and 1.5.

1.6 Scope of the thesis

This thesis aims to explore the device design strategies to employ exciplex emission in OLEDs; as emitters and as host with suitable dopants to develop simple and cost-effective devices. Firstly, the exciplex emission in selected conjugate pairs are confirmed via spectroscopic studies of the thin films, particularly the expected exciplex emission is based on their HOMO-LUMO gap at the HTM/ETM molecular interfaces. Blue exciplex emission can be combined with yellow or orange emission of fluorescent/phosphorescent/TADF dopants to achieve white emission. This approach simplifies the device architecture and leads to cost-effective device designs for WOLEDs without complex tandem structures. The thesis investigates novel

exciplex-based OLED designs by utilizing commonly available blue emitting transport molecules and the ability of their exciplex formation with suitable dopants. Efficient energy transfer from selected exciplex systems to suitable dopant materials are explored, for the development of stable and efficient WOLEDs. White emission can also be achieved by combining exciplex and excitonic emissions within a single emissive layer, without the need for expensive phosphorescent dopants. The multifunctionality of the exciplex system is explored by utilizing the strong UV-absorption and the phenomenon of SOP in the thin films of organic semiconductors. Notably, this is the first report to explore the multifunctionality of exciplex-based devices. Hence, this thesis will contribute to advancing the understanding and practical application of exciplex systems in the development of cost-effective and efficient white OLEDs, with potential implications for multifunctional optoelectronic devices.

The primary objectives of the thesis are as follows:

I. To study suitable conjugate pairs for exciplex emission from commonly used hole and electron transport materials employed in OLEDs and to explore the photophysical properties of the selected exciplex systems

II. To employ the selected exciplex combinations in OLEDs by designing simple and efficient device architectures and to explore the solution-processing method for device fabrication instead of vacuum deposition

III. To utilize the exciplex as a host for suitable dopants and to obtain white light emission

IV. To design single emissive layer WOLEDs by combining multiple exciplex systems without using high cost phosphoroscent dopants

V. To design and fabricate multifunctional devices using exciplex by utilizing the concept of surface potential in organic small molecules.

1.7 References

1. Bagher, A. M., Comparison of LED and OLED. *J Sch. J. Eng. Technol.* **2016,** *4*, 206-210.

2. Zhang, H.; Su, Q.; Chen, S., Quantum-dot and organic hybrid tandem light-emitting diodes with multi-functionality of full-color-tunability and white-light-emission. *Nat Commun* **2020,** *11* (1), 2826.

3. Ebrahim, F.; Al-Hartomy, O.; Wageh, S., Cadmium-Based Quantum Dots Alloyed Structures: Synthesis, Properties, and Applications. *Materials (Basel)* **2023,** *16* (17), 5877.

4. Yu, P.; Cao, S.; Shan, Y.; Bi, Y.; Hu, Y.; Zeng, R.; Zou, B.; Wang, Y.; Zhao, J., Highly efficient green InP-based quantum dot light-emitting diodes regulated by inner alloyed shell component. *Light Sci Appl* **2022,** *11* (1), 162.

5. Shen, J. H.; Zhu, Q. L., Stability strategies of perovskite quantum dots and their extended applications in extreme environment: A review. *Materials Research Bulletin* **2022,** *156*, 111987.

6. Tchounwou, P. B.; Yedjou, C. G.; Patlolla, A. K.; Sutton, D. J., Heavy metal toxicity and the environment. *Exp Suppl* **2012,** *101*, 133-64.

7. Chang, J. H.; Park, P.; Jung, H.; Jeong, B. G.; Hahm, D.; Nagamine, G.; Ko, J.; Cho, J.; Padilha, L. A.; Lee, D. C.; Lee, C.; Char, K.; Bae, W. K., Unraveling the Origin of Operational Instability of Quantum Dot Based Light-Emitting Diodes. *ACS Nano* **2018,** *12* (10), 10231-10239.

8. Tang, C. W.; Vanslyke, S. A., Organic Electroluminescent Diodes. *Applied Physics Letters* **1987,** *51* (12), 913-915.

9. Hong, G.; Gan, X.; Leonhardt, C.; Zhang, Z.; Seibert, J.; Busch, J. M.; Bräse, S., A brief history of OLEDs—emitter development and industry milestones. *Advanced Materials* **2021,** *33* (9), 2005630.

10. Shahnawaz; Swayamprabha, S. S.; Nagar, M. R.; Yadav, R. A. K.; Gull, S.; Dubey, D. K.; Jou, J. H., Hole-transporting materials for organic light-emitting diodes: an overview. *J Mater Chem C* **2019,** *7* (24), 7144-7158.

11. Wang, Y. P.; Li, B.; Jiang, C.; Fang, Y. F.; Bai, P. L.; Wang, Y. Q., Study on Electron Transport Characterization in TPBi Thin Films and OLED Application. *Journal of Physical Chemistry C* **2021,** *125* (30), 16753-16758.

12. Fu, C.; Lin, H. J. S. S. C., Performance enhancement of blue organic light-emitting devices by inserting BPhen: Alq3 as an n-doping electron transport layer. *Solid State Communications* **2024,** *378*, 115411.

13. Kaji, H.; Suzuki, H.; Fukushima, T.; Shizu, K.; Suzuki, K.; Kubo, S.; Komino, T.; Oiwa, H.; Suzuki, F.; Wakamiya, A.; Murata, Y.; Adachi, C., Purely organic electroluminescent material realizing 100% conversion from electricity to light. *Nat Commun* **2015,** *6* (1), 8476.

14. Kim, G. W.; Son, Y. H.; Yang, H. I.; Park, J. H.; Ko, I. J.; Lampande, R.; Sakong, J.; Maeng, M. J.; Hong, J. A.; Lee, J. Y.; Park, Y.; Kwon, J. H., Diphenanthroline Electron Transport Materials for the Efficient Charge Generation Unit in Tandem Organic Light-Emitting Diodes. *Chemistry of Materials* **2017,** *29* (19), 8299-8312.

15. Xu, Y. L.; Lv, X.; Zhu, M.; Sun, S. Q.; He, W.; Zhou, J. G.; Xie, Y. M.; Fung, M. K., Pyridine group incorporated mixed electron transporting layers for high-performance perovskite light-emitting diodes. *Materials Today Energy* **2023,** *38*, 101424.

16. Kohler, A.; Bassler, H., Fundamentals of Organic Semiconductor Devices. *Electronic Processes in Organic Semiconductors, First Edition* **2015**.

17. Monkman, A.; Interfaces, Why do we still need a stable long lifetime deep blue OLED emitter? *ACS Applied Materials* **2021,** *14* (18), 20463-20467.

18. Tankelevičiūtė, E.; Samuel, I. D.; Zysman-Colman, E., The Blue Problem: OLED Stability and Degradation Mechanisms. *Journal of Physical Chemistry Letters* **2024,** *15* (4), 1034-1047.

19. Kim, J.; Kim, J.; Kim, Y.; Son, Y.; Shin, Y.; Bae, H. J.; Kim, J. W.; Nam, S.; Jung, Y.; Kim, H.; Kang, S.; Jung, Y.; Lee, K.; Choi, H.; Kim, W. Y., Critical role of electrons in the short lifetime of blue OLEDs. *Nat Commun* **2023,** *14* (1), 7508.

20. Yoshida, K.; Manousiadis, P. P.; Bian, R.; Chen, Z.; Murawski, C.; Gather, M. C.; Haas, H.; Turnbull, G. A.; Samuel, I. D. W., 245 MHz bandwidth organic light-emitting diodes used in a gigabit optical wireless data link. *Nat Commun* **2020,** *11* (1), 1171.

21. Ouyang, M. T.; Guo, R. D.; Jiang, H.; Wang, L.; Wong, W. Y., Efficient blue and deep blue fluorescent OLEDs based on anthracene with upper-level intersystem crossing. *Journal of Luminescence* **2023,** *263*, 120069.

22. Salehi, A.; Dong, C.; Shin, D. H.; Zhu, L.; Papa, C.; Thy Bui, A.; Castellano, F. N.; So, F., Realization of high-efficiency fluorescent organic light-emitting diodes with low driving voltage. *Nat Commun* **2019,** *10* (1), 2305.

23. Xu, Y.; Liang, X.; Liang, Y.; Guo, X.; Hanif, M.; Zhou, J.; Zhou, X.; Wang, C.; Yao, J.; Zhao, R.; interfaces, Efficient deep-blue fluorescent OLEDs with a high exciton utilization efficiency from a fully twisted phenanthroimidazole–anthracene emitter. *ACS applied materials* **2019,** *11* (34), 31139-31146.

24. Jayabharathi, J.; Thanikachalam, V.; Thilagavathy, S., Phosphorescent organic light-emitting devices: Iridium based emitter materials–An overview. *Coordination Chemistry Reviews* **2023,** *483*, 215100.

25. Zhou, Z. X.; Xie, X. Y.; Sun, Z. L.; Wang, X.; An, Z. F.; Huang, W., Recent advances in metal-free phosphorescent materials for organic light-emitting diodes. *J Mater Chem C* **2023,** *11* (9), 3143-3161.

26. Benchohra, A.; Chong, J. L.; Cruz, C. M.; Besnard, C.; Guénée, L.; Rosspeintner, A.; Piguet, C., Additional Insights into the Design of Cr(III) Phosphorescent Emitters Using 6-Membered Chelate Ring Bis(imidazolyl) Didentate Ligands. *Inorganic Chemistry* **2024,** *63* (8), 3617-3629.

27. Meng, G.; Dai, H.; Wang, Q.; Zhou, J.; Fan, T.; Zeng, X.; Wang, X.; Zhang, Y.; Yang, D.; Ma, D.; Zhang, D.; Duan, L., High-efficiency and stable short-delayed fluorescence emitters with hybrid long- and short-range charge-transfer excitations. *Nat Commun* **2023,** *14* (1), 2394.

28. Qi, Y. Y.; Zhang, Z. H.; Sun, W. D.; Wu, S. H.; Liu, J. T.; Lin, Z. K.; Jiang, P. C.; Yu, H. T.; Zhou, L.; Lu, G. Z., High-efficiency narrowband multi-resonance TADF emitters the introduction of bulky adamantane units. *J Mater Chem C* **2024,** *12* (17), 6319-6325.

29. Nidhankar, A. D.; Goudappagouda; Kothavade, P.; Dongre, S. D.; Dnyaneshwar Veer, S.; Ranjan Dash, S.; Rajeev, K.; Unni, K. N. N.; Shanmuganathan, K.; Santhosh Babu, S., Thermally Activated Delayed Fluorescent Solvent-free Organic Liquid Hybrids for Tunable Emission Applications. *Chem Asian J* **2023,** *18* (13), e202300276.

30. Behera, S. K.; Costa, R. D., Emerging hyperfluorescent emitters for solid-state lighting. *J Mater Chem C* **2023,** *11* (40), 13647-13656.

31. Stavrou, K.; Franca, L. G.; Danos, A.; Monkman, A. P., Key requirements for ultraefficient sensitization in hyperfluorescence organic light-emitting diodes. *Nature Photonics* **2024,** *18* (6), 1-8.

32. Song, W.; Yook, K. S., Hyperfluorescence-based full fluorescent white organic light-emitting diodes. *Journal of Industrial and Engineering Chemistry* **2018,** *61*, 445-448.

33. Soman, A.; Sajeev, A. K.; Rajeev, K.; K, N. N., Reversible Shift from Excitonic to Excimer Emission in Fluorescent Organic Light-Emitting Diodes: Dependence on Deposition Parameters and Electrical Bias. *ACS Omega* **2020,** *5* (3), 1698-1707.

34. Wu, J.; Ameri, L.; Cao, L. Y.; Li, J., Efficient excimer-based white OLEDs with reduced efficiency roll-off. *Applied Physics Letters* **2021,** *118* (7).

35. Gupta, C. V.; Dixit, S. J. N.; Agarwal, N.; Bose, S., Voltage tunable white light generation from combined emission of monomer and electromer in phenanthroimidazole based OLED. *Journal of Photochemistry and Photobiology a-Chemistry* **2022,** *429*, 113922.

36. Cho, Y. J.; Taylor, S.; Aziz, H., Increased Electromer Formation and Charge Trapping in Solution-Processed versus Vacuum-Deposited Small Molecule Host Materials of Organic Light-Emitting Devices. *ACS Appl Mater Interfaces* **2017,** *9* (46), 40564-40572.

37. Sarma, M.; Chen, L. M.; Chen, Y. S.; Wong, K. T., Exciplexes in OLEDs: Principles and promises. *Materials Science & Engineering R-Reports* **2022,** *150*, 100689.

38. Chen, Y. S.; Lin, I. H.; Huang, H. Y.; Liu, S. W.; Hung, W. Y.; Wong, K. T., Exciplex-forming cohost systems with 2,7-dicyanofluorene acceptors for high efficiency red and deep-red OLEDs. *Sci Rep* **2024,** *14* (1), 2458.

39. Ning, Y. R.; Zhao, X.; Wu, F. J.; Wu, Y. T.; Chen, J.; Wei, F. X.; Wang, H. Y.; Chen, X. L.; Xiong, Z. H., Charge-Transfer Dynamics in OLEDs with Coexisting Electroplex and Exciton States. *Physical Review Applied* **2023,** *19* (6), 064055.

40. Zhao, D. W.; Xu, Z.; Zhang, F. J.; Song, S. F.; Zhao, S. L.; Wang, Y.; Yuan, G. C.; Zhang, Y. F.; Xu, H. H., The effect of electric field strength on electroplex emission at the interface of NPB/PBD organic light-emitting diodes. *Applied Surface Science* **2007,** *253* (8), 4025-4028.

41. Turro, N. J., *Modern molecular photochemistry*. University science books: 1991.

42. Xiao, P.; Huang, J. H.; Yu, Y. C.; Yuan, J.; Luo, D. X.; Liu, B. Q.; Liang, D., Recent Advances of Exciplex-Based White Organic Light-Emitting Diodes. *Applied Sciences-Basel* **2018,** *8* (9), 1449.

43. Zhang, M.; Zheng, C. J.; Lin, H.; Tao, S. L., Thermally activated delayed fluorescence exciplex emitters for high-performance organic light-emitting diodes. *Mater Horiz* **2021,** *8* (2), 401-425.

44. Ledwon, P., Recent advances of donor-acceptor type carbazole-based molecules for light emitting applications. *Organic Electronics* **2019,** *75*, 105422.

45. Li, J.; Li, Z.; Liu, H.; Gong, H.; Zhang, J.; Guo, Q., Advances in blue exciplex–based organic light-emitting materials and devices. *Frontiers in Chemistry* **2022,** *10*, 952116.

46. Kim, H. B.; Kim, J. J., Recent progress on exciplex-emitting OLEDs. *Journal of Information Display* **2019,** *20* (3), 105-121.

47. Singh, S. P.; Mohapatra, Y. N.; Qureshi, M.; Sundar Manoharan, S.; Manoharan, S. S., White organic light-emitting diodes based on spectral broadening in electroluminescence due to formation of interfacial exciplexes. *Applied Physics Letters* **2005,** *86* (11).

48. Goushi, K.; Yoshida, K.; Sato, K.; Adachi, C., Organic light-emitting diodes employing efficient reverse intersystem crossing for triplet-to-singlet state conversion. *Nature Photonics* **2012,** *6* (4), 253-258.

49. Su, W. M.; Li, W. L.; Xin, Q.; Su, Z. S.; Chu, B.; Bi, D. F.; He, H.; Niu, J. H., Effect of acceptor on efficiencies of exciplex-type organic light emitting diodes. *Applied Physics Letters* **2007,** *91* (4), 043508.

50. Jankus, V.; Data, P.; Graves, D.; McGuinness, C.; Santos, J.; Bryce, M. R.; Dias, F. B.; Monkman, A. P., Highly efficient TADF OLEDs: how the emitter–host

interaction controls both the excited state species and electrical properties of the devices to achieve near 100% triplet harvesting and high efficiency. *Advanced Functional Materials* **2014,** *24* (39), 6178-6186.

51. Liu, X. K.; Chen, Z.; Zheng, C. J.; Liu, C. L.; Lee, C. S.; Li, F.; Ou, X. M.; Zhang, X. H., Prediction and design of efficient exciplex emitters for high-efficiency, thermally activated delayed-fluorescence organic light-emitting diodes. *Adv Mater* **2015,** *27* (14), 2378-83.

52. dos Santos, P. L.; Dias, F. B.; Monkman, A. P., Investigation of the mechanisms giving rise to TADF in exciplex states. *The Journal of Physical Chemistry C* **2016,** *120* (32), 18259-18267.

53. Pang, Z.; Sun, D.; Zhang, C.; Baniya, S.; Kwon, O.; Vardeny, Z. V., Manipulation of Emission Colors Based on Intrinsic and Extrinsic Magneto-Electroluminescence from Exciplex Organic Light-Emitting Diodes. *Acs Photonics* **2017,** *4* (8), 1899-1905.

54. Colella, M.; Pander, P.; Monkman, A. P., Solution processable small molecule based TADF exciplex OLEDs. *Organic Electronics* **2018,** *62*, 168-173.

55. Yuan, P.; Guo, X.; Qiao, X.; Yan, D.; Ma, D., Improvement of the Electroluminescence Performance of Exciplex-Based OLEDs by Effective Utilization of Long-Range Coupled Electron–Hole Pairs. *Advanced Optical Materials* **2019,** *7* (9), 1801648.

56. Schleper, A. L.; Goushi, K.; Bannwarth, C.; Haehnle, B.; Welscher, P. J.; Adachi, C.; Kuehne, A. J. C., Hot exciplexes in U-shaped TADF molecules with emission from locally excited states. *Nat Commun* **2021,** *12* (1), 6179.

57. Wei, X. F.; Hu, T. P.; Li, Z. Y.; Liu, Y. W.; Hu, X. X.; Gao, H. L.; Liu, G. H.; Wang, P. F.; Yi, Y. P.; Wang, Y., Rational strategy of exciplex-type thermally activated delayed fluorescent (TADF) emitters: Stacking of donor and acceptor units

of the intramolecular TADF molecule. *Chemical Engineering Journal* **2022,** *433*, 133546.

58. Kesavan, K. K.; Jayakumar, J.; Lee, M.; Hexin, C.; Swayamprabha, S. S.; Dubey, D. K.; Tung, F.-C.; Wang, C.-W.; Jou, J.-H., Achieving a 32% EQE solution-processed simple structure OLED via exciplex system. *Chemical Engineering Journal* **2022,** *435*, 134879.
59. Mazzeo, M.; Pisignano, D.; Della Sala, F.; Thompson, J.; Blyth, R. I. R.; Gigli, G.; Cingolani, R.; Sotgiu, G.; Barbarella, G., Organic single-layer white light-emitting diodes by exciplex emission from spin-coated blends of blue-emitting molecules. *Applied Physics Letters* **2003,** *82* (3), 334-336.

60. Zhu, J. Z.; Li, W. L.; Han, L. L.; Chu, B.; Zhang, G.; Yang, D. F.; Chen, Y. R.; Su, Z. S.; Wang, J. B.; Wu, S. H.; Tsuboi, T. J., Very broad white-emission spectrum based organic light-emitting diodes by four exciplex emission bands. *Optics Letters* **2009,** *34* (19), 2946-2948.

61. Hung, W. Y.; Fang, G. C.; Lin, S. W.; Cheng, S. H.; Wong, K. T.; Kuo, T. Y.; Chou, P. T., The first tandem, all-exciplex-based WOLED. *Sci Rep* **2014,** *4* (1), 5161.

62. Zhao, B.; Zhang, T. Y.; Chu, B.; Li, W. L.; Su, Z. S.; Luo, Y. S.; Li, R. G.; Yan, X. W.; Jin, F. M.; Gao, Y.; Wu, H. R., Highly efficient tandem full exciplex orange and warm white OLEDs based on thermally activated delayed fluorescence mechanism. *Organic Electronics* **2015,** *17*, 15-21.

63. Angioni, E.; Chapran, M.; Ivaniuk, K.; Kostiv, N.; Cherpak, V.; Stakhira, P.; Lazauskas, A.; Tamulevicius, S.; Volyniuk, D.; Findlay, N. J.; Tuttle, T.; Grazulevicius, J. V.; Skabara, P. J., A single emitting layer white OLED based on exciplex interface emission. *J Mater Chem C* **2016,** *4* (17), 3851-3856.

64. Wei, X. Z.; Gao, L.; Miao, Y. Q.; Zhao, Y. P.; Yin, M. N.; Wang, H.; Xu, B. S., A new strategy for structuring white organic light-emitting diodes by combining

complementary emissions in the same interface. *J Mater Chem C* **2020,** *8* (8), 2772-2779.

65. Vipin, C. K.; Shukla, A.; Rajeev, K.; Hasan, M.; Lo, S. C.; Namdas, E. B.; Ajayaghosh, A.; Unni, K. N. N., White Organic Light-Emitting Diodes from Single Emissive Layers: Combining Exciplex Emission with Electromer Emission. *Journal of Physical Chemistry C* **2021,** *125* (41), 22809-22816.

66. Dong, B. Z.; Yan, J. K.; Li, G. Z.; Xu, Y. B.; Zhao, B.; Chen, L. Q.; Wang, H.; Li, W. L., High luminance/efficiency monochrome and white organic light emitting diodes based pure exciplex emission. *Organic Electronics* **2022,** *106*, 106528.

67. Li, D.; Hu, Y.; Liao, L. S., Triplet exciton harvesting by multi-process energy transfer in fluorescent organic light-emitting diodes. *J Mater Chem C* **2019,** *7* (4), 977-985.

68. Chen, Y. W.; Wu, Y. B.; Lin, C. W.; Dai, Y. F.; Sun, Q.; Yang, D. Z.; Qiao, X. F.; Ma, D. G., Simultaneous high efficiency/CRI/spectral stability and low efficiency roll-off hybrid white organic light-emitting diodes simple insertion of ultrathin red/green phosphorescent emitters in a blue exciplex. *J Mater Chem C* **2020,** *8* (36), 12450-12456.

69. Tang, X.; Pan, R.; Zhao, X.; Jia, W.; Wang, Y.; Ma, C.; Tu, L.; Xiong, Z., Full confinement of high-lying triplet states to achieve high-level reverse intersystem crossing in rubrene: a strategy for obtaining the record-high EQE of 16.1% with low efficiency roll-off. *Advanced Functional Materials* **2020,** *30* (51), 2005765.

70. Song, J.; Zhang, F.; Yang, L.; Chen, K.; Li, A.; Sheng, R.; Duan, Y.; Chen, P., Highly efficient, ultralow turn-on voltage red and white organic light-emitting devices based on a novel exciplex host. *Materials Advances* **2021,** *2* (11), 3677-3684.

71. Liehm, P.; Murawski, C.; Furno, M.; Lüssem, B.; Leo, K.; Gather, M. C., Comparing the emissive dipole orientation of two similar phosphorescent green emitter molecules in highly efficient organic light-emitting diodes. *Applied Physics Letters* **2012,** *101* (25).

72. Davidson, R.; Hsu, Y. T.; Fox, M. A.; Aguilar, J. A.; Yufit, D.; Beeby, A., Tuning Emission Lifetimes of Ir(C;N)(2)(acac) Complexes with Oligo(phenyleneethynylene) Groups. *Inorg Chem* **2023,** *62* (6), 2793-2805.

73. Park, J. W.; Cho, K. H.; Rhee, Y. M., Mechanism of Ir(ppy) Guest Exciton Formation with the Exciplex-Forming TCTA:TPBI Cohost within a Phosphorescent Organic Light-Emitting Diode Environment. *International Journal of Molecular Sciences* **2022,** *23* (11), 5940.

74. Soldano, C.; Laouadi, O.; Gallegos-Rosas, K., TCTA:Ir(ppy)(3) Green Emissive Blends in Organic Light-Emitting Transistors (OLETs). *ACS Omega* **2022,** *7* (48), 43719-43728.

75. Liu, C.-H.; Nhi, N. P. Y.; Sun, Y.-M.; Meng, H.-F.; Zan, H.-W.; Chen, L.-Y.; Huang, Z.-H.; Tian, Y.-C.; Lai, C.-S., Using light-emitting complex Ir (mppy) 3 to detect acetone from 0.5 to 100áppm by vertical-channel gas sensor. *Organic Electronics* **2022,** *106*, 106507.

76. Park, C. H.; Lee, H. J.; Hwang, J. H.; Kim, K. N.; Shim, Y. S.; Jung, S. G.; Park, C. H.; Park, Y. W.; Ju, B. K., High-performance hybrid buffer layer using 1,4,5,8,9,11-hexaazatriphenylenehexacarbonitrile/molybdenum oxide in inverted top-emitting organic light-emitting diodes. *ACS Appl Mater Interfaces* **2015,** *7* (11), 6047-53.

77. Wu, S. F.; Li, S. H.; Sun, Q.; Huang, C. C.; Fung, M. K., Highly Efficient White Organic Light-Emitting Diodes with Ultrathin Emissive Layers and a Spacer-Free Structure. *Scientific Reports* **2016,** *6* (1), 25821.

78. Li, Y. N.; Zhou, L.; Cui, R. Z.; Jiang, Y. L.; Zhao, X. S.; Liu, W. Q.; Zhu, Q.; Cui, Y. J.; Zhang, H. J., High performance red organic electroluminescent devices based on a trivalent iridium complex with stepwise energy levels. *Rsc Advances* **2016,** *6* (75), 71282-71286.

79. Li, W.; Zhao, J. W.; Li, L. J.; Du, X. Y.; Fan, C.; Zheng, C. J.; Tao, S. L., Efficient solution-processed blue and white OLEDs based on a high-triplet bipolar host and a blue TADF emitter. *Organic Electronics* **2018,** *58*, 276-282.

80. Finkenzeller, W. J.; Hofbeck, T.; Thompson, M. E.; Yersin, H., Triplet state properties of the OLED emitter Ir(btp)2(acac): characterization by site-selective spectroscopy and application of high magnetic fields. *Inorg Chem* **2007,** *46* (12), 5076-83.

81. Xiao-Bo, Z.; Fu-Xiang, W., The excitation mechanism of btp2Ir (acac) in CBP host. *Luminescence* **2017,** *32* (3), 409-413.

82. Tsuboi, T.; Tanigawa, M.; Kawami, S.; Tsuji, T., New emission band of PtOEP phosphor in organic LED devices. *Current Applied Physics* **2005,** *5* (1), 47-54.

83. Yang, L.; Chua, X. W.; Yang, Z.; Ding, X.; Yu, Y.; Suwardi, A.; Zhao, M.; Ke, K. L.; Ehrler, B.; Di, D., Photon-upconverters for blue organic light-emitting diodes: a low-cost, sky-blue example. *Nanoscale Adv* **2022,** *4* (5), 1318-1323.

84. Baranoff, E.; Curchod, B. F., FIrpic: archetypal blue phosphorescent emitter for electroluminescence. *Dalton Trans* **2015,** *44* (18), 8318-29.

85. Penconi, M.; Cazzaniga, M.; Panzeri, W.; Mele, A.; Cargnoni, F.; Ceresoli, D.; Bossi, A., Unraveling the Degradation Mechanism in FIrpic-Based Blue OLEDs: II. Trap and Detect Molecules at the Interfaces. *Chemistry of Materials* **2019,** *31* (7), 2277-2285.

86. Yao, C.; Yang, Y.; Li, L.; Bo, M.; Peng, C.; Wang, J., Not All Bis [2-(4, 6-difluorophenyl) pyridyl-N, C 2′] iridium (III) Picolinate (FIrpic) Isomers Are Unsuitable for Developing Long-Lifetime Blue Phosphorescent Organic Light-Emitting Diodes. *Journal of Physical Chemistry C* **2018,** *123* (1), 227-232.

87. Gao, K.; Liu, K. K.; Li, X. L.; Cai, X. Y.; Chen, D. J.; Xu, Z. D.; He, Z. Z.; Li, B. B.; Qiao, Z. Y.; Chen, D. C.; Cao, Y.; Su, S. J., An ideal universal host for highly

efficient full-color, white phosphorescent and TADF OLEDs with a simple and unified structure. *J Mater Chem C* **2017,** *5* (39), 10406-10416.

88. Singh, M.; Jou, J. H.; Sahoo, S.; S, S. S.; He, Z. K.; Krucaite, G.; Grigalevicius, S.; Wang, C. W., High light-quality OLEDs with a wet-processed single emissive layer. *Sci Rep* **2018,** *8* (1), 7133.

89. Kant, C.; Mahmood, S.; Katiyar, M., Large-Area Inkjet-Printed OLEDs Patterns and Tiles Using Small Molecule Phosphorescent Dopant. *Advanced Materials Technologies* **2023,** *8* (5), 2201514.

90. Chao, T. C.; Liao, J. Y.; Yeh, H. C.; Lin, J. S.; Tseng, M. R., Recent progress on Solution Processable small molecules for Organic Light-Emitting Diodes in ITRI. *Organic Light Emitting Materials and Devices Xvii* **2013,** *8829*, 201-209.

91. Tan, X. F.; Volyniuk, D.; Matulaitis, T.; Keruckas, J.; Ivaniuk, K.; Helzhynskyy, I.; Stakhira, P.; Grazulevicius, J. V., High triplet energy materials for efficient exciplex-based and full-TADF-based white OLEDs. *Dyes and Pigments* **2020,** *177*, 108259.

92. Park, Y. S.; Jeong, W. I.; Kim, J. J., Energy transfer from exciplexes to dopants and its effect on efficiency of organic light-emitting diodes. *Journal of Applied Physics* **2011,** *110* (12).

93. Park, Y.-S.; Jeong, W.-I.; Kim, J.-J. J. J. o. A. P., Energy transfer from exciplexes to dopants and its effect on efficiency of organic light-emitting diodes. **2011,** *110* (12), 124519.

94. Lee, S.; Limbach, D.; Kim, K. H.; Yoo, S. J.; Park, Y. S.; Kim, J. J., High efficiency and non-color-changing orange organic light emitting diodes with red and green emitting layers. *Organic Electronics* **2013,** *14* (7), 1856-1860.

95. Lee, J. H.; Shin, H.; Kim, J. M.; Kim, K. H.; Kim, J. J., Exciplex-Forming Co-Host-Based Red Phosphorescent Organic Light-Emitting Diodes with Long Operational Stability and High Efficiency. *ACS Appl Mater Interfaces* **2017,** *9* (4), 3277-3281.

96. Hung, W. Y.; Chiang, P. Y.; Lin, S. W.; Tang, W. C.; Chen, Y. T.; Liu, S. H.; Chou, P. T.; Hung, Y. T.; Wong, K. T., Balance the Carrier Mobility To Achieve High Performance Exciplex OLED Using a Triazine-Based Acceptor. *ACS Appl Mater Interfaces* **2016,** *8* (7), 4811-8.

97. Lim, H.; Shin, H.; Kim, K. H.; Yoo, S. J.; Huh, J. S.; Kim, J. J., An Exciplex Host for Deep-Blue Phosphorescent Organic Light-Emitting Diodes. *ACS Appl Mater Interfaces* **2017,** *9* (43), 37883-37887.

98. Feng, Y. L.; Lu, T. T.; Liu, D.; Jiang, W.; Sun, Y. M., High-performance blue phosphorescent and thermally activated delayed fluorescent solution-processed OLEDs based on exciplex host by modifying TCTA. *Organic Electronics* **2019,** *67*, 136-140.

99. Chiu, C.-H.; Al Amin, N. R.; Xie, J.-X.; Lee, C.-C.; Luo, D.; Biring, S.; Sutanto, K.; Liu, S.-W.; Chen, C.-H., A phosphorescent OLED with an efficiency roll-off lower than 1% at 10000 cd m− 2 achieved by reducing the carrier mobility of the donors in an exciplex co-host system. *J Mater Chem C* **2022,** *10* (12), 4955-4964.

100. Xia, Q.; Xiang, Y. H.; Gong, Y. J.; Li, S.; Wu, Y. S.; Wang, Z. J.; Fu, H. B., Development of a deep-blue exciplex as an emitter and a host for highly efficient and wide-color OLEDs. *J Mater Chem C* **2023,** *11* (19), 6354-6359.

101. Zhao, B.; Zhang, T. Y.; Chu, B.; Li, W. L.; Su, Z. S.; Wu, H. R.; Yan, X. W.; Jin, F. M.; Gao, Y.; Liu, C. Y., Highly efficient red OLEDs using DCJTB as the dopant and delayed fluorescent exciplex as the host. *Scientific Reports* **2015,** *5* (1), 1-8.

102. Liu, X. K.; Chen, Z.; Zheng, C. J.; Chen, M.; Liu, W.; Zhang, X. H.; Lee, C. S., Nearly 100% Triplet Harvesting in Conventional Fluorescent Dopant-Based Organic Light-Emitting Devices Through Energy Transfer from Exciplex. *Advanced Materials* **2015,** *27* (12), 2025-2030.

103. Liang, B.; Wang, J.; Cheng, Z.; Wei, J.; Wang, Y., Exciplex-Based Electroluminescence: Over 21% External Quantum Efficiency and Approaching 100 lm/W Power Efficiency. *J Phys Chem Lett* **2019,** *10* (11), 2811-2816.

104. Regnat, M.; Pernstich, K. P.; Kim, K. H.; Kim, J. J.; Nüesch, F.; Ruhstaller, B., Routes for efficiency enhancement in fluorescent TADF exciplex host OLEDs gained from an electro-optical device model. *Advanced Electronic Materials* **2020,** *6* (2), 1900804.

105. Kim, B. S.; Lee, J. Y., Engineering of mixed host for high external quantum efficiency above 25% in green thermally activated delayed fluorescence device. *Advanced functional materials* **2014,** *24* (25), 3970-3977.

106. Sun, J. W.; Lee, J. H.; Moon, C. K.; Kim, K. H.; Shin, H.; Kim, J. J., A fluorescent organic light-emitting diode with 30% external quantum efficiency. *Adv Mater* **2014,** *26* (32), 5684-8.

107. Yang, H. Y.; Zheng, C. J.; Zhang, M.; Zhao, J. W.; Zhong, P. L.; Lin, H.; Tao, S. L.; Zhang, X. H., Green solution-processed thermally activated delayed fluorescence OLEDs with improved performance by using interfacial exciplex host. *Organic Electronics* **2019,** *73*, 36-42.

108. Chen, L.; Lv, J.; Wang, S.; Shao, S.; Wang, L., Dendritic Interfacial Exciplex Hosts for Solution-Processed TADF-OLEDs with Power Efficiency Approaching 100 lm W−1. *Advanced Optical Materials* **2021,** *9* (20), 2100752.

109. Zhou, Z.; Chen, R.; Jin, P.; Hao, J.; Wu, W.; Yin, B.; Zhang, C.; Yao, J., Interplay between singlet and triplet excited states in interface exciplex OLEDs with fluorescence, phosphorescence, and TADF emitters. *Advanced Functional Materials* **2023,** *33* (5), 2211059.

110. Su, S.-J.; Cai, C.; Takamatsu, J.; Kido, J., A host material with a small singlet–triplet exchange energy for phosphorescent organic light-emitting diodes: Guest, host, and exciplex emission. *Organic electronics* **2012,** *13* (10), 1937-1947.

111. Duan, Y.; Sun, F. B.; Yang, D.; Yang, Y. Q.; Chen, P.; Duan, Y. H., White-light electroluminescent organic devices based on efficient energy harvesting of singlet and triplet excited states using blue-light exciplex. *Applied Physics Express* **2014,** *7* (5), 052102.

112. Zhang, T.; Zhao, B.; Chu, B.; Li, W.; Su, Z.; Yan, X.; Liu, C.; Wu, H.; Gao, Y.; Jin, F.; Hou, F., Simple structured hybrid WOLEDs based on incomplete energy transfer mechanism: from blue exciplex to orange dopant. *Sci Rep* **2015,** *5* (1), 10234.

113. Liu, X. K.; Chen, Z.; Qing, J.; Zhang, W. J.; Wu, B.; Tam, H. L.; Zhu, F.; Zhang, X. H.; Lee, C. S., Remanagement of Singlet and Triplet Excitons in Single-Emissive-Layer Hybrid White Organic Light-Emitting Devices Using Thermally Activated Delayed Fluorescent Blue Exciplex. *Adv Mater* **2015,** *27* (44), 7079-85.

114. Luo, D. X.; Li, X. L.; Zhao, Y.; Gao, Y.; Liu, B. Q., High-Performance Blue Molecular Emitter-Free and Doping-Free Hybrid White Organic Light-Emitting Diodes: an Alternative Concept To Manipulate Charges and Excitons Based on Exciplex and Electroplex Emission. *Acs Photonics* **2017,** *4* (6), 1566-1575.

115. Ying, S. A.; Yang, D. Z.; Qiao, X. F.; Dai, Y. F.; Sun, Q.; Chen, J. S.; Ahamad, T.; Alshehri, S. M.; Ma, D. G., Improvement of efficiency and its roll- off at high brightness in white organic light- emitting diodes by strategically managing triplet excitons in the emission layer. *J Mater Chem C* **2018,** *6* (40), 10793-10803.

116. Zhang, S.; Yao, J. W.; Dai, Y. F.; Sun, Q.; Yang, D. Z.; Qiao, X. F.; Chen, J. S.; Ma, D. G., High efficiency and color quality undoped phosphorescent white organic light-emitting diodes based on simple ultrathin structure in exciplex. *Organic Electronics* **2020,** *85*, 105821.

117. Zhang, H.; Wang, Z.; Gao, L.; Zhao, B.; Li, W., Low efficiency roll-off and high color stability pure fluorescent white organic light-emitting diode based exciplex host. *RSC Adv* **2018,** *8* (2), 954-959.

118. Ivaniuk, K.; Stakhira, P.; Helzhynskyy, I.; Kutsiy, S.; Hotra, Z.; Deksnys, T.; Volyniuk, D.; Grazulevicius, J. V.; Gorbulic, V. In *Contribution Of Fluorescence And Exciplex Emission Into Efficient White OLED*, 2020 IEEE 15th International Conference on Advanced Trends in Radioelectronics, Telecommunications and Computer Engineering (TCSET), IEEE: 2020; pp 821-824.

119. Zhao, Y.; Zhang, J.; Miao, Y.; Wei, X.; Xu, H.; Wu, Y.; Wang, H.; Li, T.; Xu, B., All-fluorescent white organic light-emitting diodes with EQE exceeding theoretical limit of 5% by incorporating a novel yellow fluorophor in co-doping forming blue exciplex. *Organic Electronics* **2020,** *83*, 105746.

120. Zhao, B.; Zhang, T.; Chu, B.; Li, W.; Su, Z.; Wu, H.; Yan, X.; Jin, F.; Gao, Y.; Liu, C. J. S. R., Highly efficient red OLEDs using DCJTB as the dopant and delayed fluorescent exciplex as the host. **2015,** *5* (1), 10697.

121. Kurban, M.; Gündüz, B., Physical and optical properties of DCJTB dye for OLED display applications: Experimental and theoretical investigation. *Journal of Molecular Structure* **2017,** *1137*, 403-411.

122. Hua, J.; Zhan, Z. L.; Cheng, Z. Y.; Cao, W. S.; Chai, Y.; Wang, X. F.; Wei, C. Y.; Dong, H.; Wang, J., High-efficiency all-fluorescent white organic light-emitting diode based on TADF material as a sensitizer. *Rsc Advances* **2023,** *13* (45), 31632-31640.

123. Wang, S. J.; Kirch, A.; Sawatzki, M.; Achenbach, T.; Kleemann, H.; Reineke, S.; Leo, K., Highly Crystalline Rubrene Light-Emitting Diodes with Epitaxial Growth. *Advanced Functional Materials* **2023,** *33* (14), 2213768.

124. Tang, X. T.; Tu, L. Y.; Zhao, X.; Chen, J.; Ning, Y. R.; Wu, F. J.; Xiong, Z. H., Realization of H-Type Aggregation in Rubrene-Doped OLEDs and Its Induced

Enhancement of Delayed Fluorescence. *Journal of Physical Chemistry C* **2022,** *126* (22), 9456-9465.

125. Xiao, J.; Yao, Y. S.; Deng, Z. B.; Wang, X. S.; Liang, C. J., Study of the characteristics of new red dopants in OLED. *Journal of Luminescence* **2007,** *122*, 639-641.

126. Yao, Y. S.; Zhou, Q. X.; Wang, X. S.; Wang, Y.; Zhang, B. W., A DCM-type red-fluorescent dopant for high-performance organic electroluminescent devices. *Advanced Functional Materials* **2007,** *17* (1), 93-100.

127. Meng, M.; Song, W.; Kim, Y. H.; Lee, S. Y.; Jhun, C. G.; Zhu, F. R.; Ryu, D. H.; Kim, W. Y., Effects of Electron Transport Material on Blue Organic Light-Emitting Diode with Fluorescent Dopant of BCzVBi. *Journal of Nanoscience and Nanotechnology* **2013,** *13* (1), 294-299.

128. Kim, N. H.; Kim, Y.-H.; Yoon, J.-A.; Lee, S. Y.; Yu, H. H.; Turak, A.; Kim, W. Y., High efficiency blue organic light emitting devices doped by BCzVBi in hole and electron transport layer. *MRS Online Proceedings Library* **2013,** *1567*, mrss13-1567-jj13-78.

129. Liu, N.; Shi, W. X.; Zhou, Y. M.; Cao, X. A., Impact of Dopant Aggregation on the EL of Blue Fluorescent Host-Dopant Emitters. *Ieee Electron Device Letters* **2019,** *40* (5), 750-753.

130. Zhang, H.; Fu, Q.; Zeng, W.; Ma, D., High-efficiency fluorescent organic light-emitting diodes with MoO 3 and PEDOT: PSS composition film as a hole injection layer. *Journal of Materials Chemistry C*
2014, *2* (45), 9620-9624.

131. Zhao, B.; Miao, Y. Q.; Wang, Z. Q.; Wang, K. X.; Wang, H.; Hao, Y. Y.; Xu, B. S.; Li, W. L., High efficiency and low roll-off green OLEDs with simple structure by utilizing thermally activated delayed fluorescence material as the universal host. *Nanophotonics* **2017,** *6* (5), 1133-1140.

132. Liu, W.; Zheng, C. J.; Wang, K.; Zhang, M.; Chen, D. Y.; Tao, S. L.; Li, F.; Dong, Y. P.; Lee, C. S.; Ou, X. M.; Zhang, X. H., High Performance All Fluorescence White Organic Light Emitting Devices with a Highly Simplified Structure Based on Thermally Activated Delayed Fluorescence Dopants and Host. *Acs Applied Materials & Interfaces* **2016,** *8* (48), 32984-32991.

133. Luo, D. X.; Chen, Q. Z.; Gao, Y.; Zhang, M. L.; Liu, B. Q., Extremely Simplified, High-Performance, and Doping-Free White Organic Light-Emitting Diodes Based on a Single Thermally Activated Delayed Fluorescent Emitter. *Acs Energy Letters* **2018,** *3* (7), 1531-1538.

134. Grybauskaite-Kaminskiene, G.; Ivaniuk, K.; Bagdziunas, G.; Turyk, P.; Stakhira, P.; Baryshnikov, G.; Volyniuk, D.; Cherpak, V.; Minaev, B.; Hotra, Z., Contribution of TADF and exciplex emission for efficient "warm-white" OLEDs. *J Mater Chem C* **2018,** *6* (6), 1543-1550.

135. Chen, L.; Chang, Y.; Shi, S.; Wang, S.; Wang, L., Solution-processed white OLEDs with power efficiency over 90 lm W(-1) by triplet exciton management with a high triplet energy level interfacial exciplex host and a high reverse intersystem crossing rate blue TADF emitter. *Mater Horiz* **2022,** *9* (4), 1299-1308.

Chapter 2

NPB:TAZ blue emitting exciplex as host for yellow and white organic light emitting diodes

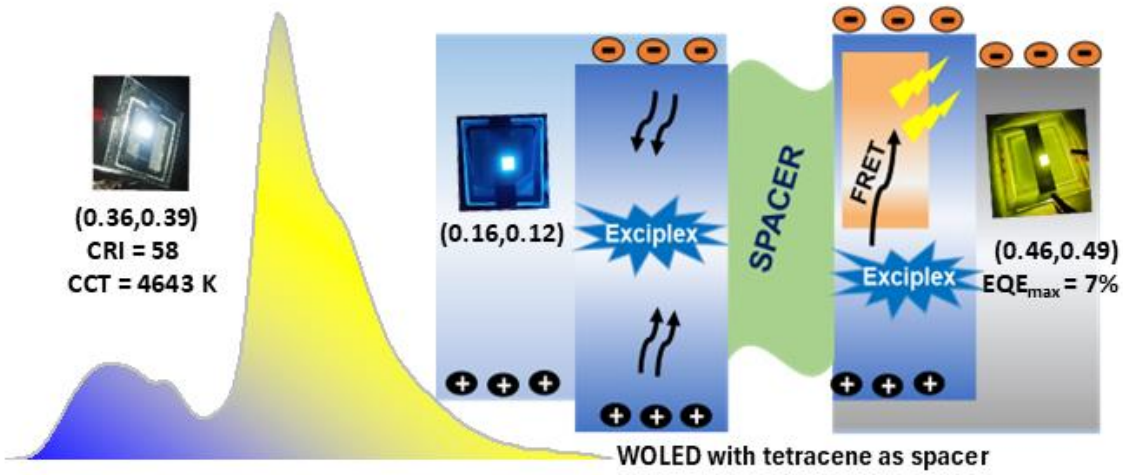

2.1 Abstract

The limited availability of wide bandgap materials for stable blue emitters is a significant challenge in organic light emitting diode (OLED) technology, limiting the quality of white emission. This issue can be addressed by employing exciplex emission in OLEDs by utilizing commercially available and relatively cheap transport materials. This work investigates the use of a standard blue emitting hole transport material (HTM) N,N' bis(naphthalen-1-yl)-N,N'-bis(phenyl)benzidine (NPB) with an electron transport material (ETM) 3-(biphenyl-4-yl)-5-(4-tert-butylphenyl)-4-phenyl-4H-1,2,4-triazole (TAZ) to obtain blue exciplex emission. Blue and yellow OLEDs with simplified device structures were designed by employing a blend layer of NPB:TAZ, serving both as a blue emitter as well as a host for the yellow phosphorescent

dopant iridium(III)bis(4-phenylthieno[3,2-c]pyridinato-N,C2')acetylacetonate (PO-01). Yellow OLED with 5% doping of PO-01 into the NPB:TAZ blend layer showed the best performance with maximum brightness of 13,070 cd/m^2 and a maximum external quantum efficiency (EQE) of 7%. Modified device architecture for white OLED (WOLED) utilizes a thin layer of tetracene as a spacer to connect the blue and yellow emitting units. This ambipolar spacer layer enhances carrier transport and controls exciton diffusion leading to balanced blue and yellow emissions. As a result, the overall white light emission properties are significantly improved, achieving Commission Internationale de l'Eclairage -1931 (CIE) coordinates of (0.36, 0.39) and a correlated color temperature (CCT) of 4643 K, giving cool white light.

2.2 Introduction

The development of stable and efficient blue emitters continues to be a critical bottleneck in the OLED industry. This challenge is primarily due to difficulties in designing wide band gap materials, thereby limiting the availability of suitable blue emitters[1-3]. The scarcity of stable blue fluorophores poses a significant challenge for achieving accurate RGB color balance in displays, underscoring the urgent need for the development of stable and efficient blue emitters and improvements in the yield of existing materials. While many blue emitting charge transport materials have not been explored due to their low quantum yield, there is a significant opportunity for breakthroughs via novel device designs that utilize these commonly available blue emitting transport molecules. In recent years, the concept of exciplex has emerged as a promising alternative emission mechanism in OLEDs[4, 5]. Exciplex emission, occurring at the interface of a HTM and an ETM, simplifies device architecture by eliminating the need for a

separate emissive layer (EML)[6, 7]. Although exciplex emission typically has a lower quantum yield, it can be effectively utilized as a host for phosphorescent, fluorescent, and thermally activated delayed fluorescence (TADF) dopants[8-10]. By identifying suitable exciplex combinations and employing innovative design strategies, it is possible to develop efficient WOLEDs without complex tandem structures[11].

NPB or NPD is extensively utilized in OLEDs[12-14] and in various other organic electronic devices including polymer photovoltaics (OPVs)[15, 16] and perovskite solar cells[17] due to its exceptional hole transport capabilities. NPB is the most widely used material in OLED applications. This prominence is attributed to its high glass transition temperature (T_g) of up to 95°C, which enhances film morphology and contributes to improved device longevity[18]. The material possesses a highest occupied molecular orbital (HOMO) energy level of 5.5 eV and a low unoccupied molecular orbital (LUMO) energy level of 2.4 eV[19, 20] and it exhibits blue fluorescence[12]. However, its poor quantum yield limits its use as a blue emitter in OLED applications. A deep blue exciplex by utilizing NPB and 1,3,5-Tris(1-phenyl-1H-benzimidazol-2-yl)benzene (TPBi) combination was reported by Jankus *et al.* in 2013[21]. Deep blue OLEDs exhibiting an EQE of 2.7% and an emission at 450 nm were fabricated. Major part of electroluminescence is harvested from triplet excitons via triplet fusion. From the comparison of electroluminescence (EL) and photoluminescence (PL) characteristics, they concluded that the charge recombination occurs in the blend layer via direct injection into the exciplex state, yielding blue emission. This result underscores the importance of using NPB with a suitable ETL in achieving efficient deep blue exciplex OLEDs. Later in 2020, Hippola *et al.* reported a bright deep blue TADF OLED, with emissive layer consisting of NPB/TPBi: triphenylphosphine oxide (PPh_3O), were PPh_3O is a novel molecule[22]. They could achieve a

brightness of 14,000 cd/m^2 with deep blue exciplex OLEDs with emission peak at approximately 435 nm and CIE coordinates of (0.1525, 0.0820). The intriguing properties of these OLEDs are linked to the presence of PPh_3O and the characteristics of the emitting layer composed of NPB and a host mixture of TPBi and PPh_3O in a 5:1 weight ratio. The intense electroluminescence is attributed to NPB/TPBi exciplexes involving triplet states through TADF, as indicated by significant quenching of PL by oxygen. The transient PL decay times for an NPB/TPBi 5:1/PPh_3O film are 43 ns in air and a weak delayed component of 2000 ns in N_2. They concluded that the slow emitting states are associated with PPh_3O aggregates interacting with NPB. Despite the limited number of studies on NPB-based exciplexes, the successful demonstration of NPB and TPBi combination necessitates more focused investigation on the same.

In this work, NPB is combined with suitable ETLs to develop efficient exciplex systems. This approach aims to exploit the excellent hole transport properties of NPB while overcoming its limitation as an emitter through the exciplex emission.

2.3 Experimental section

The devices were fabricated on pre-patterned indium tin oxide (ITO) (purchased from Kintec, Hong Kong, ITO thickness 150 nm, sheet resistance < 15 ohm/sq) coated glass substrates. These patterned ITO substrates were initially cleaned by ultra-sonication in chloroform for 15 minutes and then washed in dilute detergent solution followed by ultra-sonication in isopropanol and deionized water for 10 minutes each and dried using a hot air gun. UV- ozone cleaning for 15 minutes was done just before the fabrication of the devices. Then cleaned substrates were transferred to the evaporation chamber through the glovebox. 1,4,5,8,9,11-Hexaazatriphenylenehexacarbonitrile (HAT-CN), NPB, TAZ, Tris(8-hydroxyquinoline)

aluminium (Alq_3), Lithium Fluoride (LiF) and Al were thermally evaporated. HAT-CN was evaporated at a rate of 1 Å/s, while NPB, TAZ, and Alq_3 were each evaporated at a rate of 2 Å/s. In the co-deposited film, NPB and TAZ were simultaneously evaporated at a rate of 1 Å/s each. LiF and Al were evaporated at 0.1 Å/s and 2 Å/s, respectively. The physical vapour deposition was done in a glovebox integrated thermal evaporation system (Angstrom Engineering, Canada) at 10^{-7} torr. The thickness of the layers was measured using Dektak XT surface profilometer. After the evaporation, the devices were encapsulated inside the nitrogen filled glovebox by using a UV-curable epoxy (Epoxy Technology inc.). HAT-CN, NPB, TPBi and Alq_3 were purchased from Luminescence Technology Corp. (Lumtec), Taiwan and TAZ from Sigma-Aldrich. The absorption studies of the thin films of the materials were done using HORIBA Jobin Yvon and PerkinElmer UV/VIS/NIR Spectrometer. Emission spectra were recorded using a Fluorolog-3 spectrofluorometer (HORIBA), equipped with a 450 W xenon arc lamp. The OLED characterization system consists of a SpectraScan PR (Photo Research)-655 spectroradiometer and a Keithley 2400 source meter integrated with a PC.

2.4 Results and discussion

2.4.1 Pairing of NPB with suitable electron transport layers

The primary objective is to utilize the hole transporting ability of NPB while mitigating its low quantum yield as an emitter by utilizing exciplex emission. To achieve this, NPB is paired with suitable ETLs to form efficient exciplex systems. The commonly used ETLs in OLEDs include Alq_3[23], TPBi[24], 4,7-Diphenyl-1,10-phenanthroline (BPhen)[25], TAZ[26], 1,3-Bis[2-(4-tert-butylphenyl)-1,3,4-oxadiazo-5-yl]benzene (OXD-7)[27], etc. To identify a suitable ETL to pair with NPB, the energy levels and HOMO-LUMO gaps at the NPB/ETL interfaces were compared as shown in Figure 2.1 (a) and (b), respectively. Based on this comparison, the

NPB/TPBi and NPB/TAZ combinations are predicted to exhibit deep blue exciplex emissions. While NPB/TPBi has been previously studied, NPB/TAZ deep blue exciplex pair is selected for further study due to its unexplored nature.

(a)

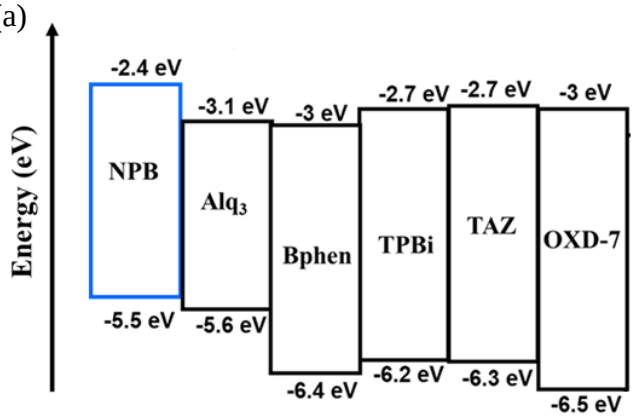

(b)

NPB/ETL	HOMO-LUMO gap at the interface (eV)
NPB/Alq_3	2.4
NPB/BPhen	2.5
NPB/TPBi	2.8
NPB/TAZ	2.8
NPB/OXD-7	2.5

Figure 2.1. (a) Energy levels of NPB and ETLs (HOMO-LUMO values obtained from https://www.ossila.com/) (b) HOMO-LUMO gaps at the NPB/ETL interfaces.

2.4.2 NPB:TAZ blue exciplex emission

The exciplex emission in the NPB:TAZ interface was investigated via spectroscopic studies. The electrons in the LUMO of TAZ and the holes in the HOMO of NPB form an excited state complex, where NPB functions as the donor and TAZ as the acceptor. The excited state species at the NPB/TAZ interface is expected to produce an emission at approximately 443 nm, based on the HOMO-LUMO gap. The molecular structures of NPB and TAZ are shown in Figure 2.2 (a). The exciplex emission at the NPB/TAZ interface is depicted in Figure 2.2 (b) in terms of energy levels, with the HTM and ETM represented by their HOMO-LUMO energy levels. The offset values at the interfaces are 0.3 eV at HOMO-HOMO and 0.8 eV at LUMO-LUMO. TAZ serves as both an efficient electron transport and a hole blocking layer[28]. Its high triplet energy level ensures the confinement of triplet excitons within the emissive layer, enhancing

device performance[29]. The low HOMO/LUMO energy levels (6.3 eV/2.7 eV) facilitate hole blocking and electron injection/transport[30, 31]. TAZ belongs to the class of triazole derivatives and is widely used in OLEDs and other organic electronic devices[32, 33].

The thin films of NPB, TAZ, and NPB:TAZ (1:1) were fabricated via vacuum deposition. The comparison of absorption and emission spectra of the thin films of the materials were done. As an excited-state complex, an exciplex lacks a ground-state counterpart. Consequently, it does not exhibit a distinct absorption spectrum, instead displays the individual absorption features of its component molecules. The absorption spectrum of the NPB:TAZ (1:1) mixed film reveals distinct absorptions for NPB and TAZ at 343 nm and 290 nm, respectively. The NPB:TAZ mixed film does not show a separate absorption peak, instead reflecting the individual absorption spectrum of NPB and TAZ. In the emission spectra, an exciplex should show a distinct emission that is significantly red shifted compared to its individual components. The emissions of NPB, TAZ and the NPB:TAZ mixture occur at 433 nm, 370 nm and 448 nm, respectively as shown in Figure 2.2 (c). The mixed film shows a distinct emission that is red shifted from the individual emissions of NPB and TAZ. This along with the absence of a distinct absorption spectrum for the blend film confirms exciplex emission.

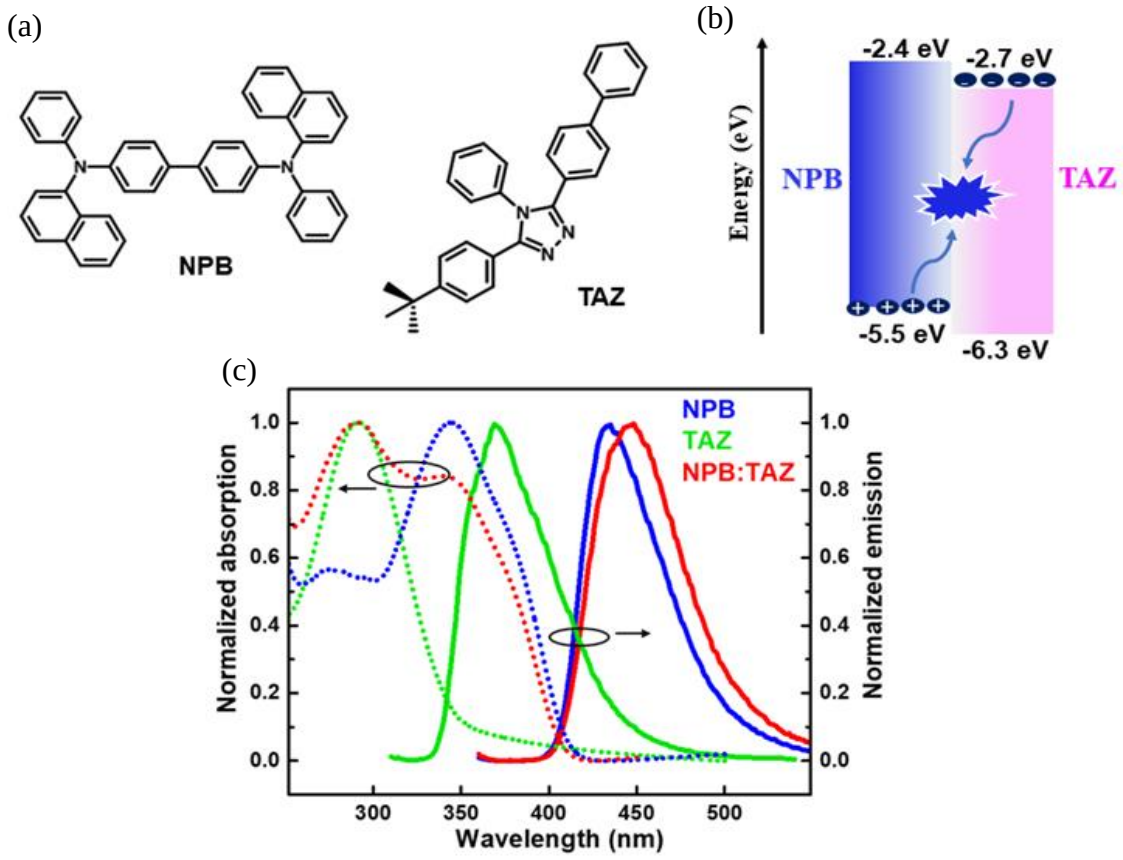

Figure 2.2. (a) Molecular structures of NPB and TAZ (b) exciplex formation at the molecular interface of NPB and TAZ in terms of energy levels (c) comparison of absorption and emission spectra of the thin films of the materials (NPB, TAZ, NPB:TAZ).

With the initial confirmation of exciplex emission, preliminary device fabrication was done. Hence, a bilayer NPB/TAZ device (B_1) was fabricated with a device architecture of ITO/HAT-CN (5 nm)/NPB (60 nm)/TAZ (40 nm)/Alq_3 (20 nm) /LiF (1 nm)/Al (100 nm) as shown in Figure 2.3 (a). A thin layer of HAT-CN (5 nm) was deposited prior to NPB to improve the hole injection, which acts as HIL. In order to balance the electron injection into TAZ, Alq_3 is incorporated in the structure, as an ETL. The J-V-L plot and the comparison of EL and PL spectra are given in Figure 2.3 (b) and (c), respectively. The device exhibited a maximum luminance of 1419 cd/m^2 with a current density of 436 mA/cm^2 at 11 V. Based on the

comparison between PL and EL spectra, the emission of TAZ can be ruled out. The EL spectrum of the device closely matches the PL spectra of both NPB and the NPB:TAZ blend, suggesting that energy transfer from TAZ to NPB is also possible.

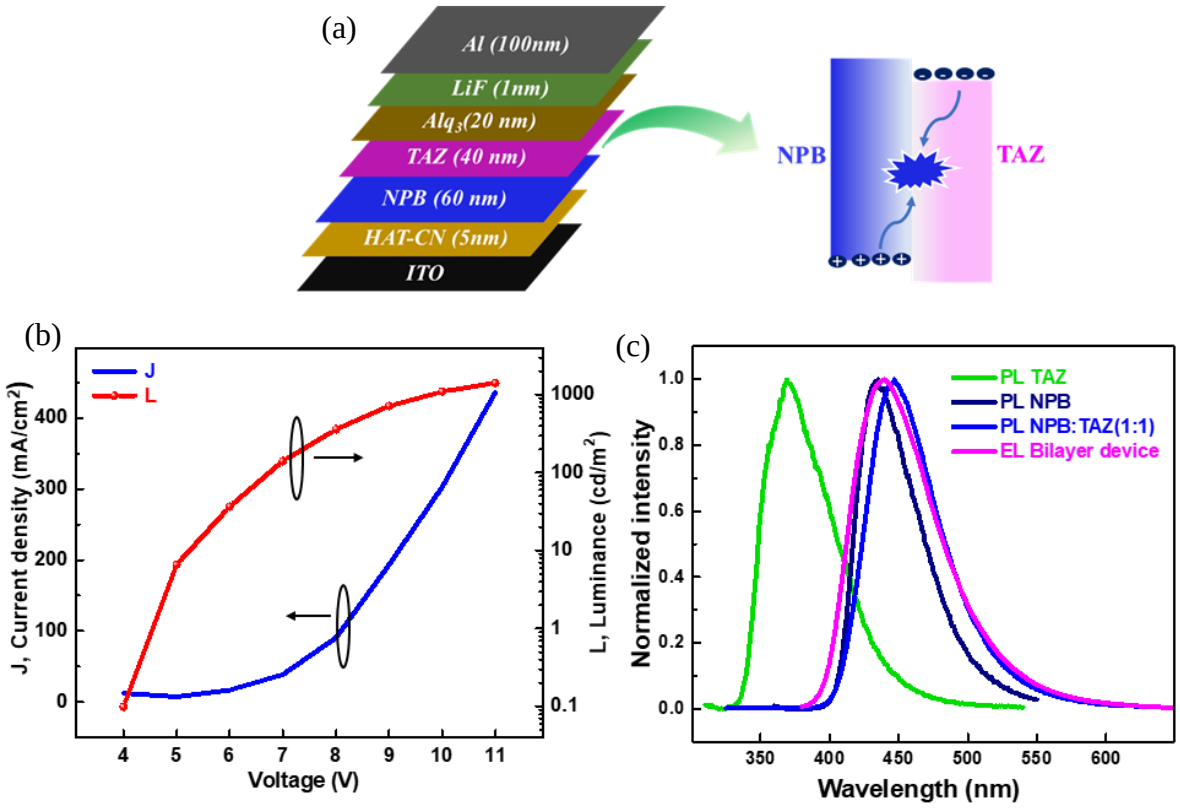

Figure 2.3. (a) Device architecture of NPB/TAZ device (b) J-V-L plot and (c) comparison of EL spectrum of the device and PL spectra of the thin films of the materials (NPB, TAZ, NPB:TAZ (1:1)).

To further investigate the lack of evidence for exciplex emission from the device characteristics, we conducted additional spectroscopic studies. Figure 2.4 (a) illustrates the spectral overlap between the absorption spectrum of NPB and the emission spectrum of TAZ, indicating possibility of energy transfer from TAZ to NPB. The PL spectra and transient decay

kinetics of NPB:TAZ thin films with 1:1 and 1:3 ratios were compared, as shown in Figure 2.4 (b) and 2.4 (c), respectively.

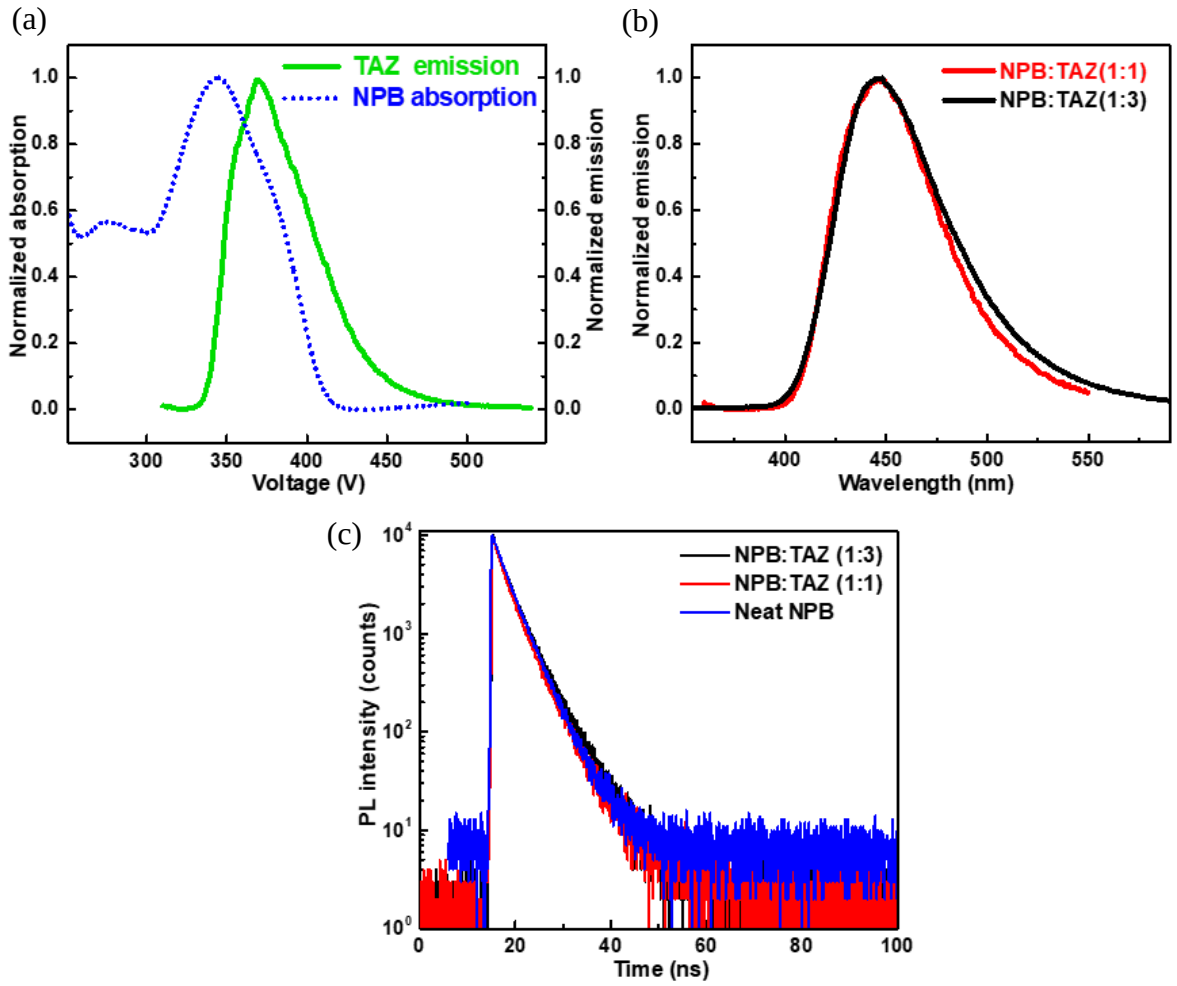

Figure 2.4. (a) Spectral overlap between emission of TAZ and absorption of NPB (b) comparison of PL spectra of NPB:TAZ (1:1, 1:3) films (c) transient decay kinetics of NPB, NPB:TAZ (1:1, 1:3) films.

The PL spectra of both films did not show any noticeable shift, although a slight improvement in the photoluminescence quantum yield (PLQY) was observed for the 1:3 ratio film, where the concentration of TAZ was increased to three times that of NPB. The transient decay kinetics revealed no delayed component in the mixed films compared to the NPB film alone. The

fluorescence decay parameters, PLQY and FWHM of the thin films are summarized in Table 2.1. These observations support the energy transfer hypothesis than exciplex emission. The spectroscopic studies of NPB:TAZ mixed film indicate that both exciplex emission and energy transfer coexist, leading to blue emission.

Thin films	**τ_1 (ns)**	**τ_2 (ns)**	**τ_{avg} (ns)**	**PLQY (%)**	**FWHM (nm)**
NPB	2.2	4.1	3.5	31	52
NPB:TAZ (1:3)	1.96	4.5	3.8	44	63
NPB:TAZ (1:1)	1.81	4.4	3.5	38	60

Table 2.1. Summary of fluorescence decay parameters (τ: fluorescence lifetime decay component), PLQY and FWHM of the thin films.

To get better insights into energy transfer from the device performance, we further fabricated devices (B_2 & B_3) with NPB:TAZ as the EML sandwiched by the pristine NPB and TAZ layers. The device architecture is shown in Figure 2.5 (a). The NPB and TAZ layers on both sides provide better charge transport and carrier confinement. Specifically, EML consists of the co-deposited layer of NPB:TAZ at 1:1 and 1:3 ratios for devices B_2 and B_3, respectively with total thickness of 15 nm. The doping ratio of NPB in TAZ in device B_3 was reduced by three times compared to B_2. It may be noted that the blend device is nothing but a device where a 15 nm blend layer is added in between the pristine NPB and TAZ layers of the bilayer device. At higher voltages, charge injection into the blend increases but charges may become trapped within the blend layer. In a bilayer structure, this trapping does not occur as charges tend to recombine either radiatively or non-radiatively at the interface. However, the trapping of carriers in the blend may promote exciplex formation. To investigate this, we analyzed the J-V-L plots of these devices as shown in Figure 2.5 (b) and observed that the bilayer device

exhibits a much higher current density compared to the blend devices. This may be due to the charge trapping as mentioned above. We observe that radiative recombination in the thin blend layer is more efficient than in the bilayer device. Consequently, the device performance indicates that the blend device outperforms the bilayer one. Among the blend devices, the 1:1 ratio device demonstrated better performance compared to the 1:3 ratio device, because the 1:1 ratio offers more molecular interfaces for exciplex formation[34]. Therefore, we can conclude that the device performance confirms NPB:TAZ exciplex emission. A maximum luminance of 1703 cd/m^2 was obtained with a current density of 245 mA/cm^2 for the 1:1 device. There was no shift in the EL spectra of the devices at 440 nm as shown in Figure 2.5 (c).

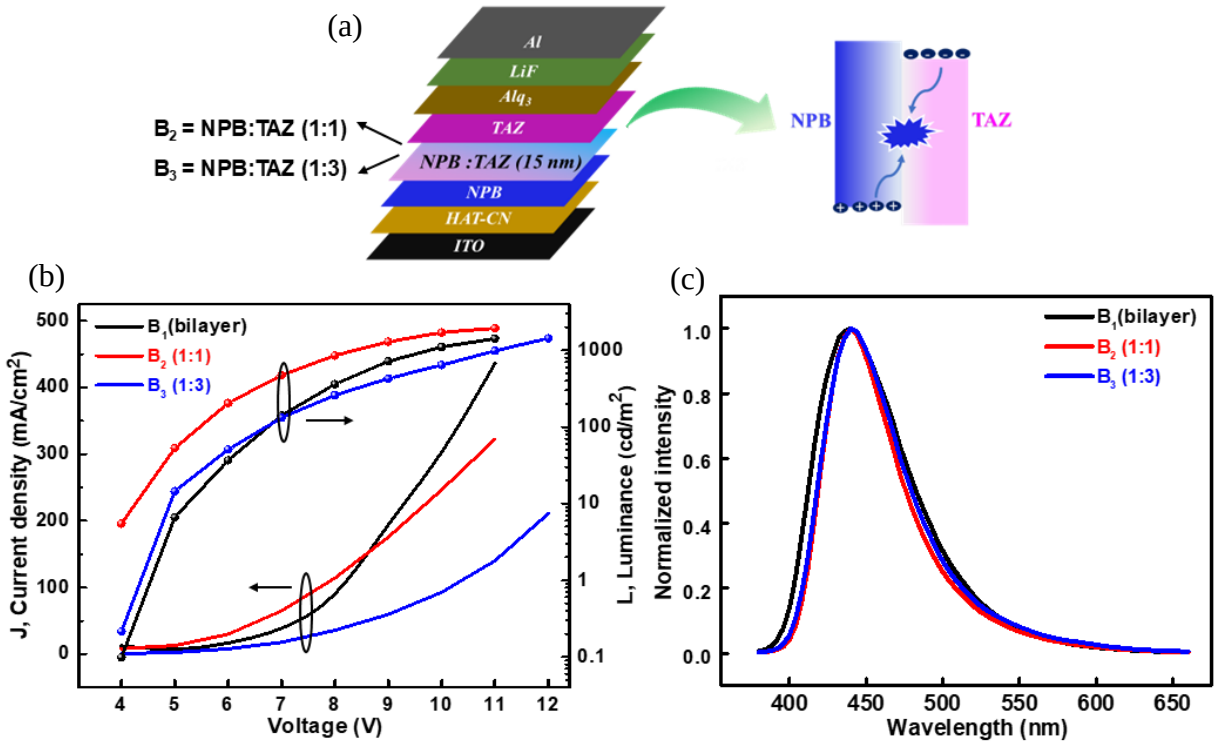

Figure 2.5. (a) Device architecture of NPB:TAZ blend devices (b) J-V-L plots and (c) EL spectra of the NPB:TAZ devices (bilayer, 1:1, 1:3).

All three devices exhibited a deep blue emission at 440 nm. The CIE coordinates of (0.16, 0.10) with a very high color purity of 91% was obtained for the 1:1 device as shown in the CIE diagram in Figure 2.6 (a). There was no variation in the CIE coordinates as shown in Figure 2.6 (b), which shows the high color stability of the device.

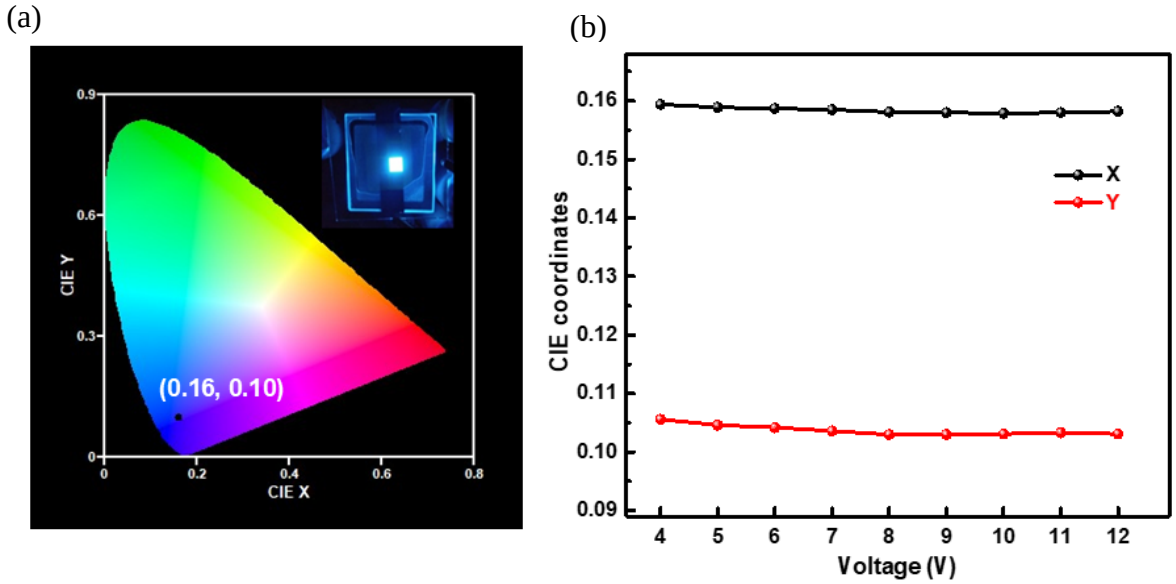

Figure 2.6. (a) CIE diagram with the inset showing the photograph of the NPB:TAZ (1:1) device (b) voltage *vs.* CIE coordinates plot of the device.

2.4.3 NPB:TAZ blue emitting exciplex as host

2.4.3.1 Yellow phosphorescent organic light emitting diodes

The core idea of this work was to develop novel device design strategies to improve the quality of white emission in OLEDs using cost-effective solutions. Exciplex host system (exciplex) can effectively transfer its energy to the dopants via Förster or Dexter energy transfer mechanisms. Therefore, a dopant was selected based on the spectral overlap of the emission of NPB:TAZ mixed film and the absorption of the dopant. Initially, a yellow phosphorescent emitter, PO-01 was selected as the dopant with NPB:TAZ exciplex host for fabricating yellow OLEDs. PO-01 is an Iridium-based yellow phosphorescent emitter used in OLEDs due to its

high quantum yield and color purity[35-37]. Figure 2.7 (a) shows the spectral overlap between the absorption of PO-01 and emission of NPB:TAZ films and Figure 2.7 (b) shows the molecular structure of PO-01 and depicts the energy transfer from exciplex to PO-01. Figure 2.7 (c) shows the yellow OLED device architecture, consisting of a doped exciplex layer in which PO-01 is doped in to NPB:TAZ (1:1). The EML configuration comprising of blue and yellow emitting units, in terms of energy levels is shown in Figure 2.7 (d).

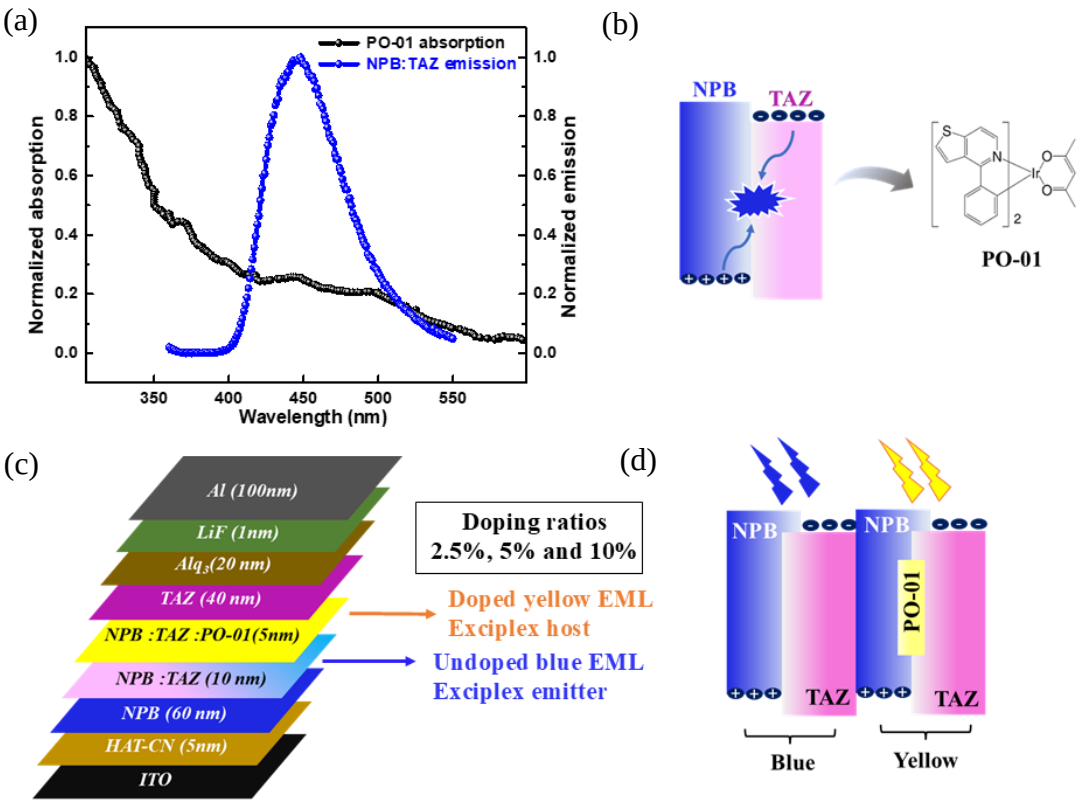

Figure 2.7. (a) Spectral overlap between the absorption of PO-01 and exciplex emission (b) illustration of energy transfer from exciplex to PO-01 (c) device architecture of PO-01 doped exciplex OLEDs (d) EML configuration of blue and yellow emitting units interms of energy levels.

The EML consists of a layer of undoped exciplex, NPB:TAZ (1:1, 10 nm) followed by the doped exciplex layer of NPB:TAZ:PO-01 (1:1, x%, 5 nm), where x = 2.5%, 5% and 10% are doping ratios of PO-01 doped into the exciplex matrix. The yellow devices are termed as $Y_{2.5\%}$, $Y_{5\%}$ and $Y_{10\%}$, with doping ratios of 2.5%, 5% and 10%, respectively. The device $Y_{5\%}$ showed the best performance with maximum brightness of 13,070 cd/m^2 and maximum EQE of 7%. The J-V-L plots, EQE and current efficiency *vs.* current density plots of the devices are shown in Figure 2.8 (a), (b) and (c), respectively. Figure 2.8 (d) compares the EL spectra of the devices, dominated by a yellow emission at around 560 nm. The yellow emission is due to the energy transfer from the exciplex to PO-01. Additionally, a blue exciplex emission around 444 nm was observed alongside the yellow emission. White emission can be achieved by properly balancing the blue and yellow emissions. When the dopant concentration was decreased to 2.5%, the relative contribution of the blue exciplex emission slightly enhanced to give a white emission with CIE coordinates (0.43, 0.46). The blue-to-yellow emission intensity ratio is the ratio of the intensities of blue and yellow emissions in the EL spectrum of the selected device. The blue-to-yellow emission intensity ratio for the $Y_{2.5\%}$ device increased to 15%, compared to 4% and 3% in the other yellow devices $Y_{5\%}$ and $Y_{10\%.}$ The summary of device performance of yellow OLEDs is shown in Table 2.2. The CIE diagram indicating the CIE coordinates of the three devices and the photographs of the $Y_{5\%}$ and $Y_{2.5\%}$ devices are shown in Figure 2.8 (e). Color temperature ranges may vary slightly depending on the specific country or region. We follow the European standards for color temperature, according to which a CCT of 2700K - 3000K is considered as warm white and 3000K - 4000K is categorized as neutral white. The cool white emission is in the range of 4000K - 6500K. Here, a neutral white light with a CCT of 3443 K and CRI of 41 was obtained for the $Y_{2.5\%}$ device.

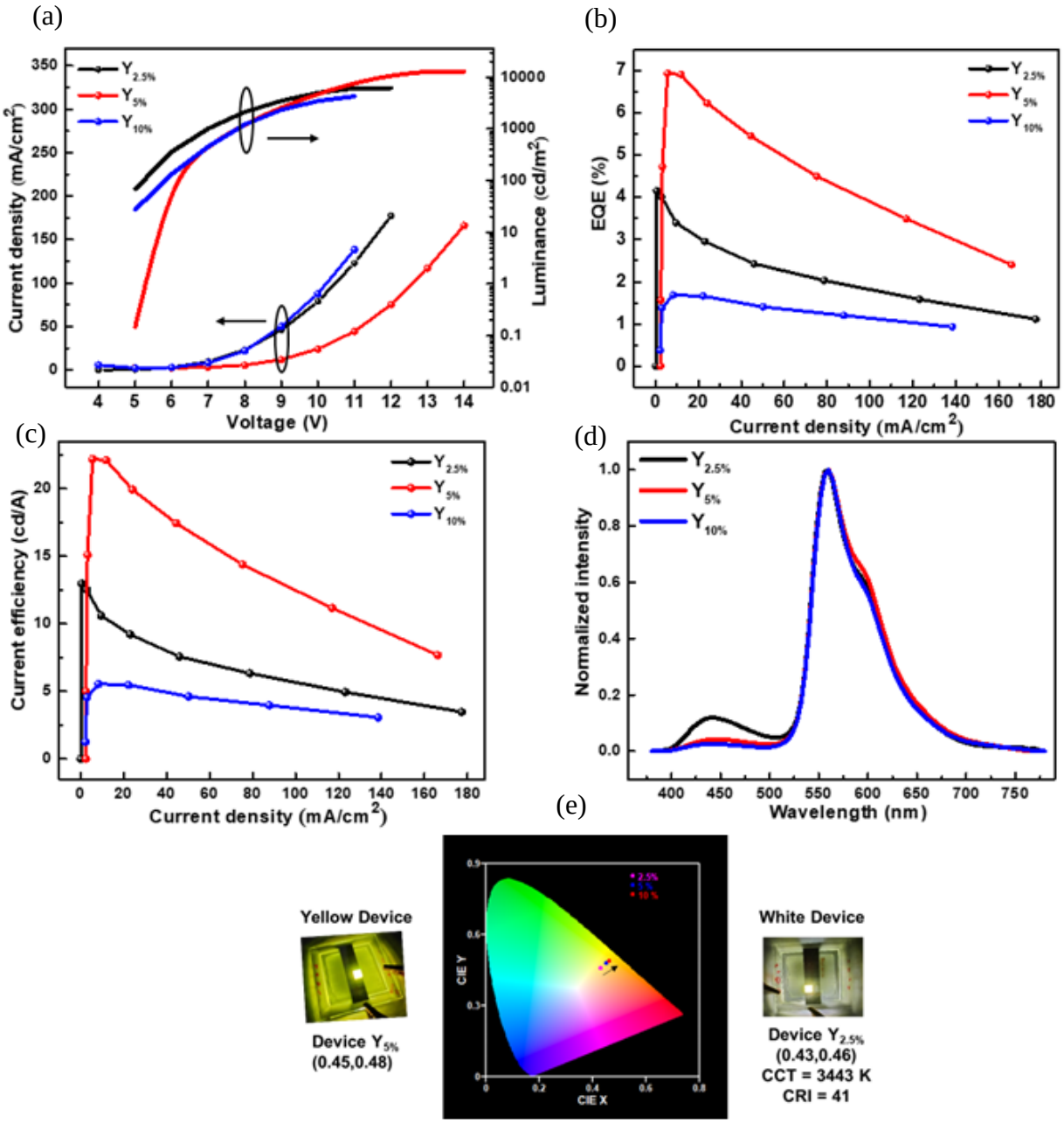

Figure 2.8. (a) J-V-L plot (b) EQE *vs.* current density plot (c) current efficiency *vs.* current density plot (d) EL spectra and (e) CIE diagram with photographs of the yellow and white devices.

Device	Luminance (cd/m^2)	Current density (mA/cm^2)	Current efficiency (cd/A)	EQE (%)	Max Luminance, max CE, max EQE
$Y_{2.5\%}$	5880 ± 104	132 ± 4.7	4.5 ± 1.70	1.40 ± 0.05	6164 cd/m^2, 13 cd/A, 4.0 %
$Y_{5\%}$	7620 ± 92	45 ± 0.44	17.0 ± 0.37	5.30 ± 0.12	13,070 cd/m^2, 22 cd/A, 7.0 %
$Y_{10\%}$	3910 ± 233	133 ± 3.9	2.94 ± 0.09	0.97 ± 0.04	4244 cd/m^2, 5.5 cd/A, 1.7 %

Table 2.2. Summary of device performance of the yellow devices at 10V and the maximum luminance, CE and EQE values.

To enhance the blue emission in the device, we increased the thickness of the NPB:TAZ blue emitting layer from 10 nm to 25 nm. As a result, the total thickness of the EML was doubled, increasing from 15 nm to 30 nm. Hence, a modified $Y_{2.5\%}$ device with 25 nm exciplex undoped layer with the EML configuration of NPB:TAZ (1:1, 25 nm)/NPB:TAZ:PO-01(1:1, 2.5%, 5 nm) was fabricated. Increasing the thickness of the blue emitting layer did not lead to an enhancement in blue emission, resulting in no significant improvement in the quality of white light compared to the $Y_{2.5\%}$ device, with a 10 nm blue layer. While the increased thickness improved the efficiency of the device, it negatively impacted the quality of the white light emission. The comparison of EL spectra of the devices and current efficiency *vs.* current density plot are given in Figure 2.9 (a) and (b), respectively.

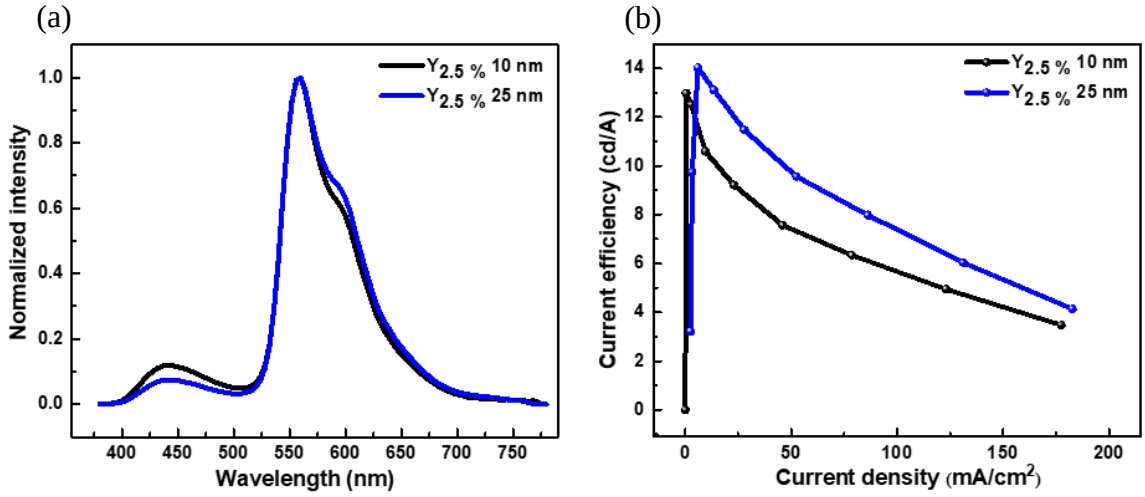

Figure 2.9. Comparison of the (a) EL spectra and (b) current efficiency *vs.* current density plots of the devices with 10 nm and 25 nm of the blue emitting unit.

As mentioned earlier, increasing the thickness of the NPB:TAZ layer to 25 nm to further enhance the blue contribution did not yield the expected results. The weak intensity of blue emission is primarily due to the difference in hole and electron mobilities of the component molecules. Due to the high hole mobility of NPB, more holes get accumulated at the HOMO of NPB in the NPB:TAZ layer. The comparatively lower electron mobility of TAZ and the longer path for electrons from cathode to reach this layer can delay electrons migration to the LUMO of TAZ in the NPB:TAZ layer. This loss of carriers can lead to decreased blue exciton formation and subsequent emission in the NPB:TAZ layer. The device architecture comprises of two emissive units with co-deposited film of NPB and TAZ. The unbalanced flow of carriers to the NPB:TAZ layer might be a reason for reduction in blue emission among the white devices.

To study the problem of carrier imbalance in the device, we fabricated the hole only and electron only devices. The device architecture was as follows: ITO/HAT-CN(5nm)/NPB(60 nm)/NPB:TAZ(50 nm)/Ag(100 nm) for the hole only device and Al(100 nm)/LiF(1 nm)/BCP(5 nm)/NPB:TAZ(50 nm)/TAZ(40 nm)/Alq_3(20 nm)/LiF(1 nm)/ Al(100 nm) for the electron only device. The comparison of the J-V characteristics of the devices are shown in Figure 2.10. The hole only devices showed much higher current density compared to electron only devices; this observation is evidence for the charge imbalance in the NPB:TAZ mixed layer.

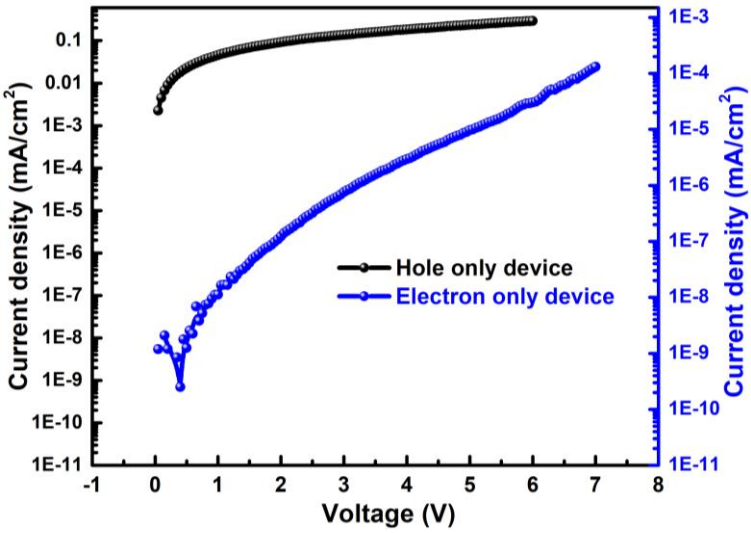

Figure 2.10. Current density *vs.* voltage plots for hole and electron only devices.

2.4.3.2 White organic light emitting diodes

2.4.3.2.1 Incorporation of charge generation layer (CGL)

To further improve the quality of white emission, it is critical to balance the blue and yellow emission. This can be done by adjusting the flow of holes and electrons toward the respective layers by incorporating a CGL between the two emitting units. A suitable CGL would provide

adequate flow of electrons and holes toward the respective units. We have therefore selected a typical fullerene (C_{60})/pentacene organic heterojunction as the CGL[38] between the blue and yellow emitting units as shown in Figure 2.11 (a). The high electron mobility of C_{60}[39] and high hole mobility of pentacene[40] can make this p-n junction an efficient CGL[41]. The balanced flow of electrons from C_{60} toward the NPB:TAZ layer is expected to enhance the blue emission. Also, the availability of holes in the NPB:TAZ:PO-01 layer is ensured by pentacene. The EML of devices with CGL has the structure, NPB:TAZ (1:1, 10 nm)/ C_{60} (15 or 10 nm)/pentacene (10 or 5 nm)/NPB:TAZ:PO-01 (5 nm, 2.5% PO-01). The device architecture is shown in Figure 2.11 (b). Two CGL devices are fabricated with two different thicknesses of C_{60} and pentacene. The thickness of C_{60} was kept slightly higher than that of pentacene to compensate the high hole mobility of pentacene compared to the electron mobility of C_{60}. However, the device performance was drastically diminished upon the incorporation of the CGL. The J-V-L plots and EL spectra of the devices are compared in Figure 2.11 (c) and (d), respectively. Hence, unlike in a normal tandem WOLED, the CGL here functioned more like a barrier. However, the percentage of blue emission in the CGL devices has slightly improved compared to that in the devices without a CGL.

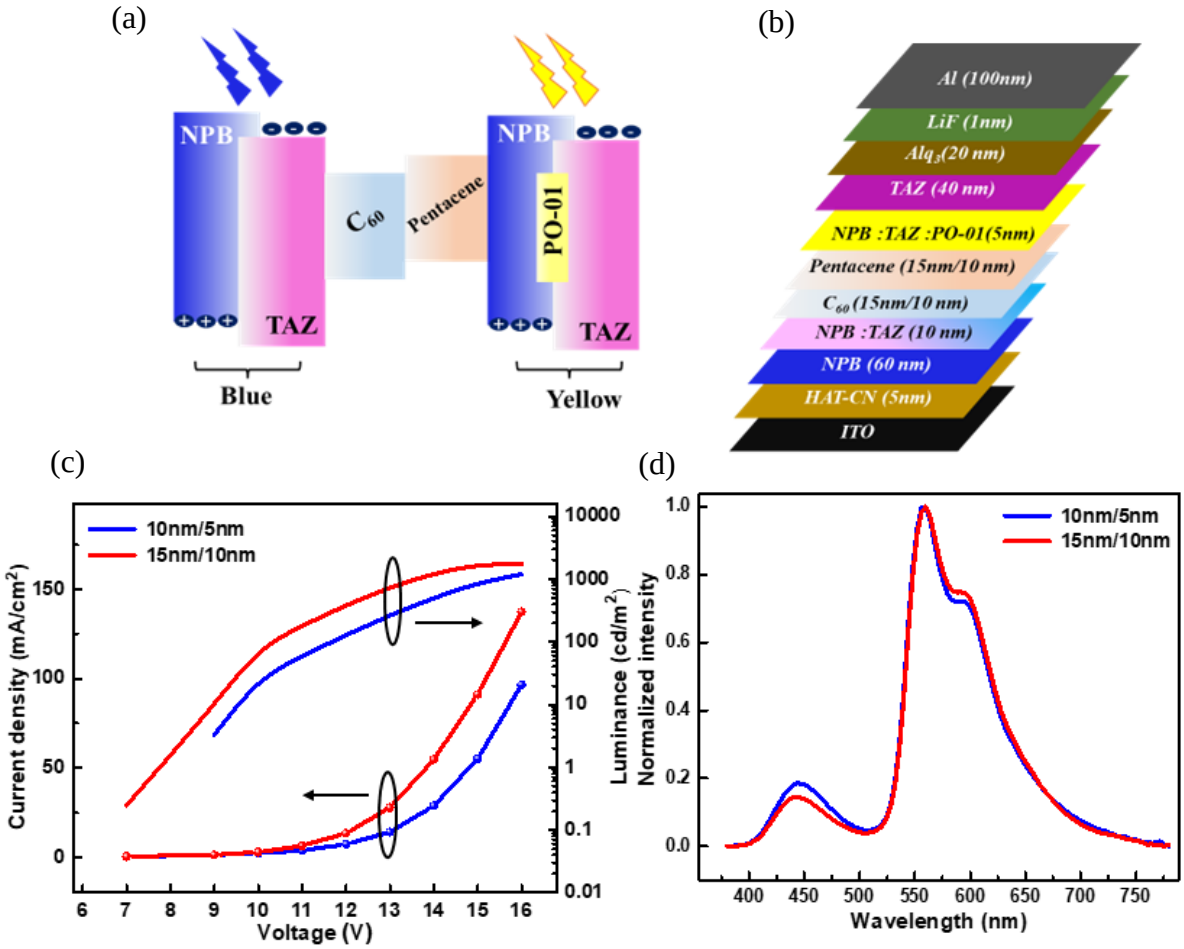

Figure 2.11. (a) EML configuration (in terms of energy levels) of the devices with CGL (b) device architecture (c) J-V-L plots and (d) EL spectra of the CGL devices.

2.4.3.2.2 Incorporation of ambipolar spacer layer

The overall performance of the devices with CGL implies the need of a separation layer other than CGL for balanced flow of carriers between the NPB:TAZ:PO-01 and NPB:TAZ units of the EML, which can be called as a spacer layer. In this context, it was further proposed that an ambipolar material would be a better choice as a spacer layer than a p-n junction. The energy levels of the spacer material should be conducive not to completely block the electrons and holes. Tetracene was selected as the spacer layer as it met the above requirements. The device architecture was modified by adding a thin layer of tetracene as a spacer layer between the

NPB:TAZ (blue emitter) and NPB:TAZ:PO-01 (yellow emitter) layers. The energy level diagram of the emissive units for the modified device architecture for WOLED is shown in Figure 2.12 (a). The device $Y_{2.5\%}$ without the spacer layer is considered as the reference device for white emission, and this device is now designated as W_1. Two spacer white devices are designed with 5nm and 10 nm of tetracene, designated as W_1 and W_2, respectively. The EML configuration of the spacer devices is NPB:TAZ (1:1, 10 nm)/tetracene (5 nm or 10 nm)/NPB:TAZ:PO-01 (5 nm, 2.5% PO-01). Tetracene devices showed a better performance compared to the devices with CGL. Increasing the thickness of tetracene layer to 10 nm did not improve the performance. The poor performance of the 10 nm spacer layer compared to that of the 5 nm shows the impact of resistance in the devices. The J-V-L plots, current efficiency and EQE *vs.* current density plots are shown in Figure 2.12 (b), (c) and (d), respectively. The devices with tetracene spacer layer indeed resulted in a higher intensity of blue emission compared to the CGL devices. The weak peak at about 484 nm could be the monomer emission of tetracene[42]. White emission with CIE coordinates of (0.36, 0.39) close to the true white point (0.33,0.33) was achieved, when 5 nm of tetracene was employed. The EL spectra and CIE diagram with a photograph of the device (W_2) are shown in Figure 2.12 (e) and (f), respectively. Cool white emission with a CRI of 58 and CCT of 4043 K was obtained.

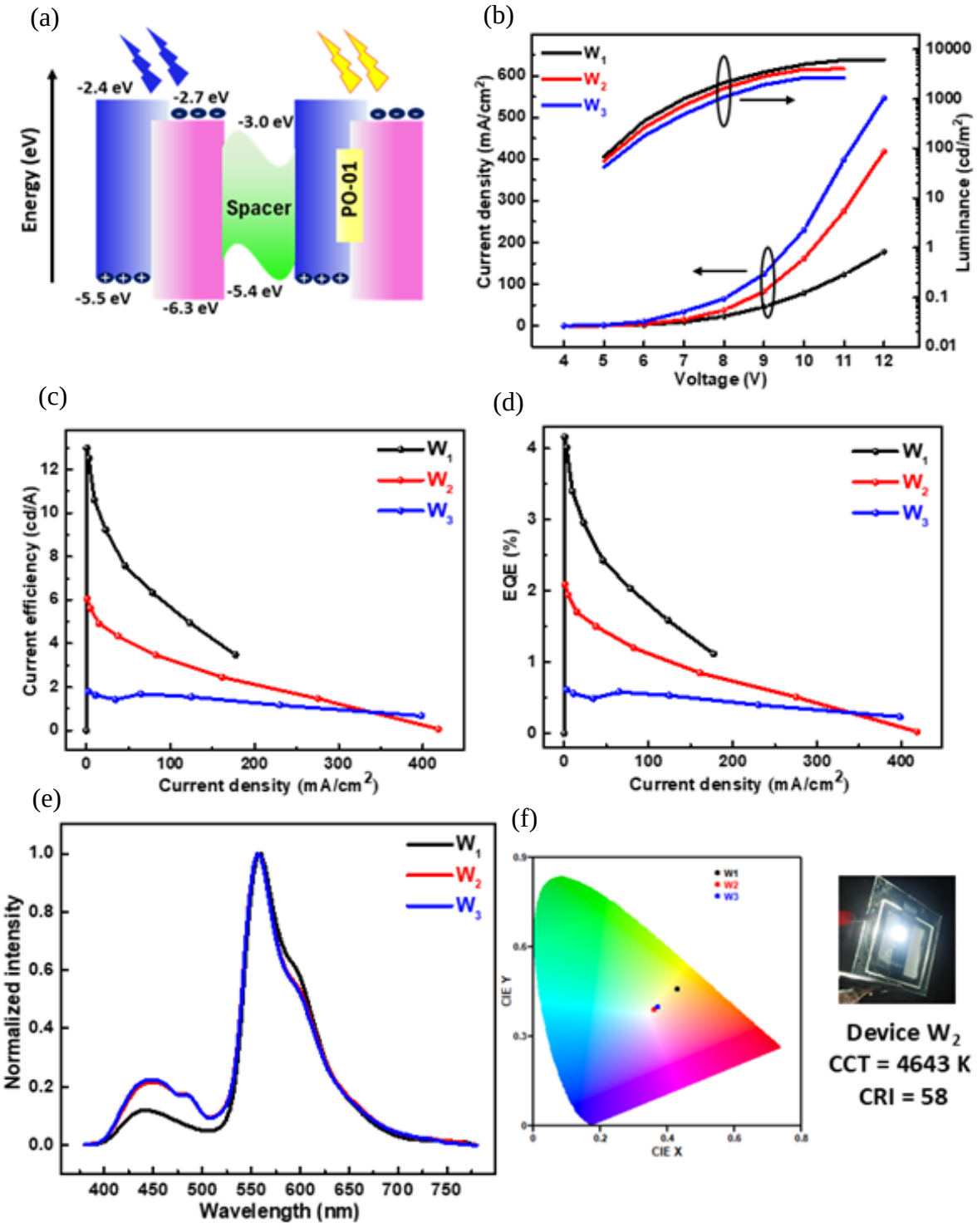

Figure 2.12. (a) EML configuration (interms of energy levels) of the devices with spacer layer (b) J-V-L plots (c) current efficiency *vs.* current density (d) EQE *vs.* current density plot and (e) EL spectra of the devices (f) CIE diagram with a photograph of the white device (W_2).

The ratios of intensities of blue and yellow emissions were compared. The ratio of blue to yellow emission intensities was increased from 12% to 23%, when the spacer layer was employed. This could be attributed to the balanced flow of carriers to NPB:TAZ layer due to the ambipolar nature of tetracene layer. The increase in current density after the addition of tetracene layer is evidence for the role of the same in the charge transport mechanism in the device. Unlike in CGL, a single layer can provide improved white light as well as device performance. The summary of performance of the WOLEDs with spacer layer is shown in Table 2.3. Hence, device architecture with a spacer layer can be considered as an alternative to complicated tandem structures. A balanced white OLED combining yellow emission from dopant and blue emission from exciplex was achieved with an ambipolar thin spacer layer.

Device	**Luminance (cd/m^2)**	**Current density (mA/cm^2)**	**Current efficiency (cd/A)**	**EQE (%)**	**Max Luminance, max CE, max EQE**
W_1	5880 ± 104	132 ± 4.7	4.5 ± 1.7	1.4 ± 0.05	6164 cd/m^2, 13 cd/A, 4 %
W_2	3180 ± 355	265 ± 8	1.27 ± 0.13	0.51 ± 0.08	4040 cd/m^2, 6.0 cd/A, 2 %
W_3	2980 ± 154	369 ± 14.6	0.47 ± 0.1	0.27 ± 0.03	2680 cd/m^2, 2 cd/A, 0.6 %

Table 2.3. Summary of device performance of the white devices at 10V and the maximum luminance, CE and EQE values.

2.4 Conclusion

A novel blue emitting exciplex system based on widely used charge transport materials, NPB and TAZ has been demonstrated which can be used both as a blue emitter and a host for a yellow dopant. By incorporating a phosphorescent dopant (PO-01) into the NPB:TAZ matrix, yellow OLED with maximum brightness of 13,070 cd/m^2 and maximum EQE of 7% was

obtained, with a doping concentration of 5% PO-01. White emission with CIE coordinates of (0.36, 0.39) and a correlated color temperature of 4643 K was realized through a novel device design, utilizing tetracene as a spacer for balanced carrier transport. This spacer separates a blue emitting unit where exciplex is the emitter and a yellow emitting unit where exciplex is the host. This approach offers a promising alternative to complex tandem structures for achieving stable white OLEDs, presenting a versatile platform for further development of exciplex-based systems, and enabling the application of custom-designed molecules for enhanced device performance.

2.5 References

1. Siddiqui, I.; Kumar, S.; Tsai, Y. F.; Gautam, P.; Shahnawaz; Kesavan, K.; Lin, J. T.; Khai, L.; Chou, K. H.; Choudhury, A.; Grigalevicius, S.; Jou, J. H., Status and Challenges of Blue OLEDs: A Review. *Nanomaterials (Basel)* **2023,** *13* (18), 2521.

2. Tankelevičiūtė, E.; Samuel, I. D.; Zysman-Colman, E., The Blue Problem: OLED Stability and Degradation Mechanisms. *Journal of Physical Chemistry Letters* **2024,** *15* (4), 1034-1047.

3. Monkman, A., Why do we still need a stable long lifetime deep blue OLED emitter? *ACS Applied Materials Interfaces* **2021,** *14* (18), 20463-20467.

4. Sarma, M.; Chen, L.-M.; Chen, Y.-S.; Wong, K.-T.; Reports, E. R., Exciplexes in OLEDs: Principles and promises. *Materials Science* **2022,** *150*, 100689.

5. Shao, J.; Chen, C.; Zhao, W.; Zhang, E.; Ma, W.; Sun, Y.; Chen, P.; Sheng, R., Recent Advances of Interface Exciplex in Organic Light-Emitting Diodes. *Micromachines (Basel)* **2022,** *13* (2), 298.

6. Kim, H.-B.; Kim, J.-J., Recent progress on exciplex-emitting OLEDs. *Journal of Information Display* **2019,** *20* (3), 105-121.

7. Wang, Q.; Tian, Q.-S.; Zhang, Y.-L.; Tang, X.; Liao, L.-S., High-efficiency organic light-emitting diodes with exciplex hosts. *Journal of Materials Chemistry C* **2019,** *7* (37), 11329-11360.

8. Lee, J. H.; Shin, H.; Kim, J. M.; Kim, K. H.; Kim, J. J., Exciplex-Forming Co-Host-Based Red Phosphorescent Organic Light-Emitting Diodes with Long Operational Stability and High Efficiency. *ACS Appl Mater Interfaces* **2017,** *9* (4), 3277-3281.

9. Anand, R. J. 한. 학. 연. 초., Thermally Activated Delayed Fluorescence Host for High Performance Organic Light Emitting Diodes. **2021,** *46* (2), 98-98.

10. Jia, L.; Jin, L.; Yuan, K.; Chen, L.; Yuan, J.; Xu, S.; Lv, W.; Chen, R.; Engineering, High-performance exciplex-type host for multicolor phosphorescent organic light-emitting diodes with low turn-on voltages. *ACS Sustainable Chemistry* **2018,** *6* (7), 8809-8815.

11. Zhang, Y.-L.; Ran, Q.; Wang, Q.; Fan, J.; Liao, L.-S., High-efficiency exciplex-based white organic light-emitting diodes with a new tripodal material as a co-host. *Journal of Materials Chemistry C* **2019,** *7* (24), 7267-7272.

12. Liu, J., Deep-blue efficient OLED based on NPB with little efficiency roll-off under high current density. *Applied Physics A* **2017,** *123*, 1-6.

13. Sharma, G.; Hashmi, S.; Kumar, U.; Kattayat, S.; Ahmad, M. A.; Kumar, S.; Dalela, S.; Alvi, P., Optical and electronic characteristics of ITO/NPB/Alq3: DCJTB/Alq3/Ag heterostructure based organic light emitting diode. *Optik* **2020,** *223*, 165572.

14. Jbbar, R.; Bahari, A.; Ahmed, D. S., Enhanced Current Efficiency of OLEDs with NPB (5 nm)/TCTA (5 nm) Multilayers Sandwiched Between ITO (Anode) and Alq 3 (50 nm)/LiF (1 nm)/Al (Cathode). *Journal of Electronic Materials* **2020,** *49*, 6276-6282.

15. Li, P.; Wu, B.; Yang, Y. C.; Huang, H. S.; De Yang, X.; Zhou, G. D.; Song, Q. L., Improved charge transport ability of polymer solar cells by using NPB/MoO3 as anode buffer layer. *Solar Energy* **2018,** *170*, 212-216.

16. Gong, W.; Xu, Z.; Zhao, S.-L.; Liu, X.-D.; Fan, X.; Yang, Q.-Q.; Kong, C., Effects of NPB anode buffer layer on charge collection in ZnO/MEH-PPV hybrid solar cells. *Chinese Physics B* **2013,** *22* (12), 128402.

17. Ma, S.; Liu, X.; Wu, Y.; Tao, Y.; Ding, Y.; Cai, M.; Dai, S.; Liu, X.; Alsaedi, A.; Hayat, T.; Cells, S., Efficient and flexible solar cells with improved stability through incorporation of a multifunctional small molecule at PEDOT: PSS/perovskite interface. *Solar Energy Materials* **2020,** *208*, 110379.

18. Dalal, S. S.; Walters, D. M.; Lyubimov, I.; de Pablo, J. J.; Ediger, M. D., Tunable molecular orientation and elevated thermal stability of vapor-deposited organic semiconductors. *Proc Natl Acad Sci U S A* **2015,** *112* (14), 4227-32.

19. Ahmed, Z.; Avila, H. C.; Carvalho, R. S.; Kai, J.; Resende, J.; Bandini, E.; Barbieri, A.; Cremona, M., Bright neodymium complexes for efficient near infra-red organic light emitting diodes. *New Journal of Chemistry* **2020,** *44* (33), 14161-14170.

20. Darzi, E. R.; Stanfield, D. A.; McDermott, L.; Kelleghan, A. V.; Schwartz, B. J.; Garg, N. K., Facile synthesis of 2-aza-9,10-diphenylanthracene and the effect of precise nitrogen atom incorporation on OLED emitters performance. *Mater Adv* **2023,** *4* (15), 3351-3355.

21. Jankus, V.; Chiang, C. J.; Dias, F.; Monkman, A. P., Deep blue exciplex organic light-emitting diodes with enhanced efficiency; P-type or E-type triplet conversion to singlet excitons? *Adv Mater* **2013,** *25* (10), 1455-9.

22. Hippola, C.; Danilovic, D.; Bhattacharjee, U.; Perez-Bolivar, C.; Sachinthani, K. N.; Nelson, T. L.; Anzenbacher, P.; Petrich, J. W.; Shinar, R.; Shinar, J., Bright Deep Blue TADF OLEDs: The Role of Triphenylphosphine Oxide in NPB/TPBi: PPh3O Exciplex Emission. *Advanced Optical Materials* **2020,** *8* (1), 0191282.

23. Fu, C.; Lin, H. J. S. S. C., Performance enhancement of blue organic light-emitting devices by inserting BPhen: Alq3 as an n-doping electron transport layer. *Solid State Communications* **2024,** *378*, 115411.

24. Wang, Y.; Li, B.; Jiang, C.; Fang, Y.; Bai, P.; Wang, Y., Study on electron transport characterization in TPBi thin films and OLED application. *Journal of Physical Chemistry C* **2021,** *125* (30), 16753-16758.

25. Kim, K. J.; Kang, S.; Kim, T., Deterioration of Li-doped phenanthroline-based charge generation layer for tandem organic light-emitting diodes. *Journal of Information Display* **2024**, 1-10.

26. Miao, Y.; Du, X.; Wang, H.; Liu, H.; Jia, H.; Xu, B.; Hao, Y.; Liu, X.; Li, W.; Huang, W., Simplified phosphorescent organic light-emitting devices using heavy doping with an Ir complex as an emitter. *RSC advances* **2015,** *5* (6), 4261-4265.

27. Yang, X.; Wu, F.-I.; Haverinen, H.; Li, J.; Cheng, C.-H.; Jabbour, G. E., Efficient organic light-emitting devices with platinum-complex emissive layer. *Applied Physics Letters* **2011,** *98* (3).

28. Gao, H.; Zhang, H.; Mo, R.; Sun, S.; Su, Z.-M.; Wang, Y., Photophysical and charge-transport properties of hole-blocking material-TAZ: A theoretical study. *Synthetic metals* **2009,** *159* (17-18), 1767-1771.

29. Xiao, L.; Qi, B.; Xing, X.; Zheng, L.; Kong, S.; Chen, Z.; Qu, B.; Zhang, L.; Ji, Z.; Gong, Q., A weak electron transporting material with high triplet energy and thermal stability via a super twisted structure for high efficient blue electrophosphorescent devices. *Journal of Materials Chemistry* **2011,** *21* (47), 19058-19062.

30. Lin, B.-Y.; Chen, C.-H.; Lin, T.-C.; Lee, J.-H.; Chiu, T.-L. In *Effect of Carrier-Transporting Layer on Blue Phosphorescent Organic Light-Emitting Diodes*, Photonics, MDPI: 2021; p 124.

31. Fan, C.; Chen, Y.; Liu, Z.; Jiang, Z.; Zhong, C.; Ma, D.; Qin, J.; Yang, C., Tetraphenylsilane derivatives spiro-annulated by triphenylamine/carbazole with enhanced HOMO energy levels and glass transition temperatures without lowering triplet energy: host materials for efficient blue phosphorescent OLEDs. *Journal of Materials Chemistry C* **2013,** *1* (3), 463-469.

32. Gessner, T.; Lennartz, C.; Schmidt, H.-W.; Thelakkat, M.; Baete, M., Triazole derivatives and use thereof in organic light-emitting diodes (OLEDs). Google Patents: 2010.

33. Ichikawa, M.; Fujimoto, S.; Koyama, T.; Miki, T.; Taniguchi, Y. In *5.3: New Triazole Derivatives as Hole-Blocking and Electron-Transporting Materials for Organic Light-Emitting Devices*, SID Symposium Digest of Technical Papers, Wiley Online Library: 2006; pp 45-48.

34. Gupta, C. V.; Dixit, S. J. N.; Agarwal, N.; Bose, S., Voltage tunable white light generation from combined emission of monomer and electromer in phenanthroimidazole based OLED. *Journal of Photochemistry and Photobiology a-Chemistry* **2022,** *429*, 113922.

35. Mu, Y.; Zhang, S.; Yue, S.; Wu, Q.; Zhao, Y., High efficiency yellow organic light-emitting diodes with optimized barrier layers. *Solid-State Electronics* **2015,** *114*, 87-89.

36. Huang, H.-L.; Chao, T.-C.; Tseng, M.-R. In *High efficient solution processed yellow phosphorescent iridium emitters*, 2010 23rd Annual Meeting of the IEEE Photonics Society, IEEE: 2010; pp 572-573.

37. Lin, Y. H.; Lin, W.-H.; Huang, Y.-S.; Wu, C.-H.; Gnanasekaran, P.; Chang, Y.-M.; Teng, S.-W.; Lu, C.-W.; Chang, C.-H.; Chang, Y. J., Highly efficient (EQE> 27%) Yellow OLEDs using spiro [fluorene-9, 9′-phenanthren-10′-one]-carbazole-based donor–acceptor–donor host materials. *Journal of Materials Chemistry C* **2023,** *11* (8), 3101-3111.

38. Deotare, P.; Chang, W.; Hontz, E.; Congreve, D.; Shi, L.; Reusswig, P.; Modtland, B.; Bahlke, M.; Lee, C.; Willard, A., Nanoscale transport of charge-transfer states in organic donor–acceptor blends. *Nature materials* **2015,** *14* (11), 1130-1134.

39. Golubev, T.; Liu, D.; Lunt, R.; Duxbury, P., Understanding the impact of C60 at the interface of perovskite solar cells via drift-diffusion modeling. *AIP Advances* **2019,** *9* (3).

40. Günther, A. A.; Widmer, J.; Kasemann, D.; Leo, K., Hole mobility in thermally evaporated pentacene: Morphological and directional dependence. *Applied Physics Letters* **2015,** *106* (23).

41. Yan, H.; Kagata, T.; Okuzaki, H., Ambipolar pentacene/C60-based field-effect transistors with high hole and electron mobilities in ambient atmosphere. *Applied Physics Letters* **2009,** *94* (2).

42. Lim, S. H.; Bjorklund, T. G.; Spano, F. C.; Bardeen, C. J., Exciton delocalization and superradiance in tetracene thin films and nanoaggregates. *Phys Rev Lett* **2004,** *92* (10), 107402.

Chapter 3

NPB:OXD-7 exciplex as a multifunctional device; blue emitting OLED and a photodetector

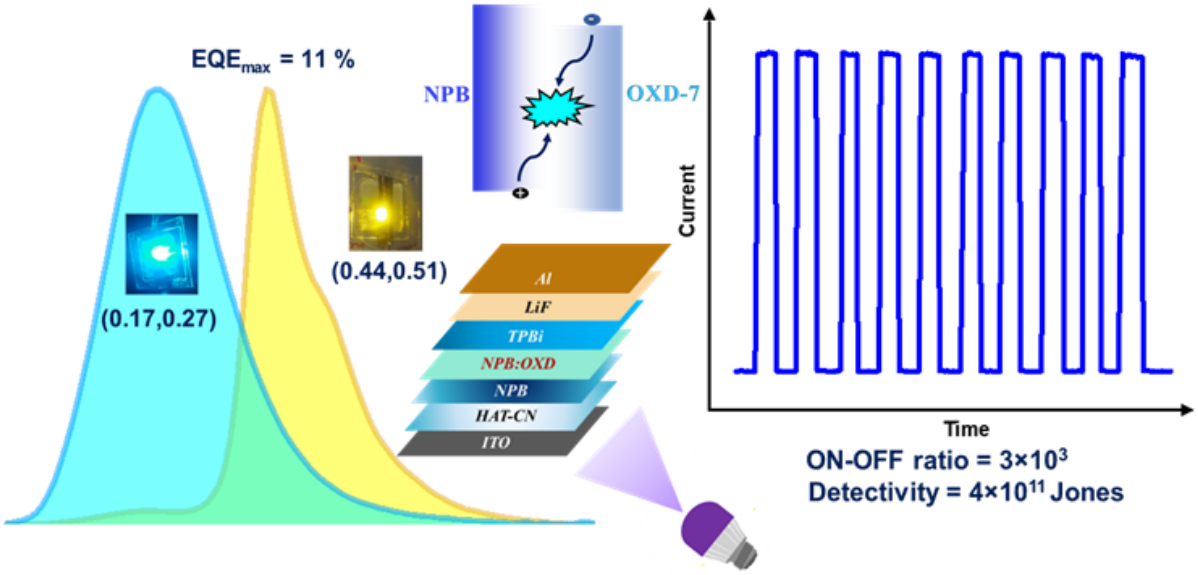

3.1 Abstract

The solution processing method for device fabrication simplifies the fabrication process and minimizes material consumption. In this chapter, solution processing method was employed to develop exciplex organic light emitting diodes (OLEDs) using the hole transport material (HTM), N,N'-Di(1-naphthyl)-N,N'-diphenyl-(1,1'-biphenyl)-4,4'-diamine)(NPB) and the electron transport material (ETM), 1,3-Bis[2-(4-tert-butylphenyl)-1,3,4-oxadiazo-5-yl]benzene (OXD-7). Introducing the yellow phosphorescent dopant Bis(4-phenylthieno[3,2-c]pyridinato-N,C2') (acetylacetonate) iridium(III) (PO-01) into the exciplex host resulted in a yellow OLED with a maximum brightness of 36,000 cd/m² and an external quantum efficiency (EQE) of 11%. In parallel, the dual functionality of the NPB/OXD-7 exciplex was also

investigated. Large surface potential of OXD-7 causes spontaneous exciplex dissociation at the NPB/OXD-7 interface. This coupled with the strong UV absorption capability of OXD-7 help generate photocurrent under UV illumination, enabling it to function as a self-powered UV detector. This allows the device to operate as both an OLED and a UV photodetector. Higher OXD-7 concentrations enhanced UV absorption and diminished exciplex emission. NPB:OXD-7(1:3) ratio device excelled as a UV detector but performed poorly as an OLED. Notably, a self-powered UV detector with a 1:3 ratio exhibited a detectivity of 4×10^{11} Jones, responsivity of 17 mA/W and an ON-OFF ratio of 3×10^{3} with a reasonable OLED performance. Integrating different functions in a single device is a significant step towards miniaturization of electronic devices.

3.2 Introduction

Exciplex-based OLEDs are particularly interesting due to their simplified device designs. While there are numerous reports on fully vacuum-deposited exciplex OLEDs[1-3], the literature on solution-processed exciplex OLEDs remains limited[4-6]. Unlike traditional vacuum deposition methods, solution processing offers several advantages including cost-effectiveness, scalability and compatibility with flexible substrates[7-10]. Precise control over the mixing and deposition of donor-acceptor blend is crucial for optimal device performance of exciplex OLEDs. Solution processing techniques such as spin coating[11, 12], inkjet printing[13, 14], slot-die coating[15] etc. can be employed to deposit the materials onto various substrates. Spin coating is commonly used due to its simplicity, ability to produce uniform films and reduced material usage. The process parameters such as concentration of the solution, rotation speed, solvent evaporation rate and annealing conditions are optimized to control the film morphology

and thickness. Optimizing these parameters can lead to significant improvements in device efficiency and stability. Additives or interfacial layers can also be added to enhance the charge injection and transport[16]. The primary challenges in the development of solution-processed OLEDs include the deposition of multilayers and the selection of appropriate solvents. Achieving uniform films and optimizing film thickness are significant factors that critically impact the performance and reliability of the devices. In this chapter our primary focus is on employing solution processing method for the fabrication of efficient exciplex OLEDs.

The concept of multifunctionality is another critical aspect recently getting emphasized in the development of organic electronic devices. Multifunctional organic electronic devices hold immense potential across a wide variety of applications, promising to revolutionize various sectors through their unique properties and capabilities[17, 18]. By considering the unique properties of organic materials, devices offering advanced functionalities integrated within a device, are referred to as multifunctional device. In this chapter, we integrate light emission (OLED) and UV detection (organic UV photodetector) capabilities within a single device. For this, we need materials with unique photophysical as well as charge transporting abilities. In this context, OXD-7 has exceptional electron transporting capabilities, primarily attributed to the electron accepting characteristics of the oxadiazole units incorporated within its molecular structure[19-21]. The presence of these oxadiazole groups of OXD-7 in conjunction with poly(9-vinylcarbazole) (PVK), an electron donating polymer, serves as one of the most widely utilized hybrid type host materials[22, 23]. This combination exploits the complementary electron donating and electron accepting properties of PVK and OXD-7, respectively, to facilitate balanced charge transport in optoelectronic devices[24]. The bulky tert-butyl units attached to the OXD-7 molecule enhance its solubility and improve film morphology, contributing to the

overall performance and stability of the resultant films. In addition to its electron transporting and film forming capabilities, OXD-7 demonstrates strong UV absorption, highlighting its potential for use in UV photodetectors.

3.2.1 Photodetectors

Photodetectors are devices that convert light into electrical signals, playing a crucial role in various scientific, industrial and consumer applications[25]. They are integral to systems that require the detection and measurement of light, such as imaging, communication, environmental monitoring, and biomedical diagnostics[26]. The Figure 3.1 illustrates the structure and working of an organic photodetector in terms of the energy levels of the molecules. It comprises of an active layer sandwiched between electron and hole extraction layers, followed by their respective electrodes.

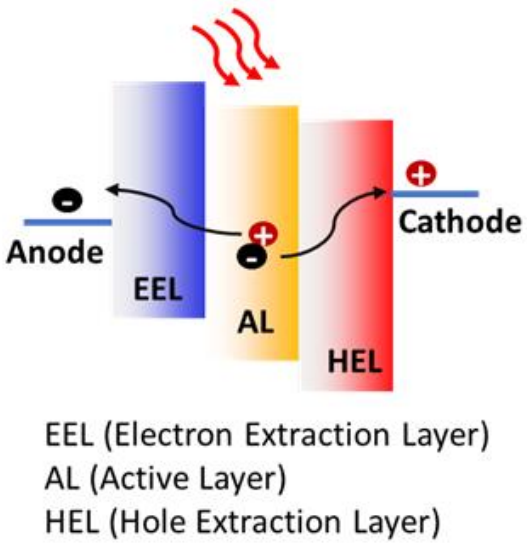

Figure 3.1. Illustration of working principle of a photodetector in terms of energy levels.

Incident photons are absorbed by the active layer, leading to exciton dissociation. The excitons dissociate into free electrons and holes at the donor acceptor interface within the active layer. Electrons are transported through the electron extraction layer towards the cathode, while holes

are transported through the hole extraction layer towards the anode. The cathode and anode collect the electrons and holes, respectively, creating a flow of photocurrent through the external circuit. The key parameters which determine photodetector performance are Responsivity (R), Detectivity (D), ON/OFF ratio, Rise time and Fall time.

Responsivity is a critical parameter that defines the efficiency of a photodetector in converting incident optical power into an electrical signal. It is the ratio of the photocurrent (I_{ph}) generated to the incident optical power (P_0) of the source lamp. Mathematically, it is expressed as in equation (1).

$$\text{Responsivity (R)} = \frac{I_{ph}}{P_0} \tag{1}$$

Responsivity is measured in units of amperes per watt (A/W) and indicates how effectively the photodetector converts incoming photons into electrical current. Detectivity is a measure of sensitivity and its ability to detect weak optical signals. It is defined as the reciprocal of the Noise Equivalent Power (NEP) as given in equation (2), normalized by the active area of the device. The detectivity (D) can also be expressed in terms of responsivity as given in the equation (3). Where q is the electron charge and J_d is the dark current density.

$$\text{Detectivity, D} = \frac{1}{NEP} \tag{2}$$

$$= \frac{R}{\sqrt{2qJ_d}} \tag{3}$$

Detectivity is measured in Jones and a higher detectivity indicates better performance in detecting low levels of light. The ON-OFF ratio is a crucial parameter that quantifies the difference in current between the illuminated (ON) and dark (OFF) states of a photodetector.

It is the ratio of the photocurrent to the dark current, which is the current that flows through the photodetector under dark condition. The ON-OFF ratio is expressed in equation (4).

$$\text{ON/OFF ratio} = \frac{I_{ph}}{I_{dark}} \quad (4)$$

A higher ON-OFF ratio indicates a photodetector with better performance, as it shows a significant increase in current upon illumination compared to the dark state. Rise time and fall time describe how quickly a device responds to a change in the input signal, which is particularly important in applications such as high-speed communication, imaging, and sensing. Rise time is the time required to reach from 10% to 90% of the maximum value of the photocurrent whereas fall time is the time required to fall from 90% to the 10% of the maximum value of the photocurrent.

3.3 Experimental section

The devices were fabricated on pre-patterned indium tin oxide (ITO) (purchased from Kintec, Hong Kong, ITO thickness 150 nm, sheet resistance < 15 ohm/sq) coated glass substrates. These patterned ITO substrates were initially cleaned by ultrasonication in chloroform for 15 minutes and then washed in dilute detergent solution followed by ultrasonication in isopropanol and deionized water for 10 minutes each and dried using a hot air gun. UV-ozone cleaning for 15 min was done just before the fabrication of the devices. Poly (3,4-ethylenedioxythiophene: polystyrene sulfonate (PEDOT:PSS) (purchased from Heraeus) was spincoated at 2500 rpm at ambient conditions. After annealing these substrates for 20 minutes at 120°C, the substrates were transferred to the wet glovebox. Mixed solution of NPB and OXD-7 in 1:1 weight ratio was prepared in chlorobenzene and spincoated at 2000 rpm inside

glovebox. The films were then annealed at 110°C for 15 minutes, followed by annealing in vacuum for 2 hours. Then substrates were transferred to thermal evaporation chamber. Electron transport layer (ETL) (OXD-7, TPBi), LiF and Al were thermally evaporated in a thermal evaporation system (Angstrom Engineering, Canada) at 10^{-7} torr. The rate of evaporation of ETL, LiF and Al were 2 Å/s, 0.1 Å/s and 2 Å/s respectively. The thickness of the layers was confirmed using Dektak XT surface profilometer. After the evaporation, the devices were encapsulated inside the nitrogen filled glovebox by using a UV-curable epoxy (Epoxy Technology inc.). TPBi was purchased from Luminescence Technology Corp. (Lumtec), Taiwan, while NPB and OXD-7 were purchased from TCI chemicals.

The absorption studies of the thin films of these materials were done using HORIBA Jobin Yvon and PerkinElmer UV/VIS/NIR Spectrometer, Lambda 950. Emission spectra were measured using a Fluorolog-3 spectrofluorometer (HORIBA), equipped with a 450 W xenon arc lamp. The surface potential mapping of the thin films was conducted using the kelvin probe microscopy by Bruker multimode 8 nanoscope atomic force microscopy (AFM). The OLED characterization system consists of a SpectraScan PR (Photo Research)-655 spectroradiometer and a Keithely 2400 source meter integrated with a PC. The photodetector characterization was done using a UV-lamp and Keithley 4200 semiconductor parameter analyzer at ambient conditions.

3.4 Results and discussion

3.4.1 Strategy for materials selection

In this chapter, NPB and OXD-7 were selected as the HTM and ETM respectively and the respective molecular structures are given in Figure 3.2 (a). According to the highest occupied molecular orbital (HOMO)- low unoccupied molecular orbital (LUMO) gap of 2.5 eV at the

interfaces, a blue exciplex emission is expected at the NPB/OXD-7 interface as illustrated in Figure 3.2 (b). The HOMO-HOMO and LUMO-LUMO offsets at the interfaces are 1 and 0.6 eV, respectively. These materials were selected because they have absorption in the UV-region; below 400 nm, and do not have any absorption in the visible. Hence, they can be considered visible-blind.

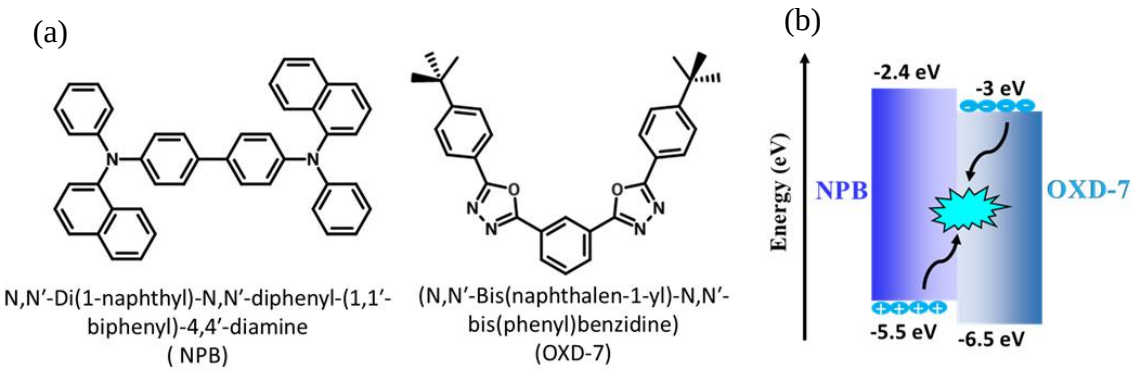

Figure 3.2. (a) Molecular structure of NPB and OXD-7 (b) exciplex formation at the molecular interface of NPB and OXD-7 in terms of energy levels.

3.4.2 Spectroscopic studies

The thin films of the materials NPB, OXD-7 and NPB:OXD-7 (1:1) were fabricated. The absorption as well as emission spectra of the thin films of the materials were compared. The absorption spectra of the NPB:OXD-7 mixed film only indicates the individual absorptions of NPB and OXD-7. The absence of a distinct absorption peak for the mixed film indicates the exciplex formation at NPB/OXD-7 interface. The comparison of absorption spectra and emission spectra are given in Figure 3.3. Whereas, in the emission spectra the mixed film exhibited a significantly red shifted and broadened emission peak. The emission of NPB, OXD-7 and NPB:OXD-7 (1:1) films are observed at 412 nm, 436 nm and 465 nm, respectively. The emission of NPB:OXD-7 mixed film is 53 nm and 29 nm redshifted from that of NPB and

OXD-7 respectively. The full width at half maximum (FWHM) values are 55 nm, 53 nm and 77 nm for NPB, OXD-7 and NPB:OXD-7(1:1), respectively. Spectroscopic studies reveal a significant red shift and broadening in the mixed film compared to NPB and OXD-7, confirming NPB:OXD-7 exciplex emission.

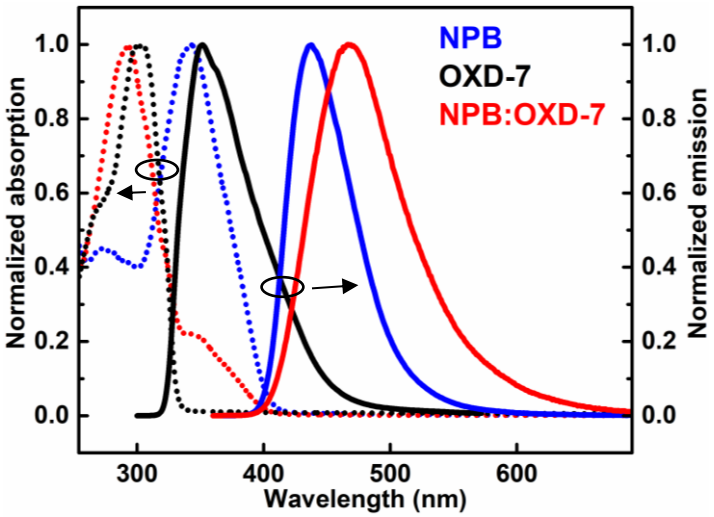

Figure 3.3. Comparison of absorption and emission spectra of the NPB, OXD-7, NPB:OXD-7 (1:1) films.

3.4.3 Device fabrication and characterization

Based on the spectroscopic studies, devices were fabricated using the NPB/OXD-7 exciplex as both an emitter and a host. The aim was to develop solution-processed exciplex OLEDs using NPB:OXD-7 combination. Solution processable devices offer several advantages, contributing to their popularity and widespread use. It reduces device fabrication complexity and material consumption. Hence, more cost effective and versatility in substrates. However, the solution processing method is not suitable for devices with multiple solution-processed layers due to the challenge of selecting solvents for depositing multiple layers of organic materials sequentially. In this chapter, solution-processed OLEDs were designed by using

NPB:OXD-7 blue emitting exciplex as an emitter as well as a host with a yellow phosphorescent dopant, PO-01.

3.4.3.1 Blue OLEDs by utilizing NPB:OXD-7 exciplex emission

Solution-processed blue exciplex OLEDs were fabricated by using a blend of NPB and OXD-7 as the emissive layer. PEDOT:PSS is used as the hole injection layer (HIL) as well as the hole transport layer (HTL), followed by the emissive layer of NPB:OXD-7 mixed film. The device configuration is as follows: ITO/PEDOT:PSS (35nm)/ NPB:OXD-7 (1:1, 35 nm)/OXD-7(45 nm)/ LiF (1nm)/Al (100 nm). EML is followed by the OXD-7 alone layer of 40 nm for better electron transport. LiF is used as electron injection layer (EIL) and Aluminum (Al) as cathode. The device architecture and detailed energy level diagram are shown in Figure 3.4 (a) and (b) respectively. PEDOT:PSS was first spin coated onto the substrate at ambient conditions. Subsequently, a NPB:OXD-7(1:1, weight ratio) mixed solution in chlorobenzene was spin coated onto the PEDOT:PSS at 2000 rpm inside a glove box. Finally, OXD-7, LiF and Al were thermally evaporated.

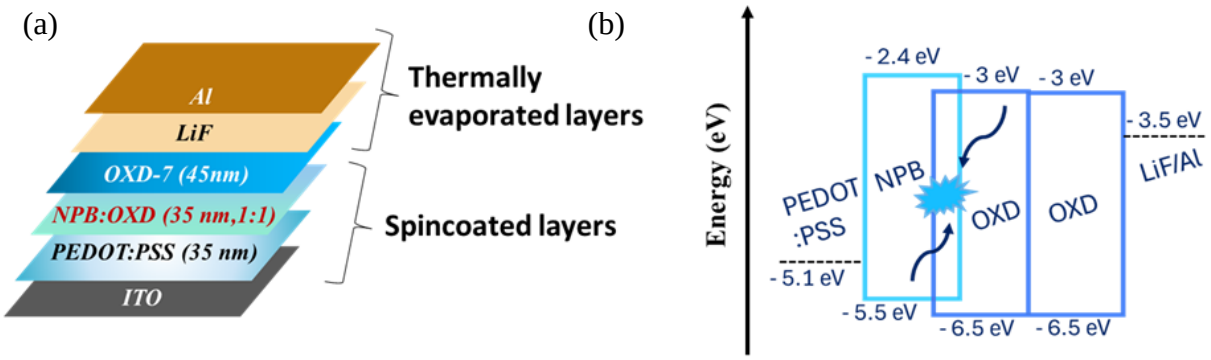

Figure 3.4. (a) Device architecture of NPB:OXD-7 blue exciplex OLED (b) detailed energy level diagram of the device and the exciplex emission at the NPB/OXD-7 interfaces in the EML.

The current density (J) - voltage (V) - luminance (L) plot and electroluminescence (EL) spectra of the device are shown in Figure 3.5 (a) and (b) respectively. The device exhibited a sky blue emission at 482 nm. The Commission Internationale de l'Eclairage-1931 (CIE) coordinates of (0.17, 0.28) remain constant with respect to the applied voltage. The variation in CIE coordinates with respect to voltage, CIE diagram and photograph of a working device are shown in Figure 3.5 (c), (d) and (e).

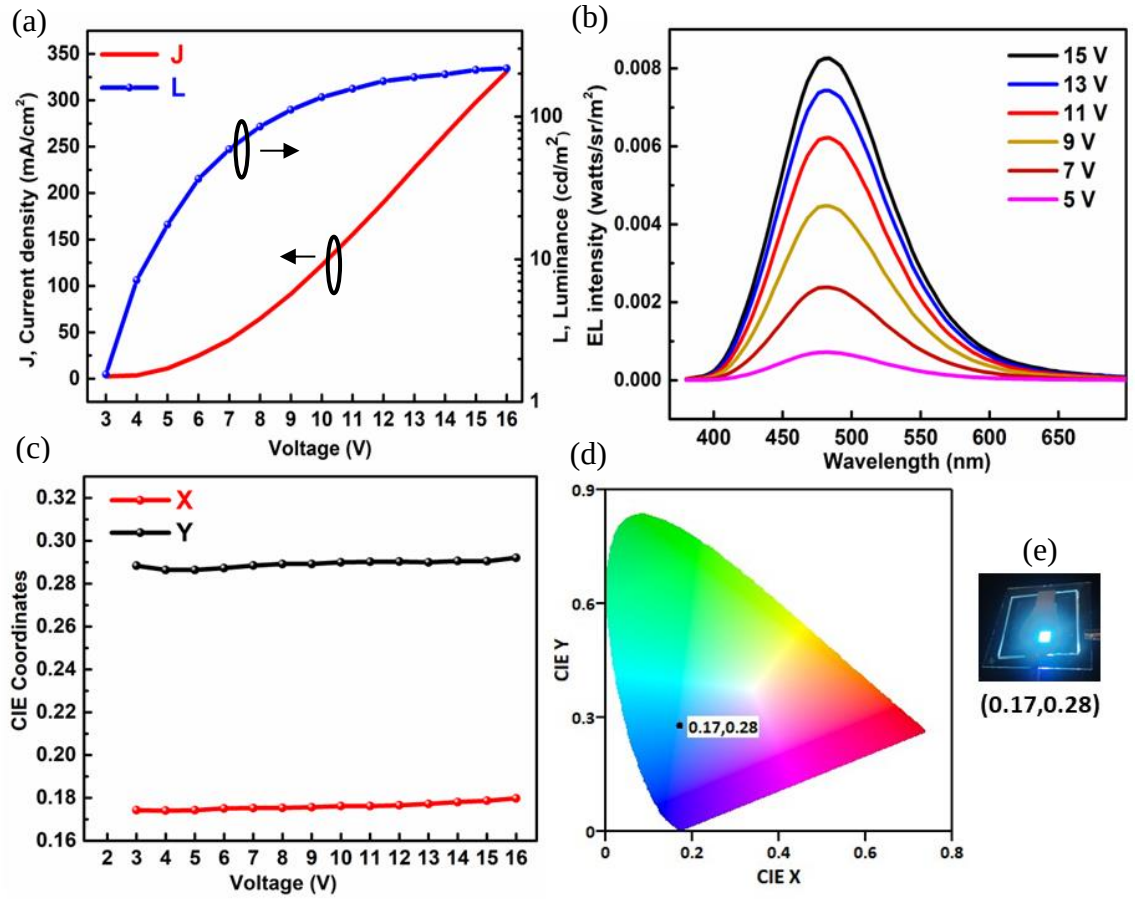

Figure 3.5. (a) J-V-L plot (b) EL spectra at different voltages (c) CIE coordinates with respect to applied voltage (d) CIE diagram and (e) photograph of the NPB:OXD-7 blue exciplex OLED.

The device exhibited a maximum luminance of 218 cd/m^2 with a current density of 330 mA/cm^2 at 16V. The low brightness could be due to the lower electron transport capability of OXD-7[24] compared to the high hole mobility of PEDOT:PSS[27]. This discrepancy can cause an imbalance in charge carrier transport, leading to inefficient recombination of electrons and holes, and consequently reducing the overall luminance. To improve the electron transport, the OXD-7 alone layer (as sole ETL) was replaced by TPBi. TPBi is an excellent electron transport material for both vacuum-deposited and solution-processed OLEDs[28, 29]. The modified device architecture is as follows: ITO/PEDOT:PSS (35nm)/ NPB:OXD-7 (1:1, 35 nm)/TPBi(45 nm)/ LiF (1nm)/Al (100 nm). The modified device architecture and detailed energy level diagram are shown in Figure 3.6 (a) and (b), respectively. The device performance has significantly improved when TPBi is used. The device exhibited a maximum luminance of 1462 cd/m^2 with a current density of 355 mA/cm^2 at 12V. The device with TPBi as the ETL demonstrates significantly higher luminance and higher current efficiency than the device with OXD-7. The luminance and CE of the device with TPBi are over three times higher than those with OXD-7. The comparison of J-V-L and current efficiency (CE) *vs.* voltage plot are shown in Figure 3.6 (c) and (d), respectively. TPBi exhibits high electron mobility[30], enabling efficient electron transport throughout the device. This reduces recombination losses and enhances overall device performance. From the comparison of the EL spectra of the devices as shown in Figure 3.6 (e), emission peak was not seen to be affected by changing the ETL. Also, both devices exhibit the same turn-on voltage of 3V, indicating that the initial energy barrier for electron injection is not affected by changing the ETL.

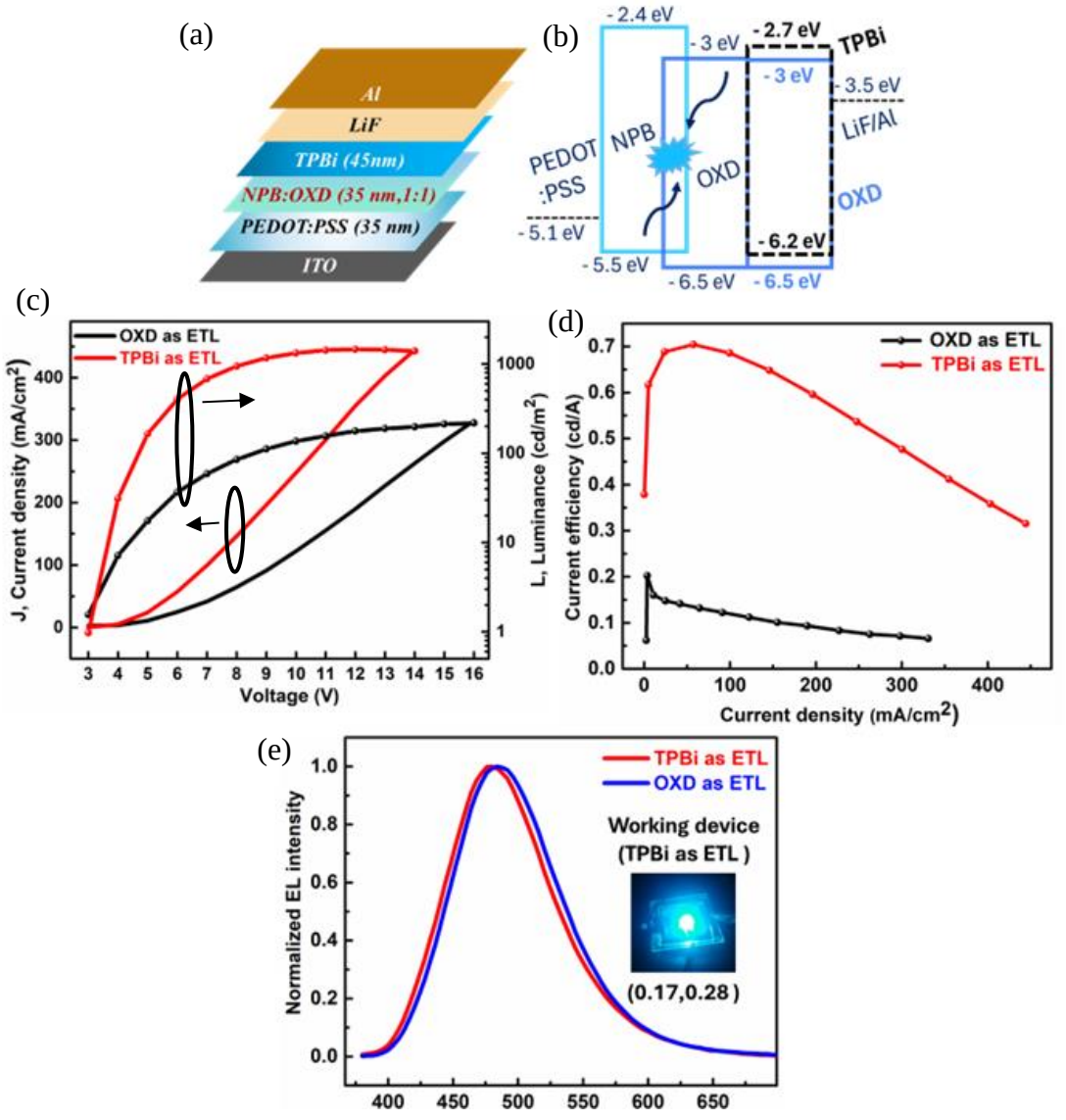

Figure 3.6. (a) Device architecture (b) detailed energy level diagram (c) J-V-L plot (d) CE *vs.* current density plot and (d) EL spectra of the NPB:OXD devices with TPBi as the sole ETL with a photograph of a working device is given in the inset.

3.4.3.2 Yellow OLEDs by utilizing NPB:OXD-7 exciplex as host

To explore the efficiency of the NPB:OXD-7 exciplex as a host with an appropriate phosphorescent dopant, solution-processed exciplex host OLEDs were designed and fabricated. Based on the spectral overlap depicted in Figure 3.7(a), PO-01 is selected as the yellow phosphorescent dopant. The device configuration is as follows: ITO/ PEDOT:PSS(35nm)/ NPB:OXD-7:PO-01(1:1, x%,35nm)/TPBi(45nm)/LiF(1nm)/Al(100nm). In the emissive layer, different weight percentages of PO-01 is doped in the NPB:OXD-7 mixed layer. The device architecture is shown in Figure 3.7(b).

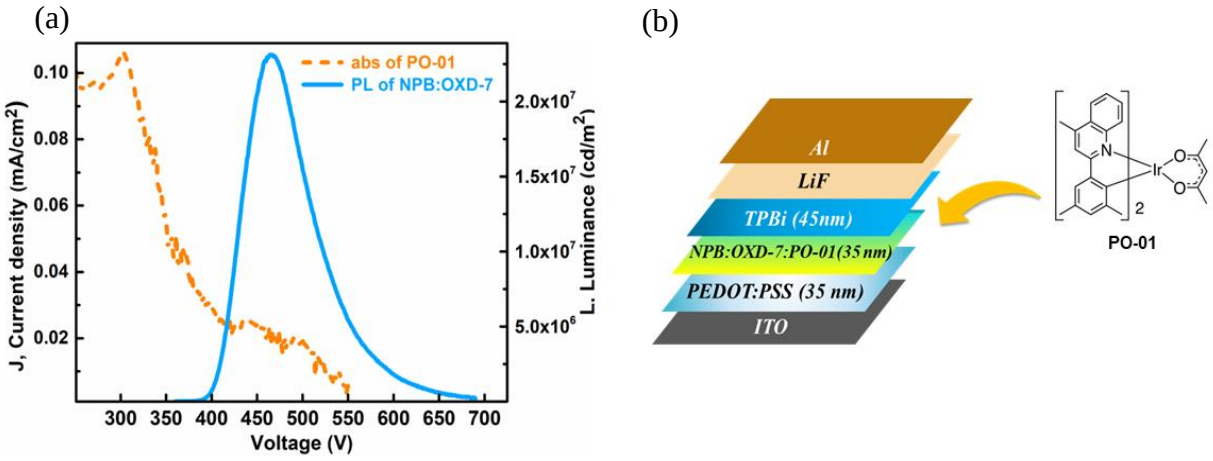

Figure 3.7. (a) Spectral overlap between absorption of PO-01 and emission of NPB:OXD-7 (1:1) thin films (b) device architecture of exciplex host OLED and the molecular structure of the yellow phosphorescent dopant PO-01.

Exciplex host devices were fabricated with x = 3%, 5%, 7% and 9% of PO-01 doped in the NPB:OXD-7 mixed layer. Maximum luminance of 36,000 cd/m^2, maximum CE of 37 cd/A and maximum EQE of 11 % were achieved for 5% doping of PO-01. It shows the efficient energy transfer occurred from the exciplex host to the phosphorescent dopant. The high quantum yield of the phosphorescent dopant, along with the bipolar nature of the exciplex host,

likely contributed to the high efficiency of the devices. The J-V-L plots are compared in Figure 3.8 (a). The EL spectra at different voltages for the device with x=5% is shown in Figure 3.8 (b). All the devices exhibited yellow emission of PO-01 at 560 nm. The device performance is summarized in the Table 3.1. The EQE and CE *vs*. current density plots of the devices are compared in Figure 3.8 (c) and (d). The CIE coordinates remain constant with respect to the applied voltage as shown in Figure 3.9 (a). The CIE diagram and photograph of a working device with 5% doping ratio are shown in Figure 3.9 (b).

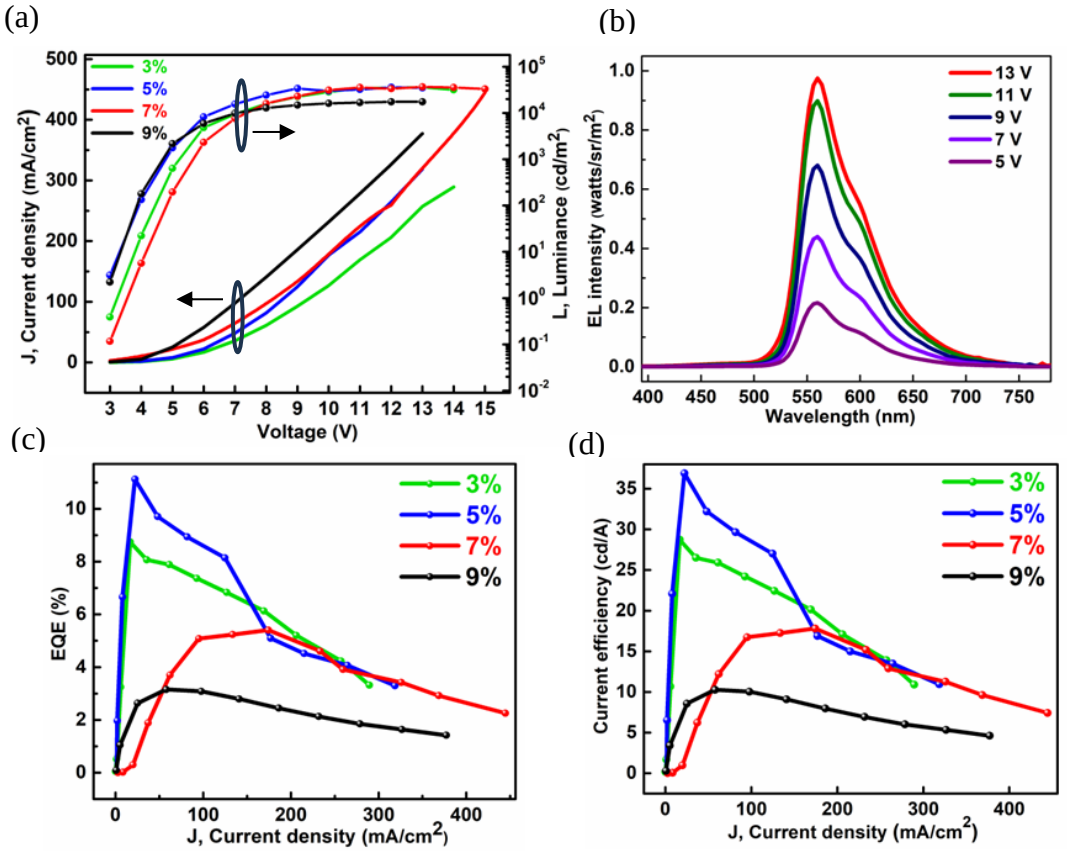

Figure 3.8. (a) J-V-L plots of the yellow devices (b) EL spectra at different voltages of the device with 5% doping (c) EQE and (d) CE *vs.* current density plots of the yellow devices.

% of PO-01	Luminance (cd/m^2)	Current density (mA/cm^2)	Current efficiency (cd/A)	EQE (%)	Max Luminance, max CE, max EQE
3%	27800 ± 537	132 ± 1.92	22.0 ± 0.32	6.55 ± 0.10	35780 cd/m^2, 26.5 cd/A, 9 %
5%	33000 ± 596	162 ± 2.76	20.9 ± 0.57	6.00 ± 0.70	35680 cd/m^2, 37.0 cd/A, 11 %
7%	31900 ±712	176 ± 3.60	17.8 ± 0.63	5.20 ± 0.08	36710 cd/m^2, 18.0 cd/A, 5 %
9%	16600 ± 435	132 ± 1.96	6.06 ± 0.26	1.93 ± 0.07	17420 cd/m^2, 10.3 cd/A, 3 %

Table 3.1. Summary of device performance at 10V and the maximum luminance, CE and EQE values of yellow solution-processed exciplex host OLEDs with different doping ratios of PO-01 into the exciplex matrix.

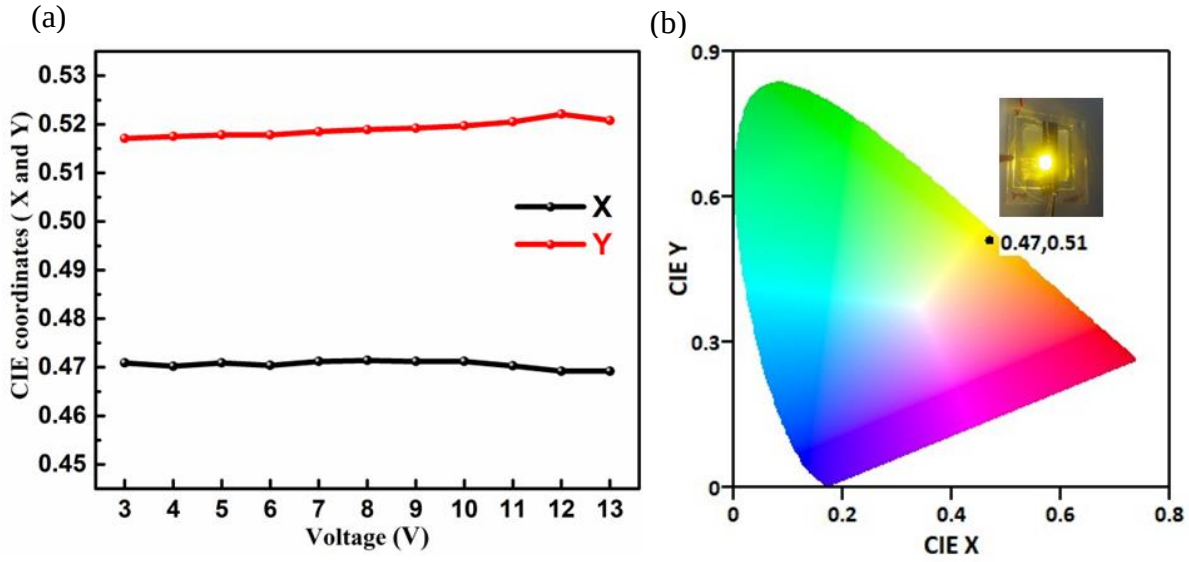

Figure 3.9. (a) CIE coordinates *vs.* voltage plot and (b) CIE diagram of the device with 5% doping of PO-01 and a photograph of a working device is given in the inset.

The lifetime testing of the best yellow device with 5% doping of PO-01 was conducted over approximately 30 hours. Throughout the test, the device was monitored at a constant current of I_0 = 0.12 mA; the initial luminance being 96 cd/m^2. The variation in the ratio of luminance

at a time to the initial luminance *vs.* operational time is shown in Figure 3.10 (a). The initial luminance was maintained for over 30 hours, indicating the high operational stability of the device. A slight increase in the initial luminance was observed, likely due to initial trap-filling processes occurring within the device. Also, the emission wavelength of the spectrum and the CIE coordinates remain stable throughout its operation as shown in the Figure 3.10 (b) and (c).

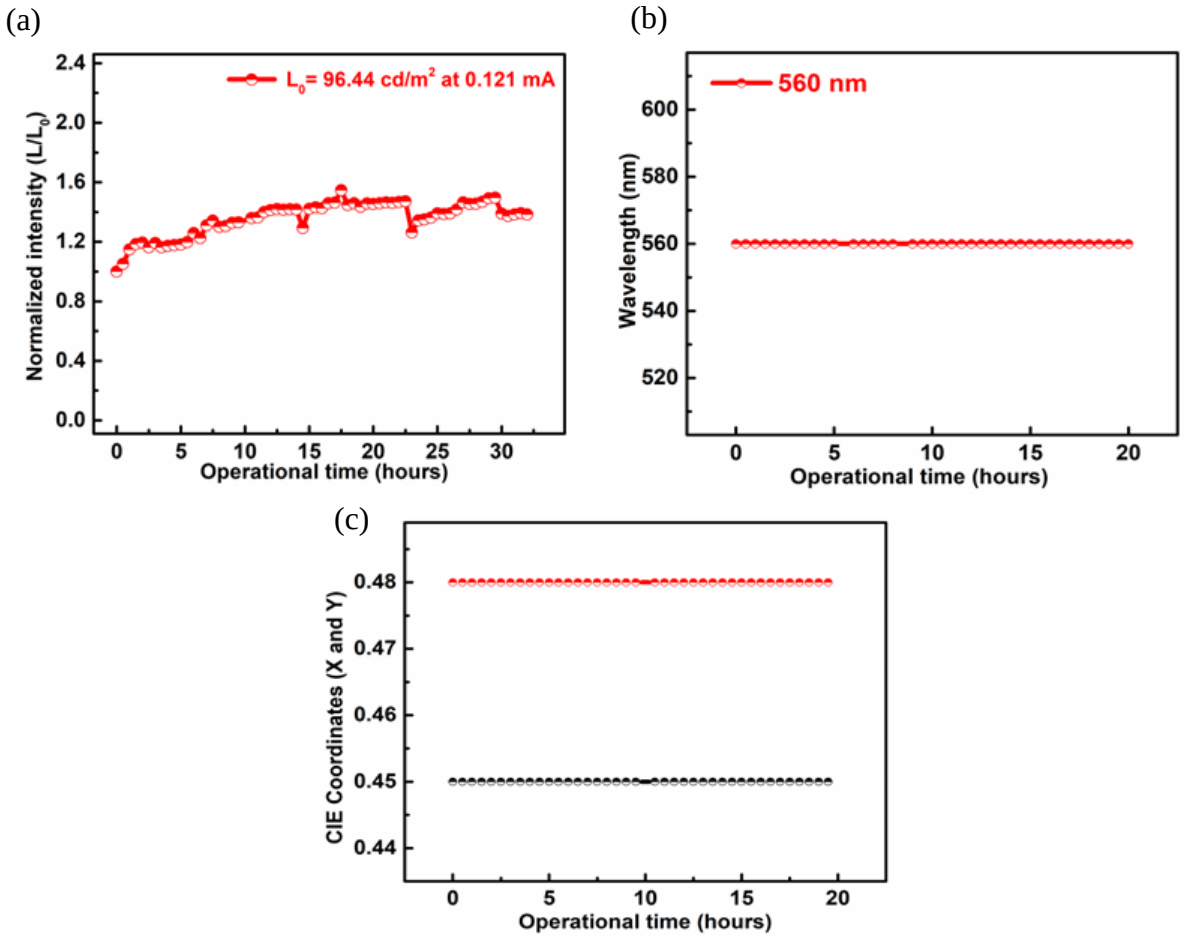

Figure 3.10. (a) Lifetime testing (L/L_0) *vs.* operational time (b) wavelength *vs.* operational time and (c) CIE coordinates *vs.* operational time of the yellow device with 5% doping of PO-01 into the NPB:OXD-7 blend film.

3.4.4 Multifunctional devices

3.4.4.1 Concept of multifunctionality

The need for integration of multifunctionality in optoelectronics has been recognized for advancing smart device technologies. From a practical perspective, multifunctional devices hold significant promise for the evolution of smart devices. The multifunctionality can be realized by combining the distinct functions of different categories of devices. An example of such integration in organic electronic devices is the incorporation of both light emission and detection functions within the same device. The fabrication and characterization of NPB:OXD-7 blue exciplex OLEDs was discussed in the previous section. Here, we are proposing a multifunctional device based on NPB:OXD-7 exciplex emission. The UV-absorption capability of NPB:OXD-7 mixed film was first investigated by Zhu *et al*. in 2014[31]. They fabricated a UV-photodetector by using NPB:OXD-7 mixed film as the active layer, exploiting the strong UV absorption of OXD-7. TiO_2, which acts as the electron extraction layer, plays a crucial role. After UV photo-excitation, the reduced work function and increased conductivity of the TiO_2 film create a low-impedance contact at the carrier-extraction layer-metal interface, facilitating the collection of photogenerated carriers at the electrodes. They did not investigate the light emission properties of the NPB:OXD-7 exciplex. Instead, they used it as the active layer specifically for UV detection. In our work, the high UV-absorption capability of OXD-7 and its exciplex forming capability with NPB are combined to create a multifunctional device. Under forward bias, exciplex emission occurs at the NPB/OXD-7 interfaces in the mixed film. Hence, device operates as an OLED under forward bias. Conversely, under reverse bias and upon UV illumination, a photocurrent is generated which can be attributed to the built-in potential at the NPB/OXD-7 interface and high UV absorption of OXD-7.

To confirm the effect of OXD-7, the UV-visible absorption spectra of mixed films with different NPB:OXD-7 ratios (1:3, 1:1, and 3:1) were compared, as shown in Figure 3.11. Both 1:1 and 3:1 films exhibit the individual absorptions of NPB and OXD-7, with OXD-7 absorption dominating in all cases. As expected, the 1:3 film shows the highest UV absorption. Increasing the concentration of OXD-7 enhances the absorption of the mixture, confirming high UV absorption properties of OXD-7.

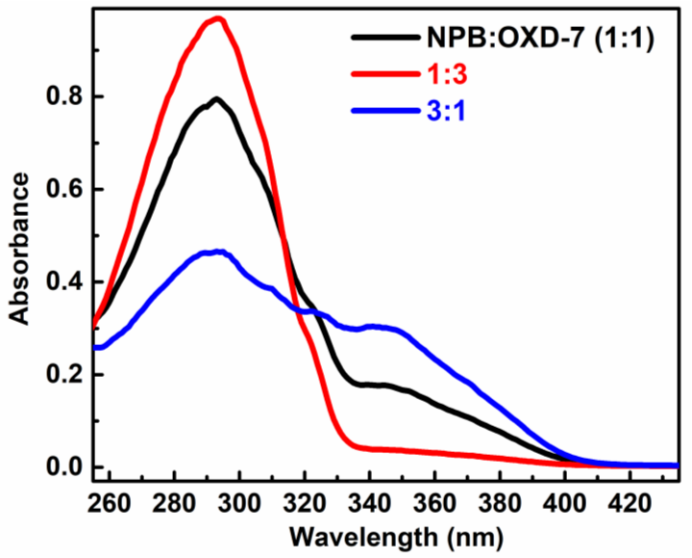

Figure 3.11. Comparison of absorption spectra of mixed films NPB:OXD-7 (1:1, 1:3 and 3:1).

3.4.4.2 Device fabrication and characterization

The high UV-absorption capability as well as exciplex emission in NPB:OXD-7 mixed film is utilized for the design of multifunctional devices. Initially, the performance of the UV detector using the NPB:OXD-7 (1:1) device was analyzed, as its exciplex emission has already been discussed in the previous sections. The photodetector characterization was done under UV-illumination and reverse bias. The IV characteristics were measured both in the dark and under 365 nm UV light. Figure 3.12 (a) illustrates the variation in dark/photocurrent density with applied voltage. The ON/OFF ratio of 26, responsivity of 4 mA/W, and detectivity of 1.76×10^{10}

Jones was obtained at 0V. The cyclic photoresponse of the device, shown in another Figure 3.12 (b), demonstrates the variation in photocurrent with operational time, revealing a rise time and fall time of 287 ms. The device demonstrated photodetector performance, with a detectivity value in the range of 10^{-10} Jones, making it suitable for UV-detection applications. Hence, the multifunctionality of the devices is confirmed with this observation.

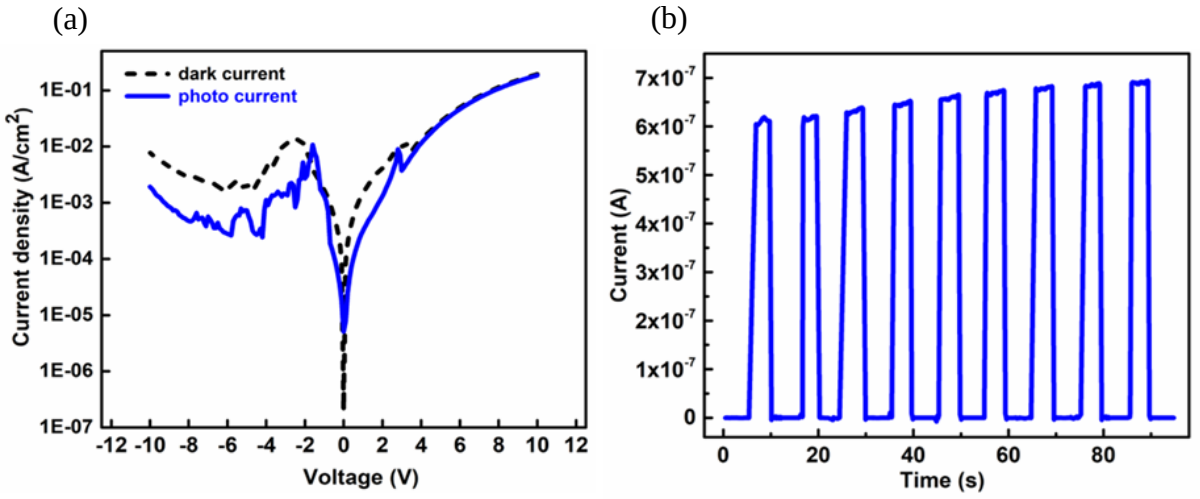

Figure 3.12. (a) Steady-state IV characteristics of dark and photocurrent under 365 nm UV light and (b) cyclic photoresponse of NPB:OXD-7 (1:1) device.

The multifunctional device proposed in this work does behave as an OLED under forward bias and as a UV-detector under reverse bias as depicted in Figure 3.13.

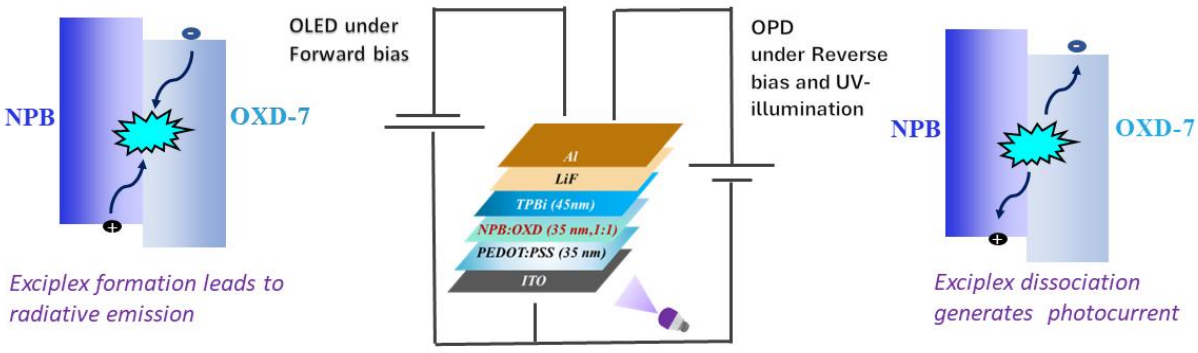

Figure 3.13. Illustration of the working mechanism of multifunctional devices.

By considering the high surface potential and UV- absorption of the OXD-7 in the mixed films, two devices were designed with emissive layers consisting of 1:3 and 3:1 ratios of NPB and OXD-7. The multifunctional exciplex devices were fabricated with the modified EMLs with the device structure of ITO/PEDOT:PSS (35nm)/ NPB:OXD-7 (1:3 or 3:1, 35 nm)/TPBi(45 nm)/ LiF (1nm)/Al (100 nm). Steady-state IV characteristics of these devices are compared in Figures 3.14 (a) and (b). The 1:3 ratio shows high ON/OFF ratio of ~ 10^3 and a high detectivity of 1.1×10^{11} Jones. The improved detector performance of 1:3 can be attributed to the higher UV-absorption of OXD-7. Whereas, the responsivity of the 3:1 device is found to be very low compared to the 1:1 and 1:3 devices. This behavior is due to the less concentration of OXD-7 in the mixture, resulting in decreased UV absorption. The cyclic photoresponses of the three devices are compared in the Figure 3.14 (c). The photodetector parameters of the devices at 0V were compared and are summarized in the Table 3.2.

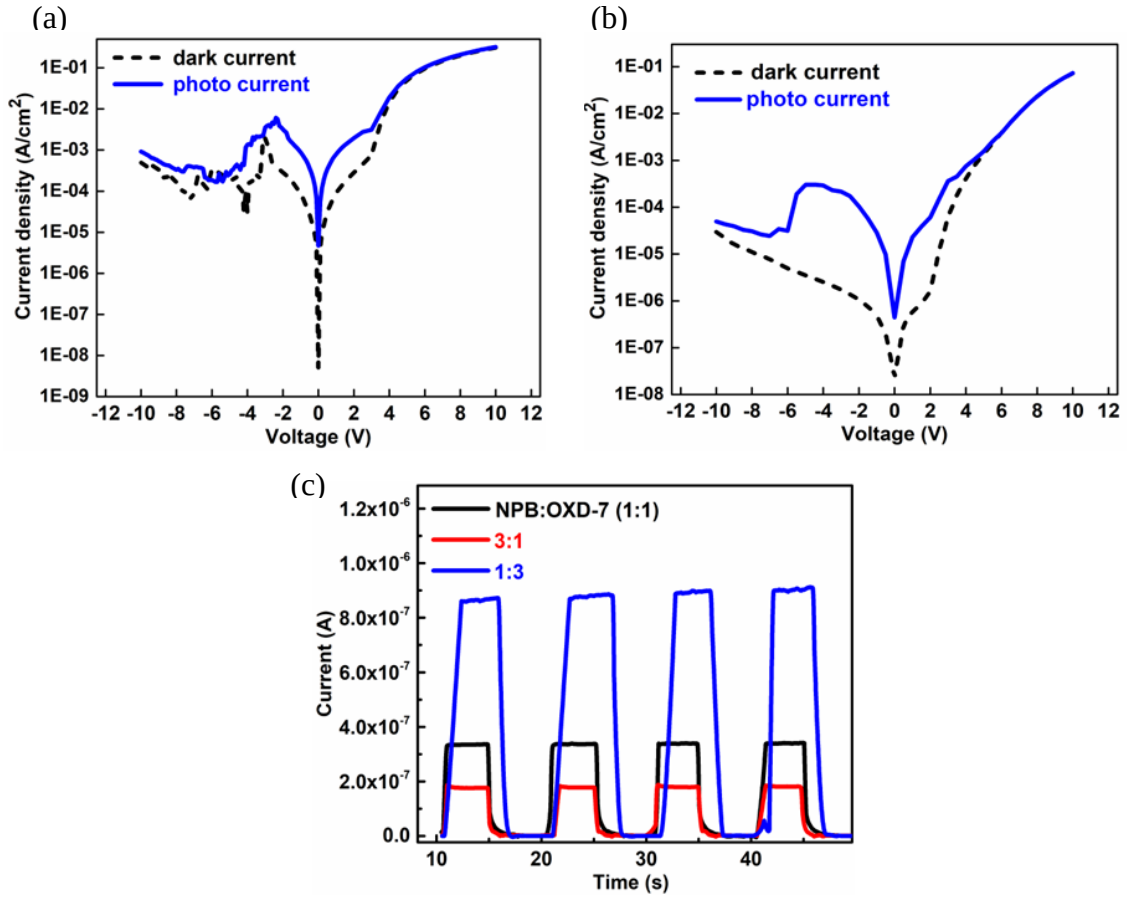

Figure 3.14. Steady state IV of dark and photo current under 365 nm UV light (a) NPB: OXD-7 (1:3) device (b) NPB:OXD-7 (3:1) devices (c) cyclic photoresponse of NPB:OXD-7 (1:1, 3:1 and 1:3) devices.

NPB:OXD-7	ON/OFF ratio	Responsivity (mA/W)	Detectivity (Jones)	Rise time	Fall time
1:1	0.26×10^{2}	4.00	1.76×10^{10}	287 ms	287 ms
1:3	0.96×10^{3}	4.30	1.00×10^{11}	191 ms	279 ms
3:1	0.18×10^{2}	0.37	4.30×10^{9}	1000 ms	382 ms

Table 3.2. Summary of the detector performance of the NPB:OXD-7 (1:1, 1:3 and 3:1) devices.

The effect of high UV absorption of OXD-7 is reflected in the UV-detector performance of these devices. Further, the OLED performance of the same devices was also analyzed. The

devices with 1:1 and 3:1 ratios exhibited comparable performance. The J-V-L plots, CE vs. current density plots and EL spectra of the devices were compared as shown in Figures 3.15 (a), (b) and (c), respectively.

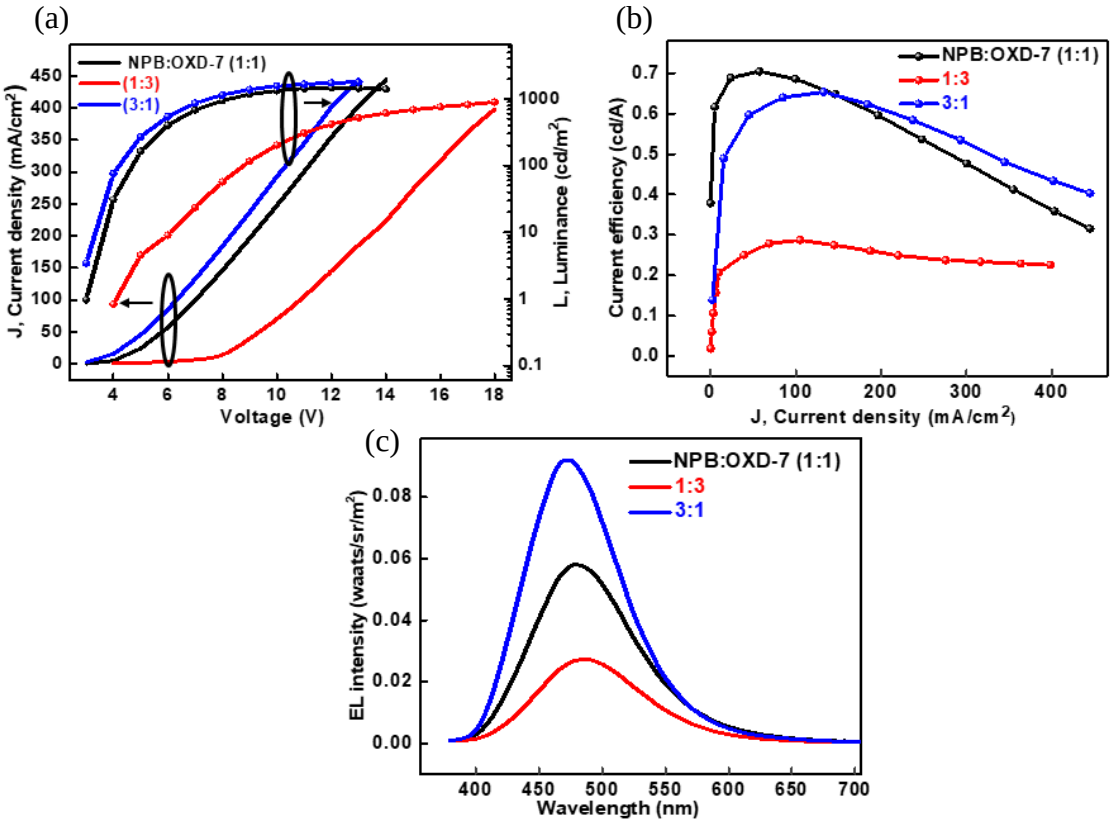

Figure 3.15. (a) J-V-L plot and (b) CE *vs.* current density plot (c) EL spectra with maximum intensities of NPB:OXD-7 (1:1, 1:3 and 3:1) devices.

The 1:3 device with more OXD-7 demonstrated a marked decrease in current density and luminance compared to 1:1 and 3:1. The variation in device performance suggests that an additional factor may be influencing the exciplex emission in the devices. This hypothesis has led to the consideration of surface potential effects in organic small molecules. This finding is crucial as it highlights that while UV absorption of OXD-7 is a significant factor, the role of surface potential cannot be ignored in understanding the device performances. Further

investigation into the surface potential and its impact on device performance is needed to fully understand the mechanisms in the devices.

3.4.4.3 Effect of spontaneous orientation polarization (SOP)

Spontaneous orientation polarization (SOP) has been observed in films of organic small molecules, which consist of randomly or horizontally oriented molecules[32]. This phenomenon is dependent on the molecular orientation within the film and occurs in molecules that possess a permanent dipole moment (PDM). The surface potential (SP) arises from the spontaneous ordering of these PDMs, a process known as SOP. In organic semiconductor films, PDM results from the symmetric structure of the molecules. The macroscopic orientation polarization in the film occurs when the average orientation of PDMs aligns in a specific direction as shown in Figure 3.16. When this PDM remains constant on average, the SP becomes directly proportional to the thickness of the film. SOP can be assessed through surface potential measurements using Kelvin-probe microscopy, typically conducted at room temperature, in the dark and under vacuum conditions[33]. This technique minimizes surface free energy by reducing the boundary effects between the vacuum and the film surface. Despite extensive research, the underlying mechanism of SOP remains unclear. Understanding SOP is crucial for optimizing the design and functionality of organic semiconductor devices. The effect of SOP on the photodetection capabilities of devices can be better understood through the study of vacuum-deposited films. SOP is more pronounced in vacuum-deposited films compared to solution-processed films, making them suitable for this investigation.

Figure 3.16. Illustration of SOP in a thin-film and development of surface potential.

Prior to device fabrication, surface potential mapping of thin films was performed to analyze their properties. Thin films of NPB, OXD-7, and a 1:1 mixture of NPB:OXD-7 were fabricated using vacuum deposition. The surface potential mapping of these films was conducted using kelvin probe force microscopy (KPFM) combined with atomic force microscopy (AFM) under ambient conditions[34]. The KPFM images with the range of surface potential values are shown in Figure 3.17 (a). The surface potential measurements indicate that the NPB film exhibits a less positive and more variable potential, whereas the OXD-7 film shows a consistent and high negative potential. The mixed film of NPB:OXD-7(1:1) demonstrates a more uniform potential, between the individual components. The results show that OXD-7 has high surface potential compared to NPB. In 2020 Adachi *et al*. have reported the role of spontaneous orientational polarization in organic donor–acceptor blends for exciton binding[35]. The behavior of exciplexes in organic semiconductor devices is significantly influenced by the presence of an electric field. Specifically, molecules with high SOP within the exciplex film generate a surface potential, which plays a crucial role in the dissociation of exciplexes. Exciplexes, which are complexes formed between excited donor and acceptor molecules is sensitive to such internal electric fields. When molecules in the exciplex film possess high SOP, they create a surface potential due to the orientation of permanent dipole moments. This surface potential

can lead to the dissociation of the exciplexes as illustrated in Figure 3.17 (b). In order to confirm the effect of SOP in photoluminescence, the photoluminescence emission spectra of the mixed films were compared as shown in Figure 3.17 (c).

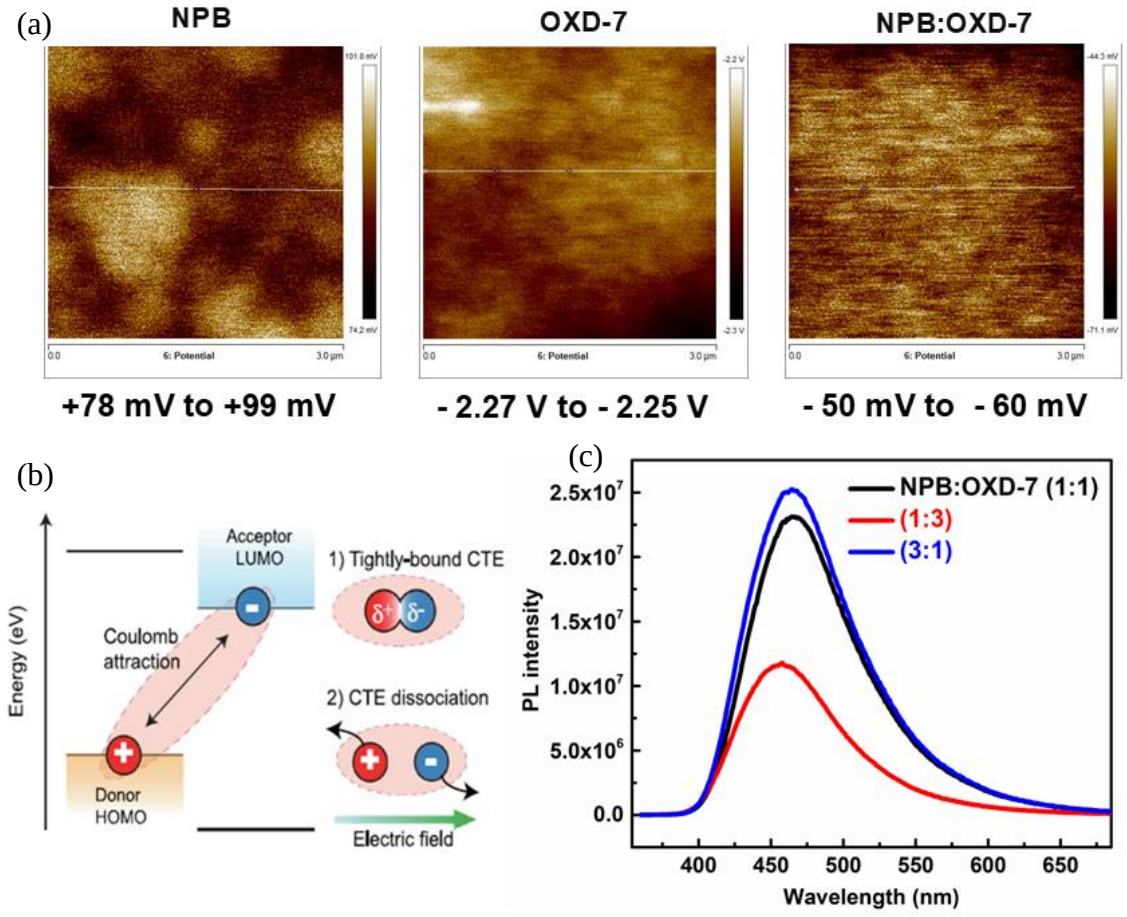

Figure 3.17. (a) Surface potential mapping images of the vacuum-deposited NPB, OXD-7 and NPB:OXD-7 thin films (b) illustration of weakening of exciplex in presence of electric field[35]. (c) comparison of photoluminescence spectra of the vacuum-deposited thin films of NPB:OXD-7 (1:1, 1:3 and 3:1).

From the photoluminescence spectra, 3:1 film showed very poor luminance compared to 1:1 and 3:1. Hence, OXD-7 with more SOP caused the dissociation of exciplex excitons resulting in reduced luminance in 1:3 film compared to the other two. The exciplex dissociation is

beneficial for organic photodetectors (OPDs) as it enhances photocurrent generation. In these devices, the dissociation of exciplexes under an electric field result in efficient charge separation and photocurrent generation. Conversely, low SOP is found to favor exciplex emission, which is desirable for OLEDs. This distinction is crucial for the design and optimization of organic multifunctional devices. By tailoring the SOP of the materials used, it is possible to enhance either the dissociation of exciplexes for OPDs or the emission of exciplexes for OLEDs, thus improving the performance of these devices for their respective applications.

3.4.4.4 Fabrication and characterization of vacuum-deposited devices

The impact of SOP is more significant in vacuum-deposited films compared to solution-processed films. Therefore, we opted for fully vacuum-deposited devices instead of using solution processing method. The modified device architecture for fully-vacuum deposited devices are illustrated in the Figure 3.18 (a). HAT-CN serves as the HIL, while an additional layer of NPB is incorporated before the emissive layer to enhance hole transport. Three devices were fabricated with co-deposited layer of NPB:OXD-7 in varying ratios as 1:3, 1:1, and 3:1. Initially, we performed OLED characterization of the devices, analyzing the J-V-L plot, current efficiency *vs.* current density plot and EL spectra as depicted in the Figure 3.18 (b), (c) and (d) respectively. The NPB:OXD-7 (3:1) device with less concentration of OXD-7 demonstrated the highest current efficiency among the three. The 1:3 device, containing a higher proportion of OXD-7, exhibited low current density and luminance, resulting in reduced efficiency. In this device, the high surface potential of OXD-7 in the mixture leads to exciplex dissociation, resulting in a reduced OLED performance.

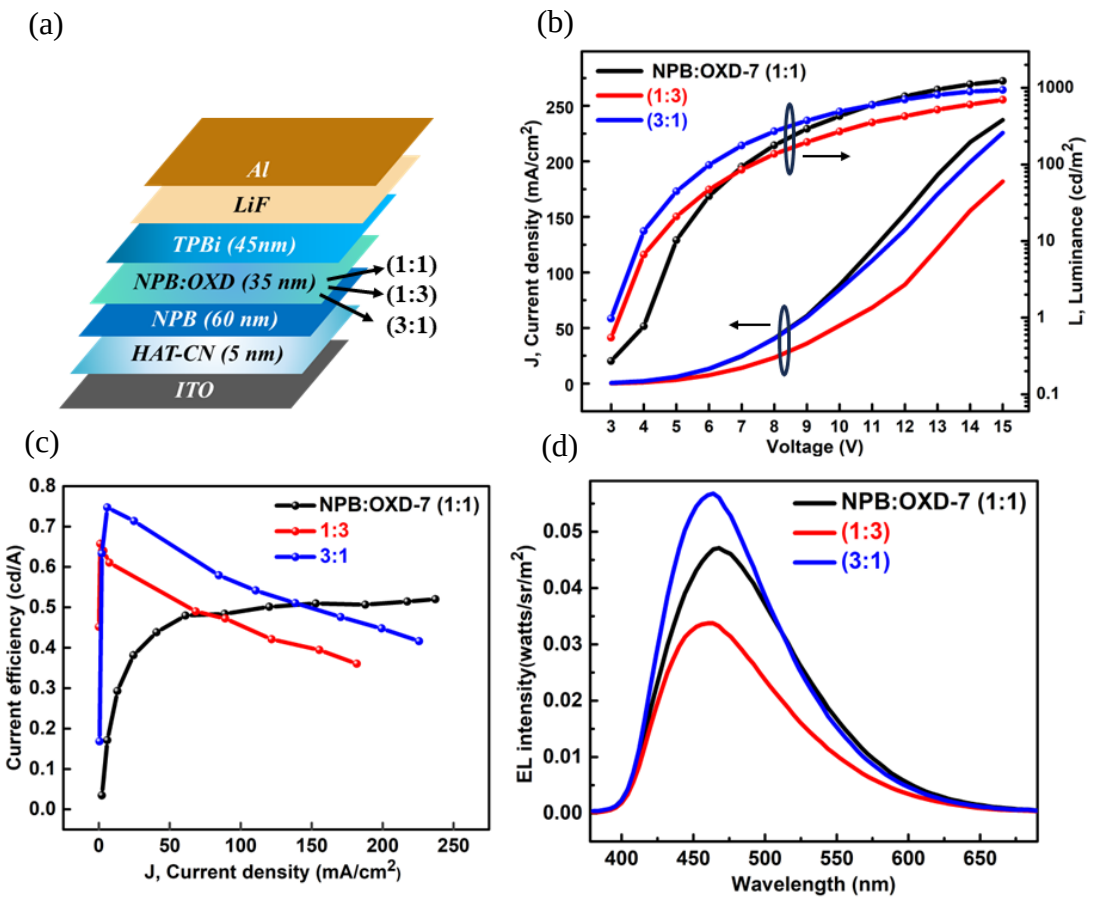

Figure 3.18. (a) Device architecture (b) J-V-L plot (c) CE *vs.* current density plot and (d) EL spectra at maximum intensities of NPB:OXD-7 (1:1, 1:3 ,3:1) vacuum-deposited devices.

Subsequently, we conducted photodetector characterization. The steady-state IV and cyclic photoresponse of the devices are presented in the Figure 3.19 (a), (b), (c) and (d) respectively.

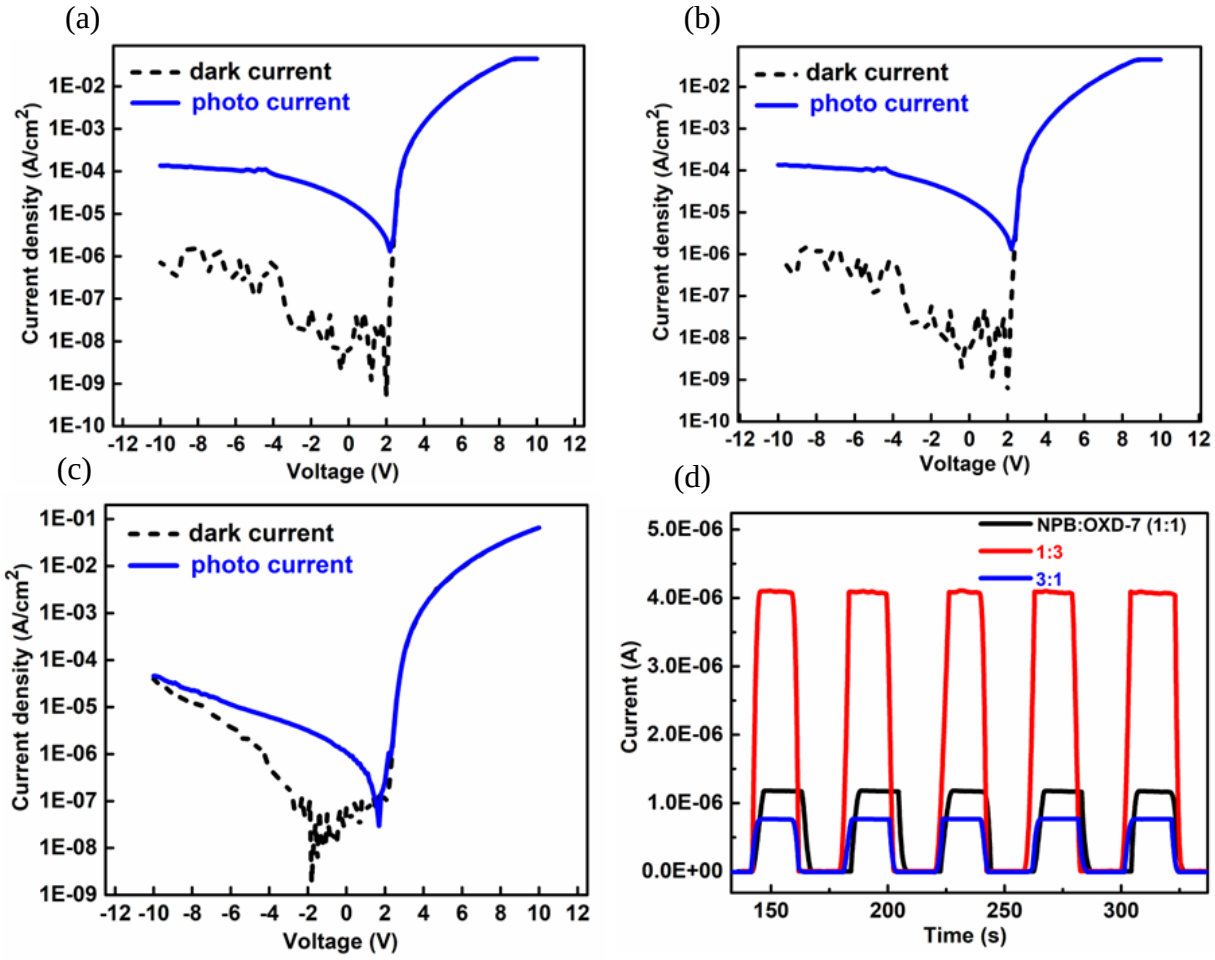

Figure 3.19. Steady state IV of dark and photo current under 365 nm UV light of the vacuum-deposited devices (a) NPB:OXD-7 (1:1) (b) 1:3 (c) 3:1 (d) comparison of cyclic photoresponse of the devices.

Among the photodetector devices, the 1:3 device showed better performance than the others, while the 3:1 device, with a lower OXD-7 content, showed the least performance. In the 1:3 device with a higher OXD-7 content, the increased SOP causes the exciplex to dissociate leading to photocurrent generation. Notably, the self-powered UV detector with a 1:3 ratio exhibited impressive performance, achieving a detectivity of 4×10^{11} Jones, a responsivity of 17 mA/W and an ON-OFF ratio of 3×10^{3} at 0V, while also maintaining satisfactory OLED performance. Comparing the OLED and photodetector performance reveals that the high SOP

of OXD-7, combined with its strong UV absorption plays a crucial role in device performance, contributing to its multifunctionality. The photodetector parameters are summarized in the Table 3.3.

NPB:OXD-7	ON/OFF ratio	Responsivity (mA/W)	Detectivity (Jones)	Rise time	Fall time
1:1	1.00×10^{2}	4.00	1.76×10^{10}	2.36 s	0.89 s
1:3	3.50×10^{3}	17.00	4.00×10^{11}	2.45 s	1.23 s
3:1	0.15×10^{2}	0.92	6.00×10^{9}	1.40 s	2.43 s

Table 3.3. Summary of the photodetector parameters at 0V of the vacuum-deposited devices.

3.5 Conclusion

In this chapter, we successfully demonstrated the dual functionality of an exciplex by using NPB, as the donor and OXD-7, as the acceptor, highlighting its potential for both OLED and UV-photodetector applications. The blue exciplex emission at the NPB/OXD-7 interface was confirmed from the spectroscopic studies. Solution-processed blue exciplex OLED was successfully fabricated. Introducing the yellow phosphorescent dopant PO-01 into the exciplex host resulted in a yellow OLED exhibiting a maximum brightness of 36,000 cd/m^2 and an EQE of 11%. The significant surface potential of OXD-7 facilitated exciplex dissociation at the NPB/OXD-7 interface with its strong UV-absorption, generating photocurrent under UV illumination. This enables the device to function dually as both an OLED and a UV photodetector, achieving a balance between exciplex emission and dissociation. Blend films of varying NPB:OXD-7 ratios (1:1, 1:3, 3:1) were studied to optimize the device performance. The high surface potential and strong UV-absorption of OXD-7, resulted in photocurrent generation. The NPB:OXD-7 (1:3) device performed better as a UV detector but showed poor

performance as an OLED. Conversely, the 3:1 device excelled as an OLED but was a poor UV detector. This study demonstrates that the NPB:OXD-7 exciplex combination holds potential for multifunctionality, enabling the devices to serve as both OLEDs and UV photodetectors. Many exciplex combinations remain unexplored, offering potential for multifunctional devices. By considering factors such as surface potential development, UV absorption, etc. in the transport materials, these combinations could be effectively utilized for enhanced device performance.

3.6 References

1. Li, J.; Li, Z.; Liu, H.; Gong, H.; Zhang, J.; Guo, Q., Advances in blue exciplex–based organic light-emitting materials and devices. *Frontiers in Chemistry* **2022,** *10*, 952116.

2. Chen, Y. S.; Lin, I. H.; Huang, H. Y.; Liu, S. W.; Hung, W. Y.; Wong, K. T., Exciplex-forming cohost systems with 2,7-dicyanofluorene acceptors for high efficiency red and deep-red OLEDs. *Sci Rep* **2024,** *14* (1), 2458.

3. Weber, D.; Morgenstern, A.; Beer, D.; Zahn, D. R. T.; Deibel, C.; Salvan, G.; Schondelmaier, D., Exciplex-driven blue OLEDs: unlocking multifunctionality applications. *Applied Physics a-Materials Science & Processing* **2024,** *130* (6), 1-11.

4. Wang, J.; Zhang, X. L.; Fan, L. X.; Zhang, X. L.; Qin, Y.; Li, R. Q.; Chen, Y. H.; Lai, W. Y.; Zhang, X. W.; Huang, W., Highly efficient solution-processed red phosphorescent organic light-emitting diodes employing an interface exciplex host. *Journal of Materials Chemistry C* **2020,** *8* (29), 9909-9915.

5. Saghaei, J.; Russell, S. M.; Jin, H.; Burn, P. L.; Pivrikas, A.; Shaw, P. E., Rivers of light—Ternary exciplex blends for high efficiency solution-processed red phosphorescent organic light emitting diodes. *Advanced Functional Materials* **2022,** *32* (8), 2108128.

6. Tsai, M.-J.; Huang, W.-L.; Chen, L.-M.; Ruan, G.-L.; Luo, D.; Tseng, Z.-L.; Wong, K.-T., Solution-processed high efficiency OLED harnessing a thermally cross-linked hole-transporting layer and exciplex-forming emission layer. *Journal of Materials Chemistry C* **2023,** *11* (3), 1056-1066.

7. Woo, J. Y.; Park, M. H.; Jeong, S. H.; Kim, Y. H.; Kim, B.; Lee, T. W.; Han, T. H., Advances in solution-processed OLEDs and their prospects for use in displays. *Advanced Materials* **2023,** *35* (43), 2207454.

8. Woo, J. Y.; Park, M. H.; Jeong, S. H.; Kim, Y. H.; Kim, B.; Lee, T. W.; Han, T. H., Advances in Solution-Processed OLEDs and their Prospects for Use in Displays (Adv. Mater. 43/2023). *Advanced Materials* **2023,** *35* (43), 2370314.

9. Wang, S. M.; Zhang, H. Y.; Zhang, B. H.; Xie, Z. Y.; Wong, W. Y., Towards high-power-efficiency solution-processed OLEDs: Material and device perspectives. *Materials Science & Engineering R-Reports* **2020,** *140*, 100547.

10. Murat, Y.; Petersons, K.; Lanka, D.; Lindvold, L.; Yde, L.; Stensborg, J.; Gerken, M., All solution-processed ITO free flexible organic light-emitting diodes. *Materials Advances* **2020,** *1* (8), 2755-2762.

11. Hamanaka, V. N.; Salsberg, E.; Fonseca, F. J.; Aziz, H., Investigating the influence of the solution-processing method on the morphological properties of organic semiconductor films and their impact on OLED performance and lifetime. *Org Electron* **2020,** *78*, 105509.

12. Uddin, A.; Teo, C. In *Fabrication of high efficient organic/CdSe quantum dots hybrid OLEDs by spin-coating method*, Organic Photonic Materials and Devices XV, SPIE: 2013; pp 140-148.

13. Kant, C.; Shukla, A.; McGregor, S. K. M.; Lo, S. C.; Namdas, E. B.; Katiyar, M., Large area inkjet-printed OLED fabrication with solution-processed TADF ink. *Nat Commun* **2023,** *14* (1), 7220.

14. Teichler, A.; Perelaer, J.; Schubert, U. S., Inkjet printing of organic electronics–comparison of deposition techniques and state-of-the-art developments. *Journal of Materials Chemistry C* **2013,** *1* (10), 1910-1925.

15. Amruth, C.; Pahlevani, M.; Welch, G. C., Organic light emitting diodes (OLEDs) with slot-die coated functional layers. *Materials Advances* **2021,** *2* (2), 628-645.

16. Leung, L. M.; Kwong, C. F.; So, S. K., Effects of additives in polymer thick film-organic light emitting diodes (PTF-OLED). *Displays* **2002,** *23* (4), 171-175.

17. Pan, T.; Liu, S.; Zhang, L.; Xie, W.; Yu, C., A flexible, multifunctional, optoelectronic anticounterfeiting device from high-performance organic light-emitting paper. *Light Sci Appl* **2022,** *11* (1), 59.

18. Chen, Y.; Yao, Y.; Turetta, N.; Samorì, P., Vertical organic transistors with short channels for multifunctional optoelectronic devices. *Journal of Materials Chemistry C* **2022,** *10* (7), 2494-2506.

19. Saghaei, J.; Leitner, T.; Mai, V. N.; Ranasinghe, C. S. K.; Burn, P. L.; Gentle, I. R.; Pivrikas, A.; Shaw, P. E., Emissive Material Optimization for Solution-Processed Exciplex OLEDs. *Acs Applied Electronic Materials* **2021,** *3* (11), 4757-4767.

20. Meer, B. B.; Sharma, D.; Tak, S.; Bisen, G. G.; Shirsat, M. D.; Girija, K. G.; Ghosh, S. S., Effect of thermal annealing on an emissive layer containing a blend of a small molecule and polymer as host for application in OLEDs. *Rsc Advances* **2023,** *13* (48), 33668-33674.

21. dos Santos, P. L.; Stachelek, P.; Takeda, Y.; Pander, P. H., Recent advances in highly-efficient near infrared OLED emitters. *Materials Chemistry Frontiers* **2024**.

22. Jankus, V.; Abdullah, K.; Griffiths, G. C.; Al-Attar, H.; Zheng, Y. H.; Bryce, M. R.; Monkman, A. P., The role of exciplex states in phosphorescent OLEDs with poly(vinylcarbazole) (PVK) host. *Org Electron* **2015,** *20*, 97-102.

23. Teixeira, F.; Germino, J. C.; Pereira, L., Wet-Deposited TADF-Based OLED Active Layers: New Approaches towards Further Optimization. *Applied Sciences-Basel* **2023,** *13* (21), 12020.

24. Kumar, M.; Pereira, L., Towards Highly Efficient TADF Yellow-Red OLEDs Fabricated by Solution Deposition Methods: Critical Influence of the Active Layer Morphology. *Nanomaterials (Basel)* **2020,** *10* (1), 101.

25. Ren, H.; Chen, J. D.; Li, Y. Q.; Tang, J. X., Recent progress in organic photodetectors and their applications. *Advanced Science* **2021,** *8* (1), 2002418.

26. Lan, Z.; Lee, M.-H.; Zhu, F., Recent advances in solution-processable organic photodetectors and applications in flexible electronics. *Advanced Intelligent Systems* **2022,** *4* (3), 2100167.

27. Niu, J. Z.; Yang, D.; Ren, X. D.; Yang, Z.; Liu, Y. C.; Zhu, X. J.; Zhao, W. G.; Liu, S. Z., Graphene-oxide doped PEDOT: PSS as a superior hole transport material for high-efficiency perovskite solar cell. *Org Electron* **2017,** *48*, 165-171.

28. Wang, Y. P.; Li, B.; Jiang, C.; Fang, Y. F.; Bai, P. L.; Wang, Y. Q., Study on Electron Transport Characterization in TPBi Thin Films and OLED Application. *Journal of Physical Chemistry C* **2021,** *125* (30), 16753-16758.

29. Zhang, L.; Lü, Z.; Wang, J., The Effect of Carrier Transport Layer on the Electroluminescent Properties of Solution-Processed Thermally Activated Delayed Fluorescent Device based on 4CzPN. *physica status solidi* **2022,** *259* (10), 2200072.

30. Chou, K.-H.; Chen, T.-H.; Huang, X.-Q.; Huang, C.-S.; Chang, C.-H.; Chen, C.-T.; Jou, J.-H. J. M. A., Seven-member-ring-based electron-transporting materials for high-efficiency OLEDs. *Materials Advances* **2023,** *4* (5), 1335-1344.

31. Zhu, H. L.; Choy, W. C. H.; Sha, W. E. I.; Ren, X. G., Photovoltaic Mode Ultraviolet Organic Photodetectors with High On/Off Ratio and Fast Response. *Advanced Optical Materials* **2014,** *2* (11), 1082-1089.

32. Noguchi, Y.; Brütting, W.; Ishii, H., Spontaneous orientation polarization in organic light-emitting diodes. *Japanese Journal of Applied Physics* **2019,** *58* (SF), SF0801.

33. Ito, E.; Washizu, Y.; Hayashi, N.; Ishii, H.; Matsuie, N.; Tsuboi, K.; Ouchi, Y.; Harima, Y.; Yamashita, K.; Seki, K., Spontaneous buildup of giant surface potential by vacuum deposition of Alq 3 and its removal by visible light irradiation. *Journal of applied physics* **2002,** *92* (12), 7306-7310.

34. Stone, A. D. D.; Mesquida, P., Kelvin-probe force microscopy of the pH-dependent charge of functional groups. *Applied Physics Letters* **2016,** *108* (23).

35. Ueda, Y.; Nakanotani, H.; Hosokai, T.; Tanaka, Y.; Hamada, H.; Ishii, H.; Santo, S.; Adachi, C., Role of spontaneous orientational polarization in organic donor–acceptor blends for exciton binding. *Advanced Optical Materials* **2020,** *8* (21), 2000896.

Chapter 4

Yellow emitting exciplex for solution-processable white organic light emitting diodes

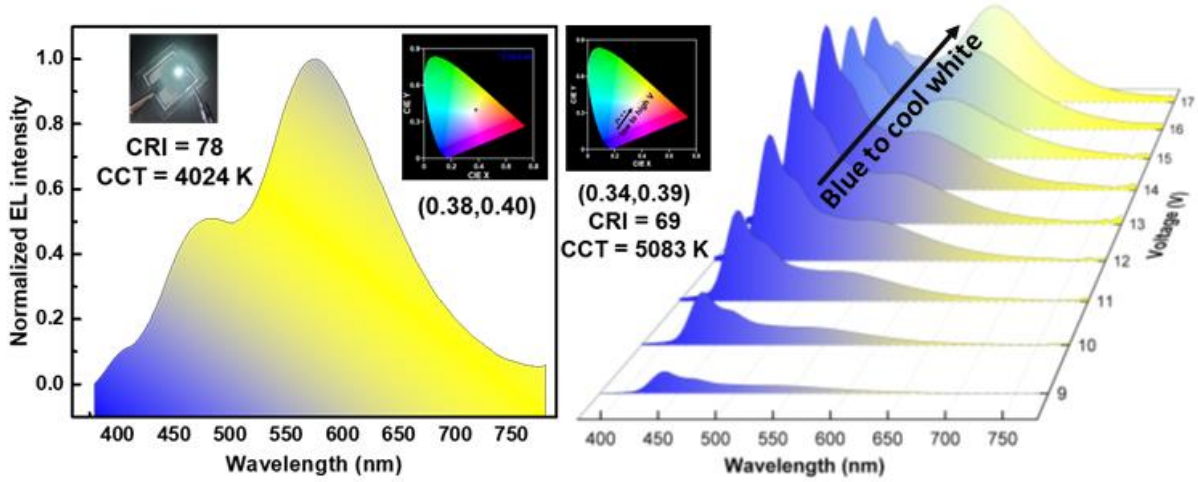

4.1 Abstract

In this chapter, we combine exciplex and excitonic emissions within a single emissive layer to achieve white emission. Two blue emitting hole transport materials (HTMs), namely, N,N'-Bis(3-methylphenyl)-N,N'-diphenylbenzidine (TPD) and Poly(9,9-dioctylfluorene-alt-N-(4-sec-butylphenyl)-diphenylamine) (TFB) were combined with a commonly used electron transport material (ETM), 2,4,6-tris[3-(diphenylphosphinyl)phenyl]-1,3,5-triazine (PO-T2T). Photoluminescence studies confirmed the exciplex emissions in TPD:PO-T2T and TFB:PO-T2T mixed films. Electroluminescence studies showed that the TPD:PO-T2T exciplex organic light emitting diode (OLED) exhibited yellow exciplex emission whereas the TFB:PO-T2T device did not have any exciplex emission; instead, it exhibited the characteristic deep blue emission of TFB. In TPD:PO-T2T device, when 2,2',2''-(1,3,5-Benzinetriyl)-tris(1-phenyl-1-H-benzimidazole) (TPBi) was used as the ETL, a blue emission from the TPD/TPBi exciplex was

obtained along with the yellow exciplex emission. Hence, white emission could be achieved by suitably combining the yellow exciplex emission of TPD:PO-T2T and the blue exciplex emission of TPD/TPBi. To optimize this, the ratios of TPD:PO-T2T in the emissive layer was varied. The TPD:PO-T2T (90:10) device achieved a maximum luminance of 3358 cd/m², a maximum current efficiency (CE) of 4.8 cd/A and a maximum external quantum efficiency (EQE) of 1.8%. Whereas, the TPD:PO-T2T (40:60) device achieved a high CRI value of 78. Subsequently, the deep blue emission of TFB was incorporated into the emissive layer to design a single emissive layer white OLED (WOLED). This device exhibited voltage-dependent emission, where the deep blue emission of TFB dominated at low voltages and the yellow exciplex emission became dominant at higher voltages. Voltage-dependent electroluminescence shows a transition from blue emission with commission internationale de l'Eclairage -1931 (CIE- 1931) coordinates of (0.24, 0.23) to cool white emission with CIE coordinates of (0.34, 0.39), color rendering index (CRI) of 69 and correlated color temperature (CCT) of 5083 K at 14V biasing.

4.2 Introduction

Over the past decade, extensive research has been conducted on OLEDs with the goal of enhancing brightness and outcoupling efficiency. Particularly, WOLEDs have obtained significant attention due to their potential applications in the lighting arena. Conventional tandem structures for WOLEDs typically employ high cost phosphorescent, fluorescent or thermally activated delayed fluorescence (TADF) emitters in complementary colors, connected via charge generation layers (CGLs)[1-4]. These high cost emitters are doped into appropriate host materials to avoid the aggregation induced quenching and to achieve better

efficiency[5-7]. However, integrating exciplex systems as both emitter and host in WOLEDs can significantly reduce the device complexity[8-13]. By using exciplex emitters of complementary colors, innovative device design strategies have been developed offering a cost-effective alternative to traditional high cost emitters in tandem WOLEDs[14-16]. Various strategies have been employed to fabricate WOLEDs, with promising approaches for reducing the number of emissive components by utilizing excimer[17, 18], exciplex[19, 20], electroplex[21] and electromer[22, 23]. In 2009, Yang *et al.* investigated the exciplex emission at the 1,1-Bis[(di-4-tolylamino)phenyl]cyclohexane (TAPC)/ Bathocuproine (BCP) interface and bilayer OLEDs were fabricated [24]. The intensity of exciplex emission increased with the thickness of the BCP layer from 10 nm to 30 nm. Combination of yellow electromer emission from TAPC as well as TAPC/BCP blue exciplex emission gives white light. The light output power *vs.* voltage plot is shown in Figure 4.1 (a). Later in 2016, Angioni *et al.* presented a novel triaryl molecule featuring a benzene-benzothiadiazole-benzene core and utilized the same in a WOLED through a combination of emissive states including exciton, electromer, exciplex and electroplex emissions[25] as shown in Figure 4.1 (b). WOLED with multiple exciplexes featuring blue and yellow-green emitting layers was reported by Beak *et al.*[26]. Blue exciplex emission at the molecular interface of tris(4-carbazoyl-9-ylphenyl)amine (TCTA) and 4,7-diphenyl-1,10-phenanthroline (BPhen) and yellow-green exciplex emissions at 4,4',4''-Tris[phenyl(m-tolyl)amino]triphenylamine (m-MTDATA)/Bphen and m-MTDATA/TPBi combinations were realized. Multiple exciplexes can control the electrical behavior of holes and electrons throughout the entire EML without any fluorescent or phosphorescent dopants. Efficiency roll-off was improved by 40% compared to WOLEDs without multiple emissive layers (EMLs) and a CRI higher than 70 was achieved at 1000 cd/m². The energy level diagram of the

WOLED is shown in Figure 4.1 (c). Pure exciplex WOLED with complementary orange and blue exciplexes have been realized using spacers by zhao *et al.* [27]. CIE coordinates of (0.31 ± 0.00, 0.37 ± 0.02) and a very high CRI of approximately 83 were acheived for the white emission. The orange and blue exciplex emissions are obtained by utilizing TAPC/PO-T2T and (1,3-Bis(N-carbazolyl) benzene) mCP/PO-T2T, respectively. The broad emission band of the exciplex contribute to a stable white light with high CRI. Later Wei *et al.* have presented a novel strategy for structuring WOLEDs by utilizing all exciplex emissions[28]. This approach involves fabricating white devices by simply depositing multiple exciplex acceptor layers on a single exciplex donor layer in a vertical arrangement. Complementary exciplex emissions are achieved at the interfaces of TAPC/TPBi and TAPC/PO-T2T. Based on this strategy, a series of WOLEDs with various arrangements of exciplex acceptor layers on the same exciplex donor layer was demonstrated. The device featuring a common HTL with two different ETLs achieved excellent two-color white emission as shown in the normalized EL spectra in Figure 4.1 (d) with a high CRI of 71 and a current efficiency of 3.17 cd/A. This new strategy effectively addresses the issues associated with using interface exciplexes when employed to achieve multi-color white emission, offering a new approach to develop all-exciplex WOLEDs. In this work, we demonstrate a simplified device architecture that combines yellow exciplex emission with blue exciplex and excitonic emissions. This design yields a high color rendering index (CRI) of 78, underscoring the cost-effectiveness and simplicity of exciplex-based WOLED designs, achieved without resorting to complex tandem structures. Moreover, a unique voltage-dependent emission phenomenon is observed upon the incorporation of a blue emitting HTM. This tunable emission characteristic highlights the potential of novel device

designs utilizing commercially available transport materials to enable color tuning in OLEDs, further emphasizing the versatility and practicality of exciplex-based systems.

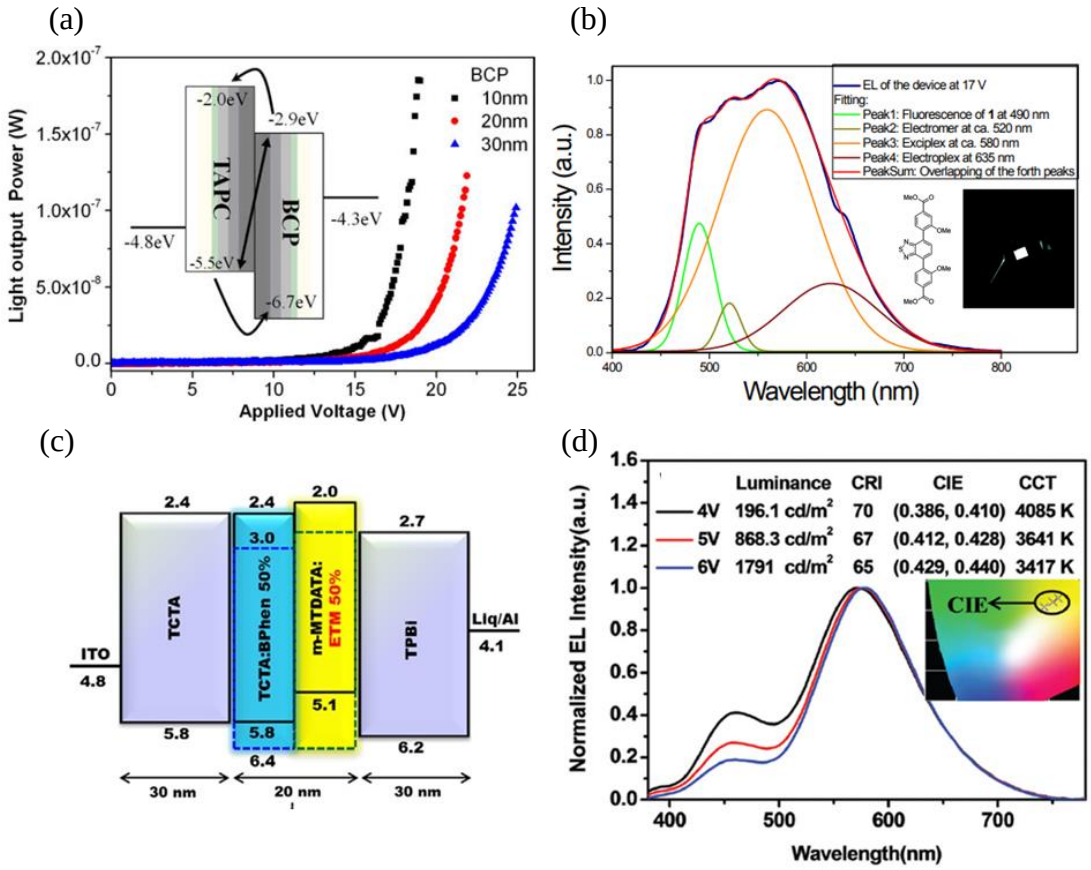

Figure 4.1. (a) The light output power *vs.* applied voltage plots of the WOLEDs by utilizing exciplex emission at TAPC/BCP interface; with varying thickness of BCP is shown. The illustration of exciplex emission in terms of energy levels is shown in the inset (adapted from ref. 24) (b) EL spectra of the WOLED by utilizing exciplex emission at the TPD/1 interface; the structure of the novel molecule and the photograph of the device is shown in the inset (adapted from ref. 25) (c) The device structure of the multiple exciplex OLED in terms of energy levels; TAPC/Bphen (blue) and m-MTDATA/Bphen and m-MTDATA/TPBi (yellow-green exciplex emissions) (adapted from ref. 26) (d) The normalized EL spectra of all-exciplex WOLED with CIE diagram shown in the inset (adapted from ref. 27).

4.3 Experimental section

The devices were fabricated on indium tin oxide (ITO) (purchased from Kintec, Hong Kong, ITO thickness 150 nm, sheet resistance < 15 ohm/sq) coated glass substrates. These patterned ITO substrates were initially cleaned by ultrasonication in chloroform for 15 minutes and then washed in dilute detergent solution followed by ultra-sonication in isopropanol and deionized water for 10 minutes each and dried using a hot air gun. UV-ozone cleaning for 15 min was done just before the fabrication of the devices. Poly(3,4-ethylenedioxythiophene:Polystyrene sulfonate (PEDOT:PSS) was purchased from Heraeus and spincoated at 2500 rpm at ambient conditions. After annealing for 20 minutes at 120°C, the substrates were transferred to the wet glovebox. Mixed solution of TPD and PO-T2T in 1:1 weight ratio was prepared in chlorobenzene and spincoated at 2000 rpm inside glovebox. Substrates were then annealed at 110°C for 15 minutes, followed by annealing in vacuum for 2 hours. The solution of TFB in different weight ratios was prepared in chlorobenzene and it was added to the TPD:PO-T2T solution in chlorobenzene at required concentrations. The substrates were then transferred to thermal evaporation chamber. ETLs (PO-T2T or TPBi), LiF, Al were thermally evaporated using a dry glovebox integrated thermal evaporation system (Angstrom Engineering, Canada) at 10^{-7} torr. The rate of evaporation of ETL, LiF and Al were done at 2 Å/s, 0.1 Å/s and 2 Å/s respectively. The thickness of the layers was confirmed using Dektak XT surface profilometer. After the evaporation, the devices were encapsulated inside the nitrogen filled glovebox by using a UV-curable epoxy (Epoxy Technology inc.). The materials TPD, TFB and TPBi were purchased from Luminescence Technology Corp. (Lumtec), Taiwan and PO-T2T from TCI chemicals.

The absorption studies of the thin films of the materials were done using HORIBA Jobin Yvon and PerkinElmer UV/VIS/NIR Spectrometer, Lambda 950. Emission spectra were measured using a Fluorolog-3 spectrofluorometer (HORIBA), equipped with a 450 W xenon arc lamp. The OLED characterization system consists of a SpectraScan PR (Photo Research) -655 spectroradiometer and a Keithley 2400 sourcemeter integrated with a PC.

4.4 Results and discussion

4.4.1 Strategy for materials selection

In this chapter, blue emitting transport materials are combined with a common ETM. TPD and TFB are selected as the HTMs. TPD is a prominent hole transport material in organic electronic devices. TPD serves as a blue-violet light emitting material or host material in phosphorescent OLEDs due to its wide energy band of approximately 3.2 eV with highest occupied molecular orbital (HOMO) and low unoccupied molecular orbital (LUMO) energy levels at 5.5 eV and 2.3 eV, respectively. TFB is a triarylamine-based semiconductor noted for its high hole mobility of 2×10^{-3} cm²/Vs and a band gap of 3.0 eV, featuring HOMO and LUMO levels of 5.3 eV and 2.3 eV, respectively. The low ionization potential and high hole mobility of TFB make it an ideal material for use as a HTL and HIL. As an interface material, TFB effectively serves as an electron blocking layer, minimizing electron leakage and reducing the possibility of exciton quenching at the interface between the active layer and charge transport layer. It is widely used in quantum dot and perovskite light emitting diodes[29, 30]. PO-T2T is selected as the electron transport material for both combinations. PO-T2T is an electron-deficient semiconducting molecule characterized by a triazine center and three diphenyl phosphines. PO-T2T efficiently forms exciplexes with electron donating host materials such as mCP[31]. These exciplexes have been shown to effectively transfer energy to blue phosphorescent

dopants, such as Bis[2-(4,6-difluorophenyl)pyridinato-C2,N](picolinato)iridium (FIrpic), facilitating triplet harvesting without energy loss[32]. With a deep HOMO level of 7.55 eV, PO-T2T also functions as an ETL and hole blocking layer (HBL) in organic electronic devices. Its electron deficient nature and high triplet energy level contribute to improved device lifetime, efficiency, and lower driving voltage when used as a universal exciplex host in combination with other electron donating materials[33, 34]. In this chapter, we introduce two exciplex combinations; TPD:PO-T2T and TFB:PO-T2T. The molecular structures and the exciplex formation at the TPD/PO-T2T and TFB/PO-T2T molecular interfaces in terms of energy levels are depicted in Figure 4.2 (a) and (b), respectively.

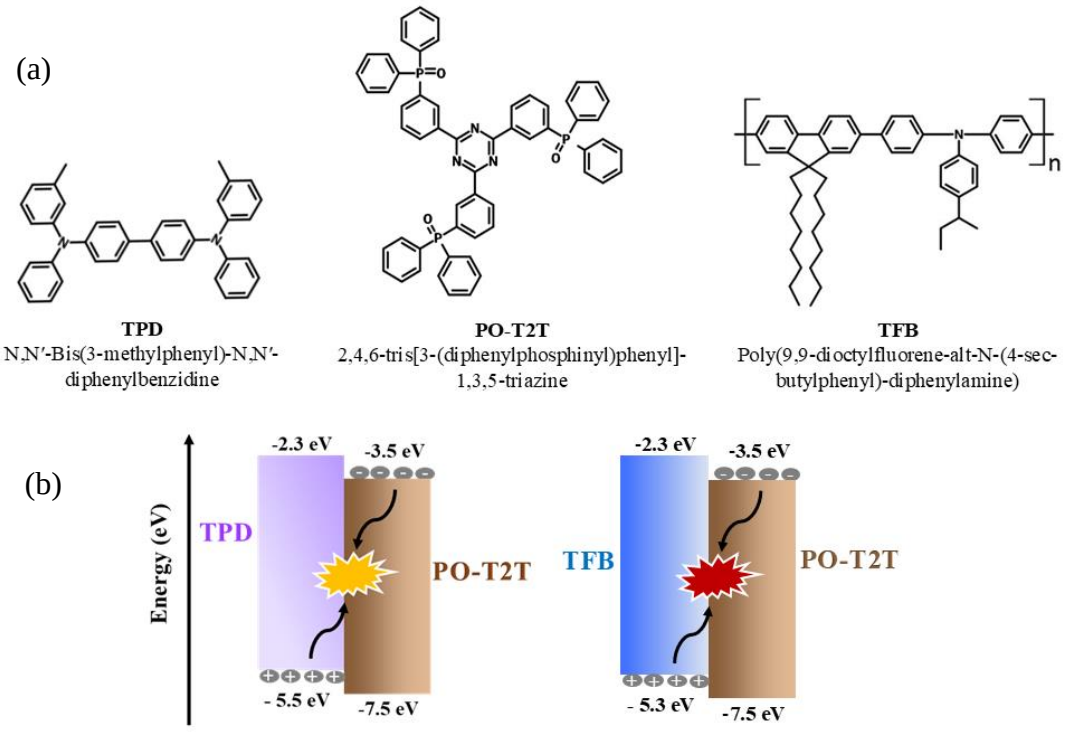

Figure 4.2. (a) Molecular structure of TPD, PO-T2T and TFB (b) schematic representation of exciplex emissions at the molecular interfaces of TPD/PO-T2T and TFB/PO-T2T in terms of energy levels.

The main goal of this work is to design a single-emissive-layer WOLED utilizing exciplex and excitonic emissions, without relying on expensive phosphorescent emitters. The aim is to achieve a non-tandem WOLED design by using only commercially available transport materials.

4.4.2 Spectroscopic studies

To confirm the exciplex emission in the selected combinations, the photoluminescence emission spectra of the thin films of the materials were compared. The emission of TPD and PO-T2T occurs at 400 nm and 375 nm, respectively. The TPD:PO-T2T (1:1) mixed film showed a significantly red shifted and broadened emission at 593 nm as shown in Figure 4.3 (a), confirms TPD:PO-T2T yellow exciplex emission. The TPD:PO-T2T mixed film indicates a feeble emission of TPD as well, the intensity of which is very low compared to that of the exciplex emission. The FWHM values of TPD, PO-T2T and TPD:PO-T2T emission spectra are 44 nm, 82 nm and 137 nm, respectively. For the materials in the second combination, the emission of TFB and PO-T2T occurs at 430 nm and 375nm, respectively. TFB:PO-T2T (1:1) mixed film showed two major emission peaks at 430 and 530 nm, respectively as shown in Figure 4.3 (b). The significantly red shifted and broadened emission at 530 nm is the green exciplex emission in TFB:PO-T2T mixture whereas the narrow blue emission peak around 430 nm is the excitonic emission of TFB. The full width at half maximum (FWHM) values of the emission peaks of TFB, PO-T2T and TFB:PO-T2T are 24 nm, 82 nm and 186 nm, respectively. Thus, exciplex emissions are confirmed in both TPD:PO-T2T and TFB:PO-T2T combinations from the photoluminescence spectra. The emission of TFB is prominently observed in the TFB:PO-T2T mixed film, whereas the emission of TPD is quite weak in the TPD:PO-T2T film. The emission of PO-T2T were completely absent in both cases. Hence, it is expected that

the exciplex emissions with the blue excitonic emissions from both combinations can be effectively utilize for the fabrication of exciplex- based WOLEDs.

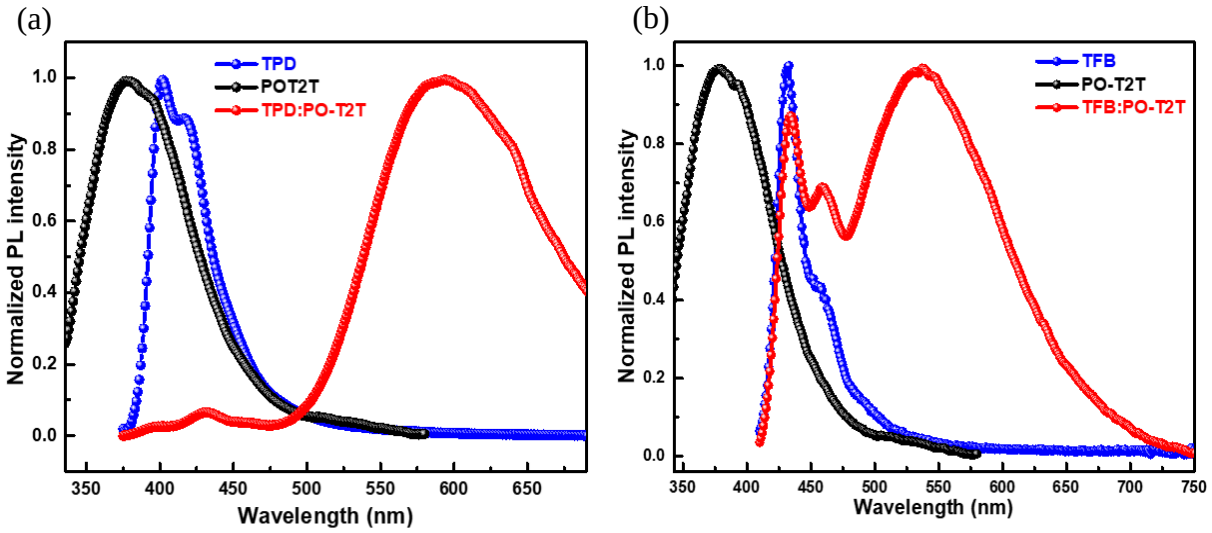

Figure 4.3. Photoluminescence emission spectra of the thin films of the materials (a) TPD, PO-T2T and TPD:PO-T2T (1:1) (b) TFB, PO-T2T and TFB:PO-T2T (1:1).

4.4.3 Device fabrication and characterization

4.4.3.1 Blue OLEDs by utilizing TPD and TFB excitonic emissions

Based on the confirmation of exciplex emissions from the photoluminescence spectra of the mixed films of TPD:PO-T2T and TFB:PO-T2T in equal ratio of thickness, we proceeded with thickness optimization and device fabrication. Prior to developing the exciplex devices, blue OLEDs were designed by utilizing the blue excitonic emissions of TPD and TFB. The device architecture is as follows; ITO/PEDOT:PSS (35 nm)/TPD or TFB (40 nm)/TPBi (40 nm)/LiF (1 nm)/Al (100 nm) (Figure 4.4 (a)). PEDOT:PSS acts as the HIL as well as HTL and TPBi acts as the ETL. For the TPD device, a maximum luminance of 983 cd/m^2 at a current density of 393 mA/cm^2 was obtained, as shown in Figure 4.4 (b). The electroluminescence (EL) spectra of the blue device with TPD as the EML exhibited multiple peaks. The split peaks around 420 nm is the characteristic emission of TPD and in addition a shoulder peak around 475 nm was

observed as illustrated in Figure 4.4 (c). This shoulder peak likely results from the exciplex emission at the TPD/TPBi interface. Based on the HOMO-LUMO gap at the TPD/TPBi interface, exciplex emission is expected to occur around 443 nm and could be red shifted to 470 nm in the EL spectra. However, the emission from TPD dominates the EL spectra more than the possible TPD/TPBi exciplex emission.

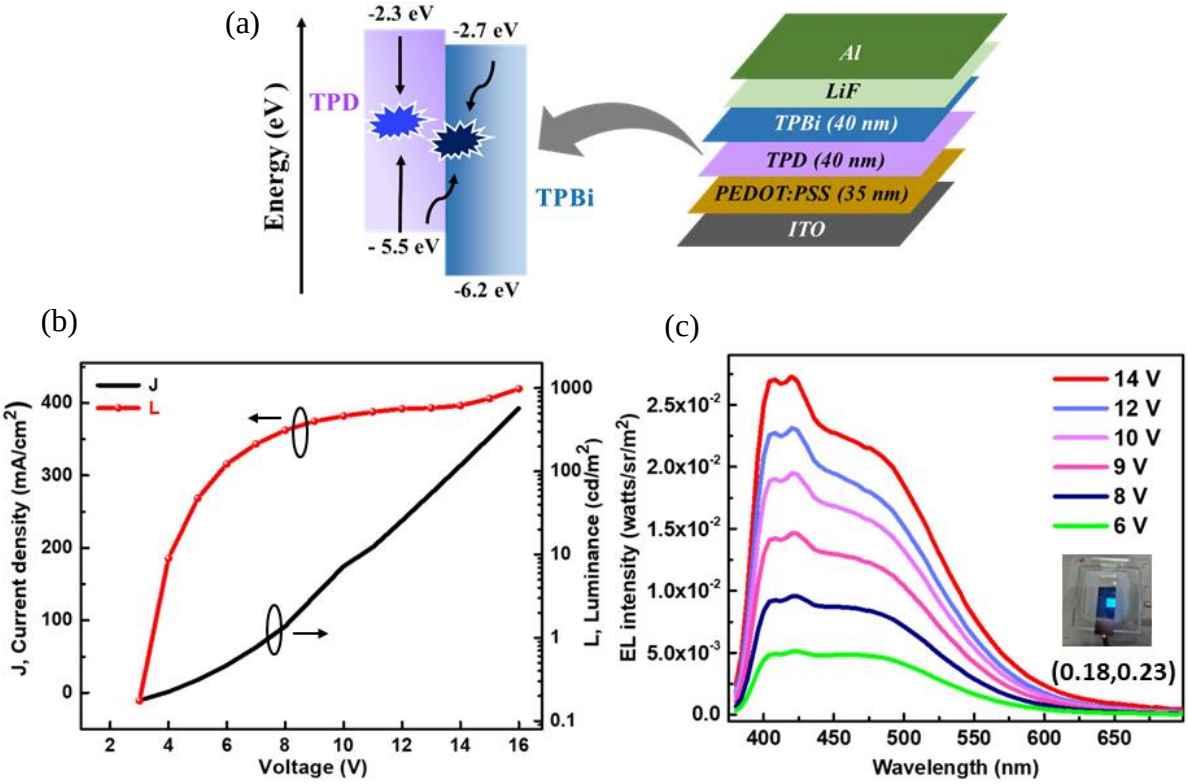

Figure 4.4. (a) The device architecture of the TPD only device with schematic representation of blue emission from TPD and exciplex emission at the TPD/TPBi interface (b) current density (J)-voltage (V)- luminance (L) plot and (c) EL spectra of the of the TPD device at varying voltages with the photograph of the device shown in the inset.

TFB device performed badly when compared to the TPD device with a luminance of 280 cd/m^2 at a current density of 393 mA/cm^2. The device exhibited a single peak of deep blue emission of TFB at 435 nm with its characteristic shoulder peak and there was no trace of any possible

TFB/TPBi exciplex emission. The device architecture with the emission mechanism, EL spectra and J-V-L plots are shown in Figure 4.5 (a), (b) and (c) respectively.

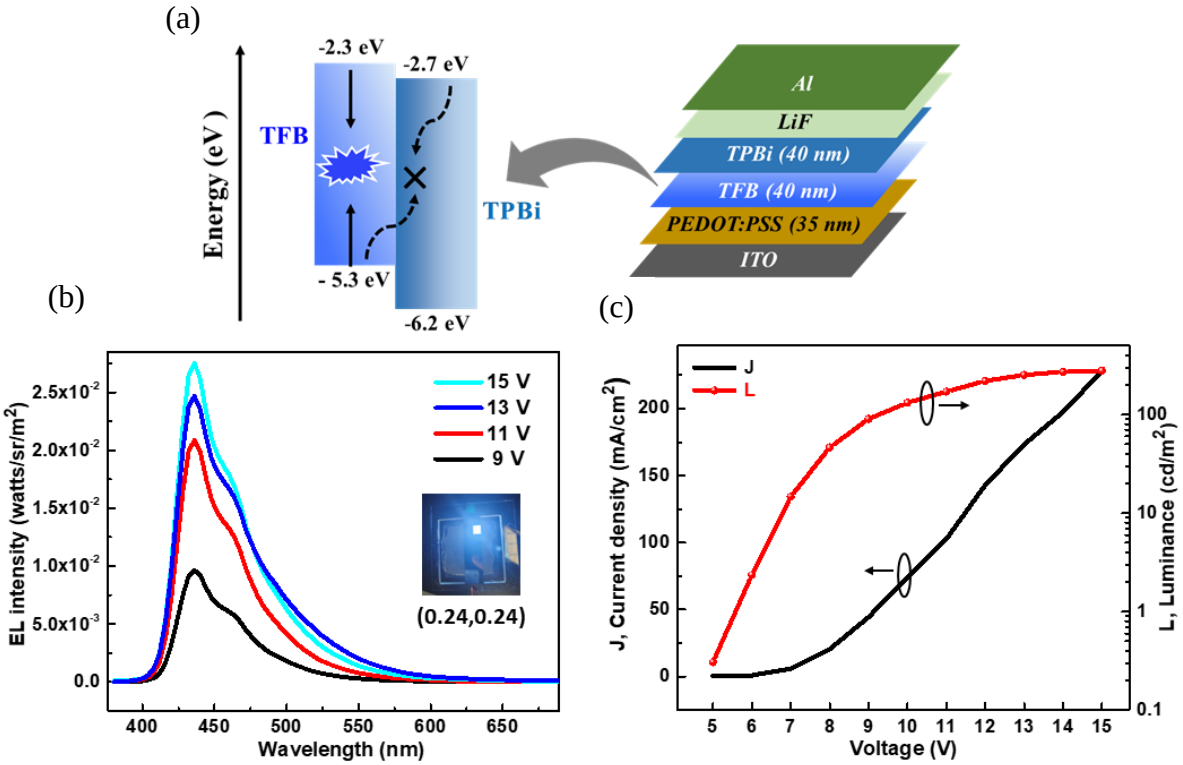

Figure 4.5. (a) The device architecture of the TFB only device with schematic representation of blue emission from TFB (b) EL spectra and (c) J-V-L plot of the TFB device.

4.4.3.2 Yellow and white OLEDs by using exciplex and excitonic emissions

4.4.3.2.1 TPD:PO-T2T exciplex WOLEDs

Based on the confirmation of exciplex emission from the photoluminescence studies, the exciplex OLEDs were fabricated via solution processing method. The device architecture with TPD:PO-T2T as the emissive layer is as follows: ITO/ PEDOT:PSS (35 nm)/ TPD:PO-T2T (1:1) (40 nm) / PO-T2T (40 nm)/ LiF (1nm)/ Al (100 nm). Initially, PO-T2T was only used as the ETL for the better charge transport to TPD:PO-T2T mixed layer from cathode. The device

architecture, energy level diagram, J-V-L plot and EL spectra of the devices are shown in Figure 4.6 (a), (b), (c) and (d) respectively.

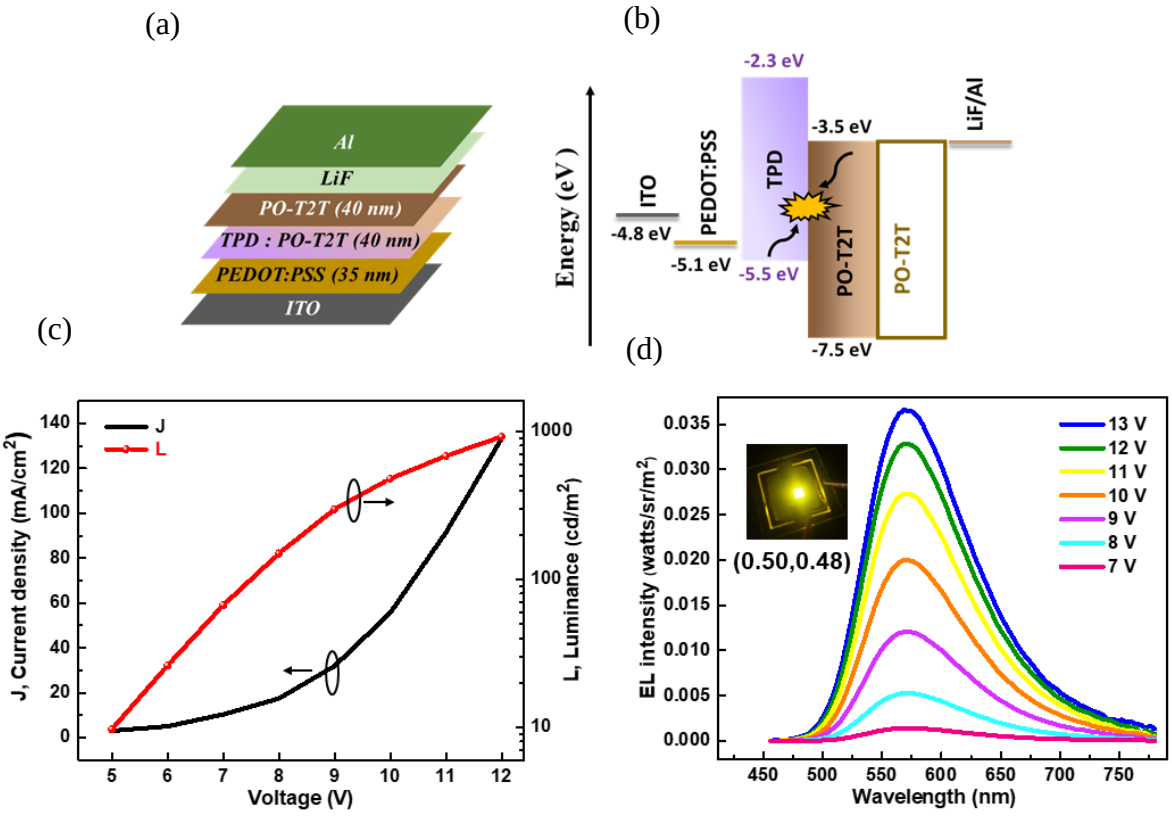

Figure 4.6. (a) Device architecture of TPD:PO-T2T exciplex device (b) energy level diagram of the device and exciplex emission at the molecular interfaces of TPD and PO-T2T in the emissive layer is depicted (c) J-V-L plot and (d) EL spectra with varying voltages and the inset picture shows the photograph of a working device of TPD:PO-T2T exciplex device.

In this typical exciplex device, only the yellow exciplex emission is observed, with the blue emission from the individual components being completely absent. The TPD:PO-T2T exciplex emission is observed at 568 nm. The device exhibited a maximum luminance of 920 cd/m^2 with a current density of 133 mA/cm^2 at 12 V. To enhance electron transport, PO-T2T was replaced by TPBi as the sole ETL. The device characteristics with two different ETLs are compared in Figures 4.7 (a) and (b).

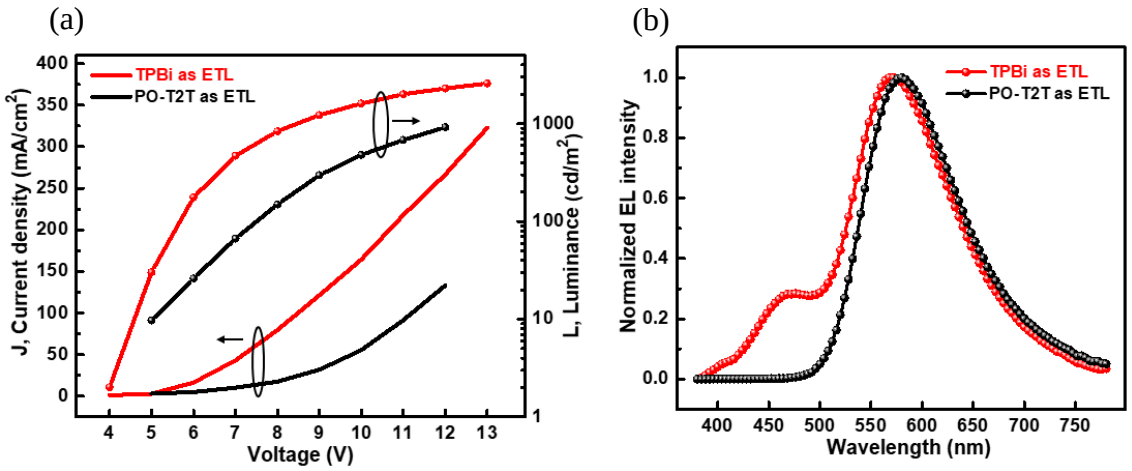

Figure 4.7. Comparison of the (a) J-V-L plot and (b) EL spectra of the TPD:PO-T2T devices with TPBi and PO-T2T as ETLs.

When TPBi is used as the ETL, there is an improvement in the current density and consequently the luminance of the device. The EL spectra showed a blue emission at 476 nm, in addition to the yellow exciplex emission. This blue emission is identified as the exciplex emission at the TPD/TPBi interface from the TPD only device as discussed earlier, which is not observed when PO-T2T is used as the ETL. Hence, combination of blue and yellow exciplex emissions results in white emission. This leads to the design of a single emissive layer WOLED which utilizes two exciplex combinations; TPD:PO-T2T bulk exciplex for yellow emission and TPD/TPBi interface exciplex for blue emission. To enhance the quality of the white light, the emissive layer was modified with different ratios of TPD:PO-T2T as shown in Figure 4.8 (a). The ratios of TPD:PO-T2T is varied to be 40:60, 60:40, and 90:10 in an attempt to balance the intensity of yellow and blue emissions. The EL spectra of the TPD:PO-T2T devices with ratios of 40:60, 50:50, 60:40 and 90:10 is shown in Figures 4.8 (b), (c), (d) and (e), respectively. CIE diagrams are given in the inset of the EL spectra and CCT and CRI index are also mentioned.

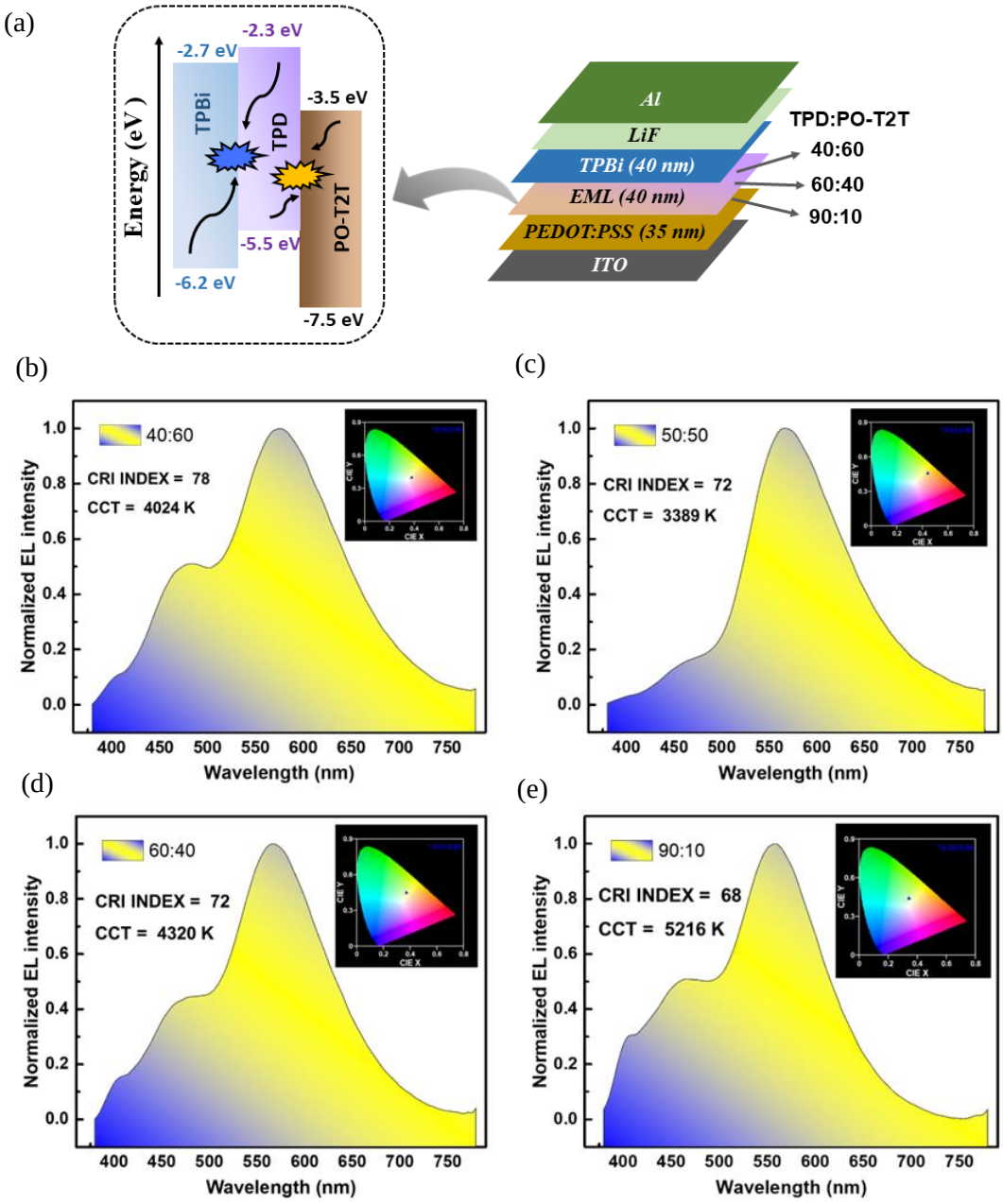

Figure 4.8. (a) Device architecture of TPD:PO-T2T exciplex WOLEDs with the illustration of yellow exciplex emission of TPD:PO-T2T and the blue exciplex emission at TPD/TPBi interface, in terms of energy levels. The EL spectra of the TPD:PO-T2T devices; (b) 40:60 (c) 50:50 (d) 60:40 and (e) 90:10 with CIE diagram, CCT and CRI index shown in the inset of EL spectra.

The EL spectra show blue and yellow emissions with varying intensities. Notably, the blue emission intensity is weak in the 50:50 device compared to the others. This happens because an equal concentration of TPD and PO-T2T results in more TPD:PO-T2T exciplex emission (yellow). For all other devices, two distinct peaks are observed in the blue region; the emission of TPD around 400 nm and the blue exciplex emission of TPD/TPBi at around 468 nm. The 90:10 device exhibited the highest blue emission intensity, while the 50:50 device showed the least as expected. The 40:60 and 60:40 devices had almost similar blue emission intensities. The CIE coordinates, ratio of blue to yellow emission intensities, CRI indices, and CCTs are compared and summarized in Table 4.1.

TPD:PO-T2T	CIE coordinates	Blue / yellow intensity ratio (%)	CRI index	CCT
40:60	(0.38,0.40)	27.08%	78	4024 K
50:50	(0.44,0.46)	08.90%	72	3389 K
60:40	(0.37,0.45)	26.50%	72	4320 K
90:10	(0.34,0.44)	37.80%	68	5216 K

Table 4.1. Summary of the emission parameters of WOLEDs with varying ratios of TPD and PO-T2T (40:60, 50:50, 60:40, and 90:10).

The 40:60 device with low concentration of TPD achieves the highest CRI value of 78. Here, low concentration of TPD creates a balance between blue and yellow exciplex emissions giving white light. The CIE coordinates for the 40:60 and 90:10 devices are closer to the true white point (0.33, 0.33). In the 90:10 device, higher concentration of TPD gives more blue emission with contribution from TPD/TPBi exciplex emission as well as emission of TPD. Hence, this

device yields the highest blue to yellow intensity ratio of 37.8%. According to European standards, a CCT of 3000K - 4000K is considered neutral white and 4000K - 6500K is categorized as cool white emission. Here, the 50:50 device provides neutral white emission, while the other devices exhibit cool white emission. The J-V-L plot and current efficiency (CE) *vs.* current density plots of the WOLEDs are presented in Figure 4.9 (a) and (b), respectively.

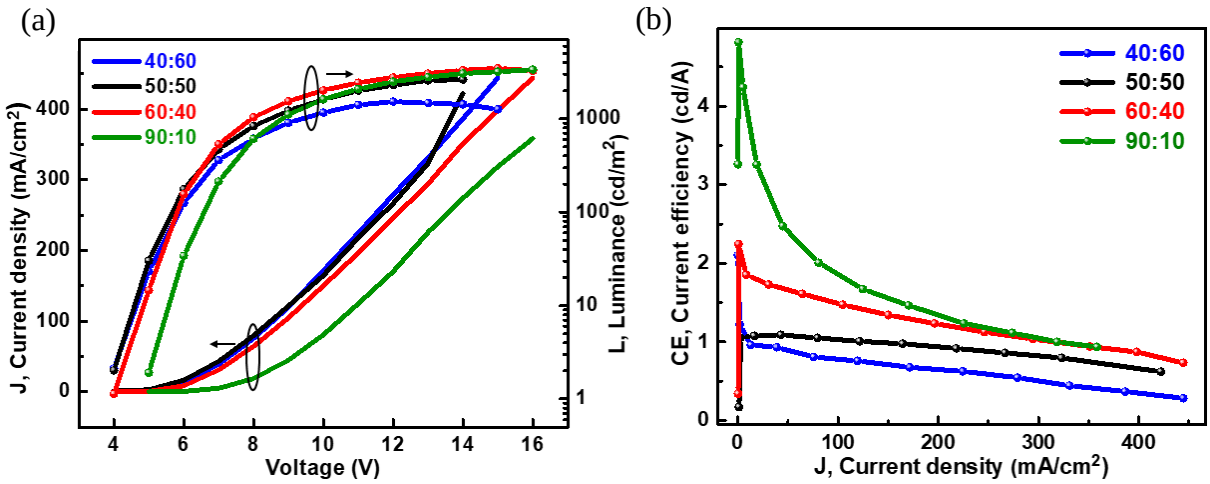

Figure 4.9. (a) J-V-L plot and (b) CE *vs.* current density plots of the TPD:PO-T2T exciplex WOLEDs with varying ratios of TPD and PO-T2T (40:60, 50:50, 60:40, and 90:10).

The 40:60 device performed badly, while the 90:10 device exhibited superior performance compared to the other devices. This indicates that a high concentration of PO-T2T diminishes device performance, whereas high concentration of TPD enhances device efficiency. The 90:10 device showed low current density due to the reduced electron mobility due to the low concentration of PO-T2T in the emissive layer. The summary of device performances at 10 V and the maximum efficiencies are provided in Table 4.2. The 90:10 device achieved a maximum luminance of 3358 cd/m², a maximum CE of 4.8 cd/A and a maximum external quantum efficiency (EQE) of 1.8%. Overall, the 90:10 device demonstrated the best performance along with the white emission.

TPD: PO-T2T	Luminance (cd/m^2)	Current density (mA/cm^2)	Current efficiency (cd/A)	EQE (%)	Max Luminance, max CE, max EQE
40:60	860 ± 13	170 ± 2.0	0.60 ± 0.03	0.23 ± 0.01	1526 cd/m^2, 2.1 cd/A, 0.95%
50:50	1480 ± 34	171 ± 66	0.90 ± 0.03	0.40 ±0.01	2625 cd/m^2, 2.25 cd/A, 0.94%
60:40	1840 ± 47	159 ± 2.5	1.12 ± 0.02	0.40 ±0.02	3474 cd/m^2, 2.24 cd/A, 0.90%
90:10	1770 ± 82	100 ± 8.5	1.83 ± 0.10	0.67 ± 0.04	3358 cd/m^2, 4.8 cd/A, 1.80%

Table 4.2. The summary of device performance of TPD:PO-T2T exciplex WOLEDs with varying ratios of TPD and PO-T2T (40:60, 50:50, 60:40, and 90:10).

4.4.3.2.2 TFB:PO-T2T Blue OLED

The TFB:PO-T2T exciplex device was fabricated using a similar architecture as the TPD:PO-T2T device, with the emissive layer consisting of a mixed film of TFB and PO-T2T. But the device exhibited a deep blue emission of TFB with no trace of TFB:PO-T2T exciplex emission. While the TFB:PO-T2T exciplex emission was clearly observed in photoluminescence, the same was completely absent in electroluminescence. This indicates that the TFB:PO-T2T exciplex cannot be electrically excited. The device architecture, energy level diagram, J-V-L plot, and EL spectra of the devices are shown in Figure 4.10 (a), (b), (c), and (d) respectively. The device efficiency significantly decreased and the turn-on voltage increased from 6 V to 8 V compared to the TFB-only device.

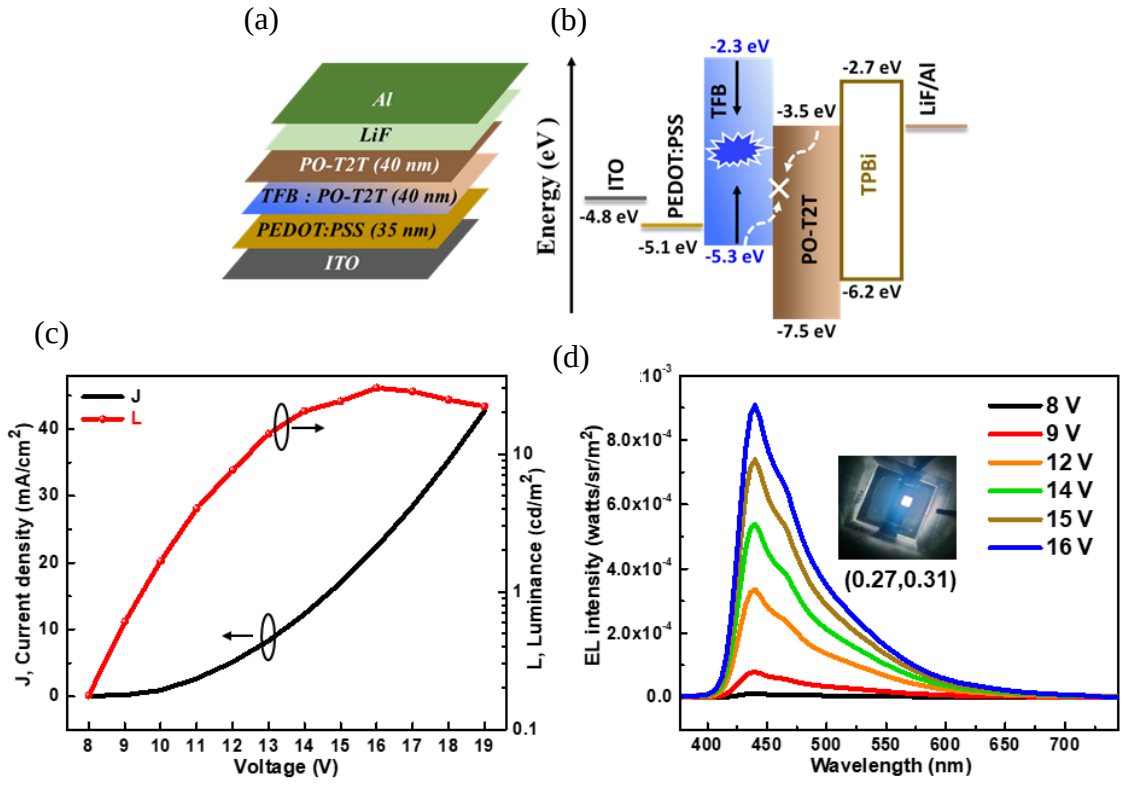

Figure 4.10. (a) Device architecture of TFB:PO-T2T exciplex device (b) energy level diagram of the device with a deep blue emission of TFB in the emissive layer is depicted (c) J-V-L plot and (d) EL spectra of the TFB:PO-T2T device.

4.4.3.2.3 Color tunable emission from a single emissive layer WOLED

Later, to enhance the quality of white emission, we propose integrating the exciplex and excitonic emissions together in a single emissive layer. The deep blue emission of TFB can be combined with the TPD:PO-T2T yellow exciplex emission to achieve white light. The device architecture for the single emissive layer WOLED is as follows: ITO/ PEDOT:PSS (35 nm)/ TPD:PO-T2T (90:10): x wt% TFB (40 nm) / TPBi (40 nm)/ LiF (1 nm)/ Al (100 nm), where x= 0.2, 0.4, and 0.6 wt%. Here, TFB is doped into the TPD:PO-T2T mixed layer in various concentrations. The yellow exciplex emission in TPD:PO-T2T with the blue excitonic emission from TFB and blue exciplex emission at TPD/TPBi interface gives a voltage

dependent white emission. The EML configuration with the emission mechanisms involved are depicted in Figure 4.11 (a) and the device architecture is shown in Figure 4.11 (b).

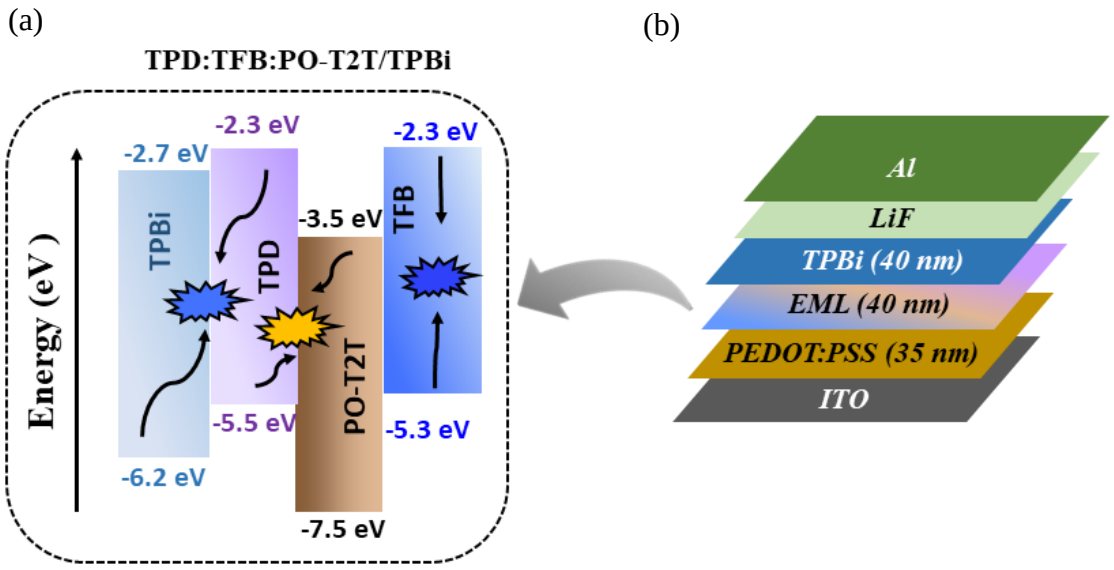

Figure 4.11. (a) EML configuration of the TFB doped TPD:PO-T2T device. yellow exciplex emission in TPD:PO-T2T, blue excitonic emission from TFB and blue exciplex emission at TPD/TPBi are depicted in terms of energy levels (b) device architecture of the TFB doped TPD:PO-T2T device.

The emissive layer consists of TPD:PO-T2T in 90:10 ratio, with varying concentrations of TFB (0.2, 0.4, and 0.6 wt%) doped into it. The EL spectra and the shift in CIE coordinates of the devices are shown in Figure 4.12 (a) - (f). The EL spectra consisted two peaks: deep blue emission from TFB at 436 nm and yellow exciplex emission at 568 nm. The blue emissions from TPD and the TPD/TPBi exciplex were completely absent. Interestingly, a voltage dependence was observed in the EL, with blue emission dominating up to 14V and then decreasing. Whereas the yellow exciplex emission is distinctly seen after 11V and became dominant at 17V. The enhancement of yellow emission at higher voltages got suppressed as the percentage of TFB in the mixture increased, indicating that the presence of TFB is

responsible for the voltage dependence. The J-V-L plots of the devices are compared in Figure 4.13 (a). The device performance was notably poor when TFB was incorporated into the emissive layer. The device with 6 wt% TFB achieved a maximum luminance of 406 cd/m² at a current density of 126 mA/cm². Additionally, an increase in the TFB concentration resulted in a decrease in the turn-on voltage.

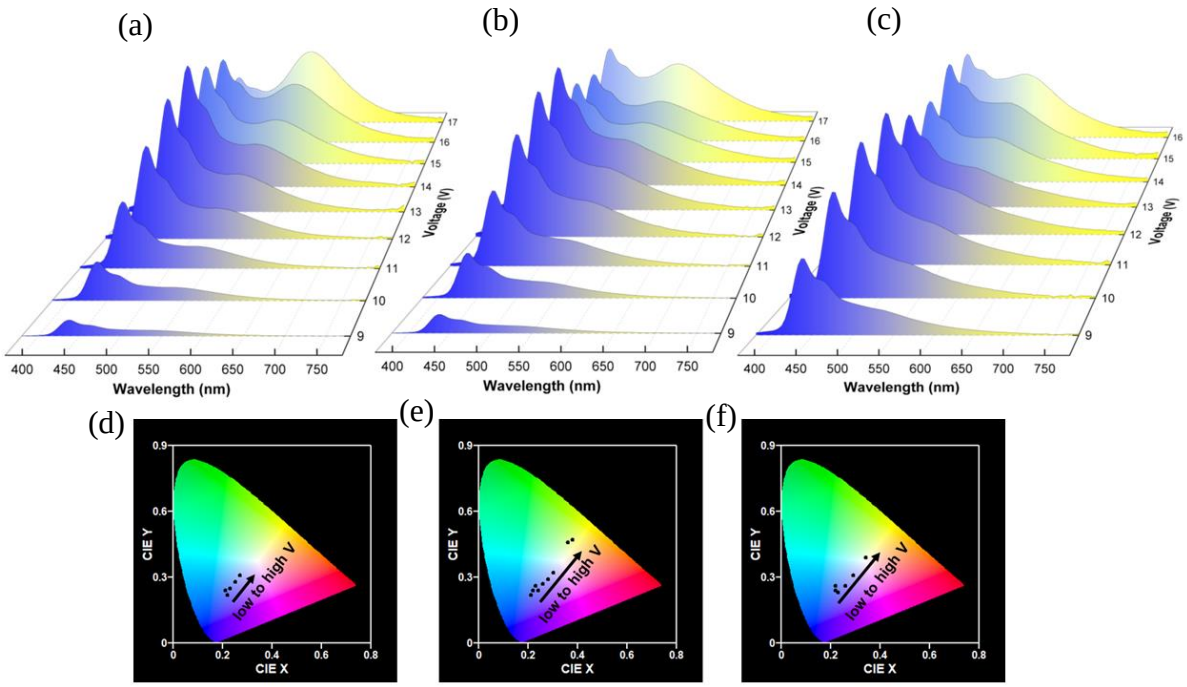

Figure 4.12. EL spectra of the devices with respect to voltage at different concentrations of TFB (a) 2 wt% (b) 4 wt% and (c) 6 wt% respectively. Variation in CIE coordinates of the devices at different concentrations of TFB (d) 2 wt% (e) 4 wt% and (f) 6 wt% respectively.

In the TFB devices discussed in the previous section, the direct excitation of TFB is always preferred and there were no exciplex emissions in TFB:PO-T2T or TFB:TPBi. Here, holes from PEDOT:PSS preferentially reach the HOMO of TFB rather than that of TPD. This might be due to a lower barrier of 0.2 eV for the holes at the PEDOT:PSS/TFB interface compared to a barrier of 0.4 eV at the PEDOT:PSS /TPD interface. The TFB:PO-T2T exciplex cannot be

electrically excited as discussed in the previous section. At lower voltages, charge carriers prefer the direct excitation of TFB leading to emission, while at higher voltages holes overcome the energy barrier to reach the HOMO of TPD causing yellow exciplex emission to become dominant. This voltage-dependent EL demonstrates a transition from blue emission with CIE coordinates (0.24, 0.23) to cool white emission with CIE coordinates (0.34, 0.39), CRI of 69 and CCT of 5083 K, respectively. The tuning of emission in the devices are depicted in Figure 4.13 (b).

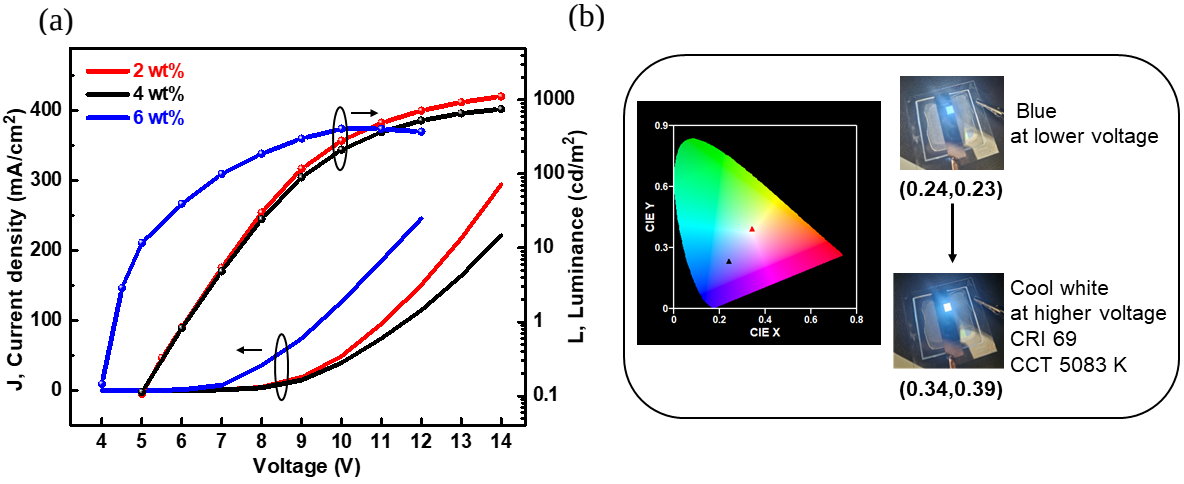

Figure 4.13. (a) J-V-L characteristics and (b) CIE coordinates showing the variation in emission and photographs of the TFB doped devices.

4.5 Conclusion

The integration of exciplex and excitonic emissions within a single emissive layer to achieve WOLEDs is demonstrated. By combining blue emitting HTMs (TPD and TFB) with PO-T2T as the ETM, confirmed exciplex emissions from the photoluminescence studies. Whereas, electroluminescence studies showed that only the TPD:PO-T2T device exhibited yellow exciplex emission and TFB:PO-T2T did not give any exciplex emission. The incorporation of TPBi in TPD:PO-T2T exciplex device allowed simultaneous blue and yellow emissions,

achieving white emission by varying the TPD:PO-T2T ratio. The optimized 90:10 device achieved high luminance of 3358 cd/m², current efficiency of 4.8 cd/A and EQE of 1.8%, while the 40:60 device had a high CRI of 78. Further Incorporation of TFB in TPD:PO-T2T device enabled a voltage-dependent emission, demonstrates a transition from blue emission of TFB at lower voltages with CIE coordinates (0.24, 0.23) to cool white emission with CIE coordinates (0.34, 0.39), CRI of 69 and CCT of 5083 K at higher voltage. In conclusion, the use of a single emissive layer device architecture, by utilizing both exciplex and excitonic emissions, successfully achieves white emission with a high CRI of 78. The TFB doped emissive layer led to the observation of voltage-dependent emission, transitioning from blue to cool white. This work paves the way for the development of efficient, high CRI WOLEDs with tunable emission properties, offering significant potential for applications in display technologies and solid-state lighting.

4.6 References

1. Yang, Z. Y.; Hsiang, E. L.; Wu, S. T., High-Performance Tandem White Micro-OLEDs for Virtual Reality and Mixed Reality Displays. *Crystals* **2024,** *14* (4), 332.

2. Miao, Y. Q.; Wei, X. Z.; Gao, L.; Wang, K. X.; Zhao, B.; Wang, Z. Q.; Zhao, B.; Wang, H.; Wu, Y. C.; Xu, B. S., Tandem white organic light-emitting diodes stacked with two symmetrical emitting units simultaneously achieving superior efficiency/CRI/color stability. *Nanophotonics* **2019,** *8* (10), 1783-1794.

3. Xiao, P.; Huang, J.; Yu, Y.; Liu, B., Recent Developments in Tandem White Organic Light-Emitting Diodes. *Molecules* **2019,** *24* (1), 151.

4. Cho, H.; Song, J.; Kwon, B. H.; Choi, S.; Lee, H.; Joo, C. W.; Ahn, S. D.; Kang, S. Y.; Yoo, S.; Moon, J., Stabilizing color shift of tandem white organic light-emitting diodes. *Journal of Industrial and Engineering Chemistry* **2019,** *69*, 414-421.

5. Kim, G. W.; Bae, H. W.; Lampande, R.; Ko, I. J.; Park, J. H.; Lee, C. Y.; Kwon, J. H., Highly efficient single-stack hybrid cool white OLED utilizing blue thermally activated delayed fluorescent and yellow phosphorescent emitters. *Sci Rep* **2018,** *8* (1), 16263.

6. Lee, J.; Lee, J. W.; Cho, N. S.; Hwang, J.; Joo, C. W.; Sung, W. J.; Chu, H. Y.; Lee, J. I., Highly efficient all phosphorescent white organic light-emitting diodes for solid state lighting applications. *Current Applied Physics* **2014,** *14*, S84-S87.

7. Tokito, S.; Tsuzuki, T.; Sato, F.; Iijima, T., High-efficiency blue and white phosphorescent organic light-emitting devices. *Current Applied Physics* **2005,** *5* (4), 331-336.

8. Hung, W. Y.; Fang, G. C.; Lin, S. W.; Cheng, S. H.; Wong, K. T.; Kuo, T. Y.; Chou, P. T., The first tandem, all-exciplex-based WOLED. *Sci Rep* **2014,** *4* (1), 5161.

9. Xu, T.; Zhou, J. G.; Fung, M. K.; Meng, H., Simplified efficient warm white tandem organic light-emitting devices by ultrathin emitters using energy transfer from exciplexes. *Organic Electronics* **2018,** *63*, 369-375.

10. Xu, T.; Zhou, J. G.; Huang, C. C.; Zhang, L.; Fung, M. K.; Murtaza, I.; Meng, H.; Liao, L. S., Highly Simplified Tandem Organic Light-Emitting Devices Incorporating a Green Phosphorescence Ultrathin Emitter within a Novel Interface Exciplex for High Efficiency. *Acs Applied Materials & Interfaces* **2017,** *9* (12), 10955-10962.

11. Zhao, B.; Zhang, T. Y.; Chu, B.; Li, W. L.; Su, Z. S.; Luo, Y. S.; Li, R. G.; Yan, X. W.; Jin, F. M.; Gao, Y.; Wu, H. R., Highly efficient tandem full exciplex orange and warm white OLEDs based on thermally activated delayed fluorescence mechanism. *Organic Electronics* **2015,** *17*, 15-21.

12. Huang, C.; Zhang, Y.; Zhou, J.; Sun, S.; Luo, W.; He, W.; Wang, J.; Shi, X.; Fung, M. K. J. A. O. M., Hybrid tandem white OLED with long lifetime and 150 Lm W− 1 in luminous efficacy based on TADF blue emitter stabilized with phosphorescent red emitter. *J Advanced Optical Materials* **2020,** *8* (18), 2000727.

13. Chiba, T.; Pu, Y. J.; Kido, J., Solution-processed white phosphorescent tandem organic light-emitting devices. *Adv Mater* **2015,** *27* (32), 4681-7.

14. Xu, X.; Zhao, Y.; Zhou, X.; Wu, Y.; He, G. J. p. s. s., High-Efficiency Nondoped White Organic Light-Emitting Diodes Based on All-Exciplex Emission. *physica status solidi* **2021,** *218* (15), 2100064.

15. Xiao, P.; Huang, J. H.; Yu, Y. C.; Yuan, J.; Luo, D. X.; Liu, B. Q.; Liang, D., Recent Advances of Exciplex-Based White Organic Light-Emitting Diodes. *Applied Sciences-Basel* **2018,** *8* (9), 1449.

16. Shao, J.; Chen, C.; Zhao, W.; Zhang, E.; Ma, W.; Sun, Y.; Chen, P.; Sheng, R., Recent Advances of Interface Exciplex in Organic Light-Emitting Diodes. *Micromachines (Basel)* **2022,** *13* (2), 298.

17. Wu, J.; Ameri, L.; Cao, L. Y.; Li, J., Efficient excimer-based white OLEDs with reduced efficiency roll-off. *Applied Physics Letters* **2021,** *118* (7).

18. Gutiérrez–Llorente, A. J. O. E., Excimer emission of Ir complex for solution processed single emitting layer white OLEDs. *Organic Electronics* **2018,** *63*, 305-309.

19. Sheng, R.; Li, A.; Zhang, F.; Song, J.; Duan, Y.; Chen, P. J. A. O. M., Highly efficient, simplified monochrome and white organic light-emitting devices based on novel exciplex host. *Advanced Optical Materials* **2020,** *8* (2), 1901247.

20. Zhang, Y. L.; Ran, Q.; Wang, Q.; Fan, J.; Liao, L. S., High-efficiency exciplex-based white organic light-emitting diodes with a new tripodal material as a co-host. *J Mater Chem C* **2019,** *7* (24), 7267-7272.

21. Wang, Y. M.; Teng, F.; Xu, Z.; Hou, Y. B.; Yang, S. Y.; Qian, L.; Zhang, T.; Liu, D. A., White emission via electroplex formation at poly(

-vinylcarbazole)/2,9-dimethyl-4,7-diphenyl-1,10-phenanthroline interface. *Applied Surface Science* **2004,** *236* (1-4), 251-255.

22. Gupta, C. V.; Dixit, S. J. N.; Agarwal, N.; Bose, S., Voltage tunable white light generation from combined emission of monomer and electromer in phenanthroimidazole based OLED. *Journal of Photochemistry and Photobiology a-Chemistry* **2022,** *429*, 113922.

23. Barah, D.; Ray, D., Broadband white electroluminescence from a dopant-free OLED comprising pure electromer and electroplex emission. *Journal of Physics D-Applied Physics* **2024,** *57* (13), 135312.

24. Yang, S. Y.; Jiang, M. X., White light generation combining emissions from exciplex, excimer and electromer in TAPC-based organic light-emitting diodes. *Chemical Physics Letters* **2009,** *484* (1-3), 54-58.

25. Angioni, E.; Chapran, M.; Ivaniuk, K.; Kostiv, N.; Cherpak, V.; Stakhira, P.; Lazauskas, A.; Tamulevicius, S.; Volyniuk, D.; Findlay, N. J.; Tuttle, T.; Grazulevicius, J. V.; Skabara, P. J., A single emitting layer white OLED based on exciplex interface emission. *J Mater Chem C* **2016,** *4* (17), 3851-3856.

26. Baek, H. J.; Lee, S. E.; Lee, H. W.; Yun, G. J.; Park, J.; Kim, W. Y.; Kim, Y. K. J. p. s. s., White Organic Light-Emitting Diodes Using Exciplex Emission with Multiple Emitting Layers. *physica status solidi* **2018,** *215* (2), 1700530.

27. Zhao, B.; Zhang, H.; Miao, Y. Q.; Wang, Z. Q.; Gao, L.; Wang, H.; Hao, Y. Y.; Li, W. L., High color stability and CRI (>80) fluorescent white organic light-emitting diode based pure emission of exciplexes by employing merely complementary colors. *J Mater Chem C* **2018,** *6* (2), 304-311.

28. Wei, X. Z.; Gao, L.; Miao, Y. Q.; Zhao, Y. P.; Yin, M. N.; Wang, H.; Xu, B. S., A new strategy for structuring white organic light-emitting diodes by combining complementary emissions in the same interface. *J Mater Chem C* **2020,** *8* (8), 2772-2779.

29. Yang, Y. T.; Wang, W. J.; Qi, S.; Sun, M. H., Optimized TFB-based perovskite quantum dot light emitting diode. *Solid State Communications* **2023,** *363*, 115102.

30. Han, Y. J.; An, K.; Kang, K. T.; Ju, B. K.; Cho, K. H., Optical and Electrical Analysis of Annealing Temperature of High-Molecular Weight Hole Transport Layer for Quantum-dot Light-emitting Diodes. *Sci Rep* **2019,** *9* (1), 10385.

31. Tseng, Z. L.; Huang, W. L.; Yeh, T. H.; Xu, Y. X.; Chiang, C. H., Thermally Activated Delayed Fluorescence in Commercially Available Materials for Solution-Process Exciplex OLEDs. *Polymers (Basel)* **2021,** *13* (10), 1668.

32. Shin, H.; Lee, J.-H.; Moon, C.-K.; Huh, J.-S.; Sim, B.; Kim, J.-J. J. A. M., Sky-Blue Phosphorescent OLEDs with 34.1% External Quantum Efficiency Using a Low

Refractive Index Electron Transporting Layer. *Advanced Materials* **2016,** *28* (24), 4920-4925.

33. Zhang, M.; Liu, W.; Zheng, C. J.; Wang, K.; Shi, Y. Z.; Li, X.; Lin, H.; Tao, S. L.; Zhang, X. H., Tricomponent Exciplex Emitter Realizing over 20% External Quantum Efficiency in Organic Light-Emitting Diode with Multiple Reverse Intersystem Crossing Channels. *Adv Sci (Weinh)* **2019,** *6* (14), 1801938.

34. Liu, W.; Pan, J. H.; Sun, Q.; Dai, Y. F.; Yang, D. Z.; Qiao, X. F.; Ma, D. G., Exciton dynamics of the efficiency roll-off of exciplex-based OLEDs and low efficiency roll-off phosphorescence OLEDs based on an exciplex as the host. *J Mater Chem C* **2024,** *12* (32), 12317-12324.

Chapter 5

Summary of the thesis and scope for future work

5.1 Summary

This thesis investigates innovative device design strategies to develop cost-effective organic light-emitting diodes (OLEDs) by utilizing the concept of exciplex emission. Three distinct exciplex combinations were identified using commercially available and relatively low-cost charge transport materials. N,N′-Di(1-naphthyl)-N,N′-diphenyl-(1,1′-biphenyl)-4,4′-diamine (NPB), a well-known hole transport material (HTM), is used with electron transport materials (ETMs), 3-(biphenyl-4-yl)-5-(4-tert-butylphenyl)-4-phenyl-4H-1,2,4-triazole (TAZ), and 1,3-bis[2-(4-tert-butylphenyl)-1,3,4-oxadiazol-5-yl]benzene (OXD-7). Both these combinations serve as blue-emitting exciplexes. The third combination, N,N′-Bis(3-methylphenyl)-N,N′-diphenylbenzidine (TPD) /2,4,6-tris[3-(diphenylphosphinyl)phenyl]-1,3,5-triazine (PO-T2T), is a yellow-emitting exciplex, where TPD is a blue-emitting HTM and PO-T2T is the ETM. The exciplex emissions were confirmed through spectroscopic studies of the thin films. The study explored solution processing method for fabricating exciplex OLEDs using NPB/OXD-7 and TPD/PO-T2T combinations. While the solution processing method does reduce fabrication complexity and material consumption, it presents challenges in depositing multiple layers.

In NPB:TAZ exciplex OLEDs, blue exciplex emission was realized and used as a host for yellow phosphorescent OLEDs. The device design consists of a double emissive layer consisting of a blue-emitting NPB:TAZ exciplex layer and the yellow-emitting doped layer.

The doped layer consists of a yellow phosphorescent emitter Bis(4-phenylthieno[3,2-c]pyridinato-N,C2') (acetylacetonate) iridium(III) (PO-01) doped into the NPB:TAZ exciplex matrix. By controlling the dopant ratio, the balanced blue and yellow emissions can be achieved, leading to white emission. To further enhance the white emission quality, a spacer layer was introduced between the blue and yellow emissive units. Tetracene, known for its ambipolar properties, was used as the spacer layer to balance carrier transport. This simplified design for exciplex-based white OLEDs provides an alternative to tandem WOLEDs, which often require complex architectures involving charge generation layers (CGLs).

A solution-processed yellow OLED was developed using an NPB:OXD-7 blue-emitting exciplex as the host material, doped with the yellow phosphorescent emitter PO-01. The device achieved a maximum brightness of 36,000 cd/m^2 and an external quantum efficiency (EQE) of 11%. Simultaneously, NPB/OXD-7 blue exciplex devices exhibited multifunctionality, operating as both OLEDs and UV photodetectors. This multifunctionality is attributed to the high surface potential and strong UV absorption properties of OXD-7. This study investigated the spontaneous orientation polarization (SOP) mechanism and the development of surface potential in organic semiconductors and its role in the dissociation of exciplex at the NPB/OXD interfaces. Notably, this is the first report on exploring multifunctional capabilities of exciplex-based devices. This research paves the way for novel multifunctional devices harnessing the unique properties of exciplex emissions.

White emission in OLEDs can be achieved by combining exciplex and excitonic emissions within a single emissive layer, without the need for expensive phosphorescent dopants. White OLED (WOLED) with a simplified device architecture is demonstrated that combines yellow emission from the TPD:PO-T2T exciplex with blue emission at the TPD/TPBi interface

exciplex combined with the excitonic emission of TPD itself. This yields a high color rendering index (CRI) of 78, underscoring the cost-effectiveness and simplicity of exciplex-based white OLED designs, achieved without resorting to complex tandem structures. Moreover, a unique voltage-dependent emission phenomenon is observed upon the incorporation of TFB, a blue-emitting polymer commonly used as HTM. Deep blue emission of TFB dominates at lower voltages, while the yellow exciplex emission prevails at higher voltages, resulting in a shift from blue to cool white emission as the voltage increases. This tunable emission characteristic highlights the potential of novel device designs utilizing commercially available transport materials to enable color tuning in OLEDs, further emphasizing the versatility and practicality of exciplex-based systems.

5.2 Scope for future work

This research highlights the potential of exciplex emissions for simplifying device architectures and achieving white emission in OLEDs while enabling multifunctional applications, offering promising pathways for the development of advanced technologies in organic electronics.

- There is significant potential in identifying new exciplex combinations using commercially available transport materials. These new combinations could lead to a wider range of emission spectra, which would be valuable in developing OLEDs with customizable color outputs, further enhancing their applicability in various display and lighting technologies.

- Blue emission remains as a critical challenge in OLED technology, particularly for efficient and stable blue OLEDs. Investigating blue-emitting HTLs, which can also function as emitters, offers a promising avenue for improving device performance. Such HTLs combined with suitable ETLs can give efficient exciplex emissions, simplifying the device architecture.
- Exploring spacer-like structures as an alternative could simplify the device designs by eliminating the need for CGLs. This approach could lead to simpler, more cost-effective devices while maintaining high efficiency and performance. By identifying suitable ambipolar materials and employing it in non-tandem WOLED designs it could be possible to optimize charge injection and transport within the emissive layer and improving overall device efficiency.
- Exciplex systems can be effectively utilized for multifunctional device applications, including light emission and photodetection. By investigating the effects of surface potential and film morphology of transport materials, it may be possible to fine-tune exciplex systems for different applications, enhancing their versatility in both OLEDs and other organic electronic devices.
- One of the main challenges in single emissive layer white OLEDs is achieving efficient carrier transport while maintaining high efficiency. By optimizing the charge injection and transport mechanisms in exciplex-based OLEDs, it may be possible to achieve high efficiencies compared to multi-layered devices, but with a much simpler architecture, making OLED fabrication more cost-effective and scalable.
- The voltage-dependent color tuning observed in exciplex-based OLEDs presents a unique opportunity for developing tunable lighting and display technologies. Further

studies could explore the underlying mechanisms of this phenomenon, offering new possibilities for dynamic display systems and smart lighting.

- Computational models and simulations can provide valuable insights into exciton dynamics, charge transport, and emission processes within exciplex based devices. These theoretical tools can help guide experimental work by predicting the behavior of new material combinations and optimizing device designs for high efficiencies, further accelerating advancements in OLED technology.

Appendix A

Fabrication and characterization of devices; techniques and instrumentation

The efficiency and longevity of devices are deeply influenced by the precision and control of the device fabrication process. Cleaning of substrates and fabrication techniques such as thin-film deposition, spin coating and encapsulation play pivotal roles in determining the uniformity, charge transport, and overall optoelectronic characteristics of the devices. Detailed characterization allows for a thorough understanding of the impact of material selection, layer thickness and interface quality on the performance of devices.

A.1 Device fabrication

A.1.1 Substrate cleaning

Substrate cleaning is the initial step in device fabrication. Contaminants and impurities on the substrate surface can significantly affect the reliability and performance of the final devices, making it essential to ensure that the surface is clean and smooth. Any contaminants can disrupt the formation of uniform and smooth films, leading to pinholes, defects, and variations in thickness. These issues can negatively impact charge transport, light emission, and overall device performance. Furthermore, contaminants may cause unwanted chemical reactions or interactions with the deposited materials, resulting in interfacial defects. The cleaning process typically involves several sequential steps to adequately prepare the substrates for subsequent film deposition and device fabrication.

The first step in substrate cleaning starts with chloroform, where the substrate is immersed in a solvent bath and will be subjected to sonication. Then these substrates will be thoroughly brush cleaned with detergent and will be washed with hot water to remove any remaining cleaning agents or residues. Subsequently these substrates will be further cleaned by sonicating in isopropyl alcohol, followed by deionized water. During sonication, ultrasonic vibrations create cavitation bubbles in the cleaning solution, which remove and agitate contaminants adhering to the substrate surface. The sonicator (Elma) is shown in Figure A.1 (a). These solvents efficiently dissolve any organic residues, oils or greases that are present on the substrate surface, as well as any leftover photoresist or other pollutants from substrate patterning. Later, the substrates are dried using a combination of hot air drying and hot plate annealing. After the drying process the substrates will be transferred to UV Ozone Cleaner (Novascan, Model. PSDP-UV 4I) (Figure A.2 (b)). In this process, the ozone generated under UV irradiation will acts as a powerful oxidizer that effectively decomposes organic contaminants that are still present on the surface and leaves behind a clean, hydrophilic surface. Finally, these substrates will be directly used for device fabrication.

Figure A.1. (a) Sonicator (b) UV-ozone cleaner

A.1.2 Thin film deposition and optimization

A.1.2.1 Spincoating

Spin coating is a commonly used deposition technique used for fabricating thin films of solution processable materials. The method involves dispensing a solution of precursor material onto a substrate and spinning it rapidly to distribute the solution uniformly across the substrate surface. Spin coating offers several advantages, including ease of use, scalability, and compatibility with different substrates. It gives good control over film thickness and morphology for a large area, which makes it suitable for large-scale production. It is also relatively less expensive and require minimal equipment and maintenance compared to other techniques. The centrifugal force generated during spinning helps to achieve uniform thin films with controlled thicknesses. The concentration of the solution, spinning speed and time of spinning determine the thickness and uniformity of the deposited film. Thickness of a spin coated film is directly proportional to the concentration of the solution and inversely proportional to the square root of spin speed[1] as in equation (1) where ω is angular velocity/spin speed and d is the final thickness of the film.

$$d = \frac{2\pi C}{\sqrt{\omega}} \qquad (1)$$

Despite its widespread use, spin coating has certain limitations, such as solvent evaporation induced defects and limited control over film uniformity and morphology. Over a large area, all materials are not compatible with spin coating due to their limited solubility in commonly used organic solvents. Optimization of spinning parameters and solvent selection is crucial in minimizing defects and achieving desired film properties. This method is well suited for lab-level fabrication but not ideal for the commercial LED production. Image of the Laurell make spin coater that we have used is shown in the Figure A.2.

Figure A.2. Spincoating unit

A.1.2.2 Thermal evaporation

Vacuum-based thermal evaporation is widely used for thin film deposition for fabricating optoelectronic devices. The material to be deposited is heated to its evaporation temperature using resistive heating method. It employs the principle of sublimation, where a solid material undergoes a phase transition directly into a vapor without passing through the liquid phase. It is done inside a vacuum chamber to avoid the exposure to atmospheric gases or other contaminants. In a vacuum chamber, the mean free path of molecules increases and at low pressures materials tend to sublime. A typical thermal evaporation consists of a vacuum chamber, crucible, heating source, substrate holder, thickness monitoring and deposition control systems. After placing the desired material in the crucible and pumping down the chamber to a high vacuum, the crucible is heated, to evaporate the material. The vaporized molecules travel freely within the chamber and condense onto the cool substrate, forming thin film. By precisely controlling the temperature and deposition time, thin films with uniform thickness and controlled composition can be achieved. A piezoelectric quartz crystal is used as

the thickness sensor. We have 6 quartz crystal sensors to control the process of deposition. The deposition of a material from a specific source requires a unique proportional integral derivative (PID) value, which is optimized through a process called autotuning. Thickness of a film is optimized via tooling and the geometric tooling factor determines the thickness of the film as given in the equation (2).

$$\text{New Tooling Factor} = \frac{\text{Measured thickness}}{\text{Actual thickness}} \times \text{given tooling factor} \qquad (2)$$

Many factors, including the substrate temperature, the distance between the source material and the substrate, and deposition rate, affect the thickness and homogeneity of the film formed. Thermal evaporation offers varied deposition rates, highly pure films with excellent film uniformity, precise control over stoichiometry and compatibility with a wide range of materials, particularly for small molecule and inorganic materials. But it requires specialized equipment, careful process control and high maintenance requirements which increase the cost and complexity of the overall fabrication process. Also, the high vacuum conditions may limit the deposition of certain materials. We have used a cryosorption pump (CTI Cryogenics 8200) to create a base vacuum ~ 10^{-7} Torr. Our evaporation chamber has 8 organic sources and 2 metal sources (inset of figure A.3). The evaporation process is controlled by the Inficon software.

A.1.2.2.1 Glovebox integrated thermal evaporation system

Gloveboxes are used in the fabrication processes where materials used must be handled in an oxygen-free environment to prevent oxidation or contamination. These gloveboxes are filled with high-purity nitrogen gas to ensure that sensitive materials, such as semiconductors or organic compounds, are protected during the fabrication process, thus enhancing the reliability and performance of the devices. Once the substrate is cleaned it will be loaded into the thermal evaporation chamber (Angstrom Inc.) maintained under ~10^{-7} Torr vacuum, integrated to the glovebox (Purelab). Figure A.3 shows the picture of a glovebox integrated thermal evaporation system that is used to fabricate all the devices in this thesis.

Figure A.3. Glovebox integrated thermal evaporation system (inset shows the internal view of the evaporation chamber).

A.1.3. Thickness optimization

After each deposition, the film thickness is measured, and the tooling factor is adjusted accordingly using equation (2). This process is repeated over multiple depositions to fix the tooling factor, ensuring that the measured thickness accurately corresponds to the actual thickness. The finalized tooling factor is obtained only after ensuring precise control over the deposition process. The thickness of the sample is measured using a Dektak XT stylus profilometer as shown in Figure A.4. The profilometer is interfaced with a computer for data acquisition and analysis. Stylus profilometer works by physically moving a probe along the surface of the film to detect and measure its height. This operates on the principle of Linear Variable Differential Transformer (LVDT), where the displacement (a non-electrical energy) is converted into electrical energy. The sample thickness is determined from the thickness profile generated after measurement using Vision 64 software.

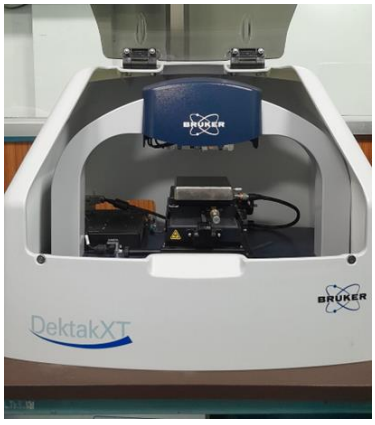

Figure A.4. Stylus profilometer

A.1.4. Encapsulation

Encapsulation eliminates several of major challenges these devices face, and is essential for ensuring their long life and performance. Encapsulation will protect the organic or inorganic semiconductor layers from atmospheric conditions, particularly moisture and oxygen. Due to

their extreme sensitivity to oxygen and moisture, these materials have a shorter operational lifetime which in turn reduces the device performance. Glass encapsulation, barrier foil encapsulation and thin film encapsulation are some of the encapsulating techniques used in general. These layers will serve as a barrier of resistance surrounding the active layers in the devices, keeping out moisture and oxygen while maintaining the material integrity and enabling them to withstand challenging operating conditions like humidity, temperature swings, and exposure to pollutants. It also helps to improve the mechanical durability of the devices by protecting them from physical damage caused by handling especially in the case of flexible or wearable applications. Overall, encapsulation of devices is essential for ensuring the long-term reliability, environmental stability, extended lifespan and performance consistency enabling their successful integration into various lighting, display and optoelectronic applications. We have used glass-based sealing caps and the UV-curable epoxy (Epo-Tek UV-curable epoxy, Epotek OG142).

A.2. OLED characterization

The characterization of an OLED involves two key instruments: a spectroradiometer and a source meter, both interfaced with a computer for data acquisition and analysis.

A.2.1 Source meter

A source meter, also known as a current-voltage (I-V) source, is an instrument that can precisely source and measure both current and voltage values in electronic circuits. The source meter can act as a power supply, providing a controlled and adjustable voltage or current to a circuit or device. It is mainly used for measuring the electrical characteristics of electronic

components like transistors, diodes, and solar cells. We have used a Keithley 2400 for our electrical measurements (Figure A.5)

Figure A.5. Keithley 2400 source meter

A.2.2 Spectroradiometer

A spectrometer is a scientific instrument used to measure the spectral properties of light, typically across a specific wavelength range. It separates incoming light into its constituent wavelengths and quantifies the intensity of each component. This allows for the precise determination of various light properties such as luminescence, electroluminescence spectra, color temperature, color rendering index etc. For the device characterizations in this thesis a PR655 spectroradiometer (Photo Research Inc.) is used as shown in Figure A.6. To prevent interference from external light, all measurements were conducted inside a black box.

Figure A.6. PR-655 Spectroradiometer

A.3. UV-photodetector characterization

The characterization of an ultraviolet (UV) photodetector includes both steady-state and transient I-V measurements, which are conducted using two key instruments: a semiconductor parameter analyzer for electrical analysis and a UV lamp for providing UV illumination.

A.3.1. Semiconductor parameter analyzer

A semiconductor parameter analyzer is an advanced instrument essential for the precise electrical characterization of semiconductor devices. Renowned for its high precision and accuracy, it can perform a variety of measurements such as current-voltage (I-V), capacitance-voltage (C-V), and pulsed I-V testing, etc. The analyzer integrates multiple Source Measurement Units (SMUs) capable of sourcing and measuring voltage and current simultaneously, catering to a wide range of current and voltage levels. It features a user-friendly graphical interface for real-time data visualization and automated testing sequences, enhancing productivity and repeatability. We have a Keithley 4200A - SCS semiconductor parameter analyzer as shown in Figure A.7.

Figure A.7. semiconductor parameter analyzer

A.3.2. UV-lamp

A UV lamp is an essential tool for providing UV radiation in various scientific applications, particularly in the characterization of optoelectronic devices such as UV photodetectors. For our measurements, we used the 6 W ENF 260C Spectroline UV Lamp with 365 nm and 254 nm wavelengths with peak UV intensity 350 $\mu W/cm^2$ and 390 $\mu W/cm^2$ at a distance of 15cm. The The current-voltage characteristics and transient photoresponse of the devices under UV illumination was recorded using a semiconductor parameter analyzer. To prevent interference from external light, all measurements were conducted inside a UV-viewing cabinet.

ABSTRACT

Name of the Student: **Ms. Kavya Rajeev** Registration No.: 10PP18A39025
Faculty of Study: Physical Sciences Year of Submission: 2024
AcSIR academic centre/CSIR Lab: CSIR-National Institute for Interdisciplinary Science and Technology (CSIR-NIIST) Name of the Supervisor: Dr. K. N. Narayanan Unni

Title of the thesis: **Exciplex OLEDs : Strategies for White Emission and Multifunctional Devices**

Organic Light Emitting Diodes (OLEDs) play a pivotal role in modern technology providing flexible and foldable displays in consumer electronics and lighting solutions. Despite their significant progress, OLEDs face challenges such as high production costs and limited lifespan, which restrict their widespread adoption. In this context, excimer, exciplex, and electroplex emissions have gathered considerable attention due to their ability to be generated using commonly used transport materials. Innovative design strategies by utilizing exciplex emissions can be employed to overcome existing limitations. This thesis explores these advancements, focusing on the role of exciplex emissions in the cost-effective fabrication of high-performance OLEDs.

Chapter 1 focuses on the recent progress in exciplex-based OLEDs, highlighting their potential for cost-effective production by avoiding the need for separate emissive layers. Exciplex emissions, generated at the molecular interface of transport materials, can serve as hosts for enabling efficient white OLED designs without the complexity of tandem structures. Reports on exciplex-based OLEDs, where exciplexes are utilized both as emitters and hosts, has been reviewed and discussed here.

Chapter 2 explores the development of simplified blue and yellow OLEDs by utilizing the exciplex emission from a blend of the blue-emitting HTL N,N' bis(naphthalen-1-yl)-N,N'-bis(phenyl)benzidine (NPB) and the ETL 3-(biphenyl-4-yl)-5-(4-tert-butylphenyl)-4-phenyl-4H-1,2,4-triazole (TAZ). The NPB:TAZ exciplex serves as both a blue emitter and a host for the yellow phosphorescent dopant, iridium(III) bis(4-phenylthieno[3,2-c]pyridinato-N,C2')acetylacetonate (PO-01). Tetracene is used as a spacer layer between the blue and yellow emitting units, controlling both exciton diffusion and carrier transport leading to white emission.

Chapter 3 investigates the dual functionality of an NPB/OXD-7 (1,3-bis[2-(4-tert-butylphenyl)-1,3,4-oxadiazo-5-yl]benzene) exciplex combination, serving both as an OLED and a UV photodetector. Solution processed devices incorporating the yellow dopant PO-01 into the exciplex host yielded high EQE. By varying the raio of NPB:OXD-7, multifunctional devices were fabricated, which function as both UV-detector and OLED. The multifunctionality is attributed to the strong UV-absorption and high surface potential of OXD-7.

Chapter 4 combines two blue emitting HTLs TPD (N,N′-Bis(3-methylphenyl)-N,N′-diphenylbenzidine) and TFB (Poly(9,9-dioctylfluorene-alt-N-(4-sec-butylphenyl)-diphenylamine) with an ETL PO-T2T (2,4,6-tris[3-(diphenylphosphinyl)phenyl]-1,3,5-triazine). The TPD:PO-T2T yellow exciplex, TPD/TPBi interface blue exciplex and blue excitonic emission of TPD are combined to fabricate White OLEDs with a high color rendering index (CRI) of 78. A voltage-dependent white emission from blue to cool white were observed after the incorporation of TFB into the emissive layer.

Chapter 5 provides a brief summary of the work done in various chapters, highlighting the key achievements and results of the research. It also outlines the future scope of this study, presenting guide lines for further exploration.

List of publications emanating from thesis work

1. **Kavya Rajeev**, C.K. Vipin, Anjali K. Sajeev, A. Shukla, S.K. McGregor, S.-C. Lo, E.B. Namdas, and K.N. Narayanan Unni, *Frontiers of Optoelectronics*. Blue emitting exciplex for yellow and white organic light-emitting diodes. 16 (2023) 46.
2. **Kavya Rajeev**, Vibhu Darshan, Anjali K. Sajeev and K.N. Narayanan Unni, Dual functional exciplex for blue organic light-emitting diodes and self-powered UV-detector. (*manuscript under preparation*)
3. **Kavya Rajeev**, Anjali K. Sajeev and K.N. Narayanan Unni, Yellow emitting exciplex for solution processable white organic light emitting diodes. (*manuscript under preparation*)

List of publications not related to thesis work

1. Anjaly Soman, Anjali K. Sajeev, **Kavya Rajeev**, and K.N. Narayanan Unni, *ACS omega*. Reversible shift from excitonic to excimer emission in fluorescent organic light-emitting diodes: dependence on deposition parameters and electrical bias. 5 (2020) 1698-1707.
2. C.K.Vipin, A. Shukla, **Kavya Rajeev**, M. Hasan, S.-C. Lo, E.B. Namdas, A. Ajayaghosh, and K.N. Narayanan Unni, *The Journal of Physical Chemistry C*. White organic light-emitting diodes from single emissive layers: Combining exciplex emission with electromer emission. 125 (2021) 22809-22816.

3. B. Hanna, L.R. Pillai, **Kavya Rajeev**, K. Surendran and K.N. Narayanan Unni, *Sensors and Actuators A: Physical*. Visible-blind UV photodetectors using a polymer/ZnO nanocomposite thin film. 338 (2022) 113495.
4. A.D. Nidhankar, Goudappagouda, P. Kothavade, S.D. Dongre, S. Dnyaneshwar Veer, S. Ranjan Dash, **Kavya Rajeev**, K.N. Narayanan Unni, K. Shanmuganathan and Santhosh Babu, *Chemistry-An Asian Journal*. Thermally Activated Delayed Fluorescent Solvent-free Organic Liquid Hybrids for Tunable Emission Applications. 18 (2023) e202300276.
5. Amrutham Linet, Aparna G Nair, **Kavya Rajeev**, Simi Achankunju, K. N. Narayanan Unni and Ishita Neogi, *Chemistry–An Asian Journal*. TICT, and Deep-Blue Electroluminescence from Acceptor-Donor-Acceptor Molecules. 19 (2024) e202400721.

List of conferences

1. A Promising Blue OLED Employing Efficient Energy Transfer Between Host And Dopant Molecules , **Kavya Rajeev**, Anjali K Sajeev, Vipin C K , K. N. Narayanan Unni*. A poster presented at International Conference on Advanced Materials (ICAM 19) held during 12-14 june 2019 at Nirmalagiri College, Kannur, Kerala, India. (Adjudged as the best poster presentation)
2. An Investigation into the Emission Mechanisms of NPB Based Blue OLEDs, **Kavya Rajeev**, K. N. Narayanan Unni*. A poster presented at National Conference on Recent Trends in Material Science and Technology (NCMST 2019) held during 18-20 December 2019 organized by Department of Chemistry, Indian Institute of Space Science and Technology, Trivandrum, Kerala, India.
3. Deep blue OLEDs Utilizing Förster Energy Transfer Between Hole Transport and Electron Transport Materials, **Kavya Rajeev**, Vipin C K , K. N. Narayanan Unni*. A poster presented at 14th International Conference on Ecomaterials (ICEM-14) held during 5-7 February,2020 at CSIR-NIIST Trivandrum, India.
4. White Orgainc Light Emitting Diodes by Utilizing Blue Exciplex as an Emitter and as a Host; Towards Cost-effective OLEDs, **Kavya Rajeev**, Vipin C K, Anjali K Sajeev, K. N. Narayanan Unni*, a Poster presentation at National Conference on “Indian Analytical Science Congress 2022”, held during March 10 - 12, 2022 at Tea County Hill Resort, Munnar, Kerala
5. Dual Functional Exciplex With a Simple Device Design for Blue, Yellow and White Organic Light Emitting Diodes, **Kavya Rajeev**, Vipin C K , Anjali K Sajeev, K. N.

Narayanan Unni*. An oral presentation at 34th Kerala Science Congress held during 10-12 February,2022 at Mar Ivanios College, Thiruvananthapuram.

6. Multifunctional Devices Utilizing the Effect of Surface Orientational Polarization (SOP) on Exciplex Excitons, **Kavya Rajeev**, Vibhu Darshan K. N. Narayanan Unni*. A poster presentation and flash talk delivered at International Conference on Chemistry and Applications of Soft Materials (CASM 2022) held during 25-27 July, 2022 at CSIR-NIIST Trivandrum, India (Adjudged as the best student flash talk).
7. Utilizing Exciplex Emission in Donor-Acceptor Combinations for OLED Applications, **Kavya Rajeev**, K.N. Narayanan Unni*. A poster presented at 15th National Symposium on Radiation and Photochemistry (NSRP-2023) held during January 5-7, 2023, at Birla Institute of Technology & Science, Pilani K K Birla Goa Campus, Zuarinagar Goa.

Abstracts for Conference Presentations

1. International Conference on Advanced Materials, ICAM-2019

Studies on the performance of NPB based deep blue OLEDS with modified device structures

Kavya Rajeev[1,2], Anjali K Sajeev[1,2], and Narayanan Unni K. N.*

[1]*Photosciences and Photonics Section, Chemical Sciences and Technology Division, CSIR–National Institute for Interdisciplinary Science and Technology (CSIR–NIIST), Thiruvananthapuram – 695019, India*

[2]*Academy of Scientific and Innovative Research (AcSIR), CSIR–NIIST, Thiruvananthapuram – 695019, India*

** Dr.Narayanan Unni K. N. Mobile: (+91) 9745300436; unni@niist.res.in

Even though the class of compounds called organic semiconductors are known since early 20th century, it is with the invention of Organic Light Emitting Diodes by Tang and Vanslyke in 1987[1], the new research area called organic electroluminescence began flourishing and now OLEDS have matured into commercial applications. Light weight, fast response, wide viewing angle, reduced processing steps and high brightness are the potential advantages of OLEDS. But air-stability and high cost are the major impediments in market penetration. Particularly, the blue OLED is a weak link in the display and lighting industry due to the lack of stability and low luminescence efficiency. Developing novel blue emitters or designing new device structures will be an ideal approach to circumvent this problem. N,N' -Bis(naphthalen-1-yl)-N,N' -bis(phenyl)-benzidine (NPB) is widely used as a hole transporting layer (HTL) in OLEDs. NPB can also act as a standard blue emitting material in OLED as well as a host for certain phosphorescent emitters[2]. However, NPB based fluorescent OLEDs have not been studied in detail because of its reported low efficiency[2]. One of the reasons for this inferior performance is the low electron mobility of NPB, which affects the charge balance in the device. With this in mind, we have fabricated an OLED with the structure ITO/HAT-CN(5nm)/NPB(60nm)/TAZ(40nm)/Alq_3(20nm)/LiF(1nm)/Al(150nm). The device exhibited deep blue emission at 440nm. Then we tried another device structure with ITO/HAT-CN(5nm)/NPB(60nm)/NPB:TAZ(15nm,1:1)/TAZ(40nm)/Alq_3(20nm)/LiF(1nm)/Al(150nm) where we incorporated an additional layer of NPB and TAZ by co-deposition. The later structure showed improved device performance. The lowest unoccupied molecular orbital (LUMO) of TAZ is close to the LUMO of NPB and hence we expect an easy electron injection into NPB, which increases the charge balance factor. An improved charge balance factor might be the reason for better device performance.

Keywords: OLED; charge balance; co-evaporation.

References

1. C. W.Tang, S. A.Van Slyke, Appl. Phys. Lett 51(12),913–915 (1987).

2. National Conference on Recent Trends in Materials Science and Technology, NCMST-2019

An Investigation into the Emission Mechanisms of NPB Based Blue OLEDs

Kavya Rajeev, K. N. Narayanan Unni*

[1]*Photosciences and Photonics Section, Chemical Sciences and Technology Division, CSIR–National Institute for Interdisciplinary Science and Technology (CSIR–NIIST), Thiruvananthapuram – 695019, India*

Kavyarajeev4@gmail.com

Although organic semiconductors were known from early 20th century, it is with the invention of OLED by Tang and Vanslyke in 1987[1] , the new research area called organic electronics began flourishing and now OLEDS have matured into commercial applications. OLEDs have many advantages over inorganic LEDs which include, color contrast, low-cost , comparatively easy processing steps, color tuning, usage of flexible substrates etc. But low air-stability, increased failure rates are the main drawbacks of the OLED industry. Researchers are aiming at improving the efficiency, life-time and cost-effectiveness of OLEDs. Blue OLEDS are so important due to their modest light emitting performances and hence a bottle neck of industrialization of OLED. NPB (N,N' -Bis(naphthalen-1-yl)-N,N' -bis(phenyl)-benzidine) is usually used as a hole transporting layer in OLEDS. NPB can also act as a standard blue emitting material in OLED. It's spectrum peaks at around 445nm with a half peak width around 60nm. But the NPB based blue OLED's efficiency is found to be very low. So the idea of an NPB based OLED device structure with high efficiency would be a great achievement. A comparative study of NPB based blue OLEDs were done with emitting layers as **1. NPB only device, 2. NPB:TAZ, 3. NPB:OXD-7**. NPB only device showed very poor performance. This may be due to the low quantum yield of NPB. Whereas for TAZ device, we got an enhanced performance. Spectroscopic studies revealed a good exchange integral between absorption of NPB and emission of TAZ. So, the enhanced performance can be attributed to the energy transfer from TAZ to NPB. In the third device, where OXD-7 is used, very low current density was observed. This may be due to the presence of trapped charges in the NPB:OXD-7 co-deposited layer.

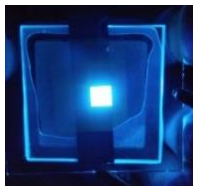

Figure 1. NPB:TAZ OLED

References

1. C. W.Tang, S. A.Van Slyke, Appl. Phys. Lett 51(12),913–915 (1987).

3. International Conference on Ecomaterials, (ICEM-14, 2020)

Deep blue OLEDs Utilizing Förster Energy Transfer Between Hole Transport and Electron Transport Materials

Kavya Rajeev,[1,2] Vipin C. K,[1] K. N. Narayanan Unni[3,*]

[1]*Photosciences and photonics, Chemical Sciences and Technology Division, CSIR-National institute for Interdisciplinary Science and Technology (CSIR-NIIST), Thiruvananthapauram,India-695019,* [2]*Academy of Scientific and Innovative Research (AcSIR), CSIR-NIIST,Thiruvananthapauram,India-695019*
Email: unni@niist.res.in

Organic Light Emitting Diodes (OLEDs) play a key role in the new generation lighting industry. Major challenges in OLED industry are stability and high cost. Researchers all over the world are addressing these same problems and exploring new emission mechanisms and novel device structures. Particularly, the blue OLED is a weak link in the display and lighting industry due to lack of stability and low luminescence efficiency. So, developing new device structures and exploring different emission mechanisms for blue OLEDs can be a major future development in this context. N,N' -Bis(naphthalen-1-yl)-N,N' -bis(phenyl)-benzidine (NPB) is widely used as a hole transporting layer (HTL) in OLEDs. NPB can also act as a standard blue emitting material in OLED as well as a host for certain phosphorescent emitters[1]. We selected two organic materials NPB and TAZ (3-(Biphenyl-4-yl)-5-(4-tert-butylphenyl)-4-phenyl-4*H*-1,2,4-triazole). We took UV-Visible absorption spectra and Photoluminescence emission spectra of the thin-films of NPB, TAZ and NPB:TAZ (co-deposited). We could observe an effective overlap between the emission spectrum of TAZ and absorption spectrum of NPB, which indicates an energy transfer between the two molecules. In this work, we are introducing a novel device structure for a deep blue OLED by utilizing the concept of Förster energy transfer mechanism between HTL and ETL materials. Here, TAZ acts as the host and NPB act as the dopant. We fabricated an OLED with NPB:TAZ (3-(Biphenyl-4-yl)-5-(4-tert-butylphenyl)-4-phenyl-4*H*-1,2,4-triazole) as the emissive layer. The device exhibited a deep blue emission at 448nm and showed a luminance of 1419 cd/m^2 at 11V with a current density of 436.25 mA/cm^2.

References

[1] Liu, J. *Appl.phys.A.Mater.Sci process*, **2017**, *123(3)*, 191.

4. Indian Analytical Science Congress (IASC-2022)

White Organic Light Emitting Diodes by Utilizing Blue Exciplex as an Emitter and as a Host ; Towards cost-effective OLEDs

Kavya Rajeev, Vipin C. K, Anjali K. Sajeev and K. N. Narayanan Unni *
Photosciences and Photonics Section, Chemical Sciences and Technology Division, CSIR-National Institute for Interdisciplinary Science and Technology (CSIR-NIIST), Thiruvananthapuram 695019, Kerala, India
Academy of Scientific and Innovative Research (AcSIR), Ghaziabad 201 002, U.P., India

Organic Light Emitting Diode (OLED) technology offers high clarity visuals and flexible large area displays. However, the cost of production is still a bottleneck in OLED industry. Here we are employing an alternate emission technique – exciplex emission – to achieve simplified device design. It points towards cost-effective fabrication of OLEDs.

Exciplex is an excited state complex formed at the interface of a hole transporting and electron transporing material. Exciplex can be used as an emitter as well as a host with suitable dopants[1]. In this work, white light emission is achieved by using a blue exciplex as an emitter as well as a host with a yellow dopant. Blue exciplex emission is observed at the interface of two transporting materials; N,N′-Bis(naphthalen-1-yl)-N,N′-bis(phenyl)benzidine (NPB) and 3-(Biphenyl-4-yl)-5-(4-tert-butylphenyl)-4-phenyl-4H-1,2,4-triazole (TAZ). The confirmation of exciplex emission is done via spectroscopic studies of the thin films[2]. In the device architecture for white emission, the emissive layer consists of an exciplex alone layer which contributes to the blue component. Whereas the exciplex host layer with a yellow phosphorescent dopant bis(4-phenylthieno[3,2-c]pyridinato-N,C2') (acetylacetonate) iridium(III) (PO-01) gives the yellow emission. An ambipolar spacer layer of tetracene inserted between the two layers provides balanced blue and yellow emission for white light. The spacer layer prevents the diffusion of exciplex excitons from the blue emitting unit to the yellow emitting one while promoting a balanced carrier flow. The WOLED shows an external quantum efficiency (EQE) of 1.2% at 1000 cd/m^2. The white light similar to day light was achieved with color coordinates (0.36,0.39) and color temperature of 4643 K.

[1] M. Sarma, K.-T. J. A. a. m. Wong, interfaces,**2018**,10, 19279.
[2] W.-Y. Hung, G.-C. Fang, S.-W. Lin, S.-H. Cheng, K.-T. Wong, T.-Y. Kuo, P.-T. J. S. r. Chou,**2014**,4, 1

5. 34th Kerala Science congress (KSC-2022)

Dual Functional Exciplex with A Simple Device Design for Blue, Yellow and White Organic Light Emitting Diodes

Kavya Rajeev[1,2], C. K. Vipin[1,2], Anjali K. Sajeev[1,2], K. N. Narayanan Unni[1,2*]

1Photosciences and Photonics Section, Chemical Sciences and Technology Division, CSIR-National Institute for Interdisciplinary Science and Technology, Thiruvananthapuram, India-695019

2Academy of Scientific and Innovative Research (AcSIR), Ghaziabad, India-201002

Smart gadgets like mobile phones, smart watches etc. have their ubiquitous presence in our daily life. In this context, cost-effectiveness of organic-opto-electronic devices like organic light emitting diodes (OLEDs), which are integral part of many consumer-electronic products, have their own importance. Complicated fabrication procedure and high cost of emitter materials are the major causes for high cost in OLED industry. In this work, we are presenting a promising method for fabrication of OLEDs by utilizing the phenomenon of exciplex emission. Exciplex emission occurs at the interface of an electron accepting and an electron donating material. Hence it avoids the need for a separate emissive layer which helps to reduce the cost-effectiveness of the device.

Here we present novel blue emitting exciplex combinations. We have selected N,N′-Bis(naphthalen-1-yl)- N,N′-bis(phenyl)benzidine (NPB) and 3-(Biphenyl-4-yl)-5-(4-tert-butylphenyl)- 4-phenyl-4H-1,2,4-triazole (TAZ); commonly used transporting materials for OLED. We could develop a promising blue exciplex OLED by using exciplex as an emitter and a yellow OLED by using exciplex as a host with a yellow phosphorescent dopant. A warm white emission has been achieved by utilizing the dual functionality of exciplex as an emitter as well as a host. The white emission is achieved via a device design strategy connecting these blue and yellow emitters using a spacer layer of tetracene, exploiting its ambipolar transport. The selection as well as confirmation methods for a suitable conjugate pair for efficient exciplex emission are a crucial task. Analysis of photoluminescence spectra, UV-visible absorption spectra and the transient PL spectra of the exciplex mixed film along with the individual films have been done to give evidences for exciplex emission. Thus, by utilizing dual-functioning of exciplex emission as well a simple device design strategy, we could achieve blue, yellow as well as white emission in OLEDs. These results address the challenges of complicated device fabrication and the lack of a stable and efficient blue emitter, providing guidelines for a cost-effective white OLED.

Keywords: Organic Light Emitting Diodes, Exciplex emission, Spacer, Deep blue exciplex, Yellow OLEDs, White light emission

6. International Conference on Chemistry and Applications of Soft Materials (CASM-2022)

Multifunctional Devices Utilizing the Effect of Surface Orientational Polarization (SOP) on Exciplex Excitons

Kavya Rajeev,[1,2] K. N. Narayanan Unni[1,2,] *
[1]*Photosciences and Photonics Section, Chemical Sciences and Technology Division, CSIR-National Institute for Interdisciplinary Science and Technology (CSIR-NIIST), Thiruvananthapuram 695019, Kerala, India.* [2]*Academy of Scientific and Innovative Research (AcSIR), Ghaziabad 201 002, U.P., India*
Email: unni@niist.res.in

Organic opto-electronic devices contribute to the major part of modern electronics. The concept of incorporating sensing, detection, emission, memory etc., within the same device has aroused considerable interest among researchers. Here, a visible light emitting UV-photodetector is presented by utilizing the effect of Surface Orientational Polarization (SOP) at the donor-acceptor interface. N,N′-Di(1-naphthyl)-N,N′-diphenyl-(1,1′-biphenyl)-4,4′-diamine (NPB) and 1,3-bis[2-(4-tert-butylphenyl)-1,3,4-oxadiazo-5-yl]benzene (OXD-7) form a conjugated pair which will give a blue exciplex emission. The high SOP nature of OXD-7 will weaken the exciplex excitons formed at the NPB/OXD-7 interface[1]. Under UV-illumination (at 365 nm), the exciplex excitons will get dissociated to give a photocurrent. Hence the same device performs as an Organic Light Emitting Diode (OLED) as well as a UV-photodetector. Exciplex emission was confirmed via spectroscopical studies of the thin-films. The bulk exciplex device gives better performance compared to the bilayer device for both OLED and OPD characteristics. An increase in OLED performance was observed when a yellow phosphorescent emitter Bis(4-phenylthieno[3,2-c]pyridinato-N,C2') (acetylacetonate) iridium(III) (PO-01) doped in NPB:OXD-7(1:1). A maximum brightness of about 14,000 cd/m^2 was achieved with a current density of 203 mA/cm^2, when 4% of PO-01 was doped into the NPB:OXD exciplex layer. In order to improve the OPD performance, the percentage of OXD-7 was increased in the bulk. An improvement in responsivity was observed, it shows the effect of high SOP of OXD-7 at the interface. For detector devices, maximum detectivity, responsivity and ON-OFF ratio were obtained as 2.26 ×10^{11} Jones, 13.33 mA/W and 1.52×10^3, respectively. Here, we are combining exciton recombination and emission within the same device. It seems paradoxical, but it can have several possibilities in near future.

References

[1] Ueda, Y.; Nakanotani, H.; Hosokai, T.; Tanaka, Y.; Hamada, H.; Ishii, H.; Santo, S.; Adachi, *Adv. Opt. Mater* , **2020,** *8 (21)*, 2000896.

7. National Symposium on Radiation and Photochemistry (NSRP-2023)

Utilizing Exciplex Emission in Donor-Acceptor Combinations for OLED Applications

Kavya Rajeev,[1,2] K. N. Narayanan Unni[1,2,] *
[1]*Photosciences and Photonics Section, Chemical Sciences and Technology Division, CSIR-National Institute for Interdisciplinary Science and Technology (CSIR-NIIST), Thiruvananthapuram 695019, Kerala, India.* [2]*Academy of Scientific and Innovative Research (AcSIR), Ghaziabad 201 002, U.P., India*
Email: unni@niist.res.in

Organic Light Emitting Diodes or OLEDs have immense applications in the display as well as lighting industry. Display is an inevitable component of smart gadgets. Here we utilize the concept of exciplex emission in OLEDs. We have selected four donor-acceptor combinations (1) N,N′-Di(1-naphthyl)-N,N′-diphenyl-(1,1′-biphenyl)-4,4′-diamine(NPB)/3 (Biphenyl-4-yl)-5-(4-tert butylphenyl)-4-phenyl-4H-1,2,4-triazole(TAZ), (2) NPB/1,3-bis[2-(4-tert-butylphenyl)-1,3,4-oxadiazo-5-yl]benzene(OXD-7), (3) Poly(9,9-dioctylfluorene-alt-N-(4-sec-butylphenyl)-diphenylamine)(TFB)/2,4,6-tris[3-(diphenylphosphinyl)phenyl]-1,3,5-triazine(PO-T2T) and (4)1,3,5-tris(carbazol-9-yl)benzene(TCP)/PO-T2T for exciplex emissions .The investigation on exciplex emission in the selected combinations were done via spectroscopic studies. The broad and significantly red-shifted emission spectra for the donor : acceptor mixed films in NPB:OXD-7, TFB:PO-T2T and TCP:PO-T2T combinations confirm exciplex emission. Whereas the absence of red-shifted emission was observed for NPB:TAZ. The comparison of excitation spectra and absorption spectra and transient decay studies of the films were also done for further confirmation of exciplex emission. Based on the spectroscopic evidences, device fabrication were done by using the selected donor : acceptor combinations. The device architecture is ITO/ Hole transporting layer (HTL)/ HTL: Electron transporting or acceptor material as a layer (ETL) /ETL /LiF/ Al. NPB:TAZ combination has exhibited the best performance with a maximum brightness of 1102 cd/m2 with a current density of 303 mA/cm2 at 10 V. This high performance can be attributed to the formation of an electroplex in NPB/TAZ combination which cannot be detected from PL studies. Other three exciplex systems exhibits weak exciplex emission which can be effectively utilized as a host rather than an emitter. Inorder to enhance the overall device performance, phosphorescent dopants such as Bis(4-phenylthieno[3,2-c]pyridinato-N,C2') (acetylacetonate) iridium(III)(PO-O1) and Tris(2-phenylpyridine)iridium(III) (Ir(ppy)3) was doped in to the exciplex matrix. The maximum performance was observed for NPB:OXD-7:PO-01 device. It showed a brightness of about 14,000 cd/m2 achieved with a current density of 203 mA/cm2, when 4% of PO-01 was doped into the NPB:OXD exciplex layer. This work has several possibilities in effectively utilizing the exciplex emission in fabricating simple and cost-effective OLEDs in near future.

1. M. Sarma, K.-T. J. A. a. m. Wong, interfaces,**2018**,10, 19279.

Frontiers of Optoelectronics (2023) 16:46
https://doi.org/10.1007/s12200-023-00101-3

Frontiers of Optoelectronics

RESEARCH ARTICLE

Blue emitting exciplex for yellow and white organic light-emitting diodes

Kavya Rajeev[1,2] · C. K. Vipin[1,2] · Anjali K. Sajeev[1,2] · Atul Shukla[3,4] · Sarah K. M. McGregor[3,5] · Shih-Chun Lo[3,5] · Ebinazar B. Namdas[3,4] · K. N. Narayanan Unni[1,2]

Received: 31 August 2023 / Accepted: 29 October 2023

Abstract
White organic light-emitting diodes (WOLEDs) have several desirable features, but their commercialization is hindered by the poor stability of blue light emitters and high production costs due to complicated device structures. Herein, we investigate a standard blue emitting hole transporting material (HTM) *N*,*N*′-bis(naphthalen-1-yl)-*N*,*N*′-bis(phenyl)benzidine (NPB) and its exciplex emission upon combining with a suitable electron transporting material (ETM), 3-(biphenyl-4-yl)-5-(4-*tert*-butylphenyl)-4-phenyl-4*H*-1,2,4-triazole (TAZ). Blue and yellow OLEDs with simple device structures are developed by using a blend layer, NPB:TAZ, as a blue emitter as well as a host for yellow phosphorescent dopant iridium (III) bis(4-phenylthieno[3,2-*c*]pyridinato-N,$C^{2'}$)acetylacetonate (PO-01). Strategic device design then exploits the ambipolar charge transport properties of tetracene as a spacer layer to connect these blue and yellow emitting units. The tetracene-linked device demonstrates more promising results compared to those using a conventional charge generation layer (CGL). Judicious choice of the spacer prevents exciton diffusion from the blue emitter unit, yet facilitates charge carrier transport to the yellow emitter unit to enable additional exciplex formation. This complementary behavior of the spacer improves the blue emission properties concomitantly yielding reasonable yellow emission. The overall white light emission properties are enhanced, achieving CIE coordinates (0.36, 0.39) and color temperature (4643 K) similar to daylight. Employing intermolecular exciplex emission in OLEDs simplifies the device architecture via its dual functionality as a host and as an emitter.

Keywords Organic light-emitting diodes · Dual functional exciplex · Spacers · Device design strategy · Blue exciplex · Yellow OLEDs · White light emission

1 Introduction

OLEDs are one of the major components in the smart electronic world. Smart displays, watches, and other electronic display gadgets employing OLEDs have an ubiquitous presence in everyday life. After the first OLED was reported in 1987 [1], rapid development enabled commercial production of OLED displays by 1997, with the technology making steady progress ever since. However, the high cost and limited life span of OLED products are considered to be the major challenges preventing their deeper market penetration. These are being addressed by efficient out-coupling techniques [2–4], novel emitter molecules [5, 6], efficient emission mechanisms such as phosphorescence [7], thermally activated delayed fluorescence (TADF) [8] and simplified device architectures [9]. However, stable and efficient blue emission is still considered a bottleneck in the OLED display industry. This is due to the challenges associated with

✉ K. N. Narayanan Unni
unni@niist.res.in

1 Centre for Sustainable Energy Technologies, CSIR-National Institute for Interdisciplinary Science and Technology, Thiruvananthapuram 695 019, India

2 Academy of Scientific and Innovative Research (AcSIR), Ghaziabad 201002, India

3 Centre for Organic Photonics & Electronics, The University of Queensland, Brisbane, QLD 4072, Australia

4 School of Mathematics and Physics, The University of Queensland, Brisbane, QLD 4072, Australia

5 School of Chemistry and Molecular Biosciences, The University of Queensland, Brisbane, QLD 4072, Australia

Published online: 14 December 2023

molecular design of wide band gap materials. Unfortunately, these design challenges are present across fluorescent, phosphorescent, and TADF materials, resulting in a scarcity of suitable materials. Furthermore, the lack of stable blue fluorophores is detrimental to application in RGB color balancing of displays. Hence, there is an urgent need to further develop stable and efficient blue emitters and to improve the yield of existing materials.

There are many blue emitting charge transport materials, which have not been explored due to their low quantum yield. Hence, novel device designs utilizing commonly available blue emitting transport molecules would provide a major breakthrough. In the past few years, excited state emission mechanisms such as exciplex (involving excited states in pairings of materials) have emerged as an alternative resource for use in OLEDs. Exciplex emission occurs at the interface of an HTM and an ETM and it provides a simple device architecture by avoiding the need for a separate emissive layer (EML). Exciplex as an emission mechanism has comparatively low quantum yield. Nonetheless, it can be effectively used as a host with phosphorescent, fluorescent [10] and TADF dopants [11]. Suitable exciplex combinations with novel design strategies can provide new routes for efficient white OLEDs (WOLEDs) without the need for complicated tandem structures. However, establishing a general criterion for the selection of conjugate pairs for efficient exciplex emission remains a complex issue. Exciplex emission can occur via electrical as well as optical excitation. The basic criterion for the selection of materials is to have a moderate offset [12] between the highest occupied molecular orbital (HOMO) energies of the HTM and ETM. Lowest unoccupied molecular orbital (LUMO) energies are also expected to have a similar offset. Exciplex emission, previously thought of as a less efficient process, has, since 2000, regained a role in OLEDs as an emitter as well as a host [13]. Most of the reported high efficiency exciplex OLEDs have utilized the exciplex as a host rather than as an emitter. Although the quantum yield for exciplex emission is quite low, proper selection of conjugate pairs can provide adequate intensity of emission.

In this work, we have addressed the issue of lack of blue emitters in OLEDs by utilizing an intermolecular excited state formed at the interface of charge transporting materials; NPB and TAZ. This exciplex was used as a blue emitter as well as a host material for a yellow emitting phosphorescent dopant (PO-01) OLEDs. An external quantum efficiency (EQE) of (6.9 ± 0.27) % @ 1000 cd/m^2 was obtained for the yellow OLED. Furthermore, white emission with CIE coordinates (0.36, 0.39) was achieved by employing tetracene as a spacer in conjunction with blue exciplex host and yellow emitting phosphorescent dopant.

2 Methods

The molecular structures of NPB, and TAZ are shown in Fig. 1a. Solid-state photophysical measurements were performed on thin films deposited on fused silica substrates. Substrates were cleaned with acetone and isopropanol followed by UV-ozone to remove organic impurities. Photoluminescence (PL) spectra were measured using a FS5 fluorescence spectrometer (Edinburgh Instruments). Absolute photoluminescence quantum yields (PLQYs) for thin film samples were measured using the same spectrometer with calibrated integrating sphere. PLQY/PL spectra of NPB and NPB:TAZ blend films were measured by exciting at 350 nm, while neat films of TAZ were excited at 300 nm. Emission lifetime was measured with the same spectrometer, and samples were excited at 375 nm using a laser diode with an instrument response function (IRF) of 150 ps.

Devices were fabricated in a nitrogen glove box-integrated thermal evaporation system (Angstrom Inc.) and the film thickness was measured using Dektak XT profilometer. Indium tin oxide (ITO) substrates were purchased from Kintec Company, Hong Kong, China and organic materials were purchased from Luminescence Technology Corp. (Lumtec), Taiwan, China. The substrates were cleaned by using a liquid detergent followed by sequential sonication in isopropanol and de-ionized water for 15 min each. After drying, the UV-ozone treated (Novascan) substrates were loaded in thermal evaporation chamber. All the layers (materials) of the device were deposited on the substrate by thermal evaporation under high vacuum ($\approx 10^{-7}$ torr) conditions. After the evaporation, the devices were encapsulated inside the nitrogen filled glovebox by using a UV-curable epoxy (Epoxy Technology Inc.). The OLED characterization system consists of a SpectraScan PR-655 spectroradiometer integrated with a Keithely 2400 sourcemeter.

3 Results and discussion

3.1 Device fabrication and characterization

3.1.1 Blue OLEDs by combining NPB and TAZ

Here we combined NPB with TAZ to create a blue emitting unit. Devices fabricated by combining NPB with TAZ could yield: excitonic emission of NPB; energy transfer between the ETL and NPB; or exciplex emission at the NPB/ETL interface. We performed spectroscopic studies of the thin

films to confirm the dominant emission mechanism in photoluminescence (PL). However, it was also critical to determine the dominant mechanism in electroluminescence and further improve the overall efficiency. The HOMO–LUMO offset values at the NPB/TAZ interface were also compared (see Fig. 1b) [14, 15]. The exciplex emission is usually favored for HOMO-HOMO/LUMO-LUMO gap ≥ 0.4 eV [16]. For the NPB:TAZ combination, the offset values are below 0.4 eV. Hence, a bilayer NPB/TAZ device (B_1) was fabricated with a device architecture of ITO/HAT-CN (5 nm)/NPB (60 nm)/TAZ (40 nm)/Alq_3 (20 nm)/LiF (1 nm)/Al (100 nm) as shown in Fig. 2a, where HAT-CN is 1,4,5,8,9,11-hexaazatriphenylenehexacarbonitrile. A thin layer of HAT-CN (5 nm) was deposited prior to NPB to improve the hole injection into NPB. To balance the hole injection into TAZ, Alq_3 was incorporated in the structure, as an electron transport layer (ETL). To get better insights into energy transfer in the process of electroluminescence, we further fabricated devices (B_2 and B_3) with NPB:TAZ as the EML sandwiched by the pristine NPB and TAZ layers. The NPB and TAZ layers on both sides provided better charge transport and carrier confinement. Specifically, EML consists of the co-deposited layer of NPB:TAZ at 1:1 and 1:3 for devices B_2 and B_3, respectively, with total thickness of 15 nm. However, the doping ratio of NPB in TAZ in device B_3 was reduced by three times compared to B_2.

The electroluminescence of the OLEDs with NPB/TAZ bilayer and blend layer (NPB:TAZ) were analyzed via device characteristics as shown in Fig. 2b, c, d. Interestingly, the current density of the bilayer device increased compared to blend devices at higher voltages as can be seen from Fig. 2b. In the bilayer device, the energy barrier for hole injection from NPB to TAZ was 0.8 eV. At higher voltages this barrier was overcome and the increased hole injection and subsequent recombination (radiative or nonradiative) may have caused the current. It may be noted that the blend device was nothing but a device where a 15 nm blend layer had been added in between the pristine NPB and TAZ layers of the bilayer device. At higher voltages, injection to the blend was increased but charges may have become trapped in the blend layer. In bilayer, this does not happen as the charges recombine either radiatively or non-radiatively at the interface. However, the trapping of carriers in the blend may have helped the exciplex formation. To study this, we looked at the luminanace (L) vs current density (J) plots of these devices as shown in Fig. S1 in the Supplementary Information (SI) and found out that compared to the blend devices, bilayer device had a much higher J value for the same L value. We believe that the radiative recombination even in the thin layer of blend layer was much more efficient than the bilayer device. However overall J, which is the sum of radiative and nonradiative currents could have been higher for the bilayer device, particularly at higher voltages.

The current density–voltage and current efficiency–voltage plots of the devices were compared. From the device characteristics, the luminance was seen to be enhanced when NPB:TAZ layer was incorporated. As shown in Fig. 2c, the current efficiency of B_2 and B_3 devices increased to 0.7 cd/A compared to that of bilayer NPB/TAZ B_1 devices, an enhancement by a factor of 2 for the NPB:TAZ blend devices. Given that exciton recombination could occur within NPB or at the NPB/TAZ interface, the effect of TAZ at the interface of NPB was investigated in detail through photophysical studies of the thin films of individual materials and their co-evaporated films, which was essential to understand the origin of PL. Hence, spectroscopic studies

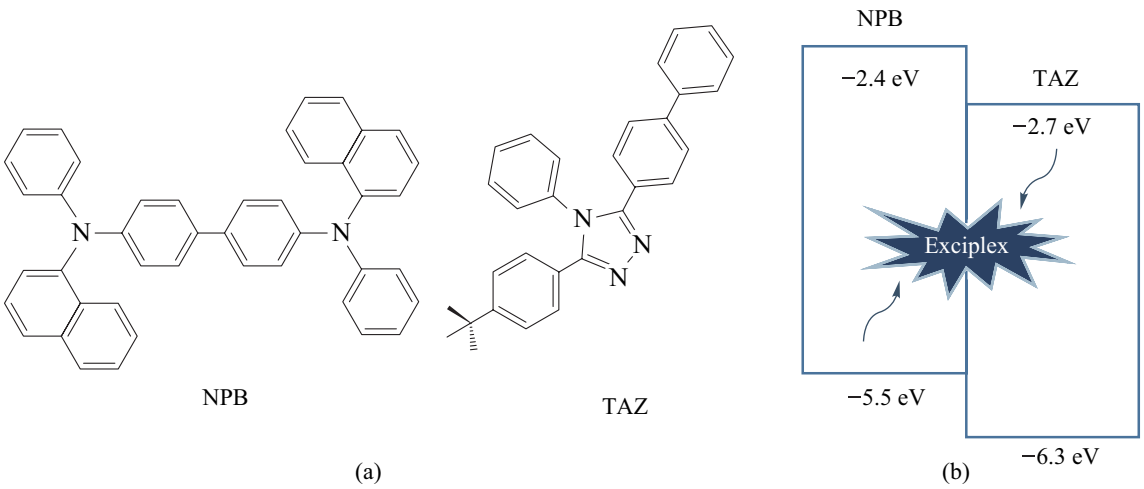

Fig. 1 **a** Molecular structures of NPB and TAZ. **b** Comparison of energy level (in eV) diagrams and mechanism of exciplex formation

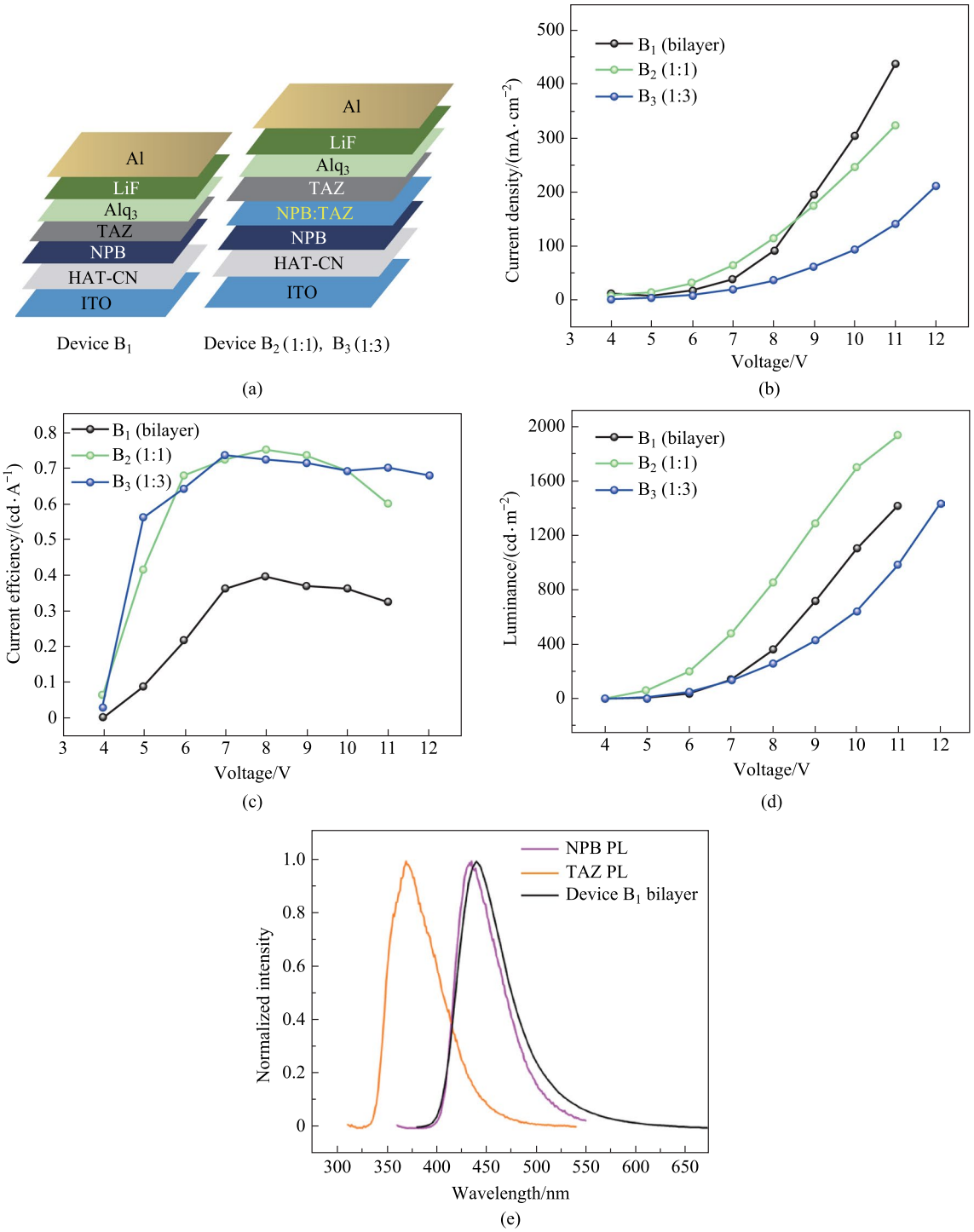

Fig. 2 **a** OLED architectures of NPB/TAZ bilayer (B_1) and NPB:TAZ (1:1 and 1:3) blend devices (for B_2 and B_3, respectively). **b** Current density vs voltage plot. **c** Current efficiency vs voltage plot. **d** Luminance vs voltage plot; **e** Comparison of photoluminescence and electroluminescence of NPB/TAZ bilayer OLED B_1 devices

were carried out to investigate whether the emission was due to energy transfer or exciplex emission in the mixed layer of NPB/TAZ. The steady-state absorption and emission spectra of the molecules were studied in the thin film state. The UV–Visible absorption spectra, as well as the emission spectra of the films of TAZ, NPB and NPB:TAZ (1:1, 1:3), are shown in Fig. S2a and b in the SI. The comparison of PL of neat films with the EL spectra of the bilayer

device is shown in Fig. 2e. The emission from TAZ can be completely ruled out as its emission spectrum was significantly different from the EL spectra. The emission spectra of NPB and blend films were not identical. The full width at half maximum (FWHM) of the PL peaks of the films of NPB, TAZ, and NPB:TAZ were 52, 54, and 63 nm, respectively. The fluorescence decay parameters of NPB, TAZ and NPB:TAZ films are shown in Table S1 in the SI. A slight red shifted emission with increase in FWHM was observed for the blend films but was not observed for the neat films. Exciplex usually leads to the red shifted emission and broadened spectrum compared to those of the individual acceptor or donor molecule. Hence, this broadness of emission in the blend films can be attributed to the exciplex formation. However, considering the absorption spectrum of NPB and photoluminescence spectrum of TAZ, energy transfer also seems likely, as there is sufficient overlap between the emission and absorption spectra of neat films of TAZ and NPB, respectively. As is shown, Fig. S2b in the SI indicates a possibility of Förster resonance energy transfer (FRET) from TAZ to NPB. We compared the PL of the NPB:TAZ blend films at two different ratios 1:1 and 1:3. The PL of TAZ was completely quenched in both 1:1 and 1:3 blend films. The PLQYs of the 1:1 and 1:3 blend films were found to be 38% and 44%, respectively. A slight enhancement in PLQYs for the 1:3 blend films again showed the possibility of energy transfer from TAZ to NPB. The transient emission properties of the blend films were found similar to that of NPB's PL as shown in Fig. S3a in the SI, with the values compared in Table S2 in the SI. Therefore, the results suggest that the energy transfer from TAZ to NPB resulted in the blue excitonic emission from NPB under optical excitation. To confirm this, we needed to rule out the chances for exciplex formation; we further studied the transient PL of the blend films by comparing them under N_2 and O_2 atmospheres as shown in Fig. S3b in the SI, with their transient decay times tabulated in Table S2. We could not detect any kind of triplet quenching in the films; hence no delayed component was observed in the transient kinetics even under N_2 atmosphere. Coupled with the almost similar PL characteristics (except for a 6% enhancement in PLQYs for 1:3 blend films), this supported the energy transfer hypothesis. The device performances are compared and summarized in Table 1.

From the spectroscopic studies of the thin-films, we could say that we have evidence for both exciplex formation and energy transfer from TAZ to NPB. The redshifted and slightly broader spectra of the blend film, compared to the spectra for the neat films, could be evidence for exciplex formation. At the same time, favorable spectral overlap between emission of TAZ and absorption of NPB and the improved PLQY of the blend film with lower concentration of NPB can be cited as supporting evidence for energy transfer from TAZ to NPB. However, the lack of delayed emission for the blend film compared to the neat films could be evidence of no exciplex formation. Hence, it appears that there is a complex mix of different mechanisms.

From the performance of blue devices, it is clear that blend devices exhibit better performance compared to the bilayer device, which may be supporting the argument in favor of exciplex formation. Bulk exciplexes are reported to be more stable than interface exciplex as more intermolecular exciplexes can be formed in the bulk, compared to the interface [17]. Also, in this study, the device with 1:1 ratio between NPB and TAZ worked better than the device with 1:3 ratio. In general, exciplexes work best with 1:1 ratio [11]. This also supports the formation of an exciplex between NPB and TAZ. However, we do not completely rule out energy transfer, though NPB is a weak emitter. In fact, both mechanisms may co-exist also.

3.1.2 Yellow and white OLEDs using phosphorescent dopant in the NPB:TAZ exciplex host

The core idea of this work was to develop novel device design strategies to improve the quality of white light in OLEDs using cost-effective solutions. A mixed host system can effectively transfer its energy to the dopants via Förster or Dexter energy transfer mechanisms. Therefore, a dopant was selected based on the spectral overlap of the emission of blend films of NPB:TAZ and the absorption of the dopant. Hence, a yellow phosphorescent dopant, PO-01, was studied as the emitter with our NPB:TAZ host as the yellow OLEDs. Figure 3a shows the spectral overlap of PO-01 and NPB:TAZ films and Fig. 3b depicts the yellow OLED device architecture, consisting of a co-evaporation of PO-01, NPB and TAZ as the EML, sandwiched

Table 1 Device performances of the blue OLEDs

Device	EML	Luminance at 10 V/(cd·m^{-2})	Current density at 10 V/(mA·cm^{-2})	EL peak/nm	Turn-on voltage/V	Maximum luminance/(cd·m^{-2})	Maximum current efficiency/(cd·A^{-1})	Maximum power efficiency/(lm·W^{-1})
B_1	NPB/ TAZ(60 nm/40 nm)	1102	303	440	3.5	1419	0.4	0.16
B_2	NPB:TAZ(1:1, 15 nm)	1703	246	440	3.6	1941	0.75	0.36
B_3	NPB:TAZ(1:3, 15 nm)	642	93	440	3.8	984	0.73	0.35

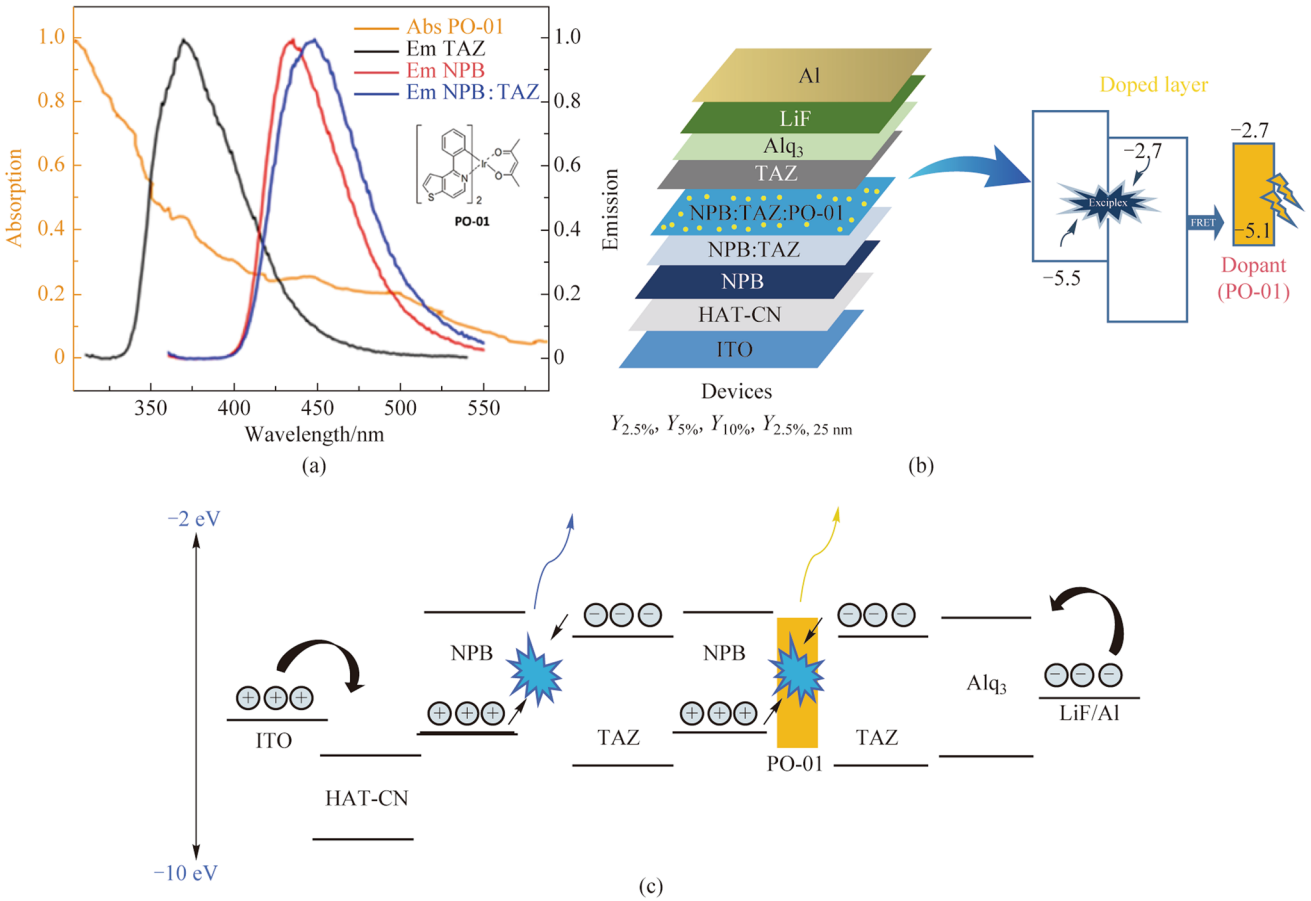

Fig. 3 **a** Spectral overlap between emission of NPB and TAZ with absorption of dopant (PO-01), with the chemical structure of PO-01 shown inset). **b** Device architecture (NPB:TAZ doped with PO-01 at 2.5%, 5% and 10%, respectively). **c** Energy level diagram showing the mechanism responsible for the yellow emission

by NPB and TAZ layers. The emissive layer consisted of a mixed layer NPB:TAZ (1:1, 10 nm) followed by the emissive layer of NPB:TAZ:PO-01 (1:1, *x*%, 5 nm), where $x = 2.5\%$, 5% and 10% for devices, $Y_{2.5\%}$, $Y_{5\%}$ and $Y_{10\%}$, respectively. The energy level diagram is shown in Fig. 3c. It was found that device $Y_{5\%}$ showed the best performance with maximum brightness of 13,070 cd/m^2 and an EQE of $(6.9 \pm 0.27)\%$ @ 1000 cd/m^2 (Fig. 4). The current efficiency vs voltage and *J*–*V*–*L* plots for the yellow devices are shown in Fig. 4a, b. Figure 4c compares the EL spectra of the devices, dominated by a yellow emission at around 560 nm, in addition to a blue emission at around 444 nm. The yellow emission is likely due to an energy transfer from the exciplex to PO-01. When the dopant concentration was decreased to 2.5%, the relative contribution of the exciplex slightly enhanced to give a warm white emission with CIE coordinates (0.43, 0.46) with a blue to yellow emission ratio of 12%. The summary of device performance of yellow OLEDs is tabulated in Tables 2 and 3 and Table S4 in the SI (with error bars). This device is more promising regarding white emission, but the blue emission is weak. To further enhance the blue contribution, we increased the thickness of the NPB:TAZ layer to 25 nm. Hence, a new device $Y_{2.5\%}$ with 25 nm blue EML as NPB:TAZ (1:1, 25 nm)/NPB:TAZ:PO-01(1:1,2.5%, 5 nm) was fabricated. It has been reported that the excitons in charge transfer (CT) states in D-A blends can diffuse much more than Frenkel excitons [18]. However, the ratio of blue to yellow emission remained at 7% with the total brightness falling compared to the device $Y_{2.5\%}$. To further study the thickness dependence of blue layer, we again increased the blue EML from 25 to 30 nm. The white quality improved but the device efficiency drastically reduced. The comparison of the current efficiency values with voltages and comparison of EL plots are given in Fig. S4a and b in the SI.

The energy level diagram in Fig. 3c shows the emission mechanisms in the yellow and blue emitting units in detail. The yellow emitting unit consists of the yellow dopant molecule in the NPB:TAZ matrix. The spectral overlap shows the chances for energy transfer from NPB:TAZ, NPB or TAZ to PO-01, yielding the yellow emission. In contrast, for charge

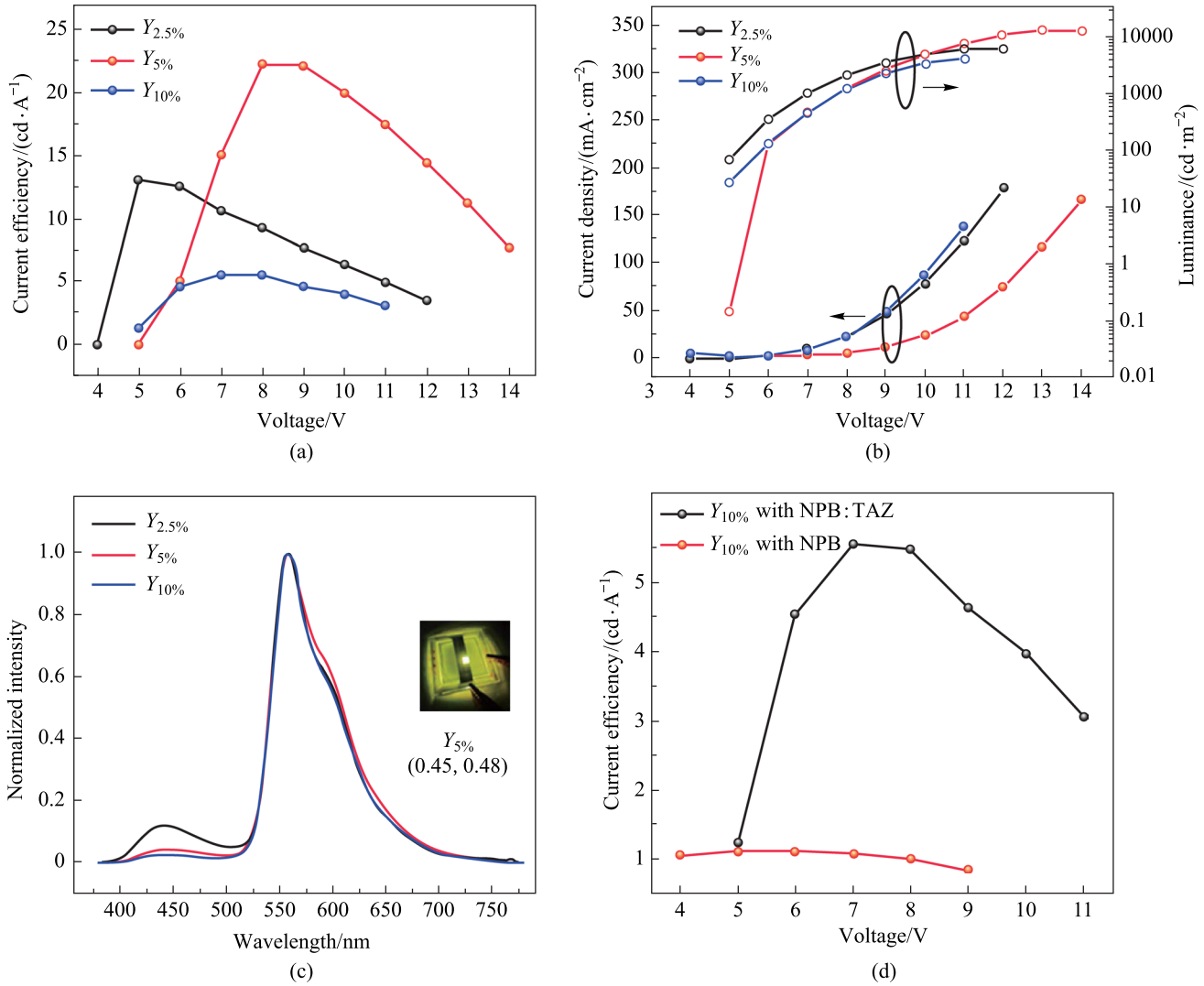

Fig. 4 **a** Current efficiency vs voltage plots for the yellow devices. **b** *J*–*V*–*L* plots. **c** EL spectra of the yellow devices. **d** Current efficiency vs voltage plots for devices with NPB and NPB:TAZ as host with 10% of PO-01

Table 2 Summary of device performance of yellow OLEDs

Device	EML	Luminance at 11 V/(cd·m^{-2})	cd/A (@ 1000 cd·m^{-2})	Turn-on voltage/V	Maximum luminance/(cd·m^{-2})	Maximum current efficiency/(cd·A^{-1})	Maximum power efficiency/(lm·W^{-1})	Maximum EQE/%
$Y_{2.5\%}$	NPB:TAZ(10 nm)/ NPB:TAZ:PO-01(1:1,2.5%, 5 nm)	6090	9.8	4.1	6164	13	8	4
$Y_{5\%}$	NPB:TAZ(10 nm)/ NPB:TAZ:PO-01(1:1,5%, 5 nm)	7750	20	4.3	13,070	22	8.7	7
$Y_{10\%}$	NPB:TAZ(10 nm)/ NPB:TAZ:PO-01(1:1,10%, 5 nm)	4240	5.47	4.8	4244	5.5	2.5	1.7
$Y_{2.5\%,\ 25\ nm}$	NPB:TAZ(25 nm)/ NPB:TAZ:PO-01(1:1,2.5%, 5 nm)	5024	13.9	5.9	7913	14	5.5	4.5

Table 3 Summary of emission parameters of yellow OLEDs

Device	EML	EL peak wavelength/nm		Ratio of blue to yellow/%
		Yellow	Blue	
$Y_{2.5\%}$	NPB:TAZ(10 nm)/NPB:TAZ:PO-01 (1:1,2.5%, 5 nm)	560	440	12
$Y_{5\%}$	NPB:TAZ(10 nm)/NPB:TAZ:PO-01 (1:1,5%, 5 nm)	560	440	4
$Y_{10\%}$	NPB:TAZ (10 nm)/NPB:TAZ: PO-01(1:1,10%, 5 nm)	560	440	3
$Y_{2.5\%,\ 25\ nm}$	NPB:TAZ(25 nm)/NPB:TAZ:PO-01 (1:1,2.5%, 5 nm)	560	444	7

injection, the holes and electrons should reach both NPB and TAZ for the yellow emission. However, given that there is a high energy barrier for transfer of holes from NPB to TAZ (0.8 eV) in the blend; the migration of holes toward the HOMO of NPB in the NPB:TAZ:PO-01 layer could have been hindered due to the presence of TAZ in the NPB:TAZ layer. Hence, NPB and TAZ in the NPB:TAZ:PO-O1 layer cannot be individually electrically excited easily.

To rule out the possibility of energy transfer from NPB to P0-01, we fabricated an equivalent device without TAZ where NPB was used as a host. The current efficiency vs voltage plots for devices with NPB and NPB:TAZ as host with 10% of PO-01 is shown in Fig. 4d. The device only showed green emission of Alq_3 instead of yellow emission. This indicates that energy transfer from NPB to the dopant is unlikely. This also showed the direct excitation of PO-01 is unlikely in the current device structure, leaving next possibility of energy transfer from exciplex to PO-01. This indeed happened while the proposed exciplex in the NPB:TAZ layer was responsible for the blue emission.

As mentioned earlier, increasing the thickness of the NPB:TAZ layer to 25 and 30 nm to further enhance the blue contribution did not yield the expected results. The slow migration of holes from the NPB alone layer toward NPB:TAZ:PO-01 layer could have been an impediment. The low *J* value of the device shows that the increased thickness of the layer resulted only in increasing the device resistance instead of enhancing the blue emission.

The weak intensity of blue emission is primarily due to the difference in hole and electron mobilities of the component molecules. Due to the high hole mobility of NPB, more holes get accumulated at the HOMO of NPB in the NPB:TAZ layer. The comparatively lower electron mobility of TAZ and the longer path for electrons from cathode to reach this layer can delay electrons migration to the LUMO of TAZ in the NPB:TAZ layer. This loss of carriers can lead to decreased blue exciton formation and subsequent emission in the NPB:TAZ layer. A similar issue can be expected for exciplex formation in the NPB:TAZ:PO-01 layer as well. But here the effect of longer path for holes from anode and low mobility of electrons in TAZ can create a balance and hence a promising white emission is to be expected. The device architecture comprises of two emissive units with co-deposited film of NPB and TAZ. Hence there will be possibility of uncontrolled flow of carriers through the co-deposited layers. This can reduce the charge balance factor and the formation of excitons. The unbalanced flow of carriers to the NPB:TAZ layer might be a reason for reduction in blue emission among the white devices. To study the problem of carrier imbalance in the device, we fabricated the hole-only and electron only devices. The device architecture was as follows: ITO/HAT-CN(5 nm)/NPB(60 nm)/NPB:TAZ(50 nm)/Ag(100 nm) for the hole-only device and Al(100 nm)/LiF(1 nm)/BCP(5 nm)/NPB:TAZ(50 nm)/TAZ(40 nm)/Alq_3(20 nm)/LiF(1 nm)/Al(100 nm) for the electron-only device. The comparison of the *J*–*V* characteristics of the devices are shown in Fig. S5 in the SI. The hole-only devices showed much higher current density compared to electron only devices; this observation is evidence for the charge imbalance in the NPB:TAZ mixed layer.

3.1.3 White OLEDs using charge generation layer and tetracene spacer

To further improve the quality of white emission, it is critical to balance the blue and yellow emission This can be done by adjusting the flow of holes and electrons toward the respective layers by incorporating a charge generation layer (CGL) between the two emitting units. A suitable CGL would provide adequate flow of electrons and holes toward the respective units. We have therefore selected a typical fullerene (C_{60})/pentacene organic heterojunction as the CGL [19]. The high electron mobility of C_{60} [20] and high hole mobility of pentacene [21] can make this p–n junction an efficient CGL [22]. The balanced flow of electrons from C_{60} toward the NPB:TAZ layer can be expected to enhance

the blue emission. Also, the availability of holes in the NPB:TAZ:PO-01 layer is ensured by pentacene. The EML of devices with CGL has the structure, NPB:TAZ (1:1, 10 nm)/C_{60} (15 or 10 nm)/pentacene (10 or 5 nm)/NPB:TAZ:PO-01 (5 nm, 2.5% PO-01). The device architecture and the energy level diagram are given in Figs. S6a and b in the SI.

The thickness of C_{60} was kept slightly higher than that of pentacene to compensate the high hole mobility of pentacene [21] compared to the electron mobility of C_{60}. However, the device performance was drastically diminished upon the incorporation of the CGL. The device *J*–*V*–*L* and EL characteristics of the devices are shown in Fig. S6c and d in the SI. Hence, unlike in a normal tandem WOLED, the CGL here functioned more like a barrier. The increase in total device thickness might also have contributed to the poor performance. However, the percentage of blue emission slightly improved in these devices compared to the same percentages without a CGL. This implies the need of a separation layer other than CGL for balanced flow of carriers between the NPB:TAZ:PO-01 and NPB:TAZ units of exciplex, which can be called as a spacer layer. In this context, it was further proposed that an ambipolar spacer material would be a better choice than a p–n junction. The energy levels of the spacer material should be conducive to not completely blocking electrons and holes. We, therefore, selected tetracene as the spacer layer as it met the above requirements. A thin layer of tetracene was used as a spacer layer between the NPB:TAZ (blue emitter) and NPB:TAZ:PO-01 (yellow emitter) layers. The energy level diagram of the emissive units for the modified device architecture for WOLED is shown in Fig. 5a. The devices with tetracene blocking layer indeed resulted in a higher intensity

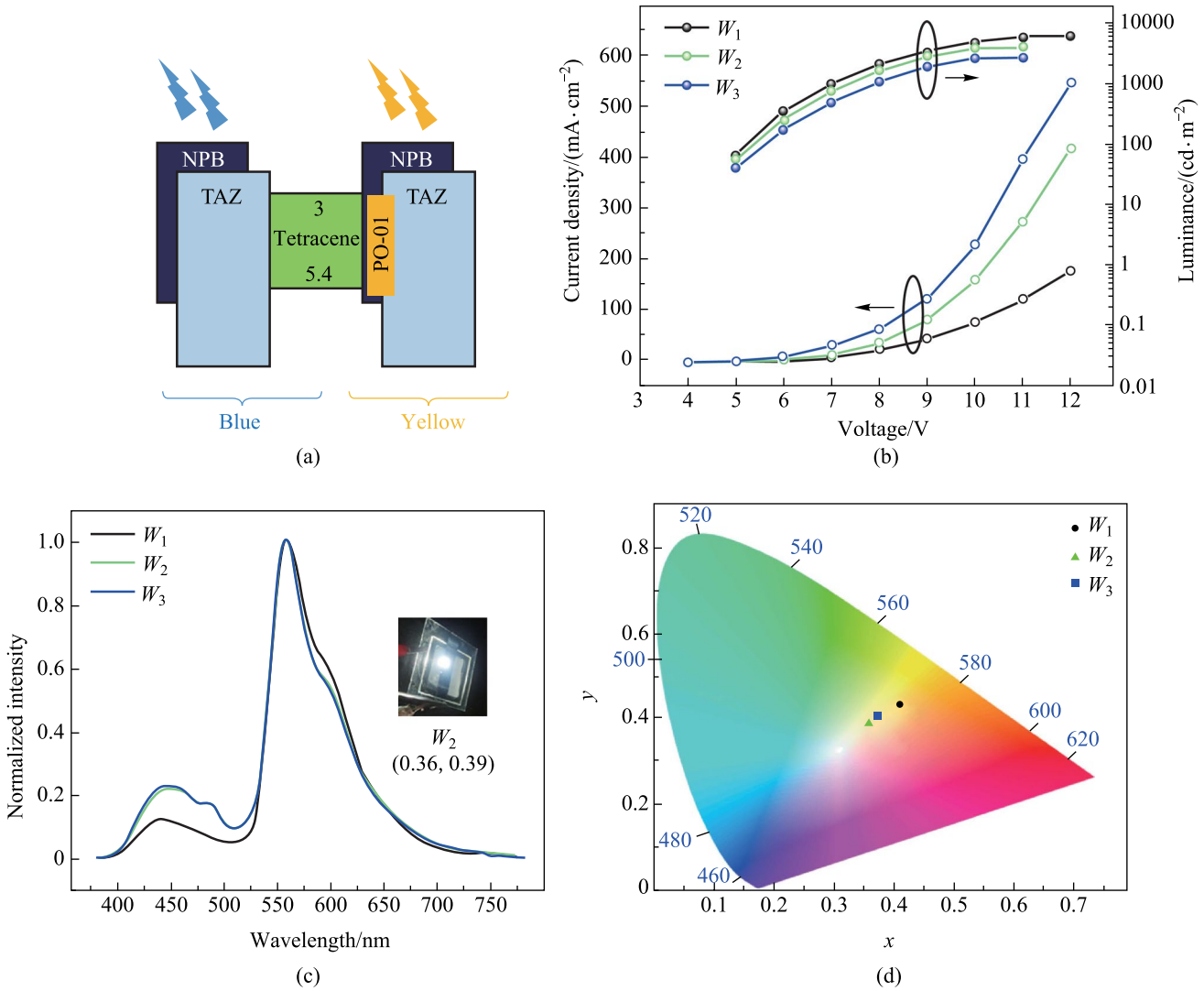

Fig. 5 **a** Energy level diagram of white OLEDs with spacer. **b** *J*–*V*–*L* characteristics. **c** EL characteristics (photograph of the white OLED (W_2) with its CIE coordinates is shown as inset). **d** CIE diagram

Table 4 Summary of device performances of the WOLEDs

Device	EML	Luminance at 11 V/(cd·m^{-2})	cd/A (@ 1000 cd·m^{-2})	Turn-on voltage/V	Maximum luminance/(cd·m^{-2})	Maximum current efficiency/(cd·A^{-1})	Maximum power efficiency/(lm·W^{-1})	Maximum EQE/%
W_1	NPB:TAZ(10 nm)/ NPB:TAZ:PO-01 (1:1,2.5%, 5 nm)	6090	9.8	4.1	6164	13	8	4
W_2	NPB:TAZ(10 nm)/Tetracene(5 nm)NPB:TAZ: PO-01(1:1,2.5%, 5 nm)	4040	4.6	4	4043	6	3.8	2
W_3	NPB:TAZ(10 nm)/ Tetracene(10 nm) NPB:TAZ: PO-01(1:1,2.5%, 5 nm)	4240	1.7	4	2675	2	1	0.6

of blue emission compared to the CGL devices. The weak peak at about 484 nm could be the monomer emission of tetracene [23]. The electroluminescence of tetracene film was around 530 nm [24], which was absent in the EL spectra. Hence, the possibility of emission from the spacer layer can be ruled out. We took the device $Y_{2.5\%}$ as the reference device for white emission, and this device is now designated as W_1. The EML of device W_2 had the structure NPB:TAZ (1:1, 10 nm)/tetracene (5 nm)/NPB:TAZ:PO-01 (5 nm, 2.5% PO-01). Increasing the thickness of tetracene layer to 10 nm (Device W_3) did not improve the performance. However, tetracene devices showed a better performance compared to performances with CGL. The poor performance of the 10 nm spacer layer compared to that of the 5 nm shows the impact of resistance in the devices. We have earlier seen that the CGL devices also fared poorly after the total device thickness increased after the insertion of the CGL. The *J*–*V*–*L* and EL characteristics are shown in Fig. 5b, c and the device performances for WOLEDs with spacer layer are summarized in Table 4. We achieved a white emission with CIE coordinates of (0.36, 0.39), when 5 nm of tetracene was employed. The CIE diagram for WOLEDs is shown in Fig. 5d. The ratios of intensities of blue and yellow emissions were compared. The intensity of blue emission was increased from 12% to 23%, when the spacer layer was employed. This could be attributed to the balanced flow of carriers to NPB:TAZ layer due to the ambipolar nature of tetracene layer. The increase in current density after the addition of tetracene layer is evidence for the role of tetracene in the charge transport mechanism in the device. Unlike in CGL, a single layer can provide improved white light as well as device performance. The efficiency comparison of the WOLEDs with CGL and spacer layer is shown in Table S3 in the SI. Hence, device architecture with a spacer layer can be considered as an alternative to complicated tandem structures. A balanced white OLED combining yellow emission from dopant and blue emission from exciplex was achieved with an ambipolar thin spacer layer.

4 Conclusion

A novel blue emitting exciplex system, utilizing commonly used charge transporting materials, NPB and TAZ, is presented. This intermolecular exciplex used as a blue emitter as well as a host for a yellow dopant to afford white light. Yellow OLEDs were fabricated by using a mixed host with a phosphorescent dopant (PO-01). An EQE of (6.9 ± 0.27)% @ 1000 cd/m^2 was obtained for the yellow OLED, with 5% of PO-01 doped into the NPB:TAZ matrix. White emission with CIE coordinates (0.36, 0.39) and color temperature of 4643 K was achieved by using a novel device design, employing tetracene as a spacer, to balance the carrier transport. The strategy presented here may be utilized for creating tailor-made molecules to realize stable and efficient blue emission, with device designs other than complicated tandem structures for obtaining white emission.

Supplementary Information The online version contains supplementary material available at https://doi.org/10.1007/s12200-023-00101-3.

Acknowledgements The authors acknowledge support by DST-SERB, Govt. of India (CRG/2020/003699). CKV and KNNU acknowledge support from DST-AISRF program of the Department of Science and Technology, Government of India (DST/INT/AUS/P-74/2017). KR acknowledges the support from Council of Scientific and Industrial Research (CSIR), Government of India for the award of a research fellowship. AKS acknowledges support from DST-INSPIRE for the award of a research fellowship.

Author contribution KR did the experimental work; made the major contribution in acquisition of data and drafted the paper. CKV and AKS helped in device fabrication and characterization. AS and SKMM carried out the photophysical studies. SCL and EBN contributed to

analysis and interpretation of the work. KNNU designed the concept of the work and interpreted the data. All authors contributed to the input to the final manuscript.

Availability of data and materials The data that support the findings of this study are available from the corresponding author, upon reasonable request.

Declarations

Competing interests The authors declare that they have no competing interests.

References

1. Tang, C.W., VanSlyke, S.A.: Organic electroluminescent diodes. Appl. Phys. Lett. **51**(12), 913–915 (1987)
2. Hippola, C., Kaudal, R., Manna, E., Xiao, T., Peer, A., Biswas, R., Slafer, W.D., Trovato, T., Shinar, J., Shinar, R.: Enhanced light extraction from OLEDs fabricated on patterned plastic substrates. Adv. Opt. Mater. **6**(4), 1701244 (2018)
3. Sajeev, A.K., Agarwal, N., Soman, A., Gupta, S., Katiyar, M., Ajayaghosh, A., Unni, K.N.: Enhanced light extraction from organic light emitting diodes using a flexible polymer-nanoparticle scattering layer. Org. Electron. **100**, 106386 (2022)
4. Zhang, Y., Biswas, R.: High light outcoupling efficiency from periodically corrugated OLEDs. ACS Omega **6**(13), 9291–9301 (2021)
5. Liu, Y., Li, C., Ren, Z., Yan, S., Bryce, M.R.: All-organic thermally activated delayed fluorescence materials for organic light-emitting diodes. Nat. Rev. Mater. **3**(4), 1–20 (2018)
6. Ma, D., Liu, R., Zhang, C., Qiu, Y., Duan, L.: High-efficiency organic light-emitting diodes based on sublimable cationic iridium (III) complexes with sterically hindered spacers. ACS Photonics **5**(8), 3428–3437 (2018)
7. Zhuang, S., Zhang, W., Yang, X., Wang, L.: A simple unilateral homogenous PhOLEDs with enhanced efficiency and reduced efficiency roll-off. Front Optoelectron. **6**(4), 435–439 (2013)
8. Li, W., Tang, J., Zheng, Y., Peng, J., Zhang, J., Wei, B., Li, X.: Improved stability of blue TADF organic electroluminescent diodes via OXD-7 based mixed host. Front Optoelectron. **14**(4), 491–498 (2021)
9. Bi, Y., Ji, J., Chen, Y., Liu, Y., Zhang, X., Li, Y., Xu, M., Liu, Y., Han, X., Gao, Q., Sun, H.: Dual-periodic-microstructure-induced color tunable white organic light-emitting devices. Front Optoelectron. **9**(2), 283–289 (2016)
10. Zhu, L., Xu, K., Wang, Y., Chen, J., Ma, D.: High efficiency yellow fluorescent organic light emitting diodes based on m-MTDATA/BPhen exciplex. Front Optoelectron. **8**(4), 439–444 (2015)
11. Sarma, M., Wong, K.T.: Exciplex: an intermolecular charge-transfer approach for TADF. ACS Appl. Mater. Interfaces **10**(23), 19279–19304 (2018)
12. Oh, E., Park, S., Jeong, J., Kang, S.J., Lee, H., Yi, Y.: Energy level alignment at the interface of NPB/HAT-CN/graphene for flexible organic light-emitting diodes. Chem. Phys. Lett. **668**, 64–68 (2017)
13. Kim, Y., Kim, J., Park, Y.: Energy level alignment at a charge generation interface between 4, 4′-bis (*N*-phenyl-1-naphthylamino) biphenyl and 1,4,5,8,9,11-hexaazatriphenylene-hexacarbonitrile. Appl. Phys. Lett. **94**(6), 063305 (2009)
14. Jankus, V., Chiang, C.J., Dias, F., Monkman, A.: Deep blue exciplex organic light- emitting diodes with enhanced efficiency; P-type or E-type triplet conversion to singlet excitons? Adv. Mater. **25**, 1455–1459 (2013)
15. Fan, C., Chen, Y., Liu, Z., Jiang, Z., Zhong, C., Ma, D., Qin, J., Yang, C.: Tetraphenylsilane derivatives spiro-annulated by triphenylamine/carbazole with enhanced HOMO energy levels and glass transition temperatures without lowering triplet energy: host materials for efficient blue phosphorescent OLEDs. J. Mater. Chem. C. **1**, 463–469 (2013)
16. Zhang, C., Lu, Y., Liu, Z., Zhang, Y., Wang, X., Zhang, D., Duan, L.: A π–D and π–A exciplex-forming host for high-efficiency and long-lifetime single-emissive-layer fluorescent white organic light-emitting diodes. Adv. Mater. **32**(42), 2004040 (2020)
17. Gu, J., Tang, Z., Guo, H., Xiao, Y., Chen, Z., Xiao, C.: Intermolecular TADF: bulk and interface exciplexes. J. Mater. Chem. C. **10**, 4521–4532 (2022)
18. Deotare, P., Chang, W., Hontz, E., Congreve, D., Shi, L., Reusswig, P., Modtland, B., Bahlke, M., Lee, C., Willard, A., Bulović, V., Van Voorhis, T., Baldo, M.A.: Nanoscale transport of charge-transfer states in organic donor–acceptor blends. Nat. Mater. **14**(11), 1130–1134 (2015)
19. Chen, Y., Chen, J., Ma, D., Yan, D., Wang, L.: Tandem white phosphorescent organic light-emitting diodes based on interface-modified C60/pentacene organic heterojunction as charge generation layer. Appl. Phys. Lett. **99**(10), 103304 (2011)
20. Golubev, T., Liu, D., Lunt, R., Duxbury, P.: Understanding the impact of C_{60} at the interface of perovskite solar cells via drift-diffusion modeling. AIP Adv. **9**(3), 035026 (2019)
21. Günther, A.A., Widmer, J., Kasemann, D., Leo, K.: Hole mobility in thermally evaporated pentacene: morphological and directional dependence. Appl. Phys. Lett. **106**(23), 233301 (2015)
22. Yan, H., Kagata, T., Okuzaki, H.: Ambipolar pentacene/C_{60}-based field-effect transistors with high hole and electron mobilities in ambient atmosphere. Appl. Phys. Lett. **94**(2), 023305 (2009)
23. Lim, S.H., Bjorklund, T.G., Spano, F.C., Bardeen, C.J.: Exciton delocalization and superradiance in tetracene thin films and nanoaggregates. Phys. Rev. Lett. **92**(10), 107402 (2004)
24. Hamid, T., Kielar, M., Yambem, S.D., Pandey, A.K.: Multifunctional diode operation of tetracene sensitized polymer: fullerene heterojunctions with simultaneous electroluminescence in visible and NIR bands. Adv. Electron. Mater. **7**(1), 2000824 (2021)

Kavya Rajeev obtained her Bachelor's degree in Physics from Nirmalagiri College, Kuthuparamba (affiliated to Kannur University, Kerala, India) in 2016 and Master's degree in Physics from Pondicherry University, India in 2018. She is currently pursuing her Ph.D. degree in the area of Organic Optoelectronic Devices at Centre for Sustainable Energy Technologies, CSIR-NIIST (Council of Scientific and Industrial Research—National Institute for Interdisciplinary Science and Technology) and AcSIR (Academy of Scientific and Innovative Research), CSIR, India. Her research focuses on investigations on exciplex based organic light emitting diodes.

C. K. Vipin obtained a M.Sc. degree in Physics from Central University of Kerala, India. In 2019, he joined CSIR- National Institute for Interdisciplinary Science and Technology (NIIST), Thiruvananthapuram, Kerala, India, as a Junior Research Fellow under the guidance of Dr. K.N. Narayanan Unni at OLED Fabrication and Characterisation Lab to work on an Indo-Australian project, "Large Area Optoelectronics for Australia and India: From Materials to Advanced Devices". Presently, he is a Ph.D. student, working under the joint guidance of Dr. K.N. Narayanan Unni and Dr. Suraj Soman and his work focuses on the fabrication and characterization of perovskite solar cells with carbon based back-electrodes.

Anjali K. Sajeev obtained her Bachelor of Science and Master of Science Dual Degree in Physics from Indian Institute of Science Education and Research in 2015. She is currently pursuing her Ph.D. in the area of Organic Optoelectronic Devices at Centre for Sustainable Energy Technologies, CSIR-NIIST (Council of Scientific and Industrial Research—National Institute for Interdisciplinary Science and Technology) and AcSIR (Academy of Scientific and Innovative Research), CSIR, India. Her main research topic is halide-based hybrid light emitting diodes.

Atul Shukla is a Postdoctoral researcher at the University of Potsdam, Germany. He completed his undergraduate degree in Chemical Engineering at the Indian Institute of Technology Roorkee in 2016 and obtained his Ph.D. degree at the University of Queensland, Australia in 2021. His research interests include using steady-state and time resolved optical spectroscopies to study optical and spin processes in organic semiconductors, with a focus on solar cell and LED applications.

Sarah K. M. McGregor is a synthetic chemist and postdoctoral research fellow at The University of Queensland, Australia, with a Ph.D. degree in Organic Chemistry. Her research has focused on the development of novel optoelectronic materials for organic solar cells, organic light-emitting diodes, and organic lasers, where she explores the intricate physical property relationships to offer crucial insights into the design of next-generation electronic devices.

Shih-Chun Lo received his D.Phil. degree from Oxford University, UK in 2000. Post his postdoctoral research at Oxford University, he joined The University of Queensland (UQ), Australia, as a lecturer in 2007, and is an Associate Professor at UQ's School of Chemistry and Molecular Biosciences. His Ph.D. work was the development of organic and organometallic semiconductors materials for organic light-emitting diodes (OLEDs) and solar cells organic as The Swire DPhil Scholar. His postdoc projects were mainly on organic light-emitting dendrimers, where he played a key role for light-emitting dendrimers being globally recognised as the third main class of light-emitting materials (alongside, small molecules & polymers). His research has focused on the development of truly frontier materials for high-performing devices, including OLEDs, clean energy generation like organic solar cells and water splitting (for hydrogen fuel), organic field-effect transistors (OFETs), organic light-emitting transistors (OLETs), organic photodetectors (OPDs) and organic lasers. He has published > 110 refereed journal articles (in e.g., *Adv. Mater.*, *Adv. Funct. Mater.*, *Adv. Opt. Mater.*, *Chem. Mater.*, *Chem. Rev.*, *Chem. Sci.*, *J. Am. Chem. Soc.*, *Nature Commun.*, *Science*), and > 70 granted patents globally.

Ebinazar B. Namdas is an associate professor in the School of Mathematics and Physics, at The University of Queensland, Australia. He completed his Ph.D. degree in Physics. He has a strong international track record in the field of organic optoelectronic materials and devices research across several platforms including transistors, light-emitting transistors, OLEDs, organic lasers, and photodetectors. He has published more than 110 papers in top international journals.

K. N. Narayanan Unni obtained his M.Sc. and Ph.D. degrees from School of Pure & Applied Physics, Mahatma Gandhi University, Kerala, India. Subsequently he received post-doctoral training at Indian Institute of Technology Bombay and University of Angers, France. Later, he joined Samtel Colour Ltd., New Delhi and led a research team to develop OLED displays in India. Subsequently, he took up the position of Principal Research Engineer at Indian Institute of Technology Kanpur and later moved to CSIR-National Institute for Interdisciplinary Science and Technology, Thiruvananthapuram, India. Currently, he is a Senior Principal Scientist and Head of Centre for Sustainable Energy Technologies at CSIR-NIIST. He is also a Professor with Academy of Scientific and Innovative Research (AcSIR), India. He is an elected Fellow of Institution of Electronics and Telecommunication Engineers, India (FIETE) and an elected Fellow of Kerala Academy of Sciences (FAS). His current research interests are organic electronics, energy materials and devices.